DISS. ETH NO. 26503

Robot-Aided Gait Assessment and Rehabilitation:

an Assist-as-Needed Approach

A thesis submitted to attain the degree of

DOCTOR OF SCIENCES of ETH ZURICH

(Dr. sc. ETH Zurich)

presented by

SERENA MAGGIONI

Laurea Magistrale in Biomedical Engineering, Politecnico di Milano

born on 30.04.1986

citizen of Italy

accepted on the recommendation of

Prof. Dr.-Ing. Robert Riener

Dr. Alejandro Melendez-Calderon

Dr. Lars Lünenburger

Prof. Dr. med. Armin Curt

2019

ABSTRACT

According to the World Health Organization (WHO), around 1.1 billion people worldwide live with a form of disability, mostly affecting mobility. Limitations in walking affect independence, quality of life and lead to several secondary complications due to immobility. To provide suitable and targeted rehabilitation to patients, we require evidence-based treatments, trained health professionals and assessments to measure and track recovery. Current assessments of sensorimotor functions are hampered by issues such as limited sensitivity and objectivity that prevent their regular use in clinical practice and limit the benefit that the patients can obtain from rehabilitation. New technologies, such as robotic gait trainers, have become a real possibility for locomotor therapy after neurological injuries. Besides offering support and guidance to the movements, they allow creating standard protocols within the training sessions and measuring objective data with the integrated sensors.

The long-term goal of this project is to develop a valid, reliable and sensitive assessment of walking activity in a robotic gait trainer that can be used in clinical practice to assess patients during every stage of rehabilitation. In this thesis, an algorithm allowing safe and objective assessment of patients' walking ability was designed and implemented in a treadmill-based robotic gait trainer. This was tested and validated on a robotic test bench and in individuals after Spinal Cord Injury against established clinical scores.

The algorithm consists of an assist-as-needed (AAN) controller that adapts the robotic support based on the patient's ability to follow a reference gait trajectory displayed on a screen. The outcome measures are the body weight support and mechanical impedance (stiffness and damping) of the hip and knee robotic joints determined by the AAN algorithm in different gait phases. The construct validity of the AAN-based assessment was evaluated using a robotic test bench simulating known neuromotor impairments: the method was sensitive enough to capture differences in the simulated impairments and allowed the identification of confounding factors such as speed and gait-phase-dependent biomechanics.

The AAN-based assessment was then evaluated in patients with Spinal Cord Injury. Each patient was assessed twice within a week to evaluate the reliability of the technique. The relationship between the AAN outcome measures and established clinical scores measuring walking ability was studied. A linear model based on only one variable (the robotic knee stiffness at terminal swing) was able to explain 74% of the variance in the 10-Meter-Walking-Test data in ambulatory patients. Adding the maximum isometric hip flexor torque as a second variable to the model increased the explained variance to >85%. The limited amount of data available from non-ambulatory patients prevented us to extend the findings to this population. Test-retest reliability was still too low for clinical application, since a change of 9.1% (between two different sessions) in the robotic knee stiffness at terminal swing would be required to indicate a significant change in walking ability.

To increase the compliance of the controller to physiological deviations of the foot trajectory from the reference, we developed a "hybrid joint/end-point space controller with AAN", combining the benefits of joint and end-point space robotic controllers. The adaptive hybrid controller shaped the end-

point (i.e. the ankle) robotic stiffness according to the direction and the magnitude of the error performed at the level of the ankle. The resulting end-point force selectively counteracted certain foot position errors while leaving the robot compliant in other directions. While additional gravity compensation was needed to support a single severely impaired patient using this controller, we demonstrated the safety and feasibility of the hybrid controller in able-bodied subjects.

Overall, we were able to design, develop and test a novel software for a treadmill-based robotic exoskeleton that can be used to quantify the robotic support required by a patient while performing gait training. The support determined by the algorithm provides information about the patient's walking ability that could be used to assess the patient's recovery, to provide motivation or to adjust the therapy accordingly. The adaptive characteristics of the software could enable a more challenging training environment that is tuned to the ability of the individual patients.

ZUSAMMENFASSUNG

Gemäss WHO leben ungefähr 1.1 Milliarden Menschen weltweit mit einer Art von Behinderung, die in den meisten Fällen die Mobilität betrifft. Gangstörungen beeinträchtigen die alltägliche Unabhängigkeit, die Lebensqualität und können zu verschiedensten Sekundärkomplikationen aufgrund von Immobilität führen. Um dem betroffenen Patienten passende und zielgerichtete Rehabilitation anzubieten, braucht es evidenzbasierte Therapien, geschulte Gesundheitsexperten und sensitive Assessments zur Verfolgung des Rehabilitationsvorganges. Heutige Assessments der sensormotorischen Funktion weisen oftmals eine limitierte Sensitivität und Objektivität auf, behindert, was deren regulären Einsatz in der Klinik limitiert. Neue Technologien, unter anderem robotische Lauftrainer, sind zu einer vielversprechenden Therapie für neurologischen Gangstörungen geworden. Neben der Möglichkeit zur gezielten Bewegungsführung, erlauben diese Lauftrainer das Etablieren von Trainingsprotokollen und die Akquise von objektiven Messdaten über integrierte Sensoren.

Das Langzeitziel dieses Projekts war die Entwicklung eines validen, zuverlässigen und sensitiven Assessments der Gehfähigkeit in einem robotischen Gangtrainer, welches in der klinischen Praxis zur Bewertung von Patienten in der Frührehabilitation eingesetzt werden kann. In dieser Doktorarbeit wurde ein Algorithmus für eine sichere und objektive Bewertung der Gehfähigkeit des Patienten ausgearbeitet, in einen robotischen Lauftrainer implementiert und validiert. Im Spezifischen wurde der Algorithmus auf einer robotischen Forschungstestplattform getestet sowie im Vergleich zu regulären klinischen Assessments in Patienten mit Rückenmarksverletzung validiert.

Der Algorithmus besteht aus einem Assist-as-Needed (AAN) Regler, welcher den robotischen Support aufgrund der Fähigkeiten des Patienten einer Gangreferenztrajektorie auf einem Bildschirm zu folgen anpasst. Die Ausgangsgrößen des AAN Algorithmus in verschiedenen Gangphasen sind die Körpergewichtsunterstützung und die mechanische Impedanz (Steifheit und Dämpfung) des robotischen Hüft- und Kniegelenks. Die Validität des AAN-basierten Assessments wurde mit einer robotischen Forschungstestplattform evaluiert, welche bekannte motorische Beeinträchtigungen simuliert hat: Die Methode war sensitiv genug um die Unterschiede zwischen den simulierten Beeinträchtigungen zu erkennen. Dies erlaubte die Identifikation von Störfaktoren wie Geschwindigkeit und gangzyklusäbhängiger Biomechanik.

Der AAN-basierte Bewertungstest wurde dann in Patienten mit Rückenmarksverletzung getestet. Jeder Patient wurde zweimal in einer Woche gemessen, um die Reliabilität der Methode zu testen. Der Zusammenhang zwischen den AAN-Messwerten und etablierten klinischen Testresultaten zur Bewertung der Gehfähigkeit wurde untersucht. Ein lineares Modell (auf einer Variable basierend (die robotische Kniesteifigkeit am Ende der Schwungphase des Beines)) war in der Lage 74% der Varianz in dem 10-Meter-Gehtest mit gehfähigen Patienten zu erklären. Wenn man das maximale isometrische Drehmoment des Hüftflexors als zweite Variable zum Model hinzugefügt wurde, erhöhte sich die erklärte Varianz auf über 85%. Die limitierte Verfügbarkeit von Daten von nicht-gehfähigen Patienten

hat uns daran gehindert, die Ergebnisse auf diese Population zu übertragen. Die Reliabilität des Assessments war zu niedrig für eine vernünftige klinische Applikation, da eine Veränderung von 9.1% (zwischen Test und Retest) in der robotischen Kniesteifigkeit am Ende der Schwungphase des Beines gebraucht würde, um einen signifikanten Unterschied in der Gehfähigkeit festzustellen.

Die Ergebnisse der klinischen Studie führten dazu, einen „hybriden Gelenks/Endpunkt Regler mit AAN" zu entwickeln, welcher die Vorteile der Gelenks- und Endpunktbasierten Regler kombiniert. Der adaptive und hybride Regler veränderte die Steifigkeit des Endpunktes (i.e. des Fußgelenks) aufgrund der Richtung und der Größe des Fehlers auf dem Gelenkslevel. Die resultierende Endpunktkraft wirkte selektiv gegen spezielle Fußpositionen, während sie in andere Richtungen transparent war. Da zusätzliche Gravitationskompensation gebraucht wurde, um einige schwerbetroffene Patienten mit diesem Regler zu unterstützen, wurde die Sicherheit und Durchführbarkeit des hybriden Reglers mit gesunden Probanden getestet.

Zusammenfassend waren wir in der Lage, eine neue Software für einen laufbandbasierten, robotischen Lauftrainer zu entwickeln und zu testen. Die Software kann genutzt werden, um die notwendige robotische Unterstützung eines Patienten während des Trainings zu berechnen. Die berechnete Unterstützung des Algorithmus gibt Informationen über die Gehfähigkeit des Patienten. Dies ist von Nutzen, um die Rehabilitation des Patienten zu bewerten, den Patienten zu motivieren und die Therapie entsprechend anzupassen. Die adaptive Gestaltung der Software könnte eine herausfordernde Trainingsumgebung ermöglichen, die an die Gehfähigkeiten des einzelnen Patienten angepasst ist.

ACKNOWLEDGEMENTS

And of course, outside the work environment, I want to thank deeply my friends in Zurich, who soon made me feel at home. My "Caro diario" Raffaele, for his warm laugh, for his ability to listen, for all the parties he is always ready to throw and the delicious Italian meals he cooks for his friends. He really made the difference for me here. I have shared my house and my stories with awesome flatmates: Andrea, with his blunt sense of humor and his theory of the sinusoidal aspects of life (we are at $\pi/2$!), Alex, and his ability to bring home the most surprising objects and Michèle, for her contagious spontaneity and the spark she puts in everything she does. Thanks also to my "acquired" flatmates of Seefeldstrasse, for hosting me and our parties multiple times. And in the last years, thanks to Luca and Michela for enriching our Zurich family with positivity, music and their warm hearts.

I moved to Zurich to start the PhD but I did not lose my friends in Italy, proof that a good friendship can stand the obstacles of time and distance: Chiara, who has shared my adventure from the courtyard of the kindergarten until that of ETH; my classmates Francesca, Rossella, Carlo and Veronica, that did not yet get bored of proposing our reunions; Francesco, whom I met again after ten years when we needed each other the most; my university colleagues Filippo and Francesca and "the Banano Tsunami protocol" that sanctioned the arrival of the summer.

I especially thank Matthias for looking at me always with a smile. His positive attitude to all the matters of life is an endless source of force, serenity, happiness and all the ingredients that I may need in life.

Grazie infine a mamma, papà e Paolo per avermi fatto sempre capire che dovunque io vada ho sempre un posto sicuro a cui tornare.

And, again, I can confirm that…

Happiness is real only when shared.

CONTENTS

Chapter 1   GENERAL INTRODUCTION

Part of the content of this chapter will be submitted for publication with the title: *"Gait features in a robotic gait trainer: what can they tell us about waking ability?",* authored by Maggioni S, Lünenburger L, Riener R, Curt A, Bolliger M, Melendez-Calderon A, in 2020.

Foreword

In this introductory chapter, I present the motivation for this work. I discuss the concrete problem that my thesis wants to solve, provide a brief state-of-the-art framework and identify the niche that this work aims to fill. I then present the objectives and synopsis of the thesis and introduce the field in which this work has developed. A comprehensive description of the state-of-the-art can be found in Chapter 2.

1.1 MOTIVATION

According to the World Report on Disability, more than one billion people worldwide live with a disability, which corresponds to 15% of the world population [1]. Ambulatory disability is the most common type of disability in the United States, affecting 5.1% of the population in the range 18-64 years old and 22.5% of the population aged 65 and over [2]. Walking impairments after a neurological injury affect around three quarters of stroke survivors [3] and the vast majority of people suffering a spinal cord injury (SCI) [4, 5]. Other common neurological causes of gait impairments are Parkinson's disease [6], multiple sclerosis [7] and traumatic brain injury [8]. In this work, we focus mainly on the SCI population, however most of the results could be applied to other neurological conditions. In 2016, there were 0.93 million new cases of SCI worldwide, and the prevalence of SCI patients currently living with the condition was 27.04 million [5]. Improvements in acute medical care after SCI have resulted in increased rates of survival and a longer life expectancy [9]. More than half of SCI survivors presents an incomplete lesion and has chances of recovering walking [4, 10]. Limitations in walking affect independence, quality of life and lead to several secondary complications due to immobility, such as joint contractures, osteoporosis and spasticity [11, 12]. Walking recovery, defined as the regaining of ability to walk independently in the community (functional walking) [13] is among the highly desired goals of the rehabilitation for patients after stroke and spinal cord injury [11, 14, 15].

The most common sensorimotor impairments after a neurological injury are muscle weakness, spasticity, reduction in joint range of motion (ROM), asymmetry (especially in stroke), sensory and proprioception deficits, balance disorders [16, 17]. In SCI, the level (cervical, thoracic, lumbar or sacral), the extent of the lesion (complete or incomplete) and the damage to specific tracts (corticospinal, dorsal column or lateral spinothalamic tract) determine the consequent impairment [17]. Patients with incomplete SCI who can achieve walking present several abnormalities with respect to able-bodied control subjects, due to the impaired proprioception, decreased voluntary muscular control, increased muscle tone and altered neural drive [17]. These patients show normally slower walking speed and longer double support duration, limited hip and knee flexion during swing and insufficient hip extension during stance [17, 18]. Spontaneous recovery can be observed within the first 2 years after injury. Extent of recovery is dependent on several factors including the severity of the lesion, overall health status, prevention of secondary complications, and rehabilitation interventions [9].

Assessing and evaluating walking-related functions and activity is needed to monitor and adapt the therapy, to motivate patients and families and to provide evidence to health insurance companies. Research on new drugs and treatments requires sensitive assessments to capture the effects. Nowadays, the assessment of walking and walking-related functions in clinical practice rely mainly on ordinal-based scores which suffer from coarseness, ceiling/floor-effects or subjectivity (to name few). Time-based assessments, such as the 10-Meter-Walking-Test (10MWT), provide useful information on overall performance, but they cannot capture the use of compensatory strategies, the quality of the gait pattern

and they cannot be administered in people who have some residual function, but cannot walk yet. More sensitive assessments, such as camera-based gait analysis, require also more time for administering, thereby taking away time from therapy, and they are not often performed.

Robotic gait trainers represent a valuable alternative for gait therapy and assessments [19–22] after neurological injury. Assessment could be combined seamlessly with therapy performed with a robotic device. Because of the assistance that the robotic gait trainer provides, assessments can be administered even if the patient is not able to perform the movement without support. The programmable logic of the device can provide standard conditions for the assessments and the information from sensors can be used to calculate objective measures.

1.2 OBJECTIVES AND SYNOPSIS

The long-term goal of this project is to develop a valid, reliable and sensitive assessment of walking activity in a robotic gait trainer that can be used in clinical practice to measure patients during every stage of rehabilitation (Figure 1.1). We envision an evaluation procedure that is: *i)* seamlessly integrated in the training, *ii)* safe and *iii)* suitable to be administered to patients ranging from mildly to severely affected (i.e. from the phase when the patient is not yet ambulatory to the phase when he/she starts to walk without assistance (Figure 1.1)). The outcome variables measured by the robotic device should relate to measures of walking function and activity commonly used in clinical practice. The assessment should be reliable and sensitive to small changes.

The specific aims of this thesis are *i)* to review current conventional and robotic assessments of walking and walking-related functions in order to understand how they can be improved and what is important to measure, *ii)* to design and implement an algorithm in a treadmill-based robotic gait trainer which allows safe and objective assessment of patients' walking ability, *iii)* to test and validate the robotic assessment on a robotic test bench and in a neurological population against established clinical scores.
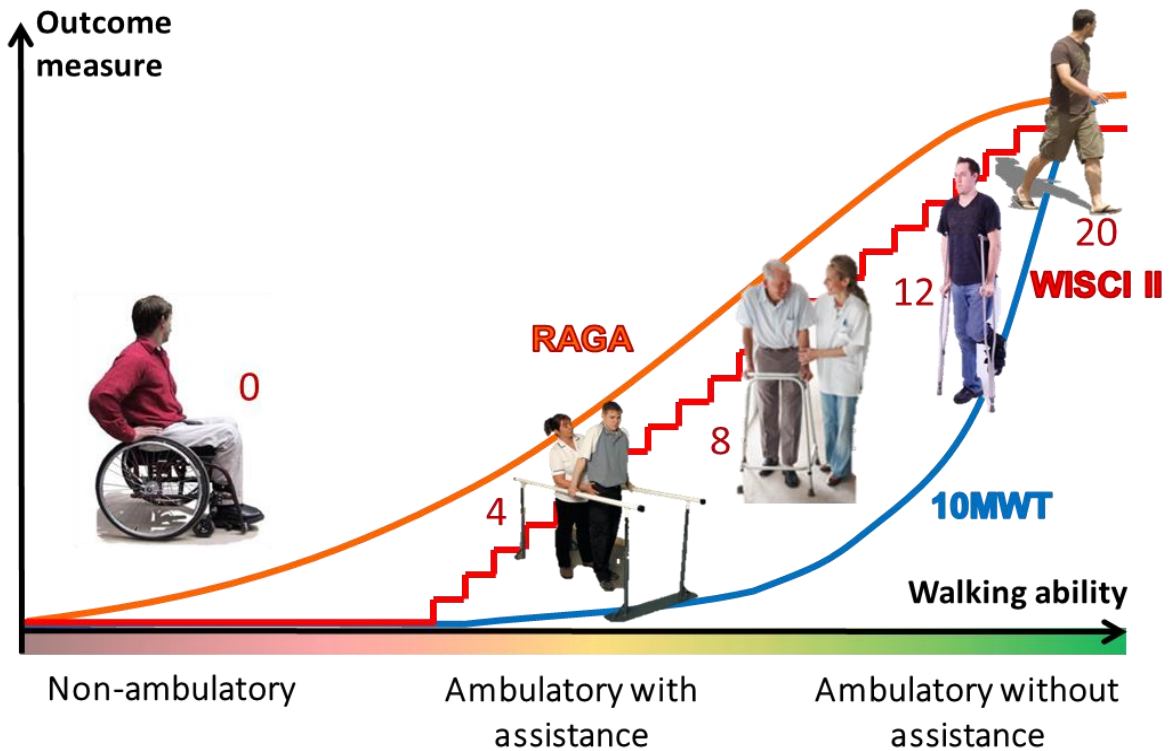
Figure 1.1: The long-term goal of this project is to develop an assessment of walking which can provide an objective, continuous outcome measure suitable to monitor the patient's walking ability in every stage of rehabilitation. The robot-aided gait assessment should relate to measures of walking-related functions and activity commonly used in clinical practice (e.g. Walking Index for SCI – WISCI II – and 10-Meter-Walking Test – 10MWT).

In this introductory chapter, the reader can find an overview of the most important concepts related to gait and gait rehabilitation, followed by a brief description of existing robotic gait trainers. I then presented why assessments are important in rehabilitation and why, despite this, they are not often used in clinical practice (Chapter 2). I framed my review in the context of the International Classification of Function, Disability and Health [23]. I also highlighted the most important psychometric properties and the statistical methods to measure them. Before proposing our idea for a robot-aided assessment of walking ability, I examined and reviewed current clinical and robotic assessment of lower limb function to identify existing shortcomings and potential use of robots to fill the gaps.

In this work, a treadmill-based robotic gait trainer, the Lokomat (Hocoma AG, Switzerland), was used to create an in-training assessment of walking ability. To achieve this goal, I developed a robot controller that adapts the support of the device to the subjects' ability to follow a pre-set physiological gait pattern, i.e. assist-as-needed [24]. The algorithm, described in Chapter 3, reduces the robotic support where possible, which encourages the patient's active movements, while maintaining a safe environment for training. This provides us with a "window" to observe and measure what the patient is actively doing during robotic training. Our hypothesis is that the robotic support set by the algorithm is proportional to the subject's impairment.

I first studied the validity of the assessment on a robotic test bench which simulates typical impairments of neurological patients (Chapter 4). These simulated test conditions allowed me to validate

the assumption that higher impairment leads to higher residual robotic support. I also realized that the impairment is visible only in some phases of the gait cycle. Afterwards, I studied the feasibility, validity and reliability of the robot-aided gait assessment (RAGA) in able-bodied subjects and people with SCI (Chapter 5). I identified there the most informative outcome measures that relates to walking ability overground.

In Chapter 6, I proposed an alternative method for developing an assist-as-needed controller in the Lokomat, based on the adaptation of the end-point rather than the joint impedance.

Chapter 7 summarizes the results, reflects on the limitations and proposes ways to overcome them in future work.

1.3 GAIT REHABILITATION

To understand how to measure 'walking ability', it is necessary to identify the main determinants and functions that are required to walk – walking-related functions. This section aims at providing clarity on the different terms used throughout this thesis.

1.3.1 Definitions

Walking can be described in different domains: *i)* the capacity of performing activities related to walking (e.g. walking without assistance, sit-to-stand); *ii)* the spatio-temporal characteristics (e.g. speed, step length, cadence, stance/swing ratio); *iii)* the "quality" of the gait pattern, which concerns the coordination of lower-limb segments and joints (e.g., intralimb coordination) [25]. In the International Classification of Functioning, Disability and Health (ICF) – see Chapter 2 for explanation - walking is addressed in two categories: in the Body Functions section (b770 – Gait Pattern Functions) and in the Activities section (d450 – Walking) [23, 26]. A list of other walking-related functions listed in the ICF classification can be found in Table 2.1. The Body Functions section refers to physiological functions of the body systems (such as proprioceptive function and muscle tone function), while the Activities section describes the execution of a task or action from an individual (e.g. walking, eating). *Impairments* are problems in the body functions or structures.

Walking ability refers to the capacity of performing the activity of *walking*, defined in the ICF as "moving along a surface on foot, step by step, so that one foot is always on the ground" [26]. The activity of walking has further specifications such as walking short and long distances, on different surfaces or around obstacles. In this thesis we focus on the basic ability of walking on level ground. To be able to perform the activity of walking, several walking-related functions are necessary (see Table 1.1 and Table 2.1). *Gait* refers to the manner or style of walking and it can be described by a cyclic series of motion patterns performed by the lower limb joints [27]. The gait cycle can be divided in phases, each one characterized by a specific function [28–30] (Figure 1.2).

1.3.2 Gait Phases
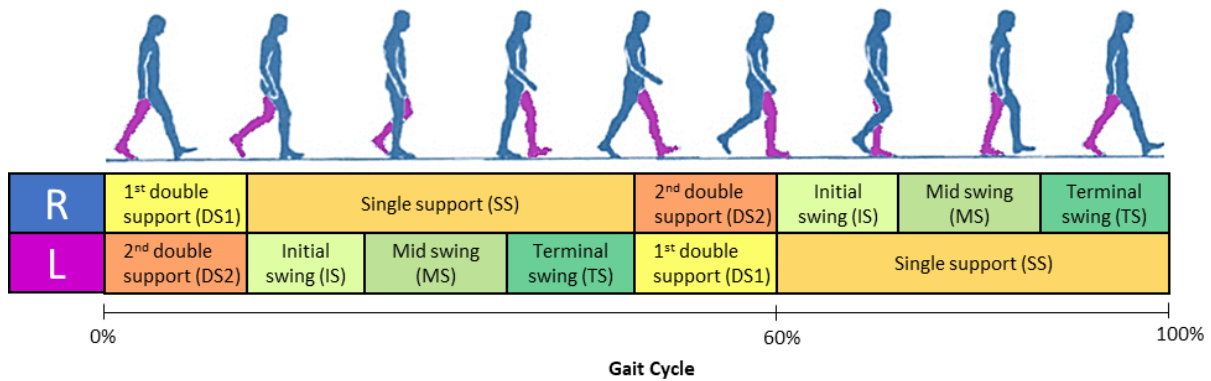
Figure 1.2: Gait cycle and its phases. Right leg (blue) and left leg (purple) phases are shifted. The gait cycle of the left leg starts when the left foot touches the ground. This event marks the start of the 2nd double support phase of the right leg.

As a convention, the gait cycle starts at 0% with the foot contact of a leg and terminates at 100% when the same foot contacts again the ground. A gait cycle can be divided into two major phases: stance and swing phases. Stance phase (from foot contact to toe-off) designates the period when the foot is on the ground. The swing phase refers to the period when the foot is in the air. Swing begins as soon as the foot is lifted from the floor (toe-off or foot-off). The stance phase further is subdivided into first double support, single support, and second double support. These phases are clearly determined by the toe-off and foot contact happening to the contralateral leg. The total stance phase occupies approximately 60% of the gait cycle. Swing can be also subdivided in three sub-phases (initial swing, mid-swing and terminal swing), but they are arbitrarily defined by dividing the swing phase in 3 equal parts [30] and different textbooks use different terminology and division.

A precise description of the events occurring in each gait phase, the graphs of the joint angles, moments and powers and the EMG activation of the numerous muscle groups involved in walking can be found in the books of gait analysis of D.A. Winter [29] and J. Perry [28].

1.3.3 Requirements for Walking

The requirements for walking are defined as the necessary conditions to achieve functional walking, which is the ability to walk independently in the community, with or without the use of devices and braces [13]. In literature, different frameworks on the requirements for walking have been proposed and we try here to summarize and synthesize them. The work of four experts in gait analysis has been reviewed: Jacquelin Perry [28], David A. Winter [29], Richard Baker [30–32] and James Gage [33]. Non-systematic discussions with five physiotherapists working in gait rehabilitation with neurological patients helped to identify which factors are addressed during gait therapy today (at least in Switzerland).

REQUIREMENTS FOR FUNCTIONAL WALKING

J. Perry	D.A. Winter		R. Baker	J. Gage	Physiotherapists
Stance phase stability	Stance phase stability, support of body weight, posture and balance		Support of body weight	Stance phase stability	Stance phase stability, support of body weight
	Control of foot trajectory	Clearance in swing	Clearance in swing	Clearance in swing	Clearance in swing
		Smooth transitions*	Smooth transitions*	Pre-positioning of foot in terminal swing**	Smooth transitions, weight shifting
			Adequate step length	Adequate step length	
Energy conservation			Energy conservation	Energy conservation	
Propulsion	Generation of mechanical energy				Propulsion
Shock absorption	Energy absorption				
					Endurance

Table 1.1: Requirements for functional walking according to J. Perry [28]*, D.A. Winter* [29]*, R. Baker* [31] *and J. Gage* [33]*. * Smooth transition from swing to stance and from stance to swing. **This requirement seems to be derived mainly from the Cerebral Palsy population, on which the book focused* [33]*. The last column shows the requirements emerged from non-systematic interviews with five physiotherapists working in neurological rehabilitation centers in the Zürich area or in the clinical applications department of Hocoma (Volketswil, ZH, CH).*

Everybody agrees on the importance of stance phase stability (including static and dynamic balance) and on the ability to support the body weight. This function is determined by the equilibrium between the alignment of the body and the muscle activation at each joint [28]. While muscle force is not a determinant of balance in able-bodied subjects, it becomes important in pathology: it has been found that when a certain level of knee extensor force is achieved (3/5 on the Manual Muscle Test (MMT)), additional strength does not seem to further contribute to gait and balance performance [16]. Muscle strength has to be enough to generate the extensor "support moment", together with the ankle and hip [29]. It is generally accepted that the maintenance of postural stability depends on the continuous integration of somatosensory, visual, and vestibular inputs, its processing, and the generation of targeted motor responses [34]. In patients with SCI, partial or complete loss of somatosensory perception and/or voluntary motor control are the main causes of balance disorders [17]. Patients with incomplete SCI who can stand show an increased postural sway during quiet standing, reduced precision during shifting of the body weight, and delayed responses to external perturbations [17]. Relearning to maintain body postures in different conditions is one of the main pillars of subacute rehabilitation [17].

The control of foot trajectory during swing plays an important role for a safe ground clearance and a smooth foot contact [29]. The trajectory of the foot during swing is a precise end-point task which depends on the multi-segment motor control of both stance and swing limbs [35]. Toe clearance is not only determined by ankle dorsiflexors and knee flexors, but it is also heavily influenced by the hip abduction of the stance leg. This factor explains why "hip hiking" (increased stance hip abduction) is so often used for compensating deficits in knee and ankle flexors in the swing leg [35]. The conditions at push-off, especially the rate of knee flexion, determine the knee flexion peak during swing phase and the consequent ability to clear the ground during swing [36]. At the transition from swing to stance (foot contact) the foot needs to be decelerated to achieve a smooth contact with the ground [35].

Step length is determined by the position where the foot lands at foot contact. The angle between the thighs at the moment of foot contact is the main determinant of step length. Secondly, if the leading knee is flexed, the step is going to be shorter. In many patients reduced range of motion of the hips is the cause of reduced step length [37].

Efficiency is the ratio between the work accomplished and the energy expended. Normal walking at comfortable speed is extremely efficient. During stance, a mechanism similar to the inverted pendulum is used to move the body mass forward and conserve energy [38, 39], similar to a "forward fall of body weight" [28]. In swing, some aspects of the motion can be modeled as a simple pendulum. This pendulum analogy, however, does not apply to the double support phase [39]. During double support, the Center of Mass (CoM) velocity is redirected from one inverted pendulum arc to the next. Energy is needed at this point and it is provided by the ankle "push-off" or by the hip "pull-off" [39][28]. Many patients with gait-related pathologies use the hip pull-off to compensate for a weak or non-existent push-off. Step length and walking velocity can be increased by increased plantarflexor power during push-off or by increased hip flexor power during pull-off [35]. The combined energetic costs of step-to-step transitions and forced leg motion (movement of the swing leg faster than achieved by simple pendulum motion) appear to account for much of the cost of human walking [39]. Efficiency is achieved only if the person moves continuously with a dynamic transition from one step to the next [38]. Throughout stance, muscle activation is only happening when body alignment creates a torque antagonistic to weight-bearing stability of the limb and trunk. As soon as an alternative mean of joint control is available, the muscles relax [28].

Limb advancement in swing is a similar mixture of momentum, gravity and direct muscle control. In mid swing the knee is extended passively. Energy is conserved if walking is achieved by reducing the amount of muscular effort required [28]. Energy conservation and energy generation are requirements that needs to be considered together, since gait is not a perfect pendulum mechanism, and thus even if part of the energy is conserved, other needs to be generated at every cycle.

The body needs to absorb mechanical energy to achieve "shock absorption" after foot contact and to decrease the forward velocity of the body. Mainly, energy absorption occurs at the knee joint during

weight acceptance and at terminal swing to decelerate the leg [29]. Loading of the weight acceptance limb similarly unloads the other limb that can prepare for swing [28].

In clinical practice, most of the requirements of walking are indeed targeted during training. However, therapists added that endurance was a necessary requirement for functional walking since patients should be able to do walk for an amount of time sufficient to carry out community activities. The ability to shift the weight from one leg to the other, despite being part of the smooth transitions, receives particular attention during rehabilitation, since the step-to-step transitions are critical for balance.

1.3.4   Rehabilitation Interventions

The recovery of ambulation after SCI has become the target of several pharmacological, rehabilitative and neuroprosthetic approaches [16, 40, 41] and the evaluation of walking recovery and of the prognostic factors influencing this function is now of major importance [4, 13, 42]. Measures of walking should target not only the walking level, but also walking characteristics, such as speed, distance and coordination [4, 18, 43, 44].

Despite the different aetiology, walking impairments present several similarities among them and it is commonly accepted that the most effective treatment for gait disorders of neurological cause is intensive, task-specific training [45–47]. This type of training is based on the activity-dependent plasticity driven by repetitive task-specific sensory input to the spinal networks [46, 48, 49]. Research studies in animals and humans show that the spinal cord integrates supraspinal and afferent information during repetitive practice and can thus improve motor output [46, 50]. Task-specific or activity-based therapy refers to interventions that provide activation of the neuromuscular system below the level of lesion with the goal of retraining the nervous system to recover a specific motor task [46]. The most prominent activity-based therapy is locomotor training. A series of guiding principles for training has emerged from the findings in basic science and has been translated to the human condition [46].

1.3.4.1   Principles of Locomotor Training

Guidelines for locomotor training provide a framework for clinical practice and constitute a reference for evaluating the potential application of any new modality and equipment for gait rehabilitation. These principles have been developed with the idea of optimizing the sensory cues and afferent inputs for walking through repetitive task practice [16, 46]:

1. Maximizing load bearing by the legs and minimizing load bearing by the upper extremities. Load bearing on the legs has been found to increase electromyographic (EMG) amplitude of the leg muscles [50]. Partial body weight support should be provided through vertical suspension, but not through hand rails or parallel bars.

2.   Optimizing the kinematics of trunk and lower extremities.   In particular, the transition from stance to swing is crucial and it can be activated by the load on the limb and the hip extension at the end of stance, which contribute to the activation pattern of leg muscles during locomotion [51]. Appropriate sensory inputs also help in the modulation of reflexes [16].

3.   Generating stepping velocities close to normal (0.75-1.25 m/s), which promotes a velocity-dependent modulation of EMG activity [46, 52].

4.   Promoting the use of reciprocal arm swing, which may help in the development of appropriate balance responses [46].

5.   Maximizing recovery strategies and minimizing compensation. Compensatory strategies such as the use of walkers or parallel bars, produce a forward flexed trunk, gait asymmetries and compensatory strategies for swing initiation such as "hip hiking" [53].

Locomotor training can be performed overground or on the treadmill, with the use of vertical suspension body weight support (BWS) systems and/or Functional Electrical Stimulation (FES) [16]. Manual locomotor training on the treadmill usually starts 4 to 6 weeks after SCI, with the help of a BWS system connected to a harness worn by the patient. The leg movements of the patient need to be manually guided by two physiotherapists sitting on either side of the patient. The therapists have the challenging task of moving the legs in a reproducible, rhythmical, and physiological manner, which is not always possible [9]. This is, however, ergonomically unfavorable and tiring work. Usually the training sessions are rather short, and in some severely affected patients, training might even be impossible [54, 55].

Therefore, since the early 2000s, robotic gait trainers have become valuable aids for the rehabilitation of walking after a neurological injury [55].

1.3.5   Robotic Gait Trainers

Robotic gait trainers can provide intensive training with a high amount of repetitions to patients with mild to severe gait impairments. The patient can train safely thanks to the robotic support. Severely affected patients, who would not be able to train otherwise, can start earlier to do rehabilitation. A single physiotherapist can perform a training with a robotic gait trainer, while at least two therapists and considerable physical effort are required for conventional locomotor training [54].

Robotic gait trainers can be classified as treadmill-based robotic exoskeletons, end-effector robots, wearable overground rigid and soft exoskeletons, overground gait trainers with mobile BWS.

Treadmill-based Exoskeleton	End-effector Robot	Wearable Rigid Exoskeleton	Wearable Soft Exoskeleton	Mobile Body Weight Support
Fixed		**Overground**		
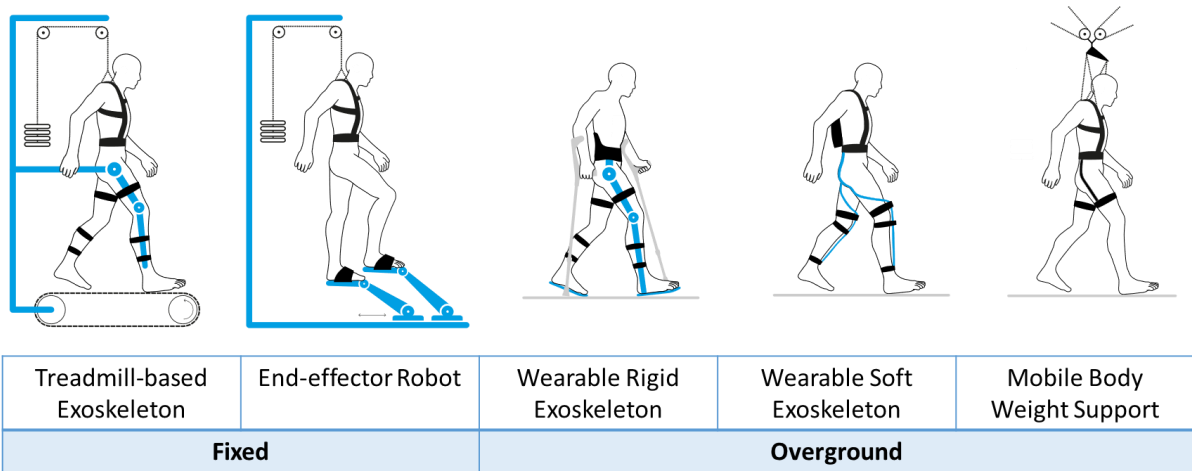
Figure 1.3: Different types of robotic gait trainers. Reproduced and edited with permission from [56], under the terms of the Creative Commons Attribution 4.0 International License (http://creativecommons.org/licenses/by/4.0/)

Treadmill-based robotic exoskeletons (e.g. Lokomat [57], Walkbot [58]) control each of the leg segments (thigh and shank) independently and are programmed to generate physiological hip and knee angular motions, i.e. similar to the gait pattern of an able-bodied individual. Normally, the robotic joints are controlled by motors whose torque can be adapted by the control logic to provide more or less guidance to each of the limb segments, while a BWS system helps maintain a good trunk posture and guarantees the support of the body. Exoskeletons are able to provide high support and movement guidance to patients that require it, therefore they are mostly indicated for people with severe gait impairments who cannot walk overground [9]. Parameters such as the amount of BWS and the impedance of the robotic joints can be adapted to challenge the patient while he/she reacquires the impaired functions.

End-effector robots typically use programmable footplates, where the feet of the patient are strapped. The movements of the footplates are controlled by the robotic system to simulate different gait patterns (e.g. level walking, stair climbing) [59]. A BWS system support the patient through a harness. The knees and hips of the patients are not directly guided, and the movement is only imposed through the foot plates. This limits the use in very severe patients who require knee and hip stabilization, but allows a more variable gait pattern [54]. Feedback is provided on the pressure applied at the foot soles. Examples of end-effector robots are the G-EO (Reha Technology, Switzerland) and the Gait Trainer GT II (Reha-Stim Medtec, Switzerland).

Rigid wearable overground exoskeletons can be worn by patients with paraplegia for limited community ambulation and for training [60]. They are untethered and battery-powered and they have actuated hip and knee joints and a passive ankle orthosis, fixed or adjustable with a spring system. They rely on crutches for supporting the body weight and maintaining balance. Rigid exoskeletons implement mostly fixed walking trajectories and react to start/stop signals provided by the user, by tilting the trunk or by moving the center of pressure. Operation modes (level walking, stairs, sit/stand) can be set via a wrist pad, by controllers on the crutches [61] or by the therapist's monitor. Age, level of injury and

number of training sessions influence the performance in using these systems [60]. The possibility of controlling the initiation and termination of the gait and of moving around makes the overground exoskeletons more challenging than treadmill-based systems. Examples of overground rigid exoskeletons are the ReWalk (ReWalk Robotics, USA) and the Indego (Parker Hannifin, USA). The HAL (Cyberdyne, Japan) implements an EMG-based control of the exoskeleton.

Soft wearable exoskeletons are the most recent development in the field as they try to overcome the issues related to weight and transportability of their rigid predecessors. The soft exoskeletons or exosuits use textile structures to interface with the human body and they are considerably more lightweight and portable. They can be designed to assist certain muscle groups during walking (e.g. hip flexors/extensors or ankle plantarflexors) [62] or to support the weight against gravity [63]. The actuators encompass multiple joints, mimicking bi-articular muscles: this allows to simplify the mechanical design of the exosuit and to reduce the number of motors needed [63]. The support provided by the exoskeleton is adjusted based on the estimated user's current posture. By supporting the user's activity, the exosuits allow weaker subjects to train functionally, but they are not able to generate 100% of the required joint torques for walking. The patients need to have a certain residual muscle function and control and contribute actively to perform the desired movements [63]. ReStore (ReWalk Robotics, USA) and Myosuit (MyoSwiss, Switzerland) are the first to commercially manufacture this type of products.

Overground gait trainers with mobile BWS can be classified further as systems with mobile base and with ceiling-mounted BWS. The former implements a motorized wheeled base with a BWS which follows the patient around in the hospital areas (e.g. Andago (Hocoma, Switzerland), Lite Run (Lite Run, USA)). The latter use a ceiling-mounted BWS system which allows movements in all the directions, but limited to a room (e.g. RYSEN (Motekforce Link, The Netherlands), FLOAT (Reha-Stim Medtec, Switzerland) [64]). These systems implement an active patient-following function, which allows the patient to train safely and freely while supported by the BWS. The therapist can concentrate on performing several therapeutic tasks with the patient (e.g. training following a path or avoiding obstacles, correcting the walking posture) without the need of physically supporting the patient to prevent falls.

The ultimate aim of the above-mentioned devices is to allow a safe and intensive training following motor learning and locomotor training principles. The choice of the device depends on the severity of the patient's condition, which determines the level of challenge of the training, and on the therapy goal.
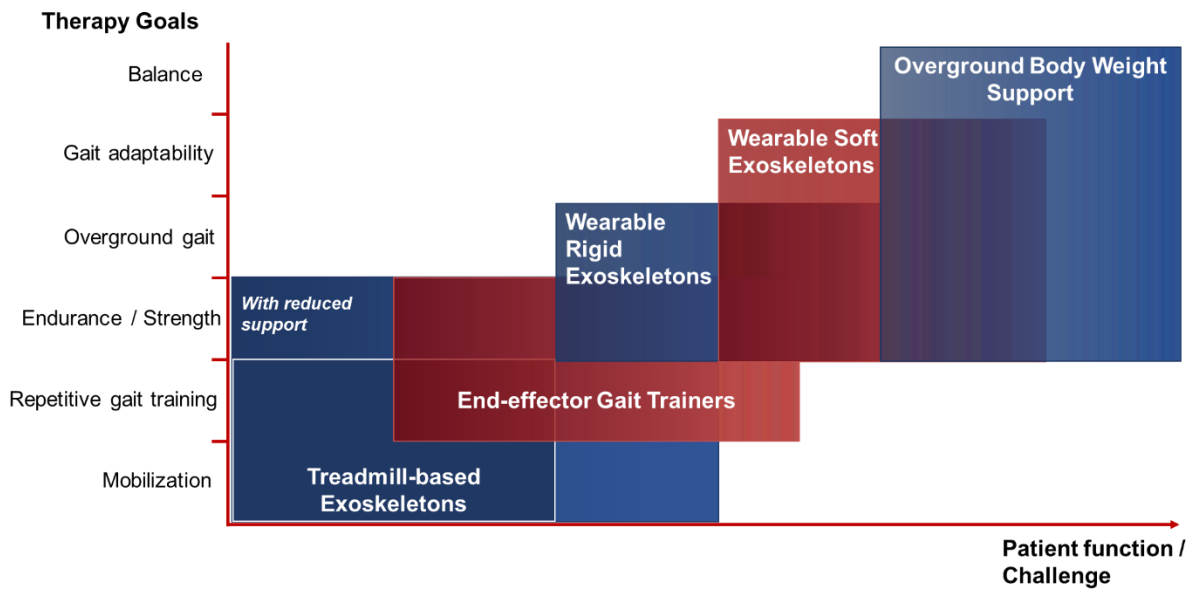
Figure 1.4: The most suitable device for each patient depends on the therapy goal and on the severity of the patient's impairment. This figure provides an overview of the devices positioned according to the most suitable therapy goal (y axis) that the device can address. On the x axis, the devices are also positioned according to the challenge that they can provide, which is proportional to the function of the patient that can train in that device. The classification provides only rough indications based on clinical observations and experience collected in the field and does not aim to be exact.

In early rehabilitation, the focus is on mobilization in a safe environment and repetitive gait movements (Figure 1.4). The patient has reduced motor functions and requires a high support to walk. Treadmill-based exoskeletons can provide high amount of repetitions in a safe environment. The challenge of the training can be increased, when possible, by tuning parameters such as BWS and guidance of the robotic joints. Reduced robotic support enables the training of endurance, muscle strength and active ROM. End-effector systems can provide more variable gait-like movements with no support to the hips and knees, which requires patients to possess anti-gravity joint stability. Rigid exoskeletons allow patients to walk overground, but the fixed trajectories and the use of crutches limit their use for balance or gait adaptability training, which are instead possible with the soft exoskeletons, which support the movements without imposing them. Overground BWS allows balance and gait adaptability training in safe conditions for people that can perform active stepping and walking. The combination with conventional therapy and transfer to daily life activities is a fundamental part of the rehabilitation.

1.3.6 Scientific Evidence and Limitations for Treadmill-based Exoskeletons

In this work, we focus on robotic gait trainers for moderately to severely impaired patients, in particular on treadmill-based exoskeletons.

The most recent Cochrane review [19] affirms that one out of seven walking dependencies in stroke survivors could be avoided if robotic gait trainers were used in addition to conventional therapy. The treatment effect was higher in the sub-group of severely impaired patients [19]. While in Spinal Cord Injury there are not such high-quality recent meta-analyses [65], several randomized controlled trials

showed the benefits of treadmill-based robotic gait trainers, alone [66–68] or in combination with other treatments [69, 70].

Robotic gait trainers provide benefits to patients in a broad range of functional levels. Severely impaired patients show benefits in bowel and bladder function [69], tone reduction [71], cardiovascular stability [72] and bone density [73]. Patients who have reacquired some walking function can be challenged further by increasing the walking speed, decreasing the BWS and the robotic support to the movements (impedance of the robotic joints relative to a predefined reference trajectory) and by motivating them to actively participating to the movements with virtual reality and feedback [74]. Robotic gait trainers can provide intensive training with high number of repetitions, which lead to better outcomes [75]. The automation of the device allows parallel training settings, where one therapist supervises more than one patient at a time.

One disadvantage of this type of robotic gait trainers, so far, is the limited physical interaction between the therapist and the patient. In conventional locomotor training, the therapist is in direct contact with the legs of the patient; he/she can provide the correct amount of support and feel whether the patient is actively participating to the training. In robot-aided locomotor therapy, the therapist adapts the robotic support via a user interface and has to rely on vision and the, usually limited, information provided by the machine to estimate the patient's function and activity. Nowadays, robotic gait trainers offer several possibilities to shape the training to the needs and severity of the patients [76], however therapists need to understand how to use these parameters and they need a way to measure the activity and assess the performance of the patient in the device and outside the device.

In the following chapters, a method for the automatic adaptation of the robotic support parameters of a treadmill-based exoskeleton will be discussed. The method can be useful *i)* to define an optimal level of robotic support for each patient, *ii)* to provide information on the patient's walking ability.

Chapter 2   ASSESSMENTS OF LOWER EXTREMITY FUNCTIONS

The content of this chapter is extracted from the following review paper and it was adapted to ensure consistency with the rest of the document and to avoid repetitions:

Maggioni, S., Melendez-Calderon, A., van Asseldonk, E. *et al.* Robot-aided assessment of lower extremity functions: a review. *J NeuroEngineering Rehabil* **13,** 72 (2016) doi:10.1186/s12984-016-0180-3. Reprinted under the terms of the Creative Commons Attribution 4.0 International License[1].

Foreword

Despite their importance in supporting clinical decision making, assessments are not often used in clinical routine and they suffer from several limitations. Before introducing the robotic assessment method developed in this thesis, I identified the existing possibilities to assess lower extremity functions and walking activity and their barriers for clinical use. Robots for rehabilitation are valuable tools for administering assessments in a standardized and objective way and several attempts have been already made in this direction. Examples of conventional and robotic assessments are presented for every walking-related function and suggestions for improvement are made.

---

[1] http://creativecommons.org/licenses/by/4.0/

2.1 INTRODUCTION

Assessments can be used for monitoring the patient's status and the recovery, to shape the therapy based on objective outcomes and to motivate the patient [77]. According to the International Classification of Functioning, Disability and Health (ICF) [23], the assessment of one's health status should include body functions, activities and participation.

Standardized sensorimotor assessments after neurological disorders can help the understanding of recovery and support the design of effective therapeutic interventions, with the ultimate goal of maximizing the patient's chances of recovery. Despite the general consensus on this statement among clinicians, neuroscientists and rehabilitation engineers, sensorimotor assessments are not routinely performed in the clinical practice [78, 79]. Duncan et al. identified four high-level determinants that impact routine assessments in practice: *i)* Knowledge, Education, and Perceived Value in Outcome Measurement (i.e. information on validity and reliability); *ii)* Support/Priority for Outcome Measure Use (i.e. organizational and management factors); *iii)* Practical Considerations (e.g. time, cost); *iv)* Patient Considerations (e.g. usefulness of the assessment to the patient's treatment). The limited use of assessments in clinical practice reduces the chances to obtain feedback on the therapeutic intervention and consequently decreases the efficiency of therapy planning and adjustment [78, 80, 81]. Objective proofs are needed to justify healthcare expenses and reimbursement from insurances [78, 80]. In research, the lack of sensitive and reliable outcome measures can hamper the results of clinical trials aimed at determining the efficacy of new treatments, if changes due to the intervention under study fail to be detected [42]. Thus, valid, reliable and sensitive assessments are useful in areas that encompass therapeutic, research and financial domains (Figure 2.1).
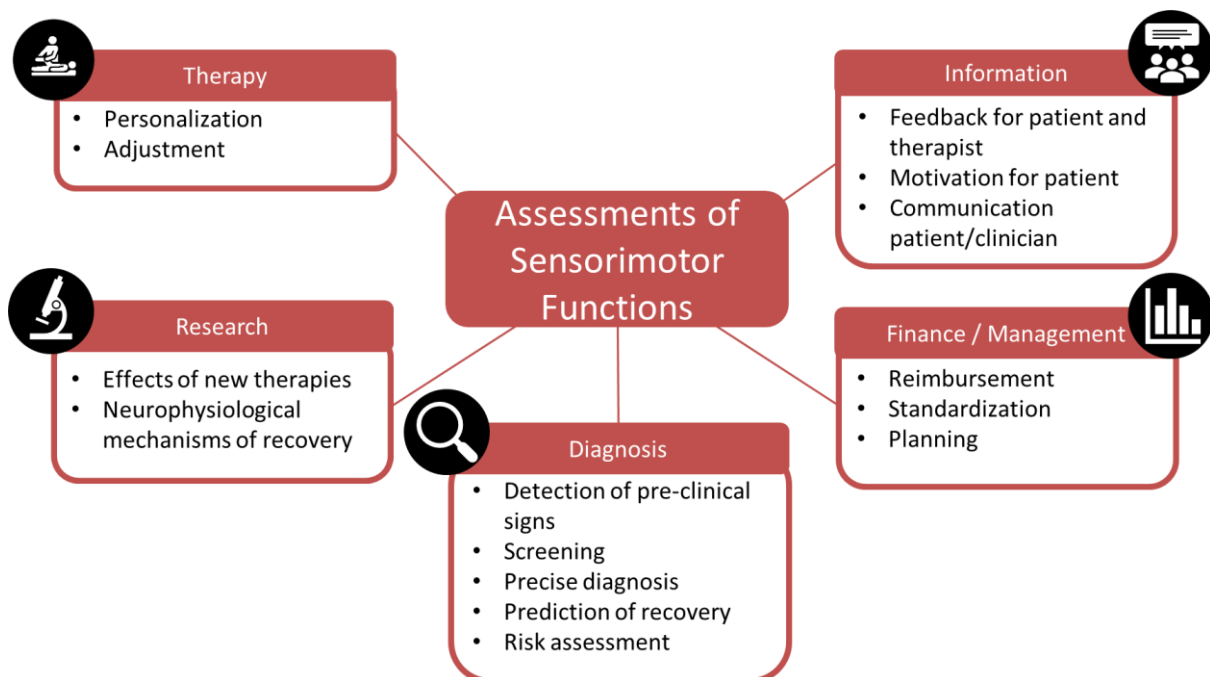
Figure 2.1: Assessments of sensorimotor functions are needed for different purposes [78, 81, 82]

The last decades have seen an increasing use of robotic devices for neurorehabilitation training in clinical centers [19, 59, 82]. Besides training, translational researchers in neurorehabilitation have proposed the use of robotic devices to overcome some of the limitations in traditional clinical assessments. Robotic devices represent an alternative method to provide more objective, sensitive, reliable and time-efficient assessments in clinical practice [82–84]. Sensors are embedded or can be easily added in robotic devices in order to provide quantitative measures of variables such as, for example, joint angles. Instrumented devices enable the recording of new variables (e.g., smoothness) that were not accessible before. Standardized assessment protocols and repeatable conditions can be achieved with the use of robotic devices. Patient's motivation, which is a factor that can influence the assessment outcomes [85], can be promoted by using virtual reality applications to provide constant engagement, along with standardized instructions. Moreover, assessments can be integrated into the training session without requiring additional setup and measurement time. Training variables (e.g., duration, number of repetitions) can also be used to provide an indication of the patient's performance and allow comparison between sessions.

However, the frequent criticism from clinicians towards these engineering solutions is that the outcome measures provided by robotic devices are too abstract, do not translate to function and lack ecological validity. Moreover, robotic devices often require a long setup time and a certain degree of technical knowledge to be operated [82]. In a typical setting, the therapist has between 30 minutes and 1 hour to deliver the therapeutic intervention. If the assessment protocol takes too much time to be performed, the solution may not be adopted. In some cases, the increase in sensitivity and reliability is discarded in favor of an existing subjective, yet time-efficient, assessment that can be applied in any clinical setting. These may be some of the reasons why robot-based assessments have not yet been integrated in clinical practice at a large scale. Therefore, future developments in rehabilitation robotics should enable the clinician to choose among a set of assessment tools according to the specific needs of the patient. We encourage engineers to develop assessment technologies that are not limited by practical constraints and administrative burdens. We believe that the barriers that prevent the translation of robotic assessments to clinical use must be understood so that they can be overtaken. Hence, to guide the development of future robotic-based assessment tools, it is fundamental that we understand the needs of the key players.

The goal of this chapter is to provide a comprehensive review of the state-of-art robot-assisted methods, with focus on the lower limb, and identify gaps in which robotic technologies can solve current issues in the assessment of sensorimotor functions. We present and discuss existing assessment methods for lower limb functions used in routine clinical practice and contrast those to state-of-the-art instrumented and robotic technologies. We also provide guidelines and recommendations for the development and validation of new sensor- and robotic-based assessment methods, taking into account the clinical needs. The review and recommendations provided in this chapter aim to guide the design of the next generation of robotic devices.

2.2 FRAMEWORK

Walking recovery is among the most desired goals of patients after a neurological injury [14, 15]. In order to maximize the recovery of the walking function, an optimal therapeutic plan should be defined and adjusted according to the patient's progress. However, the lack of quantitative and sensitive assessments of lower limb functions that can be used during every day clinical practice limits the possibility to record the patient's progress over time. For this reason, the scope of this review is constituted by measures and assessment methods that target body functions of the lower limbs, with a particular focus on those related to walking. We decided to exclude assessments of functions that, although needed for walking, are influenced by body systems other than lower limbs (e.g. balance). For a thorough review of technology-aided assessments of balance, we refer to a publication from Shirota and colleagues [86].

The methods and papers mentioned in this review were selected from an electronic search in PubMed and Google Scholar. Concerning the robotic measures, for each section we searched for the particular topic (e.g. "range of motion") and the word "robotic" OR "robot". Only papers relating to the lower extremities were considered. We looked also at the literature relevant to the robotic gait trainers and exoskeletons. The recent review from Zhang et al. (2014) [87] provided a good list of references on ankle devices. We also performed a manual search among the references considered relevant that we found in the selected articles. We aimed at a comprehensive, but not necessarily systematic or exhaustive review.

Assessments of sensorimotor functions can be discussed in the framework of a comprehensive classification for describing health and health-related states developed in 2001 by the World Health Organization. The International Classification of Functioning, Disability and Health (ICF) forms a conceptual basis for the definition, measurement and policy formulations for health and disability [23]. The main aim of the ICF is to provide decision-makers in health-related sectors with a planning and policy tool. Moreover, relevant data can be collected in a consistent and internationally comparable manner. In the ICF, limitations of function and disability are not considered to be etiology-specific but rather are seen as reflecting common manifestations of underlying health conditions [88]. In the same way, the assessments discussed in this review are not disease-specific but are applicable to different kind of populations. The ICF is a useful framework to conceive new robot-based assessment tools and to categorize existing ones. The ICF describes health and health-related states by means of three categories: functioning at the level of body or body part (Body functions and structures), the whole person (Activity), and the whole person in a social context (Participation) [23]. The functions addressed by this review are listed together with their ICF classification in Table 2.1.

LOWER LIMB FUNCTIONS AND ICF

Body functions						
Sections	Range of motion	Muscle strength	Proprioception	Joint torque coupling / synergies	Joint impedance	Walking Activity / Gait pattern
ICF chapters	b710	b730	b260	b760	b735, b7500, b7650	b770, d450
	Mobility of joint functions	Muscle power functions	Proprioceptive functions	Control of voluntary movement functions	Muscle tone functions, Stretch motor reflex, Involuntary contractions of muscles	Gait pattern functions, Walking

Table 2.1: The sections of the current review in the framework of the ICF. The ICF lists a broad range of health-related components under the categories of Body function (b), Body structures (s), Activities and Participation (d), Environmental factors (e). In each category it is possible to find a complete list of health-related components divided in chapters [26].

Rehabilitation of walking-related functions (and of any other function) requires, at the assessments of the status of the patient to correctly plan the rehabilitation interventions, it requires a common language to communicate between health professionals who will treat the patient, it requires periodic re-assessments to adapt the interventions and finally the evaluation of the performed rehabilitative interventions.

The Rehab-Cycle (Figure 2.2) is one structured problem solving approach to rehabilitation management based on the ICF [89]. The rehabilitation cycle can be subdivided in four phases:

1. Assessment: description of patient's problems and resources, setting of mutually agreed goals, determination of intervention targets

2. Assignment: allocation of relevant intervention targets and referral to responsible health professionals

3. Intervention: specific outcome measures are needed for the initial assessment and for measuring the progress and adjust the parameters of the interventions

4. Evaluation: the fulfilment of the goals defined in phase 1 is evaluated and decisions for further steps are taken.

Well-established and shared assessments are needed in every phase of the Rehab-Cycle. When measurements are not appropriate or lacking, the entire cycle can be affected with huge impact on the rehabilitation outcomes.
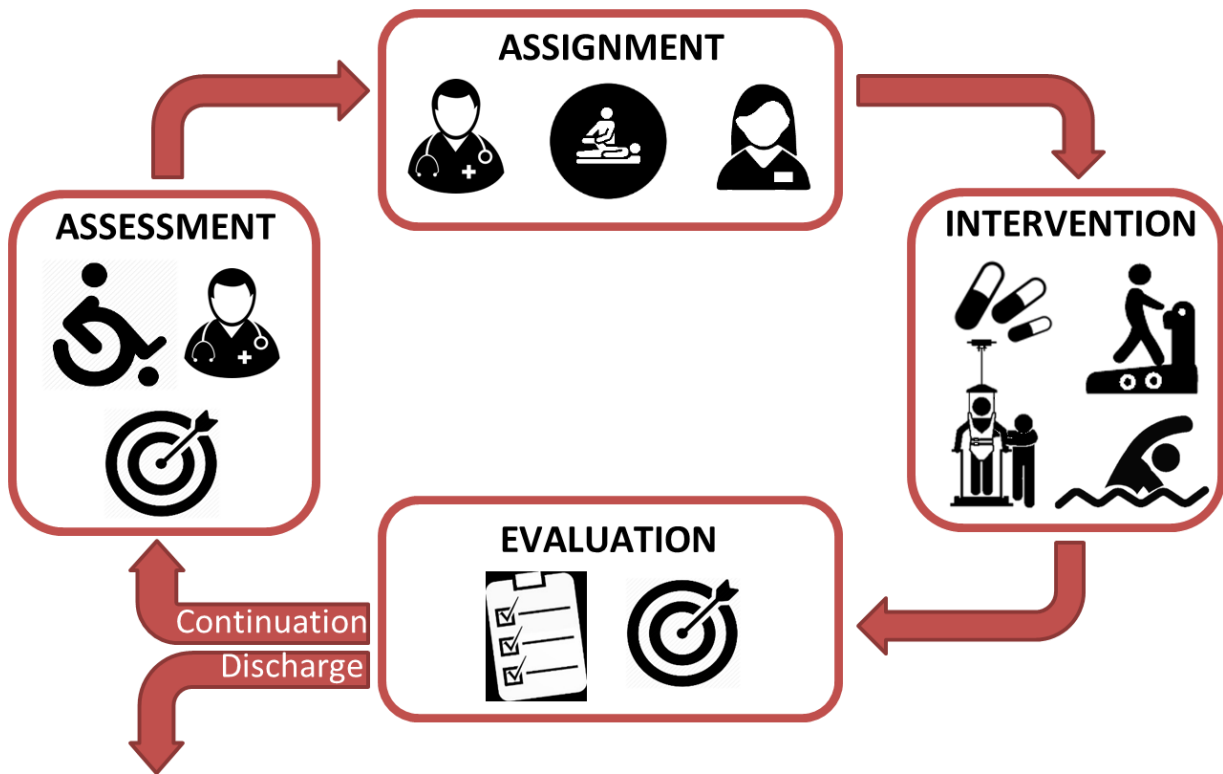
Figure 2.2: Rehab-Cycle according to [89]. *Assessments of the patient's functions, impairments and activities are required in every phase of rehabilitation.*

2.3 PSYCHOMETRIC PROPERTIES

In this section, we will present some of the most relevant statistical analyses that are commonly used to evaluate the psychometric properties of an assessment tool. One of the main challenges for the acceptance of new robot-based assessments in clinical practice is their validation. The lack of information on the validity and reliability of an assessment has been identified as one of the barriers to its use [78, 82].

Reliability must be tested first when developing a new assessment method. An instrument cannot be valid if the values it provides from repeated measurements are not consistent [90]. The most common methods to assess the reliability of an instrument in medicine and sport are the Intra-class Correlation Coefficient (ICC) and the Standard Error of Measurement (SEM). The ICC targets the relative reliability (the degree to which individuals maintain their position in a sample over repeated measurements); the SEM measures absolute reliability (the degree to which repeated measurements vary for individuals) [90]. These two methods are, therefore, complementary. ICC values are strongly influenced by the heterogeneity of the subjects (i.e. a high ICC can be obtained even if large differences between trials are present, provided that between-subjects variability is high) [91]. Results of reliability test measured with ICC in a particular population cannot be extended to a study including a different population. The SEM quantifies the precision of individual scores within the subjects [91], but its direct calculation involves the determination of the standard deviation (SD) of a large number of scores from an individual. In

practice this is not possible; therefore, the SEM is estimated (Table 2.2). SEM is independent of the population from which it was determined and it is not affected by between-subjects variability as is the ICC [91]. Absolute reliability can be also evaluated using the Bland-Altman plots [92]. Here, for each subject, the mean of two measurements is plotted against their difference.

The presence of systematic bias is confirmed when the mean of the differences between the two tests is significantly different from zero. The limits of agreement (LOA) are another measure of absolute reliability: they indicate the range where, for a new individual from the studied population, the difference between any two tests will lie with a 95% probability [90]. When the test is used to detect changes between sessions within the same individual, these changes can be considered significant only if they fall outside the LOA. Therefore, the broader the LOA, the larger the minimal detectable change (MDC) would be for a given sample size in an experiment.

Validity assessment is usually more complex because generally the "true" value of a measure is not known with absolute certainty. The general approach for validating robot-based assessments so far consisted in applying correlation between instrumented measures and clinical scores in order to find which parameters measured by robots are able to reconstruct established clinical tests (concurrent validity). However, tying the validation of an instrumented method to a score that is subjective and ordinal-based could be questionable. When a gold standard is already established (e.g. isokinetic dynamometer for muscle strength measurement), concurrent validity can be tested against it. Without such standards, validity is tested indirectly as the ability of a tool to measure the underlying theoretical construct (construct validity)[93].

Responsiveness is the ability of a test to accurately detect change when it has occurred [94]. Reliability highly influences responsiveness because real changes can be masked by the measurement error if the reliability of the test is poor. Measures characterized by a limited number of categories have intrinsically low responsiveness because large changes in status usually are required to the patient in order to change category. Ceiling and floor effects limit responsiveness at the extremes of the score range, since further improvement or deterioration cannot be monitored. The minimal clinically important difference (MCID) is a concept useful to consider the patient's perspective when dealing with assessments. It involves both a minimal amount of patient reported change and changes important enough to modify patient management [95].

PSYCHOMETRIC PROPERTIES: DEFINITION AND STATISTICAL MEASURES

Property	Definition	Measure
Reliability	Consistency of the results obtained on repeated administrations of the same test by the same person (intra-rater or test-retest) or by different people (inter-rater).	ICC: based on ANOVA statistics: between-subjects var/(between-subjects var + error), six different computational methods are possible; $0 \leq ICC \leq 1$, unitless [96, 97]. Acceptance levels for ICC depends on the application. However, a general classification of reliability has been proposed [98]: $0.00 \leq ICC \leq 0.10$ - virtually none; $0.11 \leq ICC \leq 0.40$ - slight; $0.41 \leq ICC \leq 0.60$ - fair; $0.61 \leq ICC \leq 0.80$ - moderate; $0.81 \leq ICC \leq 1.0$ - substantial. $SEM = SD \cdot \sqrt{1 - ICC}$ (SD of the scores from all subjects). SEM has the same unit of the measured variable [91]. Bland-Altman plots: mean of two measures vs their difference. LOA $= \pm 1.96 \cdot$ SD [90] Cohen's Kappa κ: percent agreement among raters corrected for chance agreement [99].
Validity	Extent to which the instrument measures what it intends to measure. Concurrent validity: degree to which the measure correlates with a gold standard. Construct validity: ability of a test to measure the underlying concept of interest.	Correlation-based methods: Pearson (r) or Spearman (ρ) correlation coefficient, ICC [100]. For continuous measures of the same data type (e.g. two methods for measuring gait speed): Root Mean Square Error (RMSE) or Bland-Altman plots against gold standard.
Responsiveness	Ability to accurately detect changes. Internal responsiveness: ability of a measure to change over a particular specified time frame. External responsiveness: extent to which changes in a measure over a specified time frame relate to corresponding changes in a gold standard [101] Minimal Detectable Change (MDC): minimal amount of change that is not likely to be due to random variation in measurement [102]. Minimal clinically important difference (MCID): smallest amount of change in an outcome that might be considered important by the patient or clinician [95]. Floor and ceiling effects: the extent to which scores cluster at the bottom or top, respectively, of the scale range.	Internal responsiveness: Cohen's effect size: observed change in score divided by the SD of baseline score. Standardized response mean (SRM): observed change score divided by SD of change score in the group. External responsiveness: ROC curves: sensitivity vs specificity based on an external criterion [101] MDC $=$ SEM $\cdot 1.96 \cdot \sqrt{2}$ [91] MCID: anchor-based (compare a change score with external measure of clinically relevant change) or distribution-based methods (based on statistical characteristics of the sample) [102]. Floor and ceiling effects: percentage of the number of scores clustered at bottom/top.

Table 2.2: Reliability, Validity, Responsiveness: Definition and Statistical methods

2.4 ASSESSMENT OF SENSORIMOTOR FUNCTIONS AFTER NEUROLOGICAL INJURIES - STATE OF THE ART

The following sections provide an overview of assessments methods for different outcome measures. For each outcome measure, its definition and relevance, the ways it is measured in clinic and in research settings are presented. For each of the available instrumented and robotic measures, the advantages over the current clinical assessments as well as points for improvement are also discussed. The tables listing the psychometric properties of clinical and technology-based assessments of lower limb functions can be found in Appendix A .

2.4.1 Range of Motion

a.   Definition of the Measure

Range of Motion (ROM) can be defined as the range, measured in degrees, through which a joint can be moved around one of its axes. Active ROM (aROM) is performed by the voluntary movement of the patient, while the assessment of passive ROM (pROM) implies that the therapist (or a robotic devices) rotates the patient's joint distal segment with respect to the proximal segment [103] while the patient tries to relax. A minimum level of joint ROM is required to perform activities of daily life in a safe and energy-efficient way [104, 105]. For example, reduced knee ROM in the sagittal plane prevents an adequate foot clearance and leads to compensatory mechanisms [106]. After a neurological injury it is common to observe a decreased ROM and a pathological behavior at the extremes of the ROM. To quantify this pathological behavior the "end feel" is sensed, which is defined as the resistance of the joint in response to a gentle overpressure applied at the end of the ROM [103]. A decreased ROM and pathological end feel can be due to weakness, spasticity, pain, tendon and muscle contractures or ectopic bone formation [107, 108].

b.   Clinical Assessment and Open Issues

The most common instrument used in clinical practice for measuring joint ROM is the universal goniometer. The therapist must place the axis of the instrument over the axis of movement of the joint, aligning the stationary arm with the proximal segment and the moveable arm with the distal segment. pROM is assessed to determine the mobility of a joint regardless of the voluntary ability of the patient and it is usually slightly greater than aROM and much greater in case of muscle weakness. aROM values can be diminished when the movement is performed against gravity, especially in weak patients. When assessing the end-feel, the therapist manually determines the type of this resistance (e.g. "hard", "soft", "firm" etc.), which is indicative of different pathologies or conditions that can affect the normal ROM of a joint [103].

Moderate to substantial intra-rater reliability and validity for ROM measurements can be achieved by means of the universal goniometer (Table A.14), but inter-rater reliability is generally lower and

highly dependent on the therapist's experience [103, 109–111]. The inter-rater reliability of pROM and of end-feel measurements is particularly critical because it depends on the torque exerted by the therapist on the patient's joint [110, 112]. Therefore, it is highly recommended that the assessment is performed by the same therapist following a rigid standardized measurement protocol [113]. Additional sources of errors in the measurements are the incorrect identification of the joint axis, the improper alignment of the goniometer arms with the body segments (also due to the movement of the joint) and the parallax error when reading the scale [103]. Moreover, the measures can be affected by compensatory motions occurring at other joints.

c.   State of the Art in Rehabilitation Robotics

Measures of ROM are obtained through angular position sensors, for which different technologies are available. Within the existing robotic devices available for *clinical use,* isokinetic dynamometers (see section *Muscle Strength*) embed ROM measurement procedures [114, 115]. Driven gait robots for treadmill walking (e.g. Lokomat [10], LOPES [9], ALEX [21], ARTHuR [117]) and exoskeletons for overground walking (e.g. Vanderbilt [118], Kinesis [119], ReWalk [120], Ekso [121], H2 [122], Vlexo [123]) usually embed potentiometers or encoders in the robotic joints to measure joint angles. Nevertheless, the only method for pROM assessment in a gait trainer available for clinical use is implemented in the Lokomat: the procedure requires the therapist to move the limbs of the patient strapped in the device [124]. For *research purposes*, several attempts to obtain instrumented measurements of the ankle joint have been made, often embedding ROM and stiffness evaluation (see section *Joint Impedance*) in the same device. For example, potentiometers were used in two ankle robots to train and assess active and/or passive plantar- and dorsiflexion ROM in stroke patients [125–127] and in a device able to assess ankle rotations in the 3 planes [128]. Another robotic ankle trainer, the Anklebot, embeds encoders to estimate the ankle dorsi-plantarflexion and inversion-eversion angles [129].

End-feel assessment, at the best of our knowledge, has not been realized yet in a lower limb device. Nevertheless, attempts to develop an instrumented end-feel assessment were made for the shoulder joint [130, 131]. The authors used a force sensor to measure the applied force and a motion tracking system to assess the joint displacement. The rationale behind this approach is that the end-feel can be interpreted as the displacement induced by a force applied at the end of the joint ROM. It is, therefore, a measure of stiffness and as such it can be quantified by applying a known force and measuring the joint displacement at the end of the ROM [131]. However, research in this field is still at an early stage and no information on validity and reliability of the measurements are available.

d.   Future Developments in Rehabilitation Robotics

Rehabilitation and assistive robots usually make use of angular position sensors in their hardware for control purposes and it would, therefore, be natural to conceive robot-aided joint ROM assessments.

The development of new technologies in rehabilitation robotics can address many of the issues of current clinical measures of joint motion. aROM measures can be improved by using robots that are able to compensate for gravity while the subject performs active movements, making the assessment independent of the body orientation with respect to gravity. Transparency of robots must be ensured by means of backdrivable actuators or particular control strategies (e.g. admittance control [132], frequency oscillators [133]). The mechanical limits of a robotic joint should be designed in order to allow a subject to reach the whole ROM. Otherwise, the measures will saturate to this limit, leading to an underestimation of the patient's ROM [83]. The stabilization of the patient's joints other than the joint of interest and the reduction of compensatory movements can be provided by mechanical fixation to the robotic device. Nevertheless, compensatory movements can be very difficult to detect, especially when they occur within the same joint under test; in this case they can only be identified from the careful eye of the examiner [134]. During the measurement of pROM and end-feel, robots can impose a standardized movement in terms of torque and/or speed [125]. This would improve the reliability of the test making it independent of the operator. Moreover, pre-defined sequences of movements can be programmed using robotic devices in order to have a standardized measurement protocol.

Exoskeletons for overground walking could potentially be used for measurements in static and dynamic conditions provided that gravity, friction and inertia are adequately compensated (see section 2.4.6). For example, a versatile passive exoskeletal research platform (Vlexo) developed to study human-robot interactions was designed to have robotic joint ROM higher than the human ROM [123]. Each degree of freedom could be blocked to avoid compensatory movement. Thanks to the high adaptability and instrumentation possibilities, it would potentially become a good tool for measuring simultaneously the ROM of hip (abd-adduction, int-ext rotation, flex-extension) and knee in static and dynamic conditions.

End-feel assessment procedures can be implemented with a similar approach as for the shoulder joint [130, 131], using for example motorized exoskeleton devices [57, 116] or ankle robots [125, 128, 129] equipped with angular position and force sensor.

Concerning the measurement technology, the most used angular sensors in robotics are potentiometers, due to their robustness, accuracy and low price. However, since they must be aligned with the joint's axis of rotation, the measures could potentially suffer from misalignments when the anatomical joint does not have a single axis of rotation or when the setup is not properly done. To overcome this issue, other sensor technologies that do not require the identification of the joint axis can be used. Flexible goniometers based on strain gauge technology are available on the market (e.g. Biometrics Ltd. – uniaxial or biaxial, [135]). The end blocks are fixed to the segments that form the joint and the angle of flexion-extension and abduction-adduction can be recorded, provided that the device is attached in a suitable plane. They have very good performances both in static and dynamic conditions [136–138], but they are at present not sufficiently robust for daily clinical usage. In wearable

applications, strain sensors [139] and optic fibers [140] have been used due to their low encumbrance and low weight, but at the moment their performance is not adequate for accurate measurements. Among the wearable sensor technologies, Inertial Measurement Units (IMUs) are promising instruments, given the good performances shown so far, especially in knee dynamic ROM measurements [141–144]. However, they require calibration and signal processing algorithms that perform sensor fusion and compensate for possible inaccuracies due to electromagnetic interferences.

Further studies are recommended to define the hardware configuration, the sensor technology and the measurement protocol that maximize the validity and reliability of the aROM, pROM and end-feel assessment in a clinical context, with the temporal and economic limitations that this implies. Wearable technologies could give an insight of the ROM that the patient is able to display in a real-life situation.

2.4.2 Muscle Strength

a.   Definition of the Measure

Muscle strength is defined as the amount of force generated by muscle contraction [145]. Muscle weakness, or the inability to generate normal levels of force, has clinically been recognized as one of the limiting factors in the motor rehabilitation of patients following stroke [146] and it is one of the major clinical manifestation in hereditary neuromuscular disorders and injuries of the spinal cord [147]. The amount of preserved voluntary muscle contraction has been proven to be highly correlated with walking ability in incomplete SCI [148] and stroke [149]. In the elderly population, lower limb muscle weakness has been associated with an increased risk of falls [150]. In the lower limbs, muscle weakness can be ascribed to disuse atrophy and to the disruption in descending neural pathways leading to inadequate recruitment of motoneuron pools [146, 151]. Assessing muscle strength is important to determine the severity of the injury, to plan the therapy and to monitor the effects of rehabilitation treatments [152].

b.   Clinical Assessment and Open Issues

In clinical practice, muscle strength is typically assessed using manual muscle testing (MMT) (e.g. Medical Research Council scale [153]). MMT grades strength according to the ability of a muscle to act against gravity or against a resistance applied by an examiner (0: no muscle contraction, 5: holds test position against maximal resistance) [152]. However, the accuracy and sensitivity of MMT is low and the same grade in MMT corresponds to a large range of absolute strength values [152]. It was reported by [152] that Beasley found that a variation of less than 25% in muscle strength for the knee extensor cannot be detected by MMT [154]. MMT is strongly influenced by the experience of the examiner, who must avoid compensatory movements by the subject and ensure a standard positioning. MMT suffers from ceiling effects, because the maximum score (5.0) is assigned before a normal level of muscle strength is truly reached [155]. MMT was found not adequate as a screening tool and insufficient in

tracking the progress of a patient undergoing therapy [156, 157]. Subtle increases in muscle strength are only detectable with instrumented methods.

Quantitative measures of muscle strength can be performed during isometric, isoinertial or isokinetic contraction. In an isometric test the subject is asked to perform a maximum voluntary contraction (MVC) against a fixed resistance and the maximum value of the force/torque is retained. In clinical practice, this test is mostly performed with a hand-held dynamometer (HHD) or myometer. The HHD is a portable force sensing device that can be placed between the hand of the examiner and the body segment to test, similar to how an examiner would perform a MMT [158]. The examiner must be able to apply a resistance equal or greater than the patient's force. Like the MMT, the myometry is, therefore, depending on the amount of resistant force the practitioner is able to apply to the segment of interest and on his ability to stabilize proximal joints [158, 159]. Nevertheless, with respect to MMT, myometry has higher sensitivity and it is less prone to ceiling effects [152]. Reliability and validity of HHD measures can be further increased by fixating the device with a belt [160, 161], so that the resistance applied against the movement is not dependent on the examiner's force. Load cells mounted on supportive frames can also be used for this purpose [162]. Isoinertial tests consist in lifting a constant load throughout the joint ROM and the outcome is the maximum load that can be lifted once (1-RM) [163]. Isoinertial tests are usually executed using sport devices, like the leg extension machine, modified in order to record the joint angle [164]. During an isokinetic contraction the joint angular velocity is kept constant by a machine, the isokinetic dynamometer. The subject is asked to forcefully contract the muscles during the whole ROM while the peak torque is calculated. This test can only be performed with a robotic device and it will be discussed in the next section. Isokinetic tests could be useful to unmask speed-dependent strength impairments [165]. Although the isokinetic dynamometer is considered the gold standard for muscle strength measurements, price, encumbrance and setup time limit its use in a clinical setting. Therefore, it was proposed to use preferably isometric or isoinertial tests in clinical practice due to their reduced cost and easiness of use [163, 164]. The three test modalities have indeed similar good construct validity (relation with physical function) and substantial test-retest reliability [164] and high correlations have been found between isometric and isokinetic torque measures, although isometric tests lead normally to higher values of muscle strength [163, 166]. It is important that users are aware that these three conditions provide different estimates of muscle strength. Nevertheless, it was demonstrated that using the HHD according to standard procedures and fixation, excellent inter and intra-tester reliability and a good correlation with the isokinetic dynamometer can be achieved [152, 158, 160, 167]. Therefore, given the cost and long measurement time (around 25 min) required by the isokinetic dynamometer, it was suggested to favor the use of HHD in clinical practice [158, 167].

c.   *State of the Art in Rehabilitation Robotics*

The most known type of device for muscle strength measures is the isokinetic dynamometer. These devices allows the measurement of joint torques in controlled conditions: isometric at selected joint

angles or isokinetic at selected angular velocities [158, 168]. A servo-controlled lever arm provides resistance to the subject's joint when it reaches a defined angular velocity ($\geq$ 0 deg/s). Different mechanical configurations allow testing of hip flexion-extension and ab-adduction, knee flexion-extension, ankle plantar-dorsiflexion and eversion-inversion. The patient's trunk and the segments proximal to the joint tested must be stabilized with straps and the axis of the dynamometer must be carefully aligned with the axis of the joint to test to avoid measurement inaccuracy [169]. In isokinetic tests the subject is asked to push "as hard and as fast as possible" while the device provides resistance to the movement of the limb so that it cannot accelerate beyond the machine's preset angular speed [170]. A continuous passive motion (CPM) has been proposed for severely impaired subjects, where the robot moves the limb and the dynamometer lever arm at a preset velocity while recording forces applied to the lever arm [85]. Reliability and validity of the isokinetic dynamometer are substantial but the high cost and the long setup time limit its use in everyday clinical practice.

In rehabilitation robotics, muscle strength has been measured integrating force sensors into the structure of exoskeletal devices for quantifying physical human-robot interaction and estimating the force exerted by the patient. Directly measuring the interaction force at the attachment points requires a load cell, placed at the connection between the cuff/orthosis and the exoskeleton link, such as in a modified version of the Lokomat [171, 172]. Otherwise, the estimation of interaction torques can be achieved through a force sensor in series with the actuators, like in the Lokomat [124] and in the ALEX [21], or through linear potentiometers for measuring the length of the springs used in the actuators of the LOPES I [116]. The torques produced at each joint are calculated online from the joint position and the linear force values. The Lokomat, in particular, allows the execution of hip and knee isometric strength tests in the sagittal plane: the patient is positioned with 30° hip flexion and 45° knee flexion and asked to flex or extend the joints against the resistance provided by the orthosis. A moderate to substantial inter- and intra-rater reliability of this method was found with patients with and without neuro-muscular disorders [84].

The ankle joint is usually measured separately from the hip and knee joints with dedicated devices used in a sitting position [87, 173]. An ankle robot constituted by a footplate fixed through a six-axis force sensor to a servomotor shaft that controls its angular position and speed was used for measuring isometric muscle strength: the subject's ankle was locked at the 0° ankle dorsiflexion, and maximal voluntary contraction was taken [125, 126]. Isometric torques of the ankle joint in different kinematic configurations were obtained from a device able to measure ankle torques around the three articular axes (plantar-/dorsiflexion, int-/external rotation and pronation/supination). The 6-DOF structure allows linear and angular displacement of the ankle with respect to the shank. Each DOF is blockable in different configurations and torques and angles can be measured [128].

d.   Future Developments in Rehabilitation Robotics

Despite the poor psychometric properties of the MMT, methods alternative to this test that can be easily integrated in a clinical setting are lacking. Robotic devices can address many of the problematics previously identified. The responsiveness of muscle strength tests is important for detecting small changes during the progression of rehabilitation. Therapy goals can be set based on the minimum force required for performing activities of daily living, like walking or sit-to-stand [174, 175]. It is important that a test is able to detect changes at least equal to the MCID. However, MCID of muscle strength changes in patients with neurological disorders have not yet been established. Ceiling effects must be avoided in order to have a measurement scale that can be used also with mildly affected patients. Robotic devices have the potential to provide more sensitive assessments thanks to the sensors embedded in their structure. Standard and repeatable testing conditions can be achieved by implementing a system for fixating the patient to the device and preventing undesired movements and by programming a standard sequence of movements that should avoid fatigue effects [176]. Moreover, assessment procedures can be integrated in a therapy session performed with a rehabilitation device without requiring additional setup time.

The isokinetic dynamometer is a first attempt to provide a state-of-the-art robotic assessment method [177]. A large body of research on this device have unraveled the possible shortcomings and studied different applications and measurement protocols. In particular, factors such as gravity compensation, damping of the system, human-machine interface and alignment of the human and robot axes of rotation have been considered in many publications [164, 168, 178]. This knowledge can be applied to the development of future robot-aided muscle strength assessments, despite the fact that the differences in hardware prevent the complete reproducibility of the results. Testing subjects with severe weakness requires particular attention because subtle levels of muscle strengths can be masked by the use of device that is too heavy for the patient or the use of a position that does not eliminate the effect of gravity [147]. Lastly, the motivation of the patient plays an important role [85] and it would be worthy to investigate how this human factor affects the outcome measures and consequently to standardize the protocol and the instructions.

2.4.3   Proprioception

a.   Definition of the Measure

Proprioception can be defined as the ability of an individual to determine joint and body movement (kinaesthesia) as well as position (statesthesia) of the body, or body segments, in space [179, 180]. It is based on sensory signals provided to the brain from muscle, joint, and skin receptors [181], with muscle spindles playing the major role [182]. Proprioceptive feedback has been demonstrated to be a key component of motor control and functional joint stability [183]. A diminished proprioceptive acuity at the ankle joint is associated with a lower unipedal stance time, which is a measure relevant for evaluating

frontal plane postural control [184]. Loss of proprioception has been reported both in neurological (e.g. stroke, SCI, peripheral neuropathy) and in orthopedic patients (e.g. knee osteoarthritis) and it has been associated with an increased risk of falls in the elderly [182].

b.   Clinical Assessment and Open Issues

Assessment of lower limb proprioception in clinical practice is based mainly on two rather simple tests: the movement detection at the big toe and the Romberg sign [182]. In the first the examiner moves the patient's toe upward or downward and asks to detect the direction and the amplitude of the movement. In the Romberg test, the subject is asked to close his eyes while standing with his feet close together. A non-specific proprioceptive deficit would usually result in the loss of balance. While useful as a quick method to detect the presence of proprioceptive abnormalities, these tests are not sensitive enough to detect mild impairments or to track changes over time. Moreover, the test at the big toe depends strongly on the pressure applied by the examiner and the amplitude of the movement imposed [185]. Furthermore, only the distal segments of the upper and lower limb are tested and no assessments of the proximal joints are performed. A more specific test, even if less used in clinical practice and mainly in upper limb examination, is the joint position reproduction or matching (JPR) [179]. In this test the patient is blindfolded and the examiner moves his/her limb to a target position. The patient is then asked to match this position either with the contralateral limb or with the same limb after it has been brought back to the starting position. This test is normally performed without any instrument and the visually observed mismatch in position is retained as a rough measure of proprioceptive precision [181, 186]. Goniometers can also be used to measure the joint angle before and after the matching but their reliability and measurement error have been shown to vary widely [187]. Items related to proprioception are included also in the sensory-related section of the Fugl-Meyer Score for stroke patients. Here small alterations in the position of hip, knee, ankle and great toe are evaluated [188]. However, the stimulus provided by the examiner is inherently subjective and sensitivity is limited to 3 levels (absent, impaired or normal proprioception).

c.   State of the Art in Rehabilitation Robotics

Instrumented tests for proprioception in lower limbs have been developed using motorized devices or isokinetic dynamometers. An overview of these experimental devices and methods can be found in [179, 189].

The classic JPR test discussed above can be easily instrumented. A machine moves the subject's limb to the target position. The subject is then asked to match this position, either by actively moving the limb or by pressing a button when the limb passively moved by the machine reaches the target position. However, it has to be taken into account that active and passive motion of the limbs are not equal in terms of sensory feedback [186]. JPR methods are not suitable for people with cognitive impairments since they are highly dependent on memory [179]. Moreover, they have been found to have

slight to moderate reliability [186]. A JPR test for assessing hip and knee joint proprioception has been implemented in the robotic gait orthosis Lokomat and tested in healthy subjects and 23 incomplete SCI subjects [185]. The subject's leg was positioned at a target hip and knee angle and then moved away to a distractor position. The subject was then asked to place the limb at the remembered target position using a joystick to control the robot. The absolute error between target and remembered position was retained as outcome measure. The test-retest reliability in SCI was found to be fair at hip joint and substantial at the knee joint but the Bland-Altman plots showed broad LOA that indicate a low sensitivity in SCI individuals. Heteroscedasticity was also reported. Nevertheless, the score correlated well with the clinical assessment of proprioception and a significant difference between SCI patients and healthy subjects was found.

A second approach for measuring proprioception is the threshold to detection of passive motion (TTDPM). In this test the body segment under test is moved by a machine in a predefined direction. The subject is asked to press a button as soon as he/she detects a movement. Movements are presented at different velocities since the proprioceptive threshold decreases with increasing speed [179, 190]. A motorized apparatus for testing hip, knee, ankle and toe detection threshold was developed by Refshauge et al. and the influence of speed and joint position on the test outcomes was studied [190, 191]. A modified isokinetic dynamometer and a chair with motorized arms have been used for assessing passive flexion/extension and varus/valgus movements of the knee in healthy subjects and osteoarthritic patients (OA) [183, 192]. From the initial posture, the servomotor rotated the knee at a constant low velocity of below or equal to 1°/s). The threshold position of detection of the movement was retained, with smaller threshold values indicating greater proprioceptive acuity. Reliability was found to be excellent both within and between raters, both for OA and healthy subjects. In both studies the subjects wore headphones and an eye mask. The TTDPM was tested also using the Lokomat [193]: hip and knee separately were moved according to a randomized order of speeds (0.5 – 4°/s), directions and catch trials (no movement). Angle and reaction time were used to calculate a movement detection score. The score presented substantial reliability and a high correlation with a clinical score of proprioception, showing better sensitivity (it is possible to measure reaction times $\geq$ 50 ms) and no ceiling effects. Faster speeds were able to elicit a response in severely impaired subjects that could not detect movements at 0.5 °/s. The TTDPM test leads generally to more precise and less variable measures of proprioception acuity than the JPR test. Interestingly, the two tests have shown no concurrent validity [186].

d.   *Future Developments in Rehabilitation Robotics*

These studies demonstrate that instrumented and robotic assessments of proprioception are feasible and present several advantages over clinical assessments of proprioception. Measures of proprioception in clinical practice are rather coarse and lack granularity. Standardization is nearly absent and the outcome of clinical tests is often a binary answer.

Lower limb robotic devices provide the possibility to maintain a high consistency in the protocol (speed, points of contact, timing) between trials. The responsiveness of the robot-based measure was demonstrated also by the ability to detect a wide range of angle errors in subjects that were judged unimpaired by the clinical assessment [185, 193]. Moreover, the influence of motor impairment on the control of lower limbs can be eliminated because the leg can be passively moved by the robot. Lastly, robotic devices can provide useful information on joints that are not normally addressed in clinical practice, where the most common examination involves only the big toe [182]. It is likely that specific information on other joints might provide an insight on different components of sensory function useful to track changes in recovery after injury [193]. On the other side, the straps of exoskeletal devices may provide additional cutaneous feedback to the subject, thus influencing the measurements [193]. When designing a new robotic device or protocol for proprioception assessment it is important to consider that the test methods (JPR or TTDPM) do not provide the same information [186]. Different versions of the protocol exist also within the same test and again their choice can highly influence the results [181]. The speed of a TTDPM test highly influences the outcome measures [179, 193] and must be accurately controlled by the robotic device. Active and passive movements are likely to activate different proprioceptive mechanisms [186].

Robot-based assessments of proprioception require longer time of administration with respect to clinical assessments, but they are able to provide reliable and sensitive information on proprioceptive acuity that allows a more detailed examination useful for diagnosis or accurate tracking of the recovery of the patient.

2.4.4 Abnormal Joint Torque Coupling and Synergies

a.   Definition of the Measure

Due to cortical damage, stroke survivors and cerebral palsy (CP) children can lose the ability to move their joints independently, which result in abnormal coupled, pathophysiological movement patterns, also called synergies. The loss of independent control of joint moments is caused by involuntary co-activation of muscles over multiple joints [172].

Brunnstrom [194] defined two often occurring pathophysiological synergies in the lower extremities:

1. Extension synergy consisting of internal rotation, adduction and extension of the hip, extension of the knee, and plantar flexion and inversion of the ankle
2. Flexion synergy consisting of external rotation, abduction, and flexion of the hip, flexion of the knee and dorsal flexion and eversion of the ankle

b.   Clinical Assessment and Open Issues

Loss of independent joint control limits the performance on activities of daily living. Therefore, in both clinical and in research settings abnormal joint torque coupling is often being assessed and this is

mostly done using the Fugl-Meyer Assessment of Physical Performance [195]. This scale has been shown to be a reliable, sensitive and valid method for the assessment of motor impairment after stroke [196–198]. However, it can be argued that for the quantification of abnormal joint torque coupling this scale lacks sensitivity due to the use of a 3-point scale (0 = cannot perform,1 = performs partially, 2 = performs fully) for the assessment of each component of torque coupling.

c.   *State of the Art in Rehabilitation Robotics*

Robotic and robot-related measures could possibly provide more accurate information. Over the last decade several studies have investigated abnormal joint torque coupling using robotic and robot-related measures [146, 172, 199–205]. The majority of these studies quantified the synergies in static situations during isometric contractions and used a similar approach. Subjects were strapped into a (robotic) device (most often the Lokomat) that constrains every movement of the concerned leg and the pelvis. The device was equipped with force sensors to measure all the interaction forces/torques that the subject exerts with this leg on the device, for instance the cuffs of the Lokomat were instrumented with 6-DOF load cells [172, 199, 200]. Participants produced isometric torques in a particular direction (primary), while torques in all other the directions (secondary) were also measured. Abnormal torque coupling was quantified as the difference in secondary torque production between healthy individuals and stroke survivors. Studies differed in the amount of joints and planes that were investigated and the position in which the coupling was assessed. Thelen et al. [202] assessed the coupling while subjects were positioned in an adjustable chair with ankle fixed to six degree- of-freedom load cell, whereas others assessed the coupling while subject where standing in the toe-off and/or mid-swing position with the test leg unloaded [146, 199–201].

Thelen et al. showed that individuals with cerebral palsy produced a knee extension moment during hip extension and vice versa whereas healthy subjects produced a knee flexion moment during hip extension and a hip flexion moment during knee extension. Quantification of abnormal joint couplings using a (robotic) device has provided evidence for different couplings. Neckel et al. [146] found that stroke survivors only showed an abnormal coupling between hip abduction and flexion and had similar couplings as found in healthy subjects for the other degrees of freedom. Cruz and Dhaher [200] observed that stroke survivor coupled knee extension with hip adduction. Tan et al. [199] found strong coupling between ankle frontal plane torque and hip sagittal plane torques and vice versa that were not present in the healthy control subjects (ankle plantar flexion with hip adduction, ankle eversion with hip extension and ankle inversion with hip flexion). Recently, Sanchez et al. [206] also found evidence for the earlier found coupling between hip extension and adduction, and ankle plantar flexion and hip adduction. So, evidence starts to accumulate that stroke survivors have abnormal coupling between hip adduction, hip extension and plantar flexion.

To our knowledge only one study has attempted to identify abnormal joint torque coupling during walking [172]. In this study participants were moved along a predetermined locomotor trajectory using

the Lokomat while interaction and ground reaction forces were measured. However, the difficulty with this setup is that it is hard to disentangle the torques required for walking and maintaining balance and those resulting from the abnormal joint torque coupling. Therefore, although assessed in a quasi-dynamic situation, the results may not be generalizable to voluntary walking.

The reliability (test-retest, inter-rater, intra-rater) has not yet been assessed for these abnormal couplings, nor has its responsiveness been determined. The criterion validity has not explicitly been investigated, however Cruz and colleagues [207] demonstrated using step wise regression that the coupling between knee extension and hip adduction was the best predictor of gait speed amongst other strength and coupling variables. None of the aforementioned studies did correlate their coupling measures with a clinical scale like the Fugl-Meyer to assess the construct validity.

d.   Future Developments in Rehabilitation Robotics

To summarize, robotic measures may be able to quantify abnormal joint torque coupling more precisely compared to clinical measures such as the Fugl-Meyer Assessment of Physical Performance. However, the reliability, responsiveness and validity of these measures need to be further investigated. Additionally, robotic assessment is still performed under static or quasi-dynamic conditions, which might not quantify well how these couplings limit walking. For assessing abnormal couplings in the upper extremities, the assessments have moved from a static approach [208] to a dynamic approach where the couplings are assessed during reaching movements using robotic devices [209]. We foresee that a similar shift will happen for the lower extremities. Integration of the principle used in the robotic assessment under static conditions in robotic gait trainers could provide the tools to assess abnormal joint torque coupling during walking.

2.4.5   Joint Impedance

a.   Definition of the Measure

In the clinical field, the term *joint stiffness* has been used to express the sensation of difficulty in moving a joint [210]. While this term is commonly used in the clinical practice, the notion of *stiffness* used in this context does not match the definition of stiffness in classical mechanics. To describe all the mechanisms that contribute to the resistance of motion, the term *impedance* is usually preferred. In motor control literature, the term mechanical impedance is defined as the dynamic operator that specifies the force an object generates in response to an imposed motion [211]. The latter definition includes all motion-dependent effects, i.e. those terms that specify the force generated by changes in position (e.g. stiffness, non-elastic forces), in velocity (e.g. viscosity, damping) and in acceleration (e.g. inertia) [212]. In biomechanics, the term *joint impedance* relates the motion of the joint and the torque acting about it [213]. Joint impedance is usually estimated by applying a torque or force perturbation and measuring the resulting change in position or applying a position perturbation and measuring the resulting change in torque of force.

Joint impedance is mainly determined by three sources: *i)* the passive biomechanical properties of the muscles, tendons and tissue around the joint and limb inertia – *passive* components; *ii)* the resistance produced by the muscles in response to reflexes [213–216] – *reflexive* components; and iii) the resistance produced by the muscle fibers due to non-reflexive, neural-driven contractions – *intrinsic* components [216]. Since the *reflexive* and *intrinsic* component are both related to muscle activation, their sum is commonly referred to as *active* component[1].

In neurological populations, an abnormal increase in joint impedance can result from spasticity, rigidity or dystonia [217]. The intrinsic and reflexive components have also been shown to be affected in neurological populations [218].

Joint impedance varies with muscle contraction [219], joint position [220–222], rotation amplitude [223], and the duration of the applied perturbation, since after approximately 30 ms cross-bridges break [224] and the contribution of cross bridge stiffness to the overall joint impedance will diminish. Joint position affects joint impedance measurements because the intrinsic component increases towards the extreme joint angles as the ligaments get more stretched. Additionally the different muscles vary their active contribution to the joint impedance depending on their length (and therefore on the corresponding joint configuration), due to the particular shape of the length-tension curve of the muscle [225]. The reflex activity is also known to be speed dependent [226] and only contributes above a threshold [227]. Finally, the task instruction given to the subject will also shape the joint impedance [228]. Most common task instructions are 'relax', 'resist the perturbation', or 'keep the force constant'.

b.   *Clinical Assessment and Open Issues*

The Modified Ashworth Scale [229] is the most widely used clinical assessment to quantify an abnormal increase in joint impedance due to excessive muscle tone. The MAS consists of moving the limb of the patient through its range of motion and rating the resistance on a 6-point scale. The MAS is widely accepted, even though the validity and reliability of the measure are questionable [230] since especially inter-rater reliability was slight to fair. Moreover, the MAS may also lack sensitivity. The MAS assess joint impedance only in passive conditions, where the subject is asked to relax, which might not be indicative for how spasticity influences dynamic movements. Another test to assess the increased resistance to movement in a more quantitative way is the pendulum test, first described by Wartenberg [231]. This test quantifies movements of the lower leg following its drop from a horizontal position by deriving the angle of first reversal, the maximal angular velocity or number of oscillations. The pendulum test has shown good convergent validity, reliability and sensitivity [232, 233]. Some limitations of this test are that it is done in relaxed conditions – which is difficult to achieve - and can only be used for the knee. Additionally, measuring equipment (electrogoniometers, inertial sensors) are needed to record the leg motion and to extract the variables.

While measurement of joint impedance in not commonly performed on the everyday clinical practice, it has implications in understanding a potential cause of impairment. For instance, Mirbagheri et al. [218] was able to isolate abnormal active contributions in spinal cord injury patients based on measurement of joint impedance of the ankle. Such measurements can also point out to different pathologies such as spasticity, rigidity or dystonia [217].

c.   *State of the Art in Rehabilitation Robotics*

As mentioned earlier, joint impedance is dependent on joint position, muscle contraction levels, and amplitude, velocity and duration of the perturbation. Therefore, the use of robotic devices is advantageous because these factors can be precisely controlled at the same time relevant signals are been recorded. Several instrumented and robotic measures have been developed to asses either the reflexive and/or intrinsic components of joint impedance [20, 127, 129, 215, 217, 234–240]. We will not review all devices and methods. In particular for the ankle joint many devices have been developed, which have recently been reviewed [87]. To assess passive joint impedance, the joint of the participant is moved by a robotic manipulator or manually over a certain angle often measured using a potentiometer while the resisting force is measured using force sensors integrated in the (robotic) device. For accessing the passive joint impedance it is important that no muscle activity is present. Therefore, the participant is asked to (try to) relax and the angular velocity is kept low to avoid the excitation of reflex contractions. In the push and pull test, the joint is moved with small increments and kept static for approximately 5 s in every position. The net moment (after removing gravity) provided by an external device to keep the segment in equilibrium is retained for each incremental position [241]. Both isokinetic dynamometers and custom made joint actuators have been used as assessment devices. With a manually operated device the passive ankle impedance could be estimated reliably in healthy subjects (ICC values between 0.71-0.85,[235]) and in CP children(ICC = 0.82, [127]). In the study of Chesworth et al. [236] a custom made torque motor system was used to assess passive joint impedance of the ankle with a comparable reliability (ICC: 0.77-0.94).

The contribution of active components (i.e. intrinsic and reflexive) to joint impedance have also been investigated using similar experimental set-ups. In a typical setup, the subject is either asked to actively resist an angular displacement or to (try to) exert a constant force. At some point, either an angular position perturbation is applied while the resisting force is measured or a force perturbation is applied and the resulting angle is measured. Impedance measured under this condition contains the three components: passive, intrinsic and reflexive. To be able to distinguish between these components, different strategies have been used. For example, in the study of McHugh et al. [238] the passive component is subtracted from the total impedance to determine the active component. Also more complex methods exist, which are based on system identification techniques. In the method of Mirbagheri et al. [215], a system identification method is applied to distinguish between intrinsic and reflexive components. In this method, pseudo-random continuous rotations of the ankle are applied, and

the ankle torque and EMG of involved muscle groups are recorded. The model consists of an intrinsic component and a unidirectional delayed velocity feedback pathway representing the reflexive component. Input to the model is ankle rotation, and the model parameters are optimized to minimize the error between the predicted and recorded torque. The EMG is used to determine the latency of the reflex component. In healthy subjects a good intra-rater (r>0.8) reliability was found [242]. De Vlugt et al. [240] used similar techniques but instead of continuous rotations, they applied ramp-and-hold ankle dorsiflexion rotations with different speed profiles. They employed a nonlinear neuromuscular model that is more complex than the one used by Mirbagheri to predict the recorded ankle torque. Results showed that stroke survivors could be distinguished from control subjects by tissue stiffness and viscosity and to a lesser extent by reflexive torque from the soleus muscle. These parameters were also sensitive to discriminate different patients, who were clinically graded by the MAS. In a subsequent study [243] these researchers adapted their model and protocol slightly by applying both ankle plantar and dorsiflexion rotations. The estimated model parameters could discriminate between patients with CP and control subjects. Soleus background activity was sensitive to MAS spasticity severity, but reflex activity was not. Preliminary data indicated that reflex activity was reduced after spasticity treatment. The between-trial (ICC: 0.76–0.99) and between-day repeatability (ICC: 0.64–0.95) was moderate to substantial for tissue stiffness and background activity, but not for reflex parameters.

A shortcoming of most of the studies on joint impedance is that the assessment is done for static or passive tasks where the participants are in a supine, prone-lying or sitting position. The ankle impedance has also been determined in more natural active conditions, such as stance [244, 245] using very fast dorsi- and plantar-flexion rotations with a motorized footplate and non-parametric impedance estimates.

Aforementioned studies and approaches all made use of dedicated assessment setups. However also robotic gait trainers can be used to derive measures of joint impedance. For instance, the Lokomat has a built-in function to assess overall joint impedance of the hip and knee joints by passively moving the limbs at different speed profiles and recording the resulting joint torque. Using this technique, a moderate correlation between joint impedance and MAS scores could be seen [20]. Koopman et al.[246] used the LOPES robotic gait trainer and multi input multi output system identification techniques to assess joint impedance of the hip and knee. Healthy subjects were assessed while in the toe-off or heel strike position and were asked to resist the movement of the device or apply no force at all. Results showed that the effect of biarticular muscles on the inter-joint impedance could not be ignored.

d.   *Future Developments in Rehabilitation Robotics*

Although research on the accuracy and reliability of robotic devices to assess joint impedance is not available for all developed devices and methods, it can be argued that the use of integrated sensors and robotic actuators will show better psychometric properties compared to the MAS score. Another advantage of robotic measures is that they can help to develop methods to estimate the active and passive or intrinsic from reflexive components, while the MAS only measures the resistance of motion but not

the underlying cause. The pendulum test could be implemented in combination with transparent devices that do not hinder the natural oscillation of the shank (e.g. soft exoskeletons). However, the reviewed robotic assessments are still performed under non-functional and static or passive conditions. Therefore, further development is necessary to be able to assess joint impedance during a dynamic task such as walking. A method to estimate joint impedance during gait is to use musculoskeletal models and using optimization techniques to estimate muscle forces that are related in the model to muscle impedance [247]. An alternative method is to apply time-varying system identification algorithms to estimate the changing impedance of the human knee over the gait cycle [248]. The ensemble-based correlation technique averages over repetitions instead as over the time cycle [249]. Averaging over repetitions and over time within a short data segment within repetition can also be combined [250] with the advantage that less repetitions are needed. A testing platform consisting of a knee perturbator has been built in order to deliver velocity perturbations during walking and record reaction torques, with the aim of determining the knee impedance using system identification techniques [251].The ensemble-based correlation technique has also been applied to estimate the modulation of the ankle impedance from the end of the stance phase to heel contact with MIT's AnkleBot [53]. However, comparing the estimated knee impedance of the ensemble-based correlation method with the model-based method [236] shows order of magnitude differences in the estimated knee impedance. Hence, more research is needed to reliably estimate the impedance of multiple joints during gait.

2.4.6   Walking Activity / Gait Pattern

a.   Definition of the Measure

Walking can be defined as a repetitious sequence of limb motions that move the body forward while simultaneously maintaining stance stability [28]. Gait refers to the manner or style of walking [27]. Gait is composed by a cyclic series of motion patterns performed by the hip, knee and ankle. The gait cycle can be divided in phases, the main ones being swing and stance [28–30]. Walking can be described according to different domains: *i)* the capacity of performing activities related to walking (e.g. walking without assistance, sit-to-stand); *ii)* the spatio-temporal characteristics (e.g. speed, step length, cadence, stance/swing ratio); *iii)* the "quality" of gait pattern, which concerns the ability to coordinate lower-limb segments and joints (e.g., simultaneous coordination of hip and knee angles) [25].

b.   Clinical Assessment and Open Issues

In clinical practice, walking is mainly assessed by examining the spatio-temporal characteristics and the capacity of performing walking-related tasks. Like the other assessments discussed in this section, measuring walking is also influenced by time constraints. Therefore, measures that are relatively easy and fast to administer are normally chosen.

Among these, the capacity of performing functional walking activities is commonly assessed using ordinal-based clinical scores. These tests have a low administrative burden and they can be useful to

grossly categorize the patients according to their walking capacity, but they are not sensitive enough to detect small improvements in locomotion [252]. The Walking Index for Spinal Cord Injury (WISCI II), for example, assigns a score between 0 and 20 based on the amount of assistance required for walking (e.g., walking with one/two crutches). Consistent floor and ceiling effects and a low responsiveness were reported [253]. Moreover, the different levels are unevenly spaced, meaning that a change of 1 point in the score has a different relevance depending on the position along the scale [252]. Several other activity-based tests were developed (e.g., Functional Ambulation Category (FAC), Dynamic Gait Index (DGI)) to assess walking function but, although very useful for gaining information on the overall walking process, they are unable to provide any detailed information on the way it is realized.

Time-based tests are often performed, since they provide quantitative measures and have shown substantial inter- and intra-rater reliability [254]. For example, in the 10-Meter-Walking-Test (10MWT) a stopwatch is used to measure the time required to walk 10 meters [255]. Thus, the test provides a measure of short-duration walking speed and it has substantial correlation with other time-based walking tests and with other walking-related functions like muscle strength of the lower limb (Table A.14) [253]. However, the information obtained with this test is limited to gait speed, which, although normally used as a surrogate measure for gait quality [256], is not able to provide information on complex alterations of walking (e.g., compensatory strategies) [257]. 10MWT and other time-based walking tests (e.g., Time-Up-and-Go, 6-Minutes-Walking-Test) present floor and ceiling effects since non-ambulatory subjects score 0 and mildly impaired patients could walk longer distances at the same speed [253]. Other spatio-temporal parameters can be obtained using more sophisticated instruments like IMUs [258–260] and pressure mats [261]. Heel strike events can be detected from an IMU placed at the lower back [262]. A more detailed step segmentation is possible if the IMUs are placed directly on the feet [263, 264]. Parameters such as step duration, step length and swing/stance time ratio can provide important additional information on gait impairments and on the progresses during recovery. For example, there is evidence that step variability (i.e. variability in stride time, stride length and gait speed) is altered in patients with neurodegenerative diseases [265]. In stroke patients, asymmetry in right and left step time and altered stance/swing time ratio were reported using IMUs [266–268]. IMU-based systems are not yet widely integrated in clinical practice, even if new systems are now commercialized (e.g. McRoberts DynaPort [269], GaitUp [270]).

It is important to evaluate the patient's gait pattern to understand whether the person is using compensatory strategies. These strategies might indeed not be visible in the spatio-temporal gait characteristics, which can be similar to physiological ones even in presence of an aberrant muscle activity [25]. This is especially important in longitudinal studies which aim at demonstrating whether improvements in walking speed are attained either by using compensatory strategies or by restoration of the pre-morbid gait patterns [81]. By using measurements able to capture the quality of the gait pattern it is possible to discriminate between the two different recovery strategies - compensation or restoration of physiological gait. However, at present the quality of the gait pattern can only be accurately assessed

using a motion tracking system and force plates. This instrumented gait analysis provides an accurate measure of joint angles, moments and powers but requires a costly equipment and a long administration time.

A major issue related to walking assessment is that non-ambulatory subjects are often assigned the lowest score in the timed test (e.g. 0 m/s in the 10MWT), irrespective of their residual lower limb functions. These subjects, therefore, cannot be assessed because of the scales' floor effect. It would be possible to assess non-ambulatory subjects indirectly by measuring other variables that correlate with walking ability, like muscle strength or balance. However, these tests are performed usually while sitting or lying, in contexts very dissimilar to walking.

c.   *State of the Art in Rehabilitation Robotics*

Driven gait robots for treadmill walking and exoskeletons for overground assistance can be used to record joint kinematics while walking in order to obtain information on the quality of the gait pattern. Robotic exoskeletons equipped with angular position sensors have been utilized to record joint kinematics during treadmill or overground walking [21, 22, 122, 271, 272].

The Lokomat and the LOPES have been used to measure hip and knee angles in various studies, where the reduced impedance of the joints allowed the subjects to impose their own gait pattern. The joints' kinematics was evaluated mainly by comparing it with a reference angular trajectory: e.g. timing error within a tunnel around the desired spatial path [273] or spatial tracking error [274]. A method to assess retraining in stroke patients based on the areal difference between a healthy reference and the patient's trajectory during the swing phase was implemented in the ALEX gait trainer [21]. However, at present, robotic gait trainers might not be the most suitable devices for performing an assessment equivalent to camera-based gait analysis, due to the influence that their mechanical constraints have on the gait pattern. Wearable and lightweight devices that do not hinder human movements are required for this purpose. Particularly suitable for this condition would be the soft lower limb exoskeletons ("exosuits") that have been recently developed to improve human-robot interaction and to allow a more natural walking pattern [63, 139, 275, 276]. In an active soft orthotic ankle device two IMUs placed on the shank and on the foot are used to compute the ankle joint angle [275]. Alternatively, strain sensors embedded in the suit spanning over a joint are used [139]. Although this is a promising approach for measurements in dynamic conditions, the sensing accuracy is at present not high enough for accurate measurements, due to relative movements between the suit and the skin of the subject. Moreover, sensor calibration is required every time a user wears the suit.

The robotic assistance required for walking has been proposed as an alternative method for assessing the walking function. For example, adaptive algorithms automatically adjust the support provided by the device based on the patient's ability to follow a predefined trajectory or to perform a specific task (e.g. foot clearance) [22, 272, 277, 278]. The algorithms update a control parameter K (usually the

impedance of the joints and the unloading of the body weight) at each walking step s based on a forgetting factor $\gamma < 1$ and on the weighted error $g \cdot e$ calculated in the previous step:

$$K_{s+1} = \gamma \cdot K_s + g \cdot e_s \qquad (2.1)$$

After a certain number of steps, the parameter K converges to a value that can be retained as a measure of the subject's impairment [279]. For example, an overall score can be obtained summing the torques required at each joint averaged during the last 10 steps [277].

d.   *Future Developments in Rehabilitation Robotics*

Robotic gait trainers and exoskeletons for overground assistance can be easily instrumented to provide kinematic and kinetic data that can be used to derive metrics useful for assessing the gait pattern and the walking function. Since these devices enable non-ambulatory patients to walk in a safe and functional manner, they allow the assessment of these category of subjects, limiting unwanted floor effects of the tests. Although these systems are expensive, they are already used in many clinical centers worldwide for providing gait training [280]. In these contexts, subjects can be tested during gait training, requiring no or little additional time. Repeatable assessment procedures can be programmed in order to standardize the testing conditions (e.g., speed, unloading of body weight). Accurate measurements of the gait pattern can be obtained if the effects of the device dynamics (i.e. weight, inertia) are minimized. Moreover, the exoskeletons should have enough degrees of freedom to avoid constraining physiological walking movements. The compliant fixation of the patient's leg to the orthosis could lead to measurement inaccuracy and errors [281], therefore standardized procedures need to be established in order to make the patient's setup in the device as independent as possible of the operator. When the transparency of the device is guaranteed by hardware design (e.g. soft exoskeletons) or by software compensation [132, 133], the robot can be used for measuring joint kinematics or spatio-temporal gait parameters. When this condition is not met or when the subject is too impaired to be able to walk without the support of the device, other assessment methods must be used. It would be misleading, in fact, to measure standard gait parameters in a robotic gait trainer that affects the patient's walking pattern. To address this problem, new outcome measures can be proposed. For example, the amount of support (i.e. joint impedance or unloading of the body weight) required to achieve a functional walking pattern can be used as an indicator of the subject's impairment. Further studies in this direction are needed to establish the concurrent validity of this outcome measure with existing clinical scores. It can be hypothesized that a correlation with clinical scores that address the amount of support required for walking (e.g. WISCI II, FAC) exists. Moreover, if the algorithm adapts the support of the device to the particular needs of the single gait phases, it would be also possible to identify specific impairments localized within the gait cycle [277]. However, the results of this method depend on the performance metric used. If a measure of the deviation from a reference trajectory is applied, the resulting support will depend also on the similarity between the prescribed trajectory and the patient's individual gait pattern. A dead band around the reference trajectory, as in [277], could partially address this problem.

2.5 DISCUSSION

Although essential for maximizing the individual therapy outcomes, the use of assessment methods in routine practice is at present insufficient. Among the reasons that contribute to this dearth, poor quality of the existing assessment scores and high administrative burden have been identified [78]. The quality of the assessment methods must be determined by studying their psychometric properties. We believe that the increasing use of robots for rehabilitation is not only beneficial for the therapy outcome, but also represents a huge opportunity for improving the assessment quality and increasing their frequency of administration. Indeed, robotic devices can be equipped with sensors for recording data useful for developing quantitative and objective assessment metrics. Secondly, robots can potentially assure the standardized execution of the assessment procedure, which is essential for reducing the measurement error and increasing the reliability. Moreover, robot-based assessments can reach higher inter-rater and intra-rater reliability if the robotic device is designed to limit fixation errors and to reduce inter-operator differences. Cuffs positioning, misalignments and different tightening of the fixation to the patient's limbs may have a huge impact on the reliability of the assessment outcomes. User-friendly and ergonomic robotic device, along with a rigorous training of the operators may contribute to solve this problem.

A known issue of the current assessments used in clinical practice is their administrative burden (mainly time-wise) that limits the frequency at which they are administered. Assessments executed with rehabilitation robotic devices can be performed during the therapy session, measuring relevant parameters directly during the training, while the patient is using the device. Robotic assessments are able not only to complement existing clinical measurements, but also to enlarge the measurable range of an impairment: because of the quantifiable assistance that robots can provide, robotic assessments can be administered even if the patient is not able to perform the movement without support [82]. Moreover, measurements that have been only subjectively addressed before (e.g., proprioception) can now be targeted by instrumented tests. New variables that were not readily accessible before (e.g., smoothness, joint coupling) become available. Further research on neurophysiological mechanisms must be encouraged to determine how these variables relate to sensorimotor functions and whether they can provide information on recovery [82]. The increased sensitivity and the reduced measurement error of the robot-based assessments can be of utmost importance when the outcome measures are used in a clinical trial aimed at demonstrating the efficacy of a new therapy. Often little can be concluded because the effects of the therapy under study are masked by high inter-subject variability or they are not captured by conventional clinical assessments [42]. Assessments able to distinguish the contribution of restoration of physiological patterns and the effect of compensatory mechanisms to the recovery will help to orient future therapeutic approaches [81]. Not least, more sensitive measurements could also contribute to increasing the motivation of the patients, when even a slight improvement can be documented.

Before starting a research study aiming at developing a new assessment method, researchers must consider several issues. First of all, an inter-disciplinary approach involving research institutes, clinical facilities and medical device manufacturers is encouraged in all the phases of development: researchers must take into account the clinical relevance of the proposed measure (is the information provided by the measure useful for adjusting the therapy?), the interpretability of the outcome parameter (what is its physiological meaning?), the feasibility of the method for both its use in clinical practice (is it safe? Are its administrative and respondent burdens reasonable?) and the manufacturability and large-scale implementation. If these steps are missing, the risk is that the assessment method will never be routinely used in the clinical practice. On the other side, it is also important that researchers go "beyond" the limits of established clinical tests by developing new and independent standards based on robotic measurements. The final aim of robotic assessments, indeed, should not be to reproduce existing clinical scales that, even if widely accepted in the clinical practice, are not comparable by their nature to instrumented and robot-based assessments [82]. Lastly, when developing assessment metrics of a same variable for different lower extremities devices, researchers should try to make the results independent of the platform on which they are obtained. In this way the same metric could be implemented in different devices and results from several studies could be compared. Even if the dynamics of the device will most likely influence some of the assessment metrics, comparative measures can be used (e.g. normalizing patient's data against healthy normative data recorded in the same device).

A crucial requirement for the acceptance of a new assessment method in the rehabilitation community is its clinical validation: reliability must be assessed with an adequate sample size and validity should be established either by comparing the score with a gold-standard - if it exists - (concurrent validity) or by studying the relationship of the new assessment score with the underlying constructs of interest (construct validity). Guidelines for the validation of new robot-based assessments should be developed to help the researchers to define adequate clinical validation studies and to use the correct statistical tools. Moreover, it is necessary to develop indications for interpreting the different scoring systems: clinicians must be able to identify whether a change in score is clinically significant or it is due to measurement error [80].

2.6 Conclusion

In this chapter, we have reviewed existing clinical and technology-based assessments for lower limb functions, and we have highlighted their shortcomings. We have then discussed how robotic devices for rehabilitation have the potential to solve these issues by providing high quality assessments (i.e. objective, reliable and valid) and by integrating the assessment procedure in a training program. Based on the existing shortcomings and on the possibilities offered by robotic technologies, we have proposed solutions and recommendations for the development of novel robot-aided assessment tools. We think that robotic assessments represent a challenging "green field" where researchers have the possibility – and the urgency – to develop methods that will have a strong impact on rehabilitation outcomes. Better

assessments of lower extremities functions will allow the clinicians to prescribe therapeutic and rehabilitation plans that optimize the individual recovery while minimizing unnecessary effort and costs [282]. We believe, therefore, that research for developing valid, reliable and responsive assessment methods is strongly needed for clinical practice, for studies on new therapies and, overall, for improving the rehabilitation outcome and decreasing the time of recovery.

Chapter 3   AUTOMATIC ADAPTATION OF ROBOTIC SUPPORT

The content of this chapter is partly extracted from two publications and it was adapted to ensure consistency within the chapter and with the rest of the document and to avoid repetitions:

Maggioni S, Lünenburger L, Riener R, Melendez-Calderon A. *Robot-Aided Assessment of Walking Function Based on an Adaptive Algorithm.* In: 2015 IEEE 14th International Conference on Rehabilitation Robotics. Singapore; 2015. p. 804–9. © 2015 IEEE. Reprinted, with permission, from the original article.

Maggioni S, Reinert N, Lünenburger L, Melendez-Calderon A. *An Adaptive and Hybrid End-Point/Joint Impedance Controller for Lower Limb Exoskeletons.* Front Robot AI. 2018; 5 October. © 2018 Maggioni, Reinert, Lünenburger and Melendez-Calderon. Reprinted under the terms of the Creative Commons Attribution 4.0 International License[2].

Foreword

The review of clinical and technology-based assessments of lower extremity functions suggested a method for the assessment of walking ability based on the automatic adaptation of the robotic support (i.e. assist-as-needed) in robotic gait trainers. We applied this concept to a treadmill-based robotic exoskeleton, the Lokomat, and we implemented a controller that adapts the impedance of the robotic joints and the body weight support based on the patient's ability to follow a physiological reference trajectory. We hypothesized that the support determined by the algorithm is proportional to the patient's impairment and can serve as an assessment of "walking ability".

---

[2] http://creativecommons.org/licenses/by/4.0/

3.1 INTRODUCTION

3.1.1 Robot-Aided Gait Assessment - Rationale

In Chapter 1, the main requirements for walking, the typical walking-related impairments after SCI and the usual rehabilitation treatment provided (locomotor training) were examined. In Chapter 2, various robot-aided assessments of lower limb functions and activity were reviewed, concluding with the assessment of walking function and gait pattern. The review of the literature found that assist-as-needed (AAN) controllers have been applied in robotic gait trainers to determine a level of robotic support as required by the patient and *proportional* to his/her impairment. Even if this type of controllers has never been used for assessment, there have been indications that the impedance profile determined by the AAN controller can converge to a characteristic profile for every patient [22, 272, 279]. With a proper selection of the parameters of Eq. 2.1, this approach could be suitable to people with mild to severe impairments and it can be performed while walking. The approach is applicable to exoskeletons and end-effector robots, therefore the knowledge gained in this thesis can be potentially generalized to other devices.

In this project, we developed an assist-as-needed (or adaptive) controller that adapts the hip and knee impedance and the body weight support (BWS) of a treadmill-based robotic exoskeleton (Lokomat®Pro V5, Hocoma AG, Switzerland) based on the ability of the subject to follow a physiological gait trajectory. We then tested this approach in eight able-body subjects to verify that it was safe, feasible and to tune the parameters of the controller. The learnings gained in this first experimental evaluation were applied before testing the algorithm with patients in Chapter 5.

Figure 3.1: LokomatPro V5. The system is composed by a treadmill, a body weight support system, an orthosis with actuated hip and knee joints and force sensors and a display to show feedback to the patient. Picture: Hocoma, Switzerland.

3.2 IMPEDANCE CONTROL IN JOINT SPACE

In this chapter we illustrate the details of a controller that adapts the impedance of the joints of a lower limb exoskeleton, the Lokomat. We model the system as a two-link exoskeleton with a shank and a thigh segment. In the swing phase, the system can be modeled as a two-segment pendulum: the upper segment is fixed to the hip center of rotation (CoR) and the end-point corresponds to the ankle position [39]. In the stance phase, the model is an inverse two-segment pendulum: after heel contact, the foot can only be moved backwards by the treadmill, hence the end-point of the kinematic chain is the hip CoR and not the ankle joint (Figure 3.2).
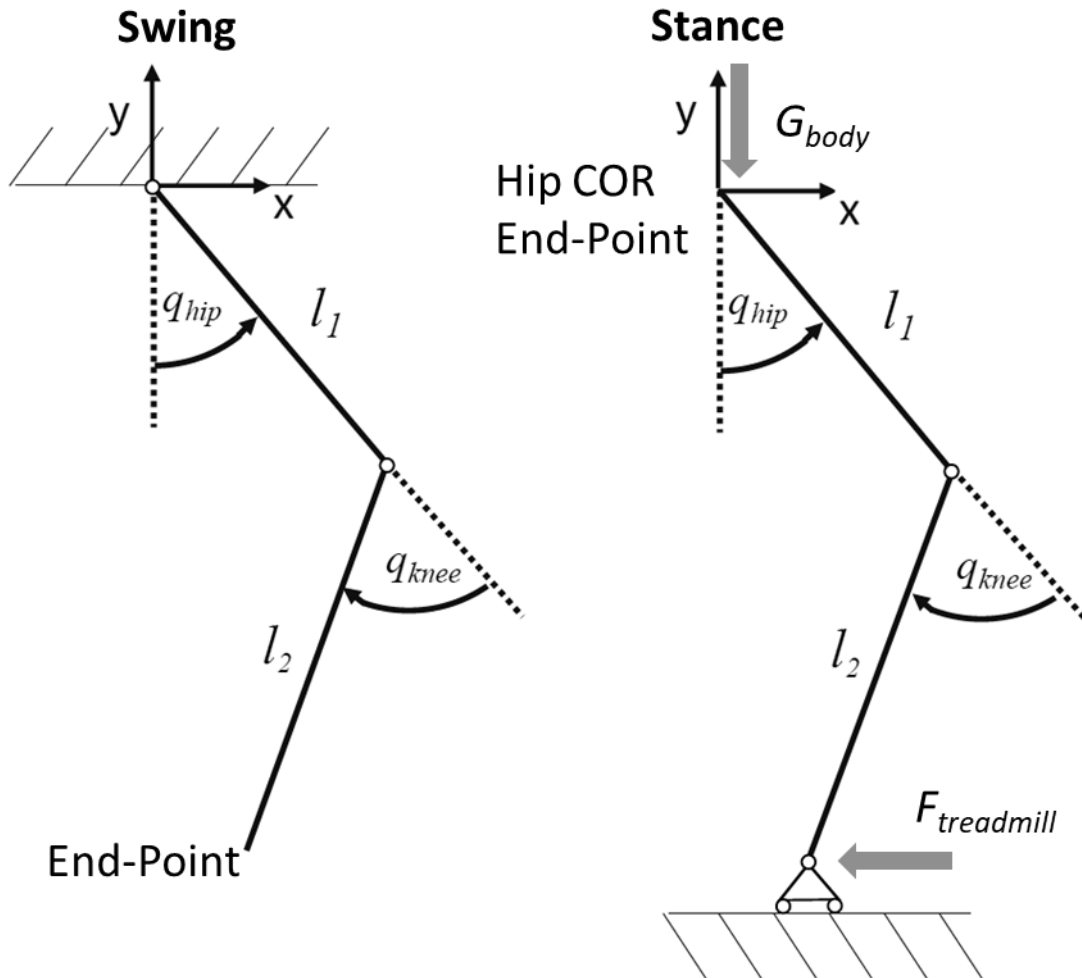
Figure 3.2: Comparison between the swing (left) and stance (right) models. During the swing phase, the ankle constitutes the end-point of the kinematic chain. During the stance phase, the end-point is the hip CoR. The force generated by the treadmill acts at the foot, whose position is constrained in the vertical direction by the treadmill. Note that the sign of the knee angle follows the anatomical convention.

For a two-link exoskeleton robot, the joint reference trajectory can be expressed as $\mathbf{q}_{ref} = [q_{hip}, q_{knee}]$, while $\mathbf{q}_{act}$ refers to the measured angles while the subject is walking. The torques $\boldsymbol{\tau}_{imp}$ to control the robotic actuators are provided by a motion controller with stiffness $\mathbf{K}_q = [K_{hip}\ 0; 0\ K_{knee}]$ and damping $\mathbf{B}_q = [B_{hip}\ 0; 0\ B_{knee}]$:

$$\boldsymbol{\tau}_{imp} = \mathbf{K}_q \cdot (\mathbf{q}_{ref} - \mathbf{q}_{act}) + \mathbf{B}_q \cdot (\dot{\mathbf{q}}_{ref} - \dot{\mathbf{q}}_{act}) \tag{3.1}$$

A control diagram is shown in Figure 3.3, where the dark elements correspond to the state-of-the-art Lokomat controller and the red elements highlight the contribution of the present work. Generally, in addition to the control torques $\boldsymbol{\tau}_{imp}$, robotic exoskeletons have a separate component $\boldsymbol{\tau}_{comp}$, which compensates the inherent robot dynamics such as gravity, friction or inertia (e.g. [283, 284]). A proportional torque controller with feedforward of the desired torque $\boldsymbol{\tau}_{des}$ is used to minimize the error $\boldsymbol{\tau}_{des} - \boldsymbol{\tau}_{int}$ [284]. The gain of this torque controller is inversely proportional to the impedance.

Joint reference trajectories $\mathbf{q}_{ref}$ can be taken from literature, e.g. [28, 29, 285], or from recordings of able-bodied subjects walking "freely" (i.e. in "transparent mode", where only $\boldsymbol{\tau}_{comp}$, but not $\boldsymbol{\tau}_{imp}$, is applied) in the same device to be controlled [55]. One challenge in joint space formulation comes with the high inter-subject variability in angular patterns, which makes it difficult to define joint reference trajectories that fit all subjects. In some exoskeletons, $\mathbf{q}_{ref}$ can be changed manually by the user within some limits [124, 286]. However, it is difficult to predict whether the subject will have adequate foot clearance and step length, since these also depend on the length of the thigh and shank segments.

3.3 ASSIST-AS-NEEDED CONCEPT

"Assist-As-Needed" (AAN) refers to a control strategy based on assisting the patient/user only as much as needed to successfully perform a predefined task [24]. One way to modulate the assistance provided by the robotic device is to modify the mechanical impedance rendered by the exoskeleton. A common AAN algorithm for an impedance controller typically updates a normalized impedance parameter P ($P \in \mathbb{R} | 0 \leq P \leq 1$), e.g. stiffness or damping, at every gait step s:

$$P_{s+1} = \gamma \cdot P_s + f(e_s) \cdot g \tag{3.2}$$

A forgetting factor, γ ($\gamma \in \mathbb{R} | 0 < \gamma \leq 1$), limits the excessive reliance on the robotic assistance provided by the motion controller (the "slacking" effect [287]). A gain g ($g \in \mathbb{R} | g > 0$) adjusts the control parameter according to an error function $f(e_s)$, f ($f: e_s \rightarrow [0,1]$), where e_s can be, for example, the kinematic deviation between the reference and actual trajectory of an exoskeleton. The function f may account for physiological kinematic variability (e.g. by defining a "deadband" around the reference trajectory [288, 289]). Note that domain of the parameters P, γ and $f(e_s)$ can be different, depending on the behavior one would like to achieve with the AAN algorithm [287], however, for the examples discussed further in this chapter we have selected the ones above.

3.3.1 Assist-as-Needed Controllers - State of the Art

There are several examples of controllers that adapt the robotic joint impedance of an exoskeleton to the subject's ability to walk - for review see: [287, 290, 291]. For example, to create a patient-cooperative strategy for the Lokomat, hip and knee impedances were adapted according to the patient's effort (as estimated by the robot force sensors) [284]. Based on a similar estimation of the subject's active contribution, Hussain adapted the joint impedance of a pneumatic-actuated exoskeleton robot [292]. However, both applications were based on forces exerted by a limited group of able-bodied subjects, which could heavily compromise their applicability in patients exhibiting clonus or spasticity. In the Lokomat, this dependence on the interaction forces was overcome by implementing an approach called "Path Control", which allows freedom of movement around predefined joint trajectories, while a virtual tunnel of adjustable width guarantees safety [273].

Other controllers adapted the end-point impedance instead of the joint impedance. In this type of controller, the parameters P adapted based on Eq. 3.2 are the end-point stiffness and damping ($\mathbf{K}_x$ and $\mathbf{B}_x$). In literature, there are several examples of end-point impedance adaptation implemented in exoskeleton and end-effector devices. Among the latter, Emken et al. adapted the end-point impedance of a robot guiding the ankle of the subject (ARTHuR) based on the position and velocity error between the reference and actual ankle trajectories [272]. Hussein et al. implemented an algorithm for adapting the width of a deadband for velocity deviations in the footplate-based Gait Trainer GT-I (Reha-Stim, Germany): based on the error between actual and desired end-effector velocity; the deadband width was either increased to allow more freedom or decreased to provide more guidance to the subject [293]. Other works instead, despite using exoskeleton devices, developed an algorithm that adapted the end-effector impedance or force field and calculated the required joint torques based on end-point information. For example, Koopman et al. developed an adaptive vertical force acting on the ankle to support foot clearance (LOPES, [22]); Banala et al. designed a force field acting on the ankle to guide the end-point along a virtual tunnel (ALEX, [289]).

3.4 Assist-as-Needed Controller in the Lokomat

In this project, we developed an AAN algorithm that automatically adapts the Lokomat actuators' impedance based on the ability of the subject to follow a reference gait trajectory. A second control loop acting in parallel adapts the BWS to the ability of the subjects to support their body weight in stance.

3.4.1 Joint Impedance Adaptation

The algorithm described by Eq. 3.2 was applied for the adaptation of the hip and knee impedance. The control parameters **P** were the stiffness **K** and the damping **B** of the hip and knee in the impedance joint controller. The gait cycle was divided in 30 windows. For each window w and for each step s the joint impedance was defined by one set of parameters, $\mathbf{K}_{s,w}$ and $\mathbf{B}_{s,w}$, which was adapted according to the weighted kinematic error performed in each window and every step.

$$K_{s+1,w} = \gamma_1 \cdot K_{s,w} + g_1 \cdot f_1(e_s)_w \tag{3.3}$$

$$B_{s+1,w} = \gamma_2 \cdot B_{s,w} + g_2 \cdot f_2(\dot{e}_s)_w \tag{3.4}$$

A set of gains $\gamma_1, \gamma_2, g_1, g_2$ were defined in order to have the impedance decrease slowly in the presence of physiological deviations and to react fast enough in case of large errors (Table 3.1).
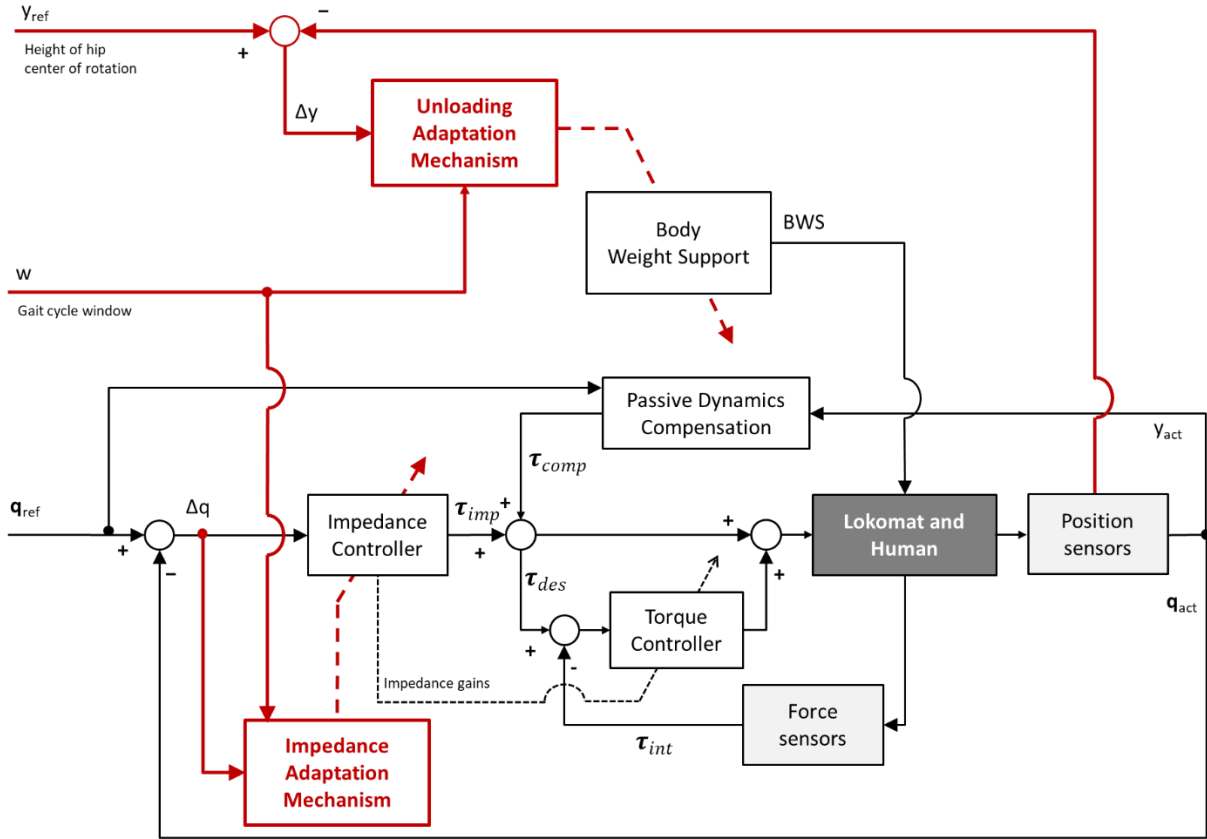
Figure 3.3: Structure of the Lokomat controller. The standard Lokomat control (black) [284] has been modified by including the impedance and unloading adaptation blocks (red). The impedance of hip and knee joints is adapted based on the error between reference (qref) and actual trajectory (qact). The unloading adaptation is based on the difference between actual (yact) and reference (yref) height of the hip center of rotation. Passive dynamics compensation is achieved through the Generalized Elasticities method [283]. © 2015 IEEE. Reprinted, with permission, from the original article [277].

In the commercial Lokomat software, **K** and **B** are always coupled to ensure that the system is overdamped [273]. In our application, we used these values as lower limits for the damping **B**, at every frame i:

$$B_{Hip}(i) = 2 \cdot \sqrt{K_{Hip}(i)} \tag{3.5}$$

$$B_{Knee}(i) = 1.5 \cdot \sqrt{K_{Knee}(i)} \tag{3.6}$$

PARAMETERS OF THE AAN CONTROLLER

Parameter	Value	Unit
$K_{Hip,1}$	1200	Nm/rad
$K_{Knee,1}$	900	Nm/rad
$B_{Hip,1}$	55.42	Nms/rad
$B_{Knee,1}$	36	Nms/rad
BWS_1	$0.7 \cdot BW$	kg
γ_1	0.9	-
γ_2	0.9	-
γ_3	0.95	-
g_1	0.1	Nm/rad
g_2	0.1	Nms/rad
g_3	20	m^{-1}
A	0.6	-
p_1	0.005	$rad^4 / N^4 m^4$
p_2	0.0005	-

Table 3.1: Parameters used in the adaptive controller equation. $K_{Hip,1}, K_{Knee,1}, B_{Hip,1}, B_{Knee,1}, BWS_1$: initial values of impedance and BWS; BW: Body Weight; $\gamma_1, \gamma_2, \gamma_3$: forgetting factors. g_1, g_2, g_3: error gains. A: steepness of the tanh function. p_1, p_2: parameters for the BWS error threshold calculation.

The estimation of the subject's performance relied on the kinematic deviation between the actual trajectory and the reference. However, individual trajectories can vary from the reference trajectory provided by the Lokomat, due to normal inter-subject variability [285, 294]. To cope with this problem, we implemented a mechanism to deal with physiological deviations that should not be considered as errors. Thresholds of maximum allowed deviations (lower th_{lo} and higher th_{hi}) are determined around the reference angular trajectory $q_{ref}(i)$ (Figure 3.4), where i refers to a sample (typically at 1kHz in the Lokomat). The error weighting function $f_1(\mathbf{e})_{s,w}$ consists of a hyperbolic tangent function of the kinematic error e_s defined for each window w (Eq. 3.8)[288]. The hyperbolic tangent function provides a smooth transition of the weighted error from 0 to 1 when $q_{act}(i)$ reaches the thresholds (Figure 3.5). The parameter A determines the slope of this transition. The gait phase specificity of the assessment is implemented by dividing the gait cycle in 30 windows w. In each window the error is calculated separately. The deviation from the reference trajectory $\mathbf{e}_i$ (Eq. 3.7) is used to calculate the mean deviation of the actual trajectory $q_{act}(i)$ in each window w and at each gait step s (Eq. 3.8). The function $f_1(\mathbf{e})_{s,w}$ is then retained as error metric for the adaptation algorithm.

$$\mathbf{e}_i = \left(q_{ref}(i) - q_{act}(i) \right) \tag{3.7}$$

$$f_1(\boldsymbol{e})_{s,w} = \frac{1}{l} \cdot \sum_{i \in w} \left(1 + \frac{1}{2} \cdot \left[tanh\big(A \cdot (\boldsymbol{e_i} - \boldsymbol{th_{hi}})\big) - tanh\big(A \cdot (\boldsymbol{e_i} + \boldsymbol{th_{lo}})\big) \right] \right) \qquad (3.8)$$

For each time point of the gait cycle, the subject's hip and knee are allowed to deviate from the reference trajectory within the deadbands defined for each joint, independently from each other. Suitable deadbands in joint-space can be defined based on normal ranges for hip and knee joint angles (e.g. taking normative data from [28, 29, 285] or from able-bodied people walking in the device). In our case, we defined deadbands ad-hoc to ensure safety in critical phases of the gait cycle (e.g. terminal swing for correct foot placement) and at the same time allow physiological variability.
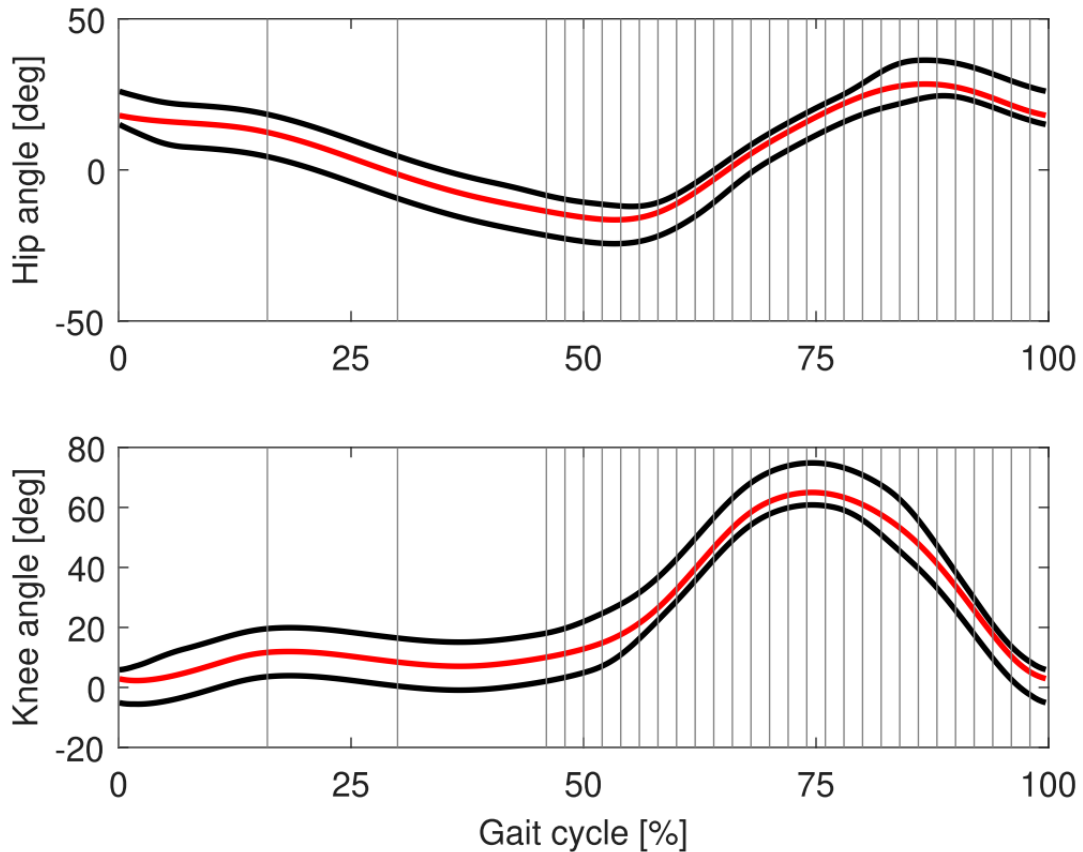
Figure 3.4: In the joint controller hip and knee deadbands are defined independently from each other, as shown in the panel A (hip angle) and B (knee angle). The reference trajectory (red) is taken from (Colombo 2000). The deadbands (black lines) are defined ad hoc to allow variability in non-critical phases of the gait cycle and ensure safety where the deviations need to be minimal. In the AAN algorithm, deviations occurring within the deadbands lead to a null error. The gait cycle is divided in 30 windows (grey lines show the windows' limits). Note that the deadbands tested in the first experimental evaluation were symmetric around the reference trajectory and equal to ± 8°.
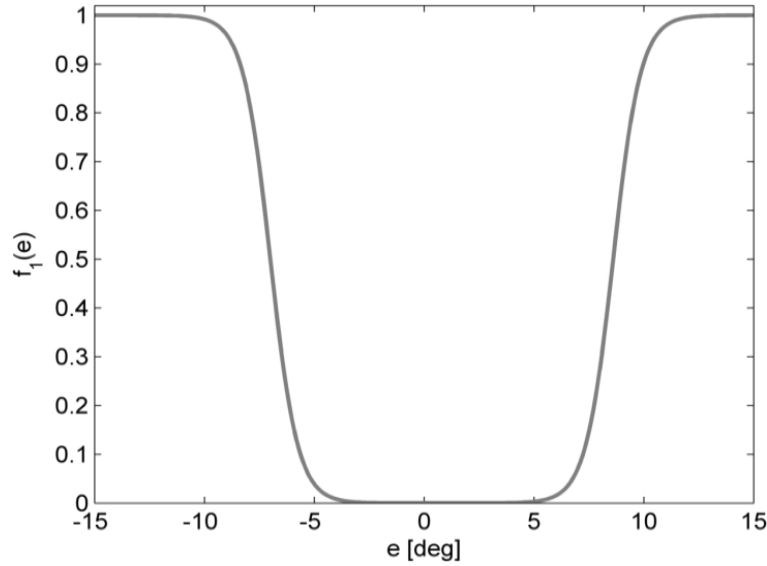
Figure 3.5: Asymmetric hyperbolic tangent function used to weight the kinematic error between actual and reference trajectory. © 2015 IEEE. Reprinted, with permission, from the original article [277].

The same approach is applied to deviations in velocity. The thresholds for lower and higher velocity error are symmetric with respect to 0. According to Eqs. 3.3 and 3.4, the impedance (stiffness **K** and damping **B**) of the joints of the device are updated for each window on each step based respectively on the position or velocity error during the previous step. The two parameters **K** and **B** are independently adapted in each window. This approach allows the support to be shaped according to the needs of the subject in different parts of the gait cycle (i.e. a selective support of the swing phase is possible) and thus the assessment of impairments occurring at particular points of the gait cycle should be possible.

3.4.2 Body Weight Support adaptation

The unloading of the body weight is adapted with a similar algorithm (Eq. 3.11). In this case the error metric is based on the difference Δy between the actual and the reference heights of the hip center of rotation(CoR) during left and right single stance, similar to the approach presented in [278]. The height of the hip CoR is estimated from the joint angles and the subject's segment lengths (Eq. 3.9). The rationale behind the choice of this metric is that the actual center of rotation of the hip will be lower than the reference height if the subject is not able to fully support his/her body weight during the stance phase.

$$y_{ref} = l_1 \cdot cos(q_{hip,ref}) + l_2 \cdot cos(q_{knee,\ ref} - q_{hip,ref}) \tag{3.9}$$

$$\Delta y_l = y_{ref,l} - y_{act,l} \tag{3.10}$$

$$BWS_{s+1,l} = \gamma_3 \cdot BWS_{s,l} + g_3 \cdot f_3(\Delta y_l); \quad l \in \{left, right\} \tag{3.11}$$

$$f_3(\Delta y_l) = \begin{cases} (\Delta y_l - th_{BWS}) \cdot BW & if\ \Delta y_l \geq th_{BWS} \\ 0 & if\ \Delta y_l < th_{BWS} \end{cases} \tag{3.12}$$

$$th_{BWS} = (l_1 + l_2) \cdot (p_1 \cdot (1 - \overline{K})^4 + p_2) \tag{3.13}$$

A threshold th_{BWS} is determined taking into account the segment lengths and the mean stiffness K on the leg l (Eq. 3.13). The threshold is higher for longer legs and lower stiffness values, since we expect higher displacements of the hip CoR in these conditions. If Δy_l is higher than the threshold, the error is multiplied by the body weight BW of the patient, to ensure an increase in BWS proportional to the patient's body weight.

3.5 FIRST EXPERIMENTAL EVALUATION

In these first tests, we checked the safety and feasibility of the adaptive controller in able-bodied subjects. We tested the appropriateness of the set of parameters of Table 3.1 and of the visual feedback provided to the subjects. We also gathered useful information on the experimental conditions in view of the tests with patients that will be performed later. We also wanted to gain insights into the repeatability of the measurements in unimpaired subjects and to determine how it could be improved. Moreover, the effects of different speeds on the assessment procedure were evaluated to test if speed can be considered a confounding factor.

3.5.1 Experiment

Eight able-bodied subjects (five males, age 35± 8 years, height 174±15 cm, weight 73±18 kg) participated in the experiment.

The protocol consisted of three conditions: fully supported walking (FULL), impedance adaptation enabled (IMP), impedance + body weight support adaptation enabled (IMP+BWS). The conditions were performed at two different speeds (Table 3.2). The adaptation of the four Lokomat joints was active simultaneously in the second and third conditions.

EXPERIMENTAL CONDITIONS

Speed \ Steps	30	60	20	60	20	60
1.8 km/h	FULL	IMP	FULL	IMP+BWS1	FULL	IMP+BWS2
2.3 km/h	FULL	IMP	FULL	IMP+BWS1	FULL	IMP+BWS2

Table 3.2: Experimental conditions. FULL: fully supported walking (100% impedance and 70% BWS), IMP: impedance adaptation enabled, IMP+BWS: impedance and BWS adaptation enabled.

The condition IMP+BWS was tested twice (IMP+BWS1 and IMP+BWS2). At each speed the subjects performed 30 steps of familiarization, followed by 60 steps in each one of the conditions. Between each trial the subjects walked with the normal Lokomat controller for 20 steps (FULL). At the beginning of each adaptive condition the impedance was set to the maximum value and it adapted to the performance of the subject from step to step. When enabled, the unloading was set initially to 70% of the body weight. The thresholds around the reference trajectory th_{lo} and th_{hi} were set symmetrically

around the reference and constant throughout the gait cycle ($\pm 8°$). During the experiment the assistive torques and the BWS provided by the Lokomat were recorded. The subjects were presented with a visual feedback on a screen positioned in front of them (Figure 3.6). They were instructed to follow the movements of a walking avatar while trying to remain inside two shaded rectangles around the thigh and the shank that indicate the reference position.

Figure 3.6: Visual feedback and instructions provided to the subjects. © 2015 IEEE. Reprinted, with permission, from the original article [277].

3.5.2 Data Analysis

The quadratic mean (RMS) value of the assistive torques over the whole gait cycle (m = sample within one gait step) was summed over the 4 joints *j*, averaged over the last 10 steps *s* of each condition presented in Table 3.2 and retained for the analysis as an index of the final level of assistance provided by the controller (Eq. 3.14).

$$T_{assist} = \frac{1}{10} \cdot \left(\sum_{s=51}^{60} \sum_{j=1}^{4} \underset{m}{RMS}\left(T_{PDm,j,s}\right) \right) \tag{3.14}$$

In the same way the *RMS* values of the parameters **K** and **B** (averaged over the 4 joints) within each step were computed in order to study their convergence. In the IMP+BWS condition the unloading *BWS* over the last 10 steps was normalized to the body weight *BW*, averaged and retained to study the final level of unloading required to the device, BWS_{avg} (Eq. 3.15).

$$BWS_{avg} = \frac{1}{10} \cdot \left(\sum_{s=51}^{60} \underset{m}{RMS}\left(\frac{BWS_{m,s}}{BW}\right) \right) \tag{3.15}$$

Kinematic data were recorded through the potentiometers embedded in the hip and knee joints of the Lokomat. The angular variability was computed for each subject as the average standard deviation of the hip and knee angles among the last 10 steps of each condition (Eq. 3.16). The error with respect to

the reference trajectory was calculated as the RMS difference between the actual trajectory of the subject and the reference (Eq. 3.17).

$$q_{var} = \frac{1}{4} \cdot \sum_{j=1}^{4} \frac{1}{M} \cdot \sum_{m=1}^{M} STD_s\left(q_{act\ m,j,s}\right) \tag{3.16}$$

$$q_{err} = \frac{1}{10} \cdot \sum_{s=51}^{60} \frac{1}{4} \cdot \sum_{j=1}^{4} RMS_m\left(q_{ref\ m,j,s} - q_{act\ m,j,s}\right) \tag{3.17}$$

3.5.3   Statistical Analysis

All the statistics was performed in Matlab (MathWorks Inc., US, version 2013b). Since the adaptation algorithm has been developed mainly for assessment purposes, it is necessary to study the reliability of the measurements in different trials [295]. The final values of the assistive torques and of the unloading of the two trials in the same condition were compared using the non-parametric Wilcoxon Signed Rank test and then examined using Bland-Altman plots [92]. The effect of speed was assessed comparing the assistive torques and the unloading between the two speeds using a Wilcoxon Signed Rank test. The angular deviations were compared using the Wilcoxon Signed Rank test. In all the tests the significance level was set at 5%.

3.5.4   Results

The adaptive algorithm shaped the **K** and **B** parameters of the controller based on the position and velocity error between the reference trajectory imposed by the Lokomat and the actual trajectory performed by the subject. The combined stiffness **K** of hip and knee reached values lower than 10% of the initial value after 30 steps in all subjects at 1.8 km/h and below 12% during the trials at 2.3 km/h. The combined damping **B** of hip and knee decreased below 27% of the initial value after 40 steps for all subjects at 1.8 km/h, but only below 35% in the trials at 2.3 km/h (Figure 3.7, right). The assistive torques reached on average 27% of the initial value in the FULL condition when the speed was set at 1.8 km/h. When walking at 2.3 km/h, the final value of the assistive torques decreased on average until the 35% of the initial value (Figure 3.7, left). The two conditions IMP and IMP+BWS did not converge to significantly different assistive torques during the final 10 steps. The BWS decreased on average to the 32% of the body weight at 1.8 km/h and to 27% at 2.3 km/h. The values of all the outcome measures measured at 50 steps after the start of the adaptation were not significantly different from the values measured at 60 steps.

The assistive torques and the unloading were not different between trials for both speeds and both conditions (IMP and IMP+BWS).
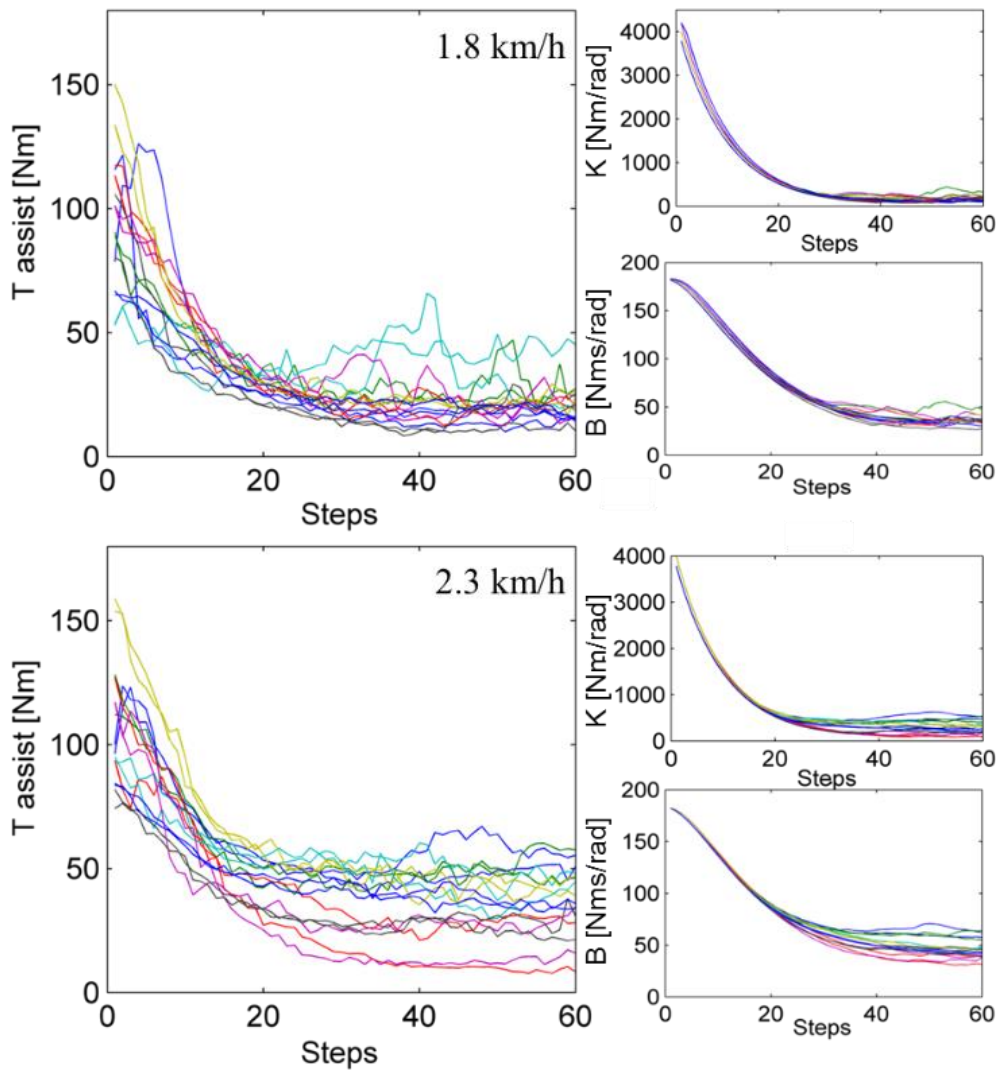
Figure 3.7: The assistive torques T_assist (left column) and the impedance (stiffness K and damping B) (right) decrease after the adaptation algorithm has been enabled. The figure shows the values obtained from the 8 subjects in the two trials that they performed at 1.8 km/h (upper panel) and at 2.3 km/h (lower panel). Data from the same subject are displayed in the same color. © 2015 IEEE. Reprinted, with permission, from the original article [277].

The Bland-Altman plots showed that although the systematic bias was not significant, the random errors lead to limits of agreement of 29.2 Nm and 43.5% (T_{assist} and BWS_{avg} at 1.8 km/h) and of 45 Nm and 10.5% (2.3 km/h) (Figure 3.9).

The kinematic variability and error increased with the reduction of the impedance of the controller (Figure 3.8). The measures q_{var} and q_{err} in the IMP and IMP+BWS conditions were significantly higher than in the last 10 steps of the FULL condition.
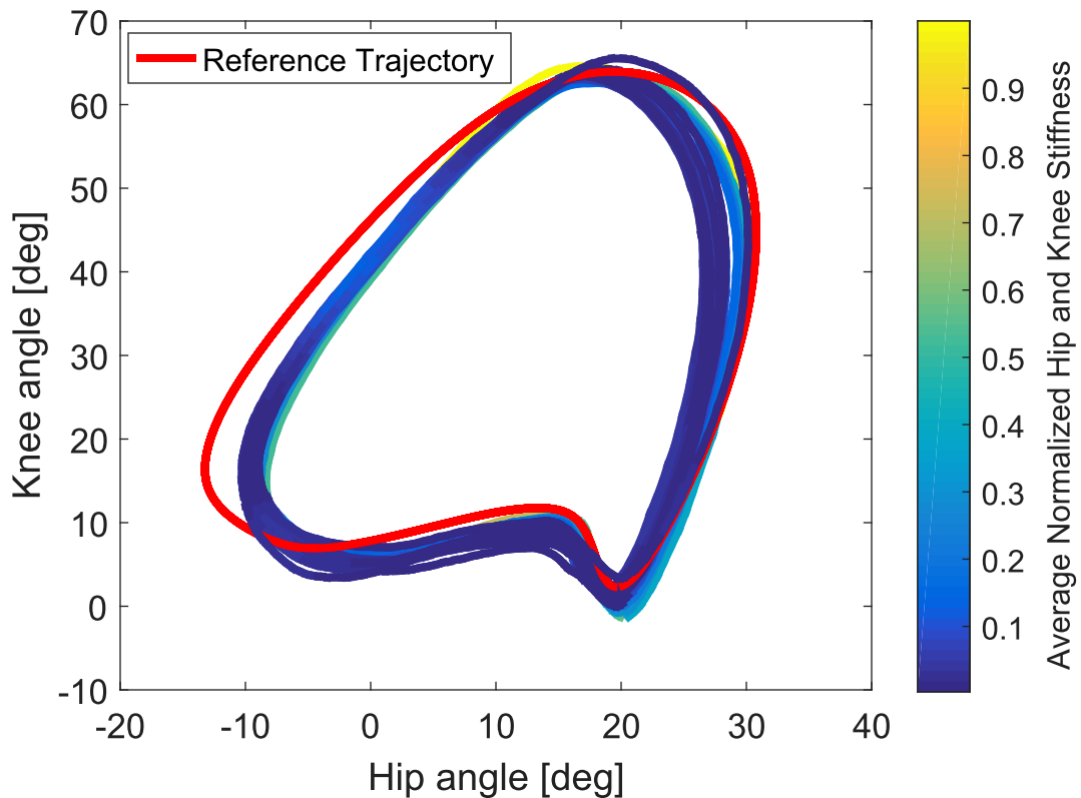
Figure 3.8: Trajectories in joint space of a subject walking in the IMP+BWS condition. The color is proportional to the normalized stiffness averaged over hip and knee. For clarity of representation, one step every three was plotted in this figure. The red line represents the reference Lokomat trajectory.

Concerning the effect of speed on the outcome measures, the results showed that the average T_{assist} over the last 10 steps during both adaptive conditions (IMP and IMP+BWS) was significantly higher at higher speed (p<0.0001 and p=0.0026). The final unloading was not significantly affected.

All the subjects well tolerated the test. 7 subjects out of 8 reported that the algorithm was smooth and comfortable, while one perceived that the effort required for walking increased consistently at low values of impedance.
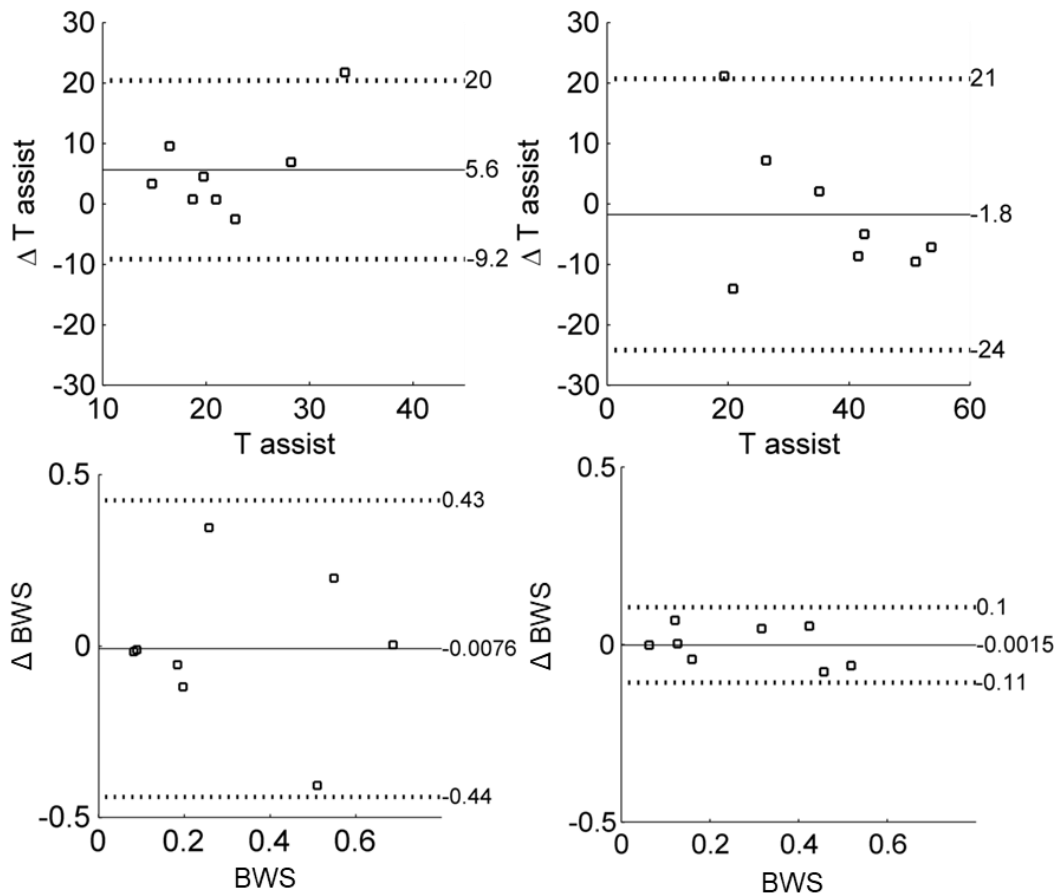
Figure 3.9: In the Bland-Altman plots the differences between the outcome measures (T_{assist} and normalized BWS) in the 2 trials are plotted against each individual's mean for the 2 tests. The results of the condition IMP+UN are presented: at 1.8 km/h on the left column and at 2.3 km/h on the right column. The bias line and random error lines forming the 95% limits of agreement are also presented on the plot. © 2015 IEEE. Reprinted, with permission, from the original article [277].

3.6 DISCUSSION

In this chapter we defined and implemented an algorithm for the assessment of walking function based on the automatic adaptation of the hip and knee impedance and the BWS in the Lokomat. In the preliminary study we tested the feasibility and repeatability of the algorithm. The results showed that the method is feasible, and it is able to reduce the robotic support during walking while following a reference trajectory. Since the participants were unimpaired, a low value of the final support was expected. The level of support dropped significantly for all subjects. The final amount of assistive torques did not reach the minimum value probably because the reference joint angular trajectories provided by the Lokomat controller were not tailored to the individual's gait pattern. The subjects were requested to follow a trajectory that was not their own and this led to kinematic errors that were captured by the assessment algorithm. These effects were minimized by adding a region around the reference trajectory where the deviations were allowed. Another reason could lie in the type of visual feedback, which showed two different moving areas around the thigh and shank segment to be followed at the same time. This may be too demanding even for unimpaired subjects. Moreover, only one leg could be shown, while the algorithm is adapting the impedance of both legs at the same time. The algorithm allowed enough freedom to the subjects to impose their own gait pattern while walking in the Lokomat

with reduced impedance, as shown by the significantly higher kinematic variability and error with respect to the non-adaptive, high-impedance controller (Figure 3.8). This indicates that physiological deviations from the angular reference trajectory were allowed by the algorithm. Shaping the reference trajectory based on anthropometric parameters (e.g. height) and on the walking speed [22] would further reduce the influence of physiological intra- and inter-subject variability.

The BWS decreased consistently, as we expected. The fact that it did not reach the minimum value (set at 5 kg) in most of the subjects could be ascribed to the error metric used for the unloading adaptation mechanism, which computes the height of the hip center of rotation from the joint angles measured by the potentiometers integrated in the orthoses. Misalignments and relative movements between the subject's and the Lokomat joints can compromise the accuracy of this measure.

The outcome measures assessed in the two trials did not show any significant systematic bias. Although the limits of agreement show the presence of a rather high random error, we expect that the values of support required by subjects with walking impairments will lie in a range significantly higher than the one showed by unimpaired subjects. We believe, thus, that it will be possible to discriminate between subjects with low and high levels of walking function. Nonetheless, we think that it is necessary to reduce the amplitude of the random error in order to provide a sensitive assessment tool that can be used to assess intra-individual differences and monitor the progression of the walking recovery of the individual patient. We propose some ways to address this problem: first, the visual display of the reference trajectory should be adapted. We hypothesize that the display of a reference foot trajectory will improve the ability of the subject to track the reference trajectory. Secondly, the adaptation should occur at one leg at a time, so that the subject can concentrate only on the leg under test. Thirdly, looking at the stiffness and damping may lead to better results, since these values are less affected by instantaneous position and velocity errors than the assistive torques are. Lastly, a longer familiarization phase should be granted to the subjects before the measurements.

Before this assessment method can be applied to clinical practice, a proper inter- and intra-rater reliability study is required and every attempt of standardizing the task execution should be made. Experiments with subjects with gait disabilities are needed to test whether the algorithm will be able to discriminate between different levels of gait impairment and to determine its validity and sensitivity.

Speed was proven to be a confounding factor for this type of assessment method. We noticed that at higher speed the assistive torques were significantly higher and so was the inter-subject variability. To address this issue, a fixed value of speed will be chosen for future experiments and results will be only compared within the same speed.

Since the assistive torques did not differ between conditions IMP and IMP+BWS, we conclude that the latter condition is more suitable for further testing of the assessment algorithm. The adaptation of the BWS not only guarantees a safer training (an increased support can act when the impedance does

not provide enough assistance during stance), but it can also provide an important measure related to weight bearing ability. Given that impedance and BWS values do not differ between 50 and 60 steps after the start of the adaptation, we will in the future reduce the adaptive task to 50 steps, to avoid fatigue and shorten the length of the test protocol.

The outcome measures of this novel walking assessment methods will be *i)* the residual stiffness and damping after adaptation and *ii)* the amount of BWS after adaptation. The hypothesis is that these parameters converge to a value individual for each subject that is representative of the support needed (and indirectly of the level of impairment).

We highlight that the proposed algorithm could allow the detection of impairments localized at particular points of the gait cycle. After considering the possibilities and constraints that the Lokomat imposes and the behavior of the AAN software previously described, we narrowed down the list of measurable requirements for functional walking to: support of body weight, clearance in swing, smooth transitions, adequate step length and propulsion (Table 3.3). We hypothesized that these functions could be observed in the Lokomat when the support is reduced with the AAN algorithm. This hypothesis will be tested in 0, by simulating impairments on a robotic test bench, and in Chapter 5, by testing the AAN-based assessment in subjects with Spinal Cord Injury.

REQUIREMENTS FOR FUNCTIONAL WALKING MEASURABLE IN THE LOKOMAT

Requirements for Walking		Proposed AAN-based Outcome Measures
Support of body weight		Residual BWS
Control of foot trajectory	Clearance in swing	Residual joint impedance in swing
	Smooth transitions	Residual joint impedance at push-off (2nd double support) and foot contact (terminal swing)
Adequate step length		End-point position error at foot contact
Propulsion		Residual joint impedance at 2nd double support and in swing phase

Table 3.3: Requirements for functional walking which could be measured in the Lokomat with the AAN-based assessment and proposals for outcome measures.

3.7 CONCLUSION

Based on the literature review of Chapter 2 and on the state of the art of the controllers used in rehabilitation robotics, we implemented an assist-as-needed controller in a treadmill-based exoskeleton, the Lokomat, to assess walking function during training. As hypothesized, the impedance of the joints and the BWS decreased step by step until reaching a convergence value. The random error affecting the measurements needs to be reduced for further applications, by undertaking some changes to the protocol:

only one leg will be tested at a time, the clarity of the visual feedback will be increased, the residual stiffness and damping in the separate gait phases will be used instead of the torques as outcome measures, a longer familiarization time will be granted. We confirmed that speed affects the outcome measures but adapting simultaneously joint impedance and BWS does not affect the value of the residual joint torques. The proposed changes will be implemented in the next studies presented in Chapter 4 and 5.

Chapter 4 TECHNICAL VALIDATION

The content of this chapter is partly extracted from the following publication and it was adapted to ensure consistency within the chapter and with the rest of the document and to avoid repetitions:

Foreword

When developing a novel controller for gait trainer devices, it is critical to test it in patients. Tests in able-bodied subjects can only partially address questions related to safety but they cannot provide a realistic simulation of the patients' impairments. To collect preliminary, reliable information on the validity of our approach in a controlled condition, we developed a robotic test bench to simulate a human-like behavior with superimposed impairment. We tested whether the AAN controller previously developed could assess correctly the characteristics of the simulated human leg.

4.1 INTRODUCTION

Robot assisted rehabilitation is a field in expansion. Based on the shortcomings and areas of improvement identified in the first generation of robotic devices, new solutions have been proposed and will likely be proposed in the near future [82, 291]. Moreover, current research aims at employing robotic devices not only in therapy, but also for providing reliable and sensitive assessment of function, activity and impairment [77, 82, 296].

Every time a new algorithm is developed, the challenge is, first, to guarantee stability and safety in human applications, and second, to determine whether it does what it claims to do (e.g. construct validity in the case of an assessment algorithm). Performing preliminary validation experiments with human subjects poses several issues: *i)* for ethical reasons, the experiments cannot be too long and physically demanding, *ii)* humans are inherently variable and they are affected by fatigue or other factors that are unpredictable or uncontrollable, *iii)* humans are widely heterogeneous, *iv)* experiments with patients require even more caution since the risk of adverse events is higher than in unimpaired individuals, *v)* it is difficult and time-demanding to find large cohort of patients with a certain impairment. In the case of robot-assisted assessments, it is crucial to validate the method against a gold-standard (concurrent validity). It is often the case, however, that no valid alternative measures exist. Furthermore, test-retest reliability studies require that the tests are performed under the same conditions. Lastly, confounding factors that could affect the outcome measures should be isolated and their effects studied and eliminated when possible.

An approach to address the issues encountered in the testing of algorithms for rehabilitation devices consists in robotic testing. Haptic devices, rendering biomechanical properties of human motion, can serve as platforms for testing algorithms in a systematic way. Robots can be used for simulating human-like conditions in a repeatable and controlled way, eliminating the inherent variability of the human behavior. The initial phases of the development process of a new device or software could be time- and cost-efficient, since no tests in humans would be required. Furthermore, hazardous conditions can be tested with a robot without hesitation. Lastly, other parameters can be readily available (e.g. joint torques of the simulated human limb).

In the last years robotic testing has been applied in a diversity of applications. For instance, Richter et al. [297] developed a 2 DOF robot to which a transfemoral prosthesis can be attached. The study was able to provide insight about the compensation that a patient would need to apply to reproduce normal gait while wearing that specific prosthesis. In [298], Melendez-Calderon and colleagues developed a haptic simulator of a human upper limb; such simulator allowed the authors to systematically investigate how therapists perceive different simulated impairments - something that is not possible if testing is done directly with human subjects or in computer simulations.

In this chapter, we propose a novel method for testing training and assessment algorithms for lower limb rehabilitation robots. Until now, development and testing of the devices have been based solely on experiments in humans, that, although necessary, present several problems, especially at early stages of development. The method described here exploits the mechanical structure of a robotic gait trainer to simulate a human leg affected by impairments typical of the neurological population. Such a test bench can be used for testing the effects of different algorithms. Although here we use the Lokomat, this method can be broadly applied on any other robotic device. The biomechanical model of a human leg is discussed and an approach to simulate healthy and impaired conditions is described. Preliminary results on the evaluation of the novel algorithm for the assessment of walking in a robotic gait trainer (RAGA) [277], discussed in Chapter 3, are presented.

4.2 METHODS

4.2.1 Robotic Setup

We took advantage of the structural configuration of the Lokomat to build a bio-inspired test bench for evaluating the behavior of new algorithms implemented in lower limb rehabilitation robots. In our proposed scenario, one robotic orthosis is controlled to behave as a human leg (we will refer to it as *simulated human leg*), while the second orthosis (the *test orthosis*) is controlled with the algorithm under test. The two orthoses are then rigidly connected using two aluminum bars, simulating a physical attachment of the robot to the user's leg without the confounding effects of compliant cuffs (Figure 4.1). In our case, we want to test the validity of the AAN-based assessment presented in Chapter 3. The test orthosis provides guidance to the simulated human leg and assesses its performances, like it would do when connected to a human leg. In this way, a known behavior (e.g. a typical pathological behavior) can be programmed in the simulated human leg and we can study whether the test orthosis correctly captures what was simulated. The great advantage of this approach is that we know with certainty the input provided to the system and we can study its effects on the outcome measures in a straightforward manner.
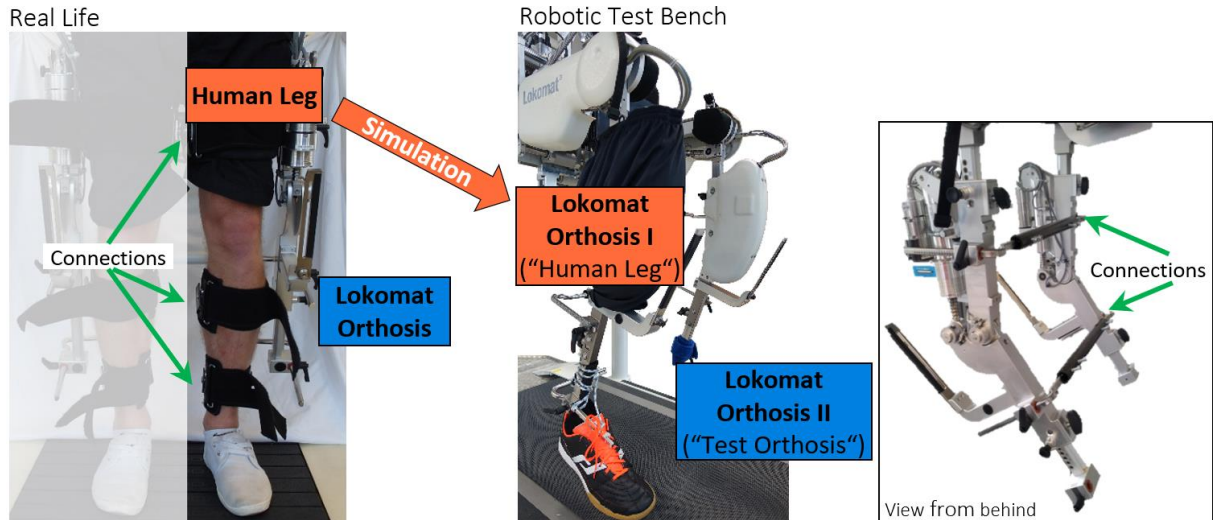
Figure 4.1: Hardware of the robotic test bench: the Lokomat Orthosis I simulates a human leg (orange). The Lokomat Orthosis II implements the algorithm under test (blue). The connections between the two Lokomat legs simulates the cuffs connecting the human leg to the Lokomat orthosis in real life.

4.2.2 Haptic Simulation of a Human Leg

Human motion can be modeled as a combination of feedback and feedforward control [299–301]. We took a simplified assumption that the central nervous system (CNS) controls the leg motion by sending feedforward commands and to compensate for its dynamics, the CNS (active) and musculoskeletal properties (intrinsic) produces a restoring force that can be modeled as feedback.

A Lokomat orthosis is constituted by two rigid segments that - to an extent - have similar dimensions, weight and inertia of a human leg modeled. The hip and knee joints are actuated by linear drives and they can be programmed. As a proof of concept, we took advantage of such structural characteristics and developed a bio-inspired controller that made a robotic orthosis generate a "human-like" motion. The Lokomat is normally controlled with a proportional-derivative (PD) controller [284], which is not adequate to reproduce the properties of a human limb. We added, therefore, a feed-forward (FF) component to simulate more realistically the normal and pathological human behavior. We designed a controller that considers the rigid body dynamics of a friction-compensated Lokomat orthosis (acting as a physical leg), with *i)* a feedback (FB) loop simulating spinal reflexes and muscle-tendon visco-elasticity properties and *ii)* a feedforward (FF) stage simulating motor commands from higher brain centers (Figure 4.2). The hip and knee torques acting the Lokomat orthosis are then:

$$\boldsymbol{\tau_{leg}} = \begin{bmatrix} \tau_{hip} \\ \tau_{knee} \end{bmatrix} = \boldsymbol{\tau_{FB}} + \boldsymbol{\tau_{FF}} \tag{4.1}$$

The torque generated by such FB and FF loops were tuned to generate a compliant "human-like" motion. In this proof of concept, we simulated a leg motion during swing; therefore, interaction forces and impact with the ground were not considered.

A) Controller structure of the bio-inspired robotic test bench

B) Controller structure of AAN-based assessment algorithm
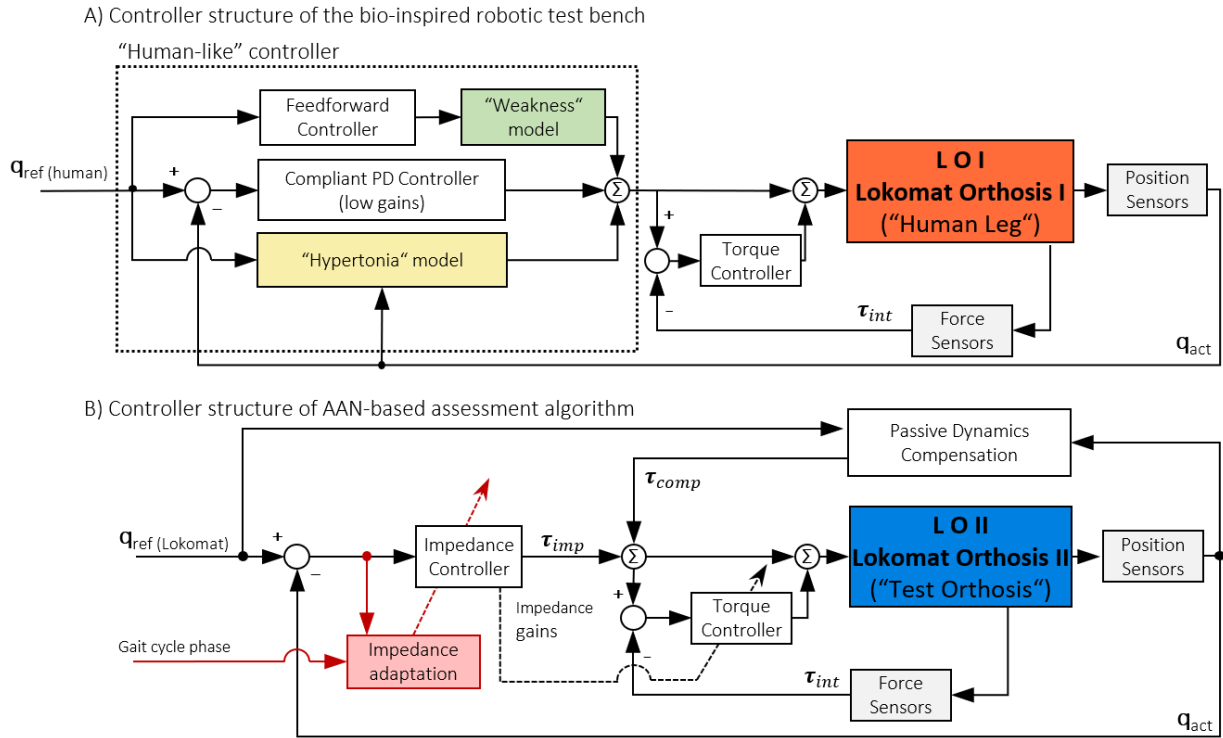
Figure 4.2: A) The Lokomat Orthosis I (LOI) is used to model a human-like behavior through a combination of FB and FF controllers. The FF controller includes gravity, inertia, Coriolis and friction compensation. Abnormal neuro-mechanics is added to the simulation. B) Control diagram of the AAN-based Assessment software, which is the software under test in this application example. More details on the AAN-based Assessment software can be found in Chapter 3. The two orthoses are mechanically connected via two rigid bars. © 2016 IEEE. Reprinted and modified, with permission, from the original article [302].

4.2.3 Feedback Controller

To our knowledge, there has been little research in estimating knee, and especially hip, impedance during walking. Pfeifer [303] reported knee active stiffness estimates during swing ranging from ~60 to ~200 Nm/rad assuming no co-contraction; intrinsic stiffness was estimated at 35 – 45 Nm/rad [304]. We implemented a compliant feedback PD controller (Eq. 3.1), with stiffness $\mathbf{K} = [K_{hip}, 0; 0, K_{knee}]$; $K_{hip} = 60$ Nm/rad, $K_{knee} = 45$ Nm/rad (B gains were tuned to guarantee stability of the system and damping $\mathbf{B} = [B_{hip}, 0; 0, B_{knee}]$; $B_{hip} = 15.5$ Nms/rad, $B_{knee} = 10.1$ Nms/rad).

The relatively low gains of this controller, and their similar magnitude to estimated values of stiffness in humans, ensure that external perturbations are handled in a compliant way, closely resembling human behavior. However, it is to be expected that, given low FB gains, the actual trajectory does not completely follow a predefined trajectory. The addition of a FF controller enables the *simulated human leg* to generate a "human-like" walking motion with low stiffness.

4.2.4 Feedforward Controller

A parametric FF controller requires knowledge of the plant to be controlled. To an extent, parameters like mass, center of mass, moment of inertia, etc. could be obtained from CAD models of the robotic device. However, such estimations are usually not perfect and other parameters such as friction are not accessible. Therefore, in order to tune the FF controller, so as to generate a "human-like" motion, we

used an adaptive feedforward controller (AFFC), as presented in [305]. With such approach, one can "teach" the *simulated human leg* how to follow a desired trajectory when connected to a (dynamic compensated) *test orthosis* – simulating walking with the robotic device (Figure 4.3).

To implement the AFFC, we first modeled the *simulated human leg* connected to a *test orthosis* as one double pendulum, assuming a rigid connection between the two orthoses (Figure 3.2, Swing phase model). The torques that the *simulated human leg* generates to move itself and the connected *test orthosis* are given by:

$$\boldsymbol{\tau_{leg}} = \boldsymbol{\tau_{FF}} + \boldsymbol{\tau_{FB}} = \boldsymbol{H(q)} \cdot \ddot{q} + \boldsymbol{C(q, \dot{q})} + \boldsymbol{G(q)} + \boldsymbol{F(\dot{q})} + \boldsymbol{\tau_{FB}} \tag{4.2}$$

where, $\boldsymbol{H(q)}$ corresponds to the inertia, $\boldsymbol{C(q, \dot{q})}$ to Coriolis and Centripetal forces, $\boldsymbol{G(q)}$ to the gravity and $\boldsymbol{F(\dot{q})}$ to friction. As the AFFC algorithm requires the model to be linear in the parameters to be identified, Eq. 4.2 was expressed as:

$$\boldsymbol{\tau_{leg}} = \boldsymbol{\tau_{FF}} + \boldsymbol{\tau_{FB}} = \boldsymbol{\Phi(q, \dot{q}, \ddot{q})} \cdot \lambda + \boldsymbol{\tau_{FB}}, \tag{4.3}$$

where the vector λ condenses all unknown parameters such as masses, centers of mass, moments of inertia, viscous and static friction, etc. and the matrix $\boldsymbol{\Phi}$ only depends on joint position, velocity and acceleration (see Appendix B for details on linearization). Such parameters, initially set to 0, are identified in real-time according to gradient descent of the tracking error function

$$E = \left(\boldsymbol{\tau_{leg}} - \boldsymbol{\Phi} \cdot \lambda\right)^{\boldsymbol{2}}, \tag{4.4}$$

from which the AFFC learning rule is derived [305]:

$$\lambda_{i+1} = \lambda_i + \boldsymbol{L} \cdot \boldsymbol{\Phi}\left(\boldsymbol{q_{ref}}, \dot{\boldsymbol{q}}_{\boldsymbol{ref}}, \ddot{\boldsymbol{q}}_{\boldsymbol{ref}}\right)^{\boldsymbol{T}} \cdot \boldsymbol{\tau_{FB}} \tag{4.5}$$

where *i* corresponds to the time step of the real-time controller (running at 1kHz); $\boldsymbol{L}$ to a learning factor matrix; $\boldsymbol{\tau}_{FB}$ to the feedback torque; and $\boldsymbol{q}_{ref}$ to the desired walking hip and knee trajectory to be achieved by the *simulated human leg*.
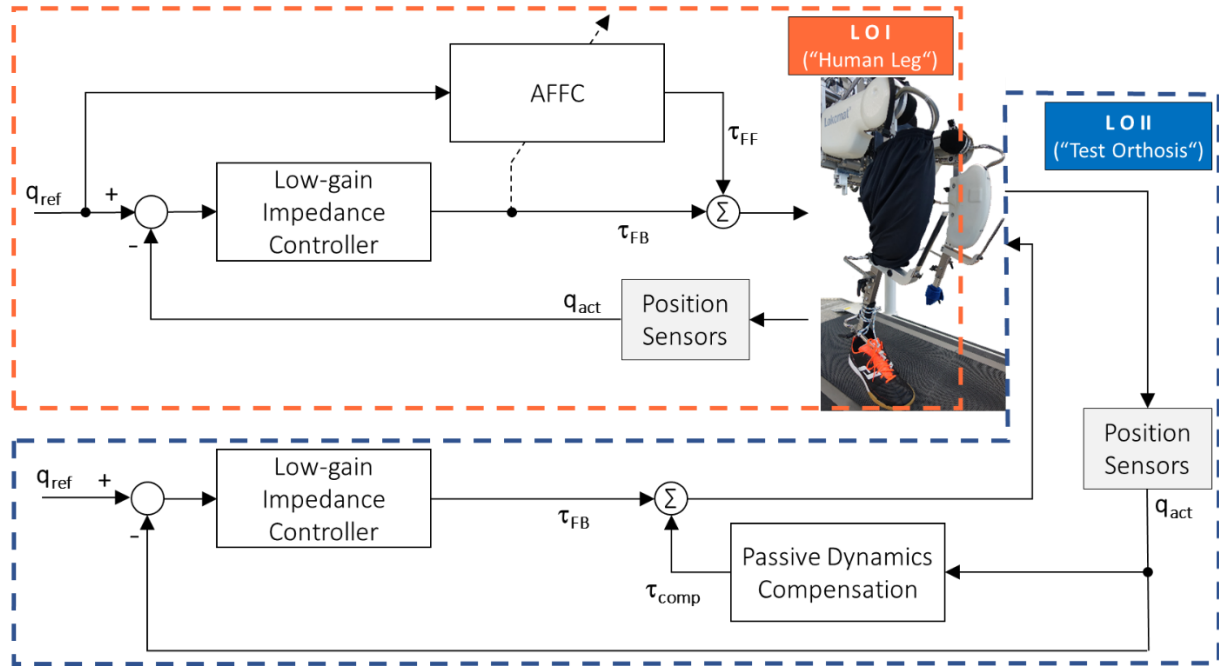
Figure 4.3: Control diagram of the robotic setup while the AFFC adapts the parameter vector λ. The simulated human leg "learns" to walk while connected to LO II, simulating a human leg walking attached to the Lokomat orthosis. LO II is controlled with an impedance controller with low gains, while its inertia, gravity and friction are compensated. The torque controller was omitted from diagram for the sake of simplicity, but it is active for both legs.

Here, we identified the parameters λ necessary to enable the *simulated human leg* to execute a walking pattern with FF and low FB torques at different speeds - 1.5, 1.8 and 2.3 km/h - by running the adaptation law three times (one per speed tested – some parameters in λ are speed-dependent). The algorithm adapted until *i)* the root mean square (RMS) of the tracking error, $q_{ref} - q$, within a walking step *s* (or gait cycle), e_s, was lower than or equal to 2.5° for both the hip and the knee joints (Eq. 4.6); and ii) the change in RMS of the tracking error between the last 50 steps and the current step was lower than 0.2° (Eq. 4.7). The first criterion ensures the tracking of the walking pattern within physiological variability, while the second criterion guarantees that the parameters are chosen after convergence. Once these criteria had been satisfied, the adaption was terminated and the last values of λ were chosen for the FF controller in the following experiments.

$$RMS(e_s) \leq 2.5°; \tag{4.6}$$

$$\|RMS(e_{s-50:s-1}) - RMS(e_s)\|_\infty < 0.2°. \tag{4.7}$$

4.2.5 Haptic Simulation of Abnormal Limb Neuro-Mechanics

4.2.5.1 *Weakness*

One of the most common impairments after a neurological injury is muscle weakness. Muscle weakness can be a consequence of disuse atrophy and disruption in descending neural pathways leading to inadequate recruitment of motoneuron pools [146, 151]. In this paper, we model weakness as an activation failure due to decreased inputs from cortico-spinal pathways [151]. Therefore, to simulate diminished efferent inputs (with preserved reflex pathways), we multiplied the FF torque commanding

the simulated human leg by a gain $W \leq 1$ that set the severity of the "simulated weakness" (Figure 4.2A) in a range between 0 and 100% of the maximum FF torque:

$$\boldsymbol{\tau_{FF,W}} = W \cdot \boldsymbol{\tau_{FF}}. \tag{4.8}$$

Note that different ways of modeling weakness are possible depending on the assumptions for the underlying cause of the impairment.

4.2.5.2 Spastic-Like Behavior

Another common impairment after neurological injury is increased muscle tone, that can be due to spasticity, rigidity or dystonia [268, 306]. In literature, spastic-like behaviors are usually modeled as velocity dependent torques, active when the joint angular velocity exceeds a certain threshold [307, 308] or velocity dependent stiffness [298]. Here, we modeled a "spastic-like" impairment active at the level of the knee joint by adding a torque τ_h to the torques controlling the simulated human leg (Figure 4.2A). τ_h is generated by a velocity-dependent stiffness $K_h(\dot{q})$:

$$K_h(\dot{q}) = 0.5 \cdot K_{max}\big(1 + tanh\big(b \cdot (\dot{q} - \dot{q}_{th})\big)\big) \tag{4.9}$$

$$\tau_h = S \cdot K_h(\dot{q}) \cdot (q_{rest} - q) \tag{4.10}$$

K_h is negligible as long as the velocity is lower than a certain threshold $\dot{q}_{th}$. b defines the width of the transition phase of the velocity threshold. τ_h forces the knee joint to a resting angle q_{rest}, corresponding to an almost fully extended knee. A gain S was used to simulate different severities of the hypertonic impairment. The parameters were fine-tuned with the help of an experienced physical therapist in order to achieve a faithful haptic simulation of a spastic-like behavior of the knee joint.

4.2.6 Test of AAN-Based Assessment Using the Robotic Test Bench

We applied this method for testing the AAN-based Assessment– described in Chapter 3. The controller was developed based on an assist-as-needed framework [272]. At each walking step, the software adapts the support of the gait trainer (i.e. the impedance of the hip and knee joints) based on the ability of the subject to follow a physiological reference trajectory. The hypothesis is that the level of residual support determined by the device after 40 steps is proportional to the subject's impairment. To test the construct validity of this method we need determine whether the residual support provided by the *test orthosis* (where the AAN algorithm is implemented) is proportional to the impairment (weakness or spastic-like behavior) simulated on the *human leg*. Using a rigid connection between the two Lokomat orthoses, we deployed the AAN software on the test orthosis to *assess* what we simulated. To estimate the residual support determined by the AAN we considered two different outcome measures: an overall RMS of the assistive torques throughout the gait cycle, as in [277], and the gait phase-dependent impedance (we considered only the stiffness K in this study), which provides information on the required support in specific parts of the gait cycle. We tested different severity of simulated impairment at three different speeds, as shown in Table 4.1.

EXPERIMENTAL CONDITIONS

Severity Speed	0 %	25%		50%		75%		100%	
V1 = 1.5km/h	N	W	S	W	S	W	S	W	S
V2 = 1.8km/h	N	W	S	W	S	W	S	W	S
V3 = 2.3km/h	N	W	S	W	S	W	S	W	S

Table 4.1: Experimental conditions tested on the robotic test bench. At each speed, "normal" (0 % impairment) and four severities of simulated weakness (W) and spastic-like impairment (S) were tested.

4.3 RESULTS

4.3.1 Simulated Human Leg

4.3.1.1 *Identification of FF Parameters*

The AFFC was able to identify three set of parameters λ for walking at three different speeds – 1.5, 1.8 and 2.3 km/h. The converged values and the combination with a compliant FB controller allowed the *simulated human leg* to follow a desired walking reference trajectory with an overall angular error of less than or equal to 2.5° after convergence (Figure 4.4). Figure 4.5 shows the hip and knee angle of the rendered simulated leg. Note how a combination of FB with low gains and FF closely match the performance of healthy subjects walking in the Lokomat with low impedance.
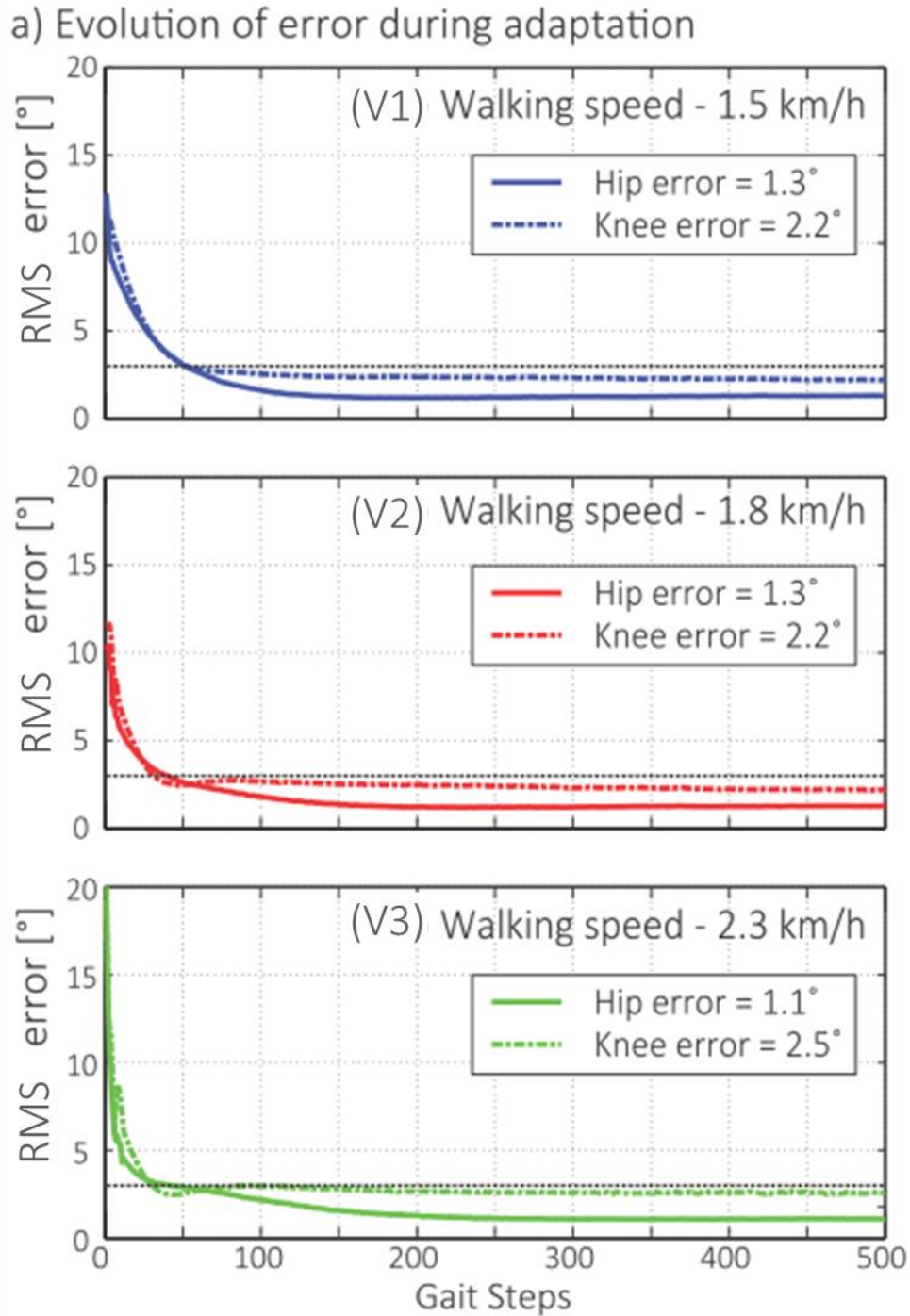
Figure 4.4: The AFFC adapts the λ parameters step by step. The RMS error between q_{ref} and q_{act} reaches convergence at V1, V2 and V3, both for the hip (continuous line) and for the knee (dashed line), below 2.5°. As soon as the criteria in Eq. 4.6 and 4.7 are satisfied in step $\bar{s}$, the vector $\lambda_{\bar{s}}$ is saved and used in the FF controller in the following experiment. © 2016 IEEE. Reprinted, with permission, from the original article [302].
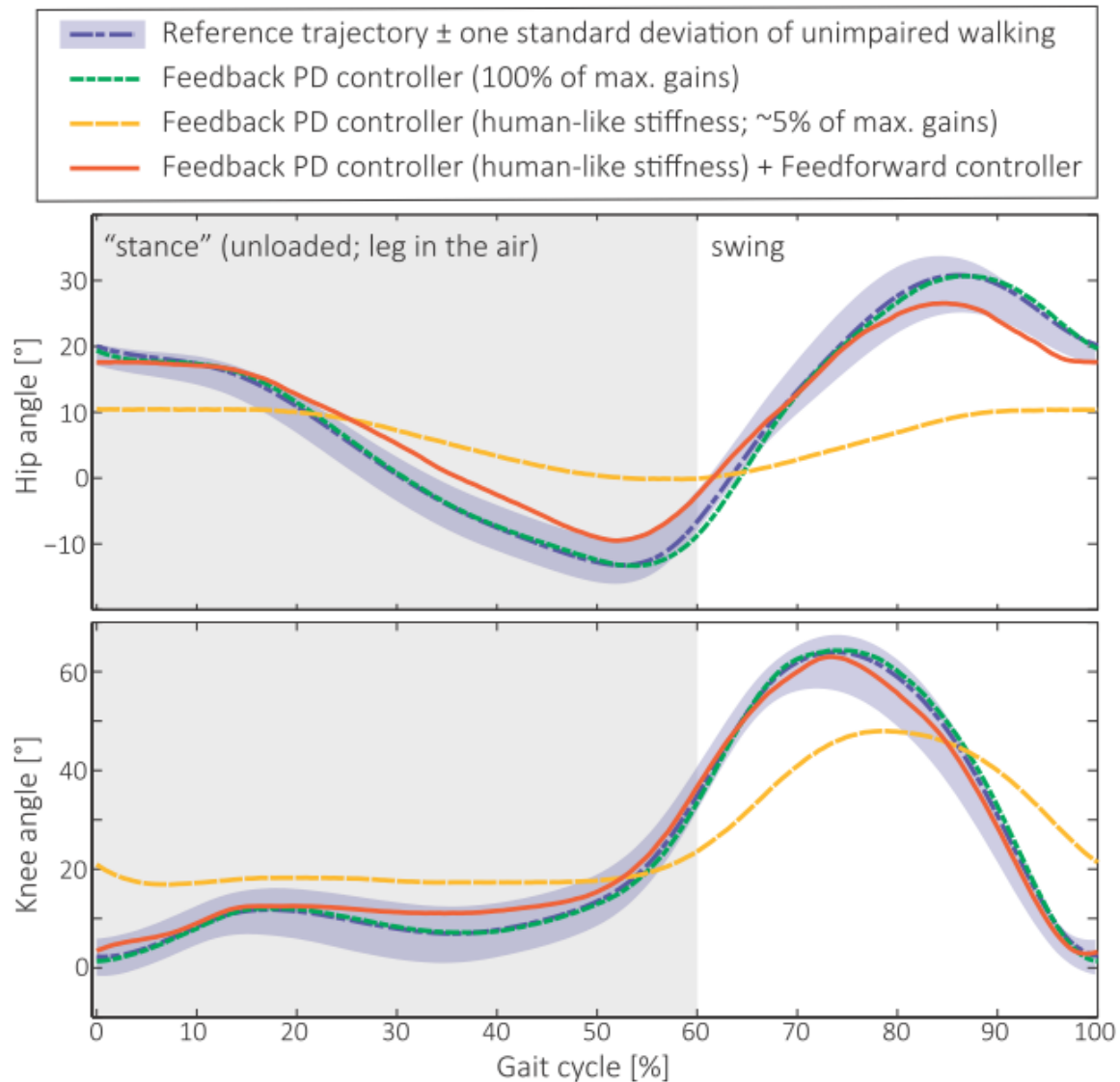
Figure 4.5: Hip and knee angles generated from different contributions of FB and FF controllers at 1.8 km/h. The shaded area shows values of physiological variability around the reference trajectory of 10 unimpaired subjects walking in the Lokomat in "low impedance" mode. © 2016 IEEE. Reprinted, with permission, from the original article [302].

4.3.1.2 Haptic Simulation of Abnormal Limb Neuro-Mechanics

The simulation of weakness led to walking trajectories with reduced Range of Motion (ROM) during swing, as could be expected in subjects with reduced muscle force [268]. An experienced physiotherapist confirmed that the rendering of "spastic-like" impairment provided a realistic haptic feedback in response to a manual stretch at different speeds.

4.3.2 Assessing Abnormal Biomechanics with AAN-Based Assessment

We hypothesized that the AAN-based assessment algorithm would provide a final residual impedance proportional to the simulated impairment. To verify this, we rendered different severities of weakness and spastic-like behavior at three different speeds and we studied the corresponding outcome measures obtained with the AAN-based assessment. In this study we considered only the results relative to swing phase, since our model at present does not render the ground reaction forces.

4.3.2.1   Weakness

Four levels of weakness severity were simulated by progressively reducing the contribution of the FF part of the controller (Table 4.1). For each speed and for each simulated severity, the knee stiffness profile of the *test orthosis* at the 40th step is presented (Figure 4.6a). In the case of the gait phase-dependent stiffness K we can notice that the support was required in two specific phases of the gait cycle, namely initial swing and terminal swing. The peaks of K increased monotonically with increased simulated weakness severity. Similarly, the overall support torque increased proportionally to the simulated weakness. Speed caused an offset but did not affect the monotonicity of the measures (Figure 4.6b).

a) Gait-dependent support (stiffness) for different levels of "weakness"

b) Overal support (torque) for different levels of "weakness"
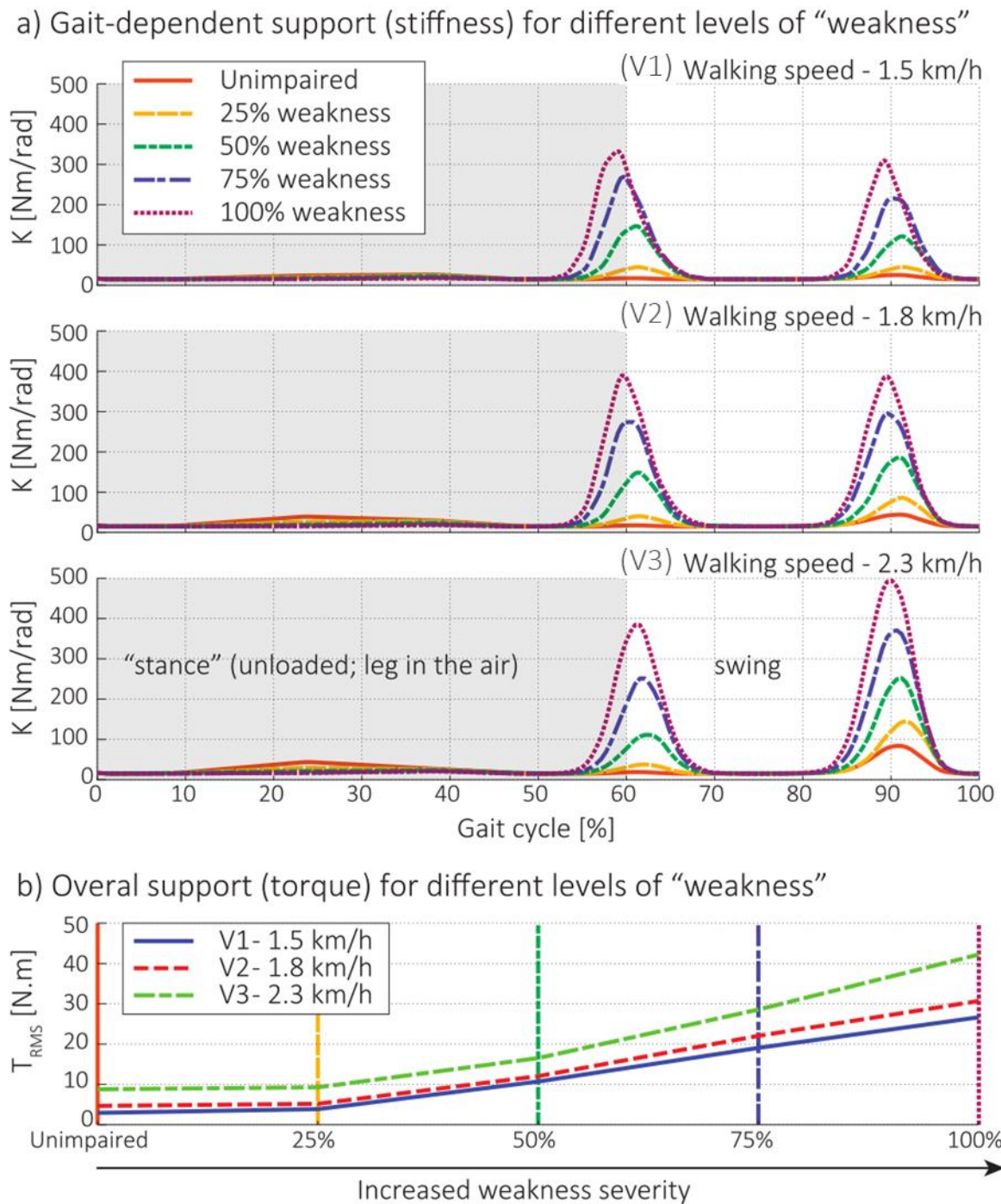
Figure 4.6: Results of AAN-based assessment algorithm from the simulation of weakness for different levels of simulated severity and at three different speeds: (a) gait phase-dependent stiffness of the test orthosis (knee); (b) overall measure of assistive torques (knee). © 2016 IEEE. Reprinted, with permission, from the original article [302].

4.3.2.2 Spastic-Like Behavior

Concerning the spastic-like behavior, the results showed more complex characteristics. The gait phase-dependent stiffness presented two different patterns (Figure 4.7a). In early swing the residual support to the *simulated human leg* provided by the *test orthosis* increased proportionally to the simulated spastic-like behavior. Conversely, at the end of swing, the simulated impairment improved the walking performance of the *simulated* (impaired) *human leg*, helping in decelerating the leg.

Therefore, the resulting stiffness provided by the AAN-based assessment decreases with increased simulated severity of the spastic-like behavior. If we look instead at the overall torque provided by the AAN algorithm, we notice that this outcome measure is not proportional to the simulated severity of the spastic-like behavior. Also, in this condition speed causes an offset that led to increased overall assistive torques with higher speeds (Figure 4.7b).

a) Gait phase-dependent support (stiffness) for different levels of "spastic-like behavior"
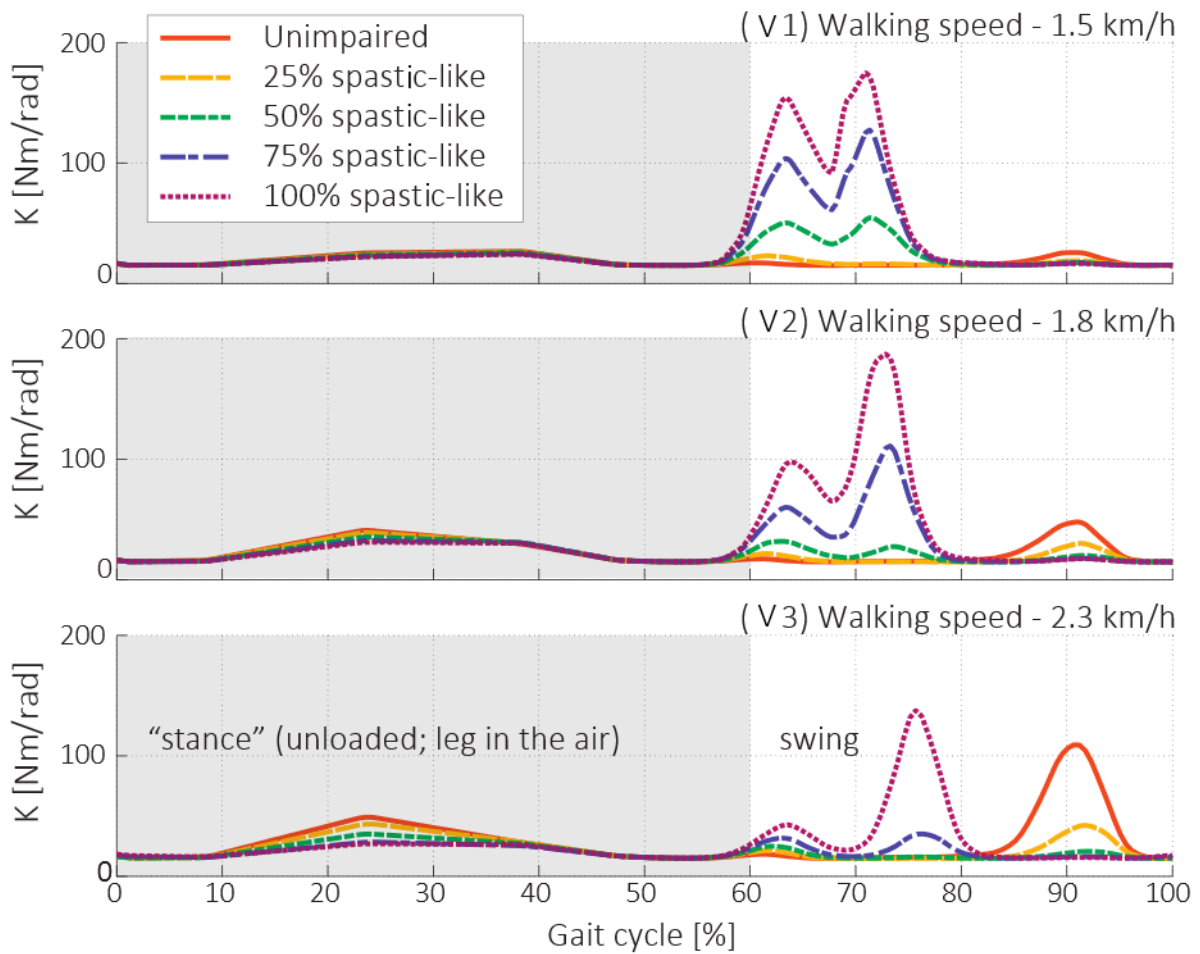
b) Overall support (torque) for different levels of "spastic-like behavior"
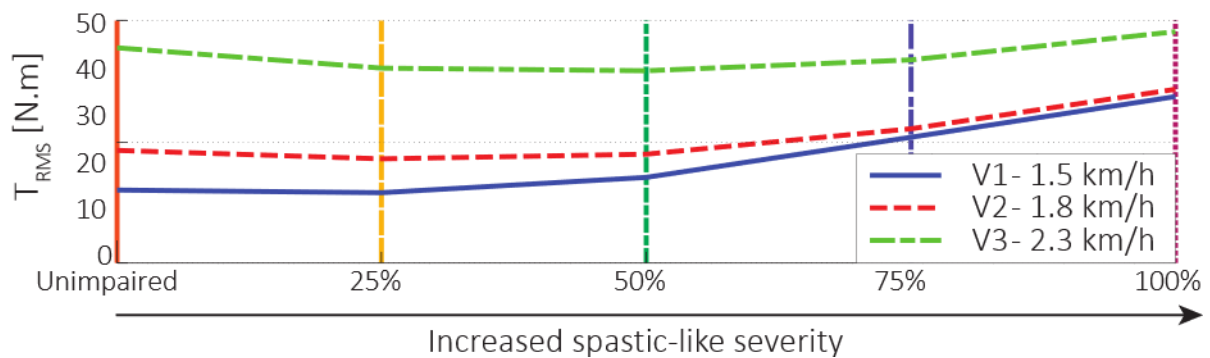
Figure 4.7: Results of AAN-based assessment algorithm from the simulation of spastic-like behavior for different levels of simulated severity and at three different speeds: (a) gait phase-dependent stiffness of the test orthosis (knee); (b) overall measure of assistive torques (knee). © 2016 IEEE. Reprinted, with permission, from the original article [302].

4.4 DISCUSSION

In this chapter we presented a novel bio-inspired test bench for testing assessment and training algorithms for rehabilitation robots. A feedback-feedforward controller is used to simulate a human-like leg behavior on a robotic two-link orthosis. In this application, a *simulated human leg,* consisting of a robotic orthosis controlled by a bio-inspired controller, is connected to another robotic orthosis, *test orthosis*, in which the control and assessment algorithms of a robotic gait trainer are deployed. In this particular study, we evaluated a software developed for assessing the walking function of a patient, the AAN-based assessment algorithm [277]. The aim of the test was to verify whether the assumptions underlying this method, such as bigger robotic support for more severe impairments, are correct and whether we could determine confounding factors that we may encounter in further experiments with humans. Here we show, that the AAN-based assessment, under the conditions presented, is able to correctly discriminate between simulated impairments.

4.4.1 Example of Use – Learnings about AAN-Based Assessment

Although the bio-inspired model presented here is a simplistic representation of the complex biomechanics and control exhibit by humans, such approach allows us to systematically test different methods and gain information on confounding factors that can otherwise be misinterpreted if such methods were tested directly on humans. Simulating a known impairment reduces the causes of uncertainty and allows to perform tests in controlled conditions in order to study the different sources of errors and variability and try to control for them.

The outcome measures of the AAN-based assessment reflected the simulated severity of the impairment. In the case of simulated weakness, we identified in which phases the presence of an impairment can be mostly detected (i.e. initial swing and terminal swing). Interestingly, the data reflects the gait literature, where it is known that muscle activity at the level of the hip and knee joint is mainly required to start the swing of the leg and to decelerate it before heel strike [29, 309]. Very low energy is required in mid swing provided that the initial conditions in generating knee flexion at toe-off are met [310].

In the case of spastic-like behavior, we were able to detect an unexpected behavior occurring at terminal swing, where the AAN algorithm detected decreasing stiffness of the *test orthosis* with increasing simulated severity on the *simulated human leg* (i.e. less robotic support was required for higher severity of the impairment). It has been suggested that spasticity can be beneficial for walking because it can partially compensate for the lack of supraspinal drive in spinal cord injured subjects [311]. Although this effect was mainly noticed during the stance phase of walking, we speculate that spasticity could also aid walking during terminal swing, where active energy is required to decelerate the leg.

Since we were in control of the conditions that we were simulating, we could tune and isolate different impairments and study how these, separately, impacted on the outcome measures of the

assessment algorithm. We noticed that the effects of simulated weakness on the outcome measures of the AAN-based assessment was visible in a different phase of the gait cycle with respect to the effects of the spastic-like behavior. This information may help in the interpretation of the data that will be obtained from human subjects.

This study also gave useful insights on which AAN outcome measure to select to best describe the impairment. Although the overall assistive torques provided by the AAN software were able to differentiate between levels of weakness, they were not be able to identify the level of impairment when the spastic-like behavior was present. Therefore, it is important to consider always the gait phase-dependent values of the stiffness to have a correct indication of the subject's impairment.

Another important factor to consider is the walking speed. As discussed in [277], speed causes an offset in the AAN outcome measures, possibly due to the bigger role of passive dynamics generating the swing motion. Therefore, to avoid confounding factors when experimenting the AAN-based assessment in humans, one should not mix results obtained at different speeds.

The great advantage of the method presented here is that we could perform several tests in different controlled conditions without involving human subjects. This allowed us to have a fast testing process that, even if it cannot substitute final testing in humans, was able to provide us with important information on how to interpret those data.

4.5 CONCLUSION

Robotic test benches provide a powerful method for the initial tests of new devices and algorithms for rehabilitation robots. It can expedite the development process of novel devices and algorithms and ensure that the version that will be tested on subjects will be free of issues that pertain to the technical implementation. The methodology presented here can be generalized potentially to any device (for upper and lower limb) and it can be applied for testing any kind of robotic algorithms, both for assessment and for training (see [312] for another application of this same test bench).

In the case of robot-aided assessments, robotic testing is a useful technique to perform a first test on construct validity. Confounding factors, such as speed and co-presence of different impairments, can be isolated and studied separately.

In this chapter we presented a simple model of weakness and spastic-like behavior, but other biomechanical models could be rendered in the device. For example, neuromusculoskeletal models created with OpenSim (NCSRR, USA) [313] can be used to calculate the joint torques generated in presence of a certain musculoskeletal impairment and used to control the robotic device. The simulation of the interaction with the ground during stance phase would complete the simulation of human walking presented in this study. Moreover, it would be possible to study how a robotic system reacts to simulated disturbances typical of human variability.

The possibility to simulate a repeatable and controlled input can be used for the benchmarking of different rehabilitation robots and algorithms because they can be tested in the same known conditions. In the future, the phase of robotic testing can be a standard step in the development of new rehabilitation robots.

Chapter 5   CLINICAL VALIDATION

Part of the content of this chapter will be submitted for publication with the title: *"Gait features in a robotic gait trainer: what can they tell us about waking ability?",* authored by Maggioni S, Lünenburger L, Riener R, Curt A, Bolliger M, Melendez-Calderon A, in 2020.

Foreword

After testing in able-bodied subjects and on a robotic test bench simulating neuromotor impairments, the novel Assist-as-Needed (AAN) controller is finally applied in patients affected by Spinal Cord Injury. The aim of this clinical study is to establish the relationship between the AAN outcome measures and the patients' walking ability, as measured by standard clinical scores, timed tests and isometric torque measures. Validity and intra-rater reliability of the AAN-based assessment are evaluated in 3 visits where the patients are assessed twice with the AAN-based assessment and once with standard scores. The measures able to provide more information on walking ability are identified.

5.1 INTRODUCTION

One aim of this thesis is to develop a quantitative and objective evaluation of walking ability that *i)* can be used during training and *ii)* enables objective, valid, reliable and sensitive measurements. This should be applicable to patients with mild to severe gait impairments. For this purpose, we developed an adaptive controller in a treadmill-based robotic exoskeleton, the Lokomat (Chapter 3). Our hypothesis is that the level of robotic support (a combination of robotic joint impedance and body weight support) determined by the algorithm is proportional to the patient's level of walking impairment. The adaptive software was first tested in able-bodied subjects (Chapter 3). Those pilot tests were useful to evaluate several aspects and led to some changes in the controller and to the experimental protocol prior to tests in Spinal Cord Injury patients that will be presented later in this chapter. We also evaluated the system's performance in assessing different types of typical walking impairments on a biomimetic robotic test bench (0). This technical validation confirmed that the method can capture different levels of impairment and that the outcome measures are affected by speed. It also showed that the impairment is only visible in some gait phases, likely those with higher motor control demands. It was also shown that there are factors (such as increased joint stiffness) that cause a non-linear relationship between impairment and AAN outcome measures.

In this Chapter, we present the results of testing the adaptive software in patients with SCI. We performed a study including 15 subjects with SCI and 12 able-bodied subjects. Our aim was to study how the parameters of the controller adapted to the patients' impairment and how they related to "walking ability" in the real world, i.e. walking overground, without a robotic device, as measured by standard clinical scores. Before the study, patients were assessed using clinical scores measuring walking activity, balance and muscle force. The subjects walked in the Lokomat with the experimental AAN software. The robotic support values determined by the algorithm in several gait phases were used as features to assess patient's walking ability. We wanted to understand which features captured in a robotic gait trainer could provide the most relevant information about gait. In the future, these features could be used to develop an objective assessment of walking ability which clinicians may use to assess the patient's progress and to adapt the training, especially by focusing on the features where the patient still has deficits.

5.2 METHODS

5.2.1 AAN Controller in the Lokomat

The AAN controller developed in this study adjusts *i)* the mechanical impedance of the robot's hip and knee joints throughout the different gait phases and *ii)* the body weight support (BWS). The robotic hip and knee joint impedances are adapted based on the patient's ability to follow a physiological gait pattern displayed on a screen. The BWS is adapted according to the height difference of the hip center

of rotation (CoR) [278]. The controller is based on an assist-as-needed concept implemented in the Lokomat, as described in detail in [277, 314] and in Chapter 3 of this thesis.

The first experimental evaluation performed in able-bodied subjects indicated that some changes should be applied to the experimental protocol. We allowed the subjects to have a familiarization visit where they could try the AAN software in the same week of the two experimental visits. We shortened the adaptive task to 50 steps to limit the occurrence of fatigue and limit the time required for the assessment. The visual feedback was modified to increase clarity of the information: the shaded areas were replaced by a line showing the ankle trajectory that the subjects were asked to follow. The reference and actual position along the trajectory were indicated, respectively, with a blue and a green/red dot (indicating if the kinematic error was within (green) or outside (red) the deadbands). The foot trajectory performed in the last step was shown in orange. The adaptive task was limited to one leg at a time, to ensure a proper display of the reference and actual trajectory and reduce the cognitive and motor demand on the patients performing the task.

Before starting the experiments with patients, we performed a pilot test with one subject affected from a complete SCI (ASIA A). This was considered as "worst-case scenario", since the patient was functionally on the lower end of the spectrum of patients that we would include in our study. The assessment task was considered very challenging by the patient, and it was possible to perform only after some modifications, that we decided then to implement in the following study. We increased the maximum value of BWS to 80% of the body weight, although maintaining 70% as starting value of the adaptive algorithm. The deadbands around the reference trajectory were reduced as shown in Figure 3.4. These less permissive deadbands were particularly narrow in critical phases of the gait cycle such as foot contact. We increased the number of steps of full support between the adaptive tasks to 40, to ensure that patients could rest between assessment tasks, which were perceived as quite physically demanding.

5.2.2 Population

The study was carried out at Balgrist Campus, Zurich, Switzerland and was approved by the Kantonale Ethikkommission Zürich (KEK-ZH-Nr. 2015-0020) and by Swissmedic (2014-MD-0035). A total of 27 subjects participated in this study: fifteen participants with a complete or incomplete SCI (age 54±12, eleven males) and twelve unimpaired controls (age 43±15, seven males). The inclusion criteria were: >1 year post Spinal Cord Injury or persons without history of walking impairments. The exclusion criteria were: presence of contraindications to Lokomat training (a complete list can be found at https://www.hocoma.com/legal-notes/ or in the Lokomat user manual); inability or unwillingness to provide written informed consent or follow study procedures.

PATIENTS CHARACTERISTICS

ID	Sex	Age	AIS	Level	WISCI II	10MWT [m/s]	TUG [s]	BBS	FAC	Notes / Comorbidities
P22	M	57	D	T12	20	1.89	4.80	56	5	-
P24	M	49	D	C2	20	1.69	5.15	56	5	Neuropathic pain
P25	M	68	D	C2	20	1.19	8.64	52	5	Polytrauma with head contusion bleeding / mild cognitive deficit
P26	M	38	D	C7	16	0.23	32.03	23	3	-
P27	M	30	D	C6	11	0.19	74	15	1	Musculoskeletal and neuropathic pain
P37	M	53	A	T11	8	0	NA	7	0	Polytrauma
P40	M	54	D	C4	20	1.78	6.88	56	5	Chronic right lumboischialgia
P42	M	65	D	C2	20	1.33	10.71	53	5	Diabetic polyneuropathy
P43	F	51	D	T5	20	1.27	8.63	56	5	-
P44	M	56	D	C4	0	0	NA	6	0	Multiple Sclerosis
P45	F	74	A	T10	0	0	NA	6	0	-
P46	F	67	D	T4	16	0.64	12.89	46	3	-
P47	M	43	C	T12	12	0.28	38.94	21	2	-
P48	F	56	D	L1	13	0.29	65.94	10	3	-
P49	M	47	C	ND	0	0	NA	7	0	-

Table 5.1: Subject characteristics for the patient group. NA: Not Applicable (these patients could not perform the timed walking tests). ND: Not Determined (missing data in the ASIA score sheet did not allow to determine the level of lesion precisely).

ABLE-BODIED SUBJECTS CHARACTERISTICS

ID	Sex	Age	10MWT [m/s]	TUG [s]
S28	M	52	2.10	3.86
S29	M	29	2.14	5.77
S30	F	29	1.38	6.09
S31	F	25	1.97	5.30
S32	F	29	1.61	5.19
S33	M	53	2.59	4.44
S34	M	37	1.78	4.74
S35	F	61	2.34	3.78
S36	M	64	1.82	3.95
S38	M	45	2.01	4.06
S39	M	64	2.44	4.08
S41	F	26	2.61	4.91

Table 5.2: Subject characteristics for the able-bodied group

EXPERIMENTAL PROTOCOL

Visit 1	Visit 2	Visit 3
Clinical assessments	AAN-based assessment	AAN-based assessment
L-FORCE	TLX Questionnaire	TLX Questionnaire
Familiarization		

Table 5.3: Visits of the clinical experiment

The study protocol consisted of three visits within 7 days (Table 5.4). During the first visit, a set of clinical assessments was carried out, followed by a familiarization phase with the AAN algorithm. The assessments focused on: gait speed, balance, assistance required for walking, muscle force, functional status.

OTHER ASSESSMENTS INCLUDED IN THE PROTOCOL

Domain	Name of test	Abbreviation
Gait speed	10 Meter Walking Test Time Up-and-Go Test	10MWT [254] TUG [254]
Balance	Berg Balance Scale Time Up-and-Go Test	BBS [315] TUG [254]
Muscle strength	L-FORCE – Lokomat isometric joint torque assessment (hip/knee, flexion/extension) Manual Muscle Test	LF [84] MMT [316]
Assistance required for walking	Walking Index for Spinal Cord Injury Functional Ambulation Category	WISCI II [254] FAC [315]
Functional status	ASIA impairment scale	AIS [317]

Table 5.4: Clinical assessments included in the experiment. All the assessments were performed during the first visit.

In the able-bodied (AB) control group, only the 10MWT, TUG and L-FORCE were conducted. During the Lokomat familiarization phase, the subjects were set up in the Lokomat for a practice session. The settings were adjusted until the most physiological and comfortable gait pattern was found. No data was recorded but the Lokomat optimal settings (cuff size, leg length, hip and knee offset and range of motion) were retained for the next two sessions. An isometric joint torque assessment (L-FORCE) [84] was performed in the Lokomat before the subjects started to walk. The L-FORCE assesses sequentially hip and knee joint of the left and right leg, testing both flexion and extension torques. The subjects walked in the Lokomat with a speed of 1.9 km/h with full robotic support (40 steps) and then using the adaptive controller (50 steps) (Table 5.5). The subjects received instructions on the task: they were requested to follow the blue trajectory in space and in time (the blue dot indicated the desired position at every instant) (Figure 5.1), first with one leg and then with the other. After each run with the adaptive controller, the Lokomat support was set back to the initial conditions (100% guidance force and 70% BWS).
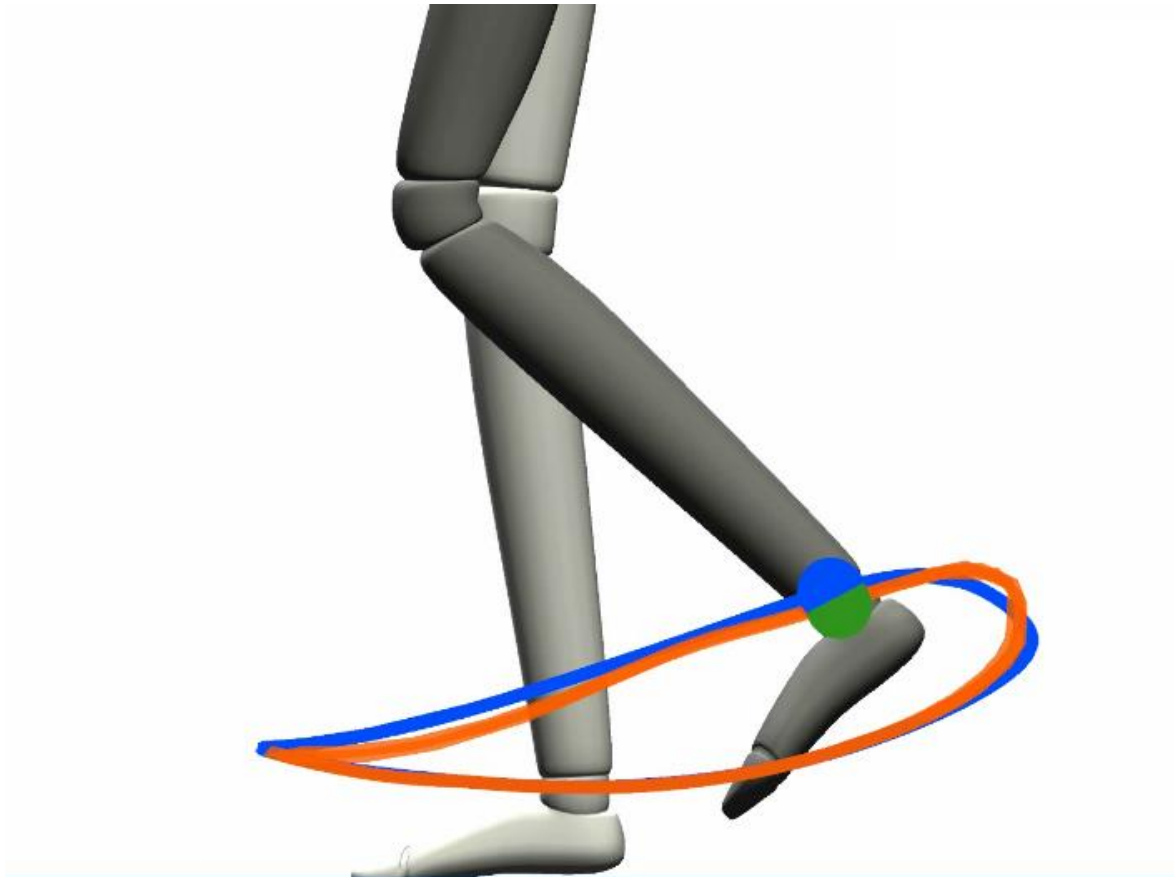
Figure 5.1: Visual feedback provided to the subjects. The reference trajectory and reference position are shown in blue, while the actual trajectory is shown in orange. The actual position is indicated by a green dot when the error is in a physiological range, changing to red when the error is outside the dead bands defined in the adaptive controller.

During the second and third visit the adaptive algorithm was used and data was recorded. Next, the adaptive software was executed at 1.6, 1.9 and 2.2 km/h. Only the middle speed was analyzed in this study. Left leg and right leg were tested separately, according to the sequence shown in Table 5.5. The leg tested first in every subject was randomly chosen between left and right.

EXPERIMENTAL PROTOCOL

Steps	**40**	**50**	**40**	**50**
Task	Max support (100% GF and 70% BWS)	Adaptive impedance leg 1 + Adaptive BWS	Max support (100% GF and 70% BWS)	Adaptive impedance leg 2 + Adaptive BWS

Table 5.5: Experiment sequence

At the end of each visit, the subjects were asked to fill out a questionnaire. The questionnaire included a general Lokomat user questionnaire and the NASA Task Load Index (TLX - see Appendix D).

5.3 DATA PREPARATION

Data analyses and statistics were done with Matlab R2016b. Steps were divided and segmented in 6 gait phases (Figure 5.2) using the heel strike and toe-off instants as described in [318]. The swing phase was divided in three sub-phases according to gait literature [30].

Figure 5.2: Gait step divided in 6 gait phases: first double support, single stance, second double support, initial swing, mid swing and terminal swing. For every gait phase the stiffness K and the damping B (except in DS1 and SS) are calculated as the average between left and right leg.

The impedance of the robotic joints and the BWS decrease following an exponential decay, until a point where the error prevents a further decrease. For each gait phase, the robotic impedance of hip and knee joint (K hip, K knee, B hip, B knee) was averaged and modeled as exponential decay to filter out any noise. The average over the last 5 modeled steps of each adaptive task (left and right leg adaptation) was calculated, and afterwards averaged over the left and right task. The modeled BWS averaged on the last 5 steps of each adaptive task was also calculated and normalized by body weight. The residual impedance is used as an indicator of the support required for walking in the different gait phases. The stiffness K was adapted based on spatial deviation from the predefined trajectory [277, 314]. Thus, K reflects the additional support required to follow the reference trajectory in space. The damping B was adapted based on errors in velocity and reflects, therefore, the additional support required to follow the trajectory with an adequate speed. We did not consider the damping B in DS1 and SS since the speed error is not relevant for these phases. The residual BWS indicates the support required during stance phase. The residual impedance and the BWS were then averaged among left and right task. For each subject, a dataset for the second visit and a dataset for the third visit were considered.

The L-FORCE results for each joint and each direction were averaged over left and right leg and normalized by body weight. For each joint and direction, the maximum value among all the subjects was found and used to normalize all the other subjects' values. The correlations between the different L-FORCE measures were studied using the Spearman correlation coefficient.

5.4 What are the Most Representative Robotic Variables that Explain Walking Ability?

5.4.1 Methods

Our first aim was to identify which are the most representative variables measurable in the Lokomat that relate to walking ability (as measured by the 10MWT and TUG) in patients with SCI. Linear regression was used as an exploratory technique to identify the best predictor(s) of walking speed, rather than to determine an accurate prediction model [319]. Only ambulatory patients, i.e. patients that had a speed higher than 0 m/s in the 10MWT, were included in this analysis (n=11).

We included all the variables listed in Figure 5.2 and we used Lasso (Least Absolute Shrinkage and Selection Operator) as a variable selection algorithm [320]. Lasso is a least-square regression method that adds a penalty term equal to the sum of the absolute values of the coefficients, multiplied by a parameter δ. The addition of the penalty term forces the coefficients of the linear model to shrink and set some coefficients to 0. We used the function *lasso* in Matlab R2016b with a 5-fold cross-validation to determine the parameter δ.

As summarized in Table 5.6, we included two observations per patient (data from visit 2 and visit 3) and we implemented a bootstrapping procedure to study if the predictors selected via Lasso were consistent (Bolasso) [321, 322]. We reported the results from 1000 bootstrap replications in Appendix C . At every replication, we selected at random *n-3* subjects without replacement, choosing for each randomly selected subject at every run either the observation from visit 2 or the observation from visit 3. By selecting for each subject only one observation among the two, we tried to limit the effect of having two dependent observations in the same pool. We obtained 1000 vectors of coefficients. We selected only the predictor(s) whose coefficient was different from 0 in at least 60% of the replications.

We then generated unregularized linear models using the *fitlm* function within a second bootstrap loop to determine the Confidence Interval (CI) of the coefficients and the regression line and the Prediction Interval (PI) for new observations. At every bootstrap replication, *n-3* subjects were selected without replacement as explained above. We decided to include two observations per subject, although breaking the assumption of independence of the observations, since we were mainly interested in identifying the most important predictors of walking speed, rather than providing exact values for the accuracy of the models. We decided anyway to present also the values of the coefficients of the model to give an idea of the association between the selected predictor(s) and the predicted variables.

We repeated the same procedure described above for predicting the TUG. The data from the TUG were reciprocated, to have them in a similar form to the data of the 10MWT, which are expressed as speed. This allows the TUG data of patients who could not perform the test to be expressed as numeric value (0 s^{-1}).

Steps for Selecting the Predictor(s)

1. Run Lasso on 1000 bootstrap samples (Bolasso)

    1.1. select *n-3* subjects without replacement at every run

    1.2. for every subject, select randomly either observation from visit 2 or observation from visit 3

    1.3. Run Lasso on the selected sample and save the vector of coefficients β

2. Select all the variables with coefficient ≠ 0 in ≥ 60 % of the cases

Steps for Bootstrap Evaluation of the Model

3. Run *fitlm* on 1000 bootstrap samples

    3.1. select *n-3* subjects without replacement at every run

    3.2. for every subject, select randomly either observation from visit 2 or observation from visit 3

    3.3. run *fitlm* on the selected sample and save β, Adj. R^2 and residuals

4. Calculate the average model coefficients β and their CI, the CI of the mean and the PI for new observations

---

Table 5.6: Steps for the selection of predictor(s) and evaluation of the model

5.4.2 Results

5.4.2.1 Prediction of 10MWT

In 1000 bootstrap replications of Lasso, the variable K knee TS (knee stiffness at terminal swing) was selected 87.3% of the time (see Appendix C.1.1 for percentage of selection of all the variables). We used only this predictor to generate the unregularized linear model to predict the 10MWT in ambulatory patients. K knee TS was a significant predictor of speed in the 10MWT (β = -7.933, Confidence Interval (CI) = [-11.072, -6.189], $p < 0.001$). The coefficient in the model was negative, meaning that the higher the support required from the knee at terminal swing, the lower was the speed measured in the 10MWT. The adjusted R^2 for the model generated from all the observations was 0.738 (CI = [0.420, 0.936]) and the average Prediction Interval (PI) was 1.410 m/s.
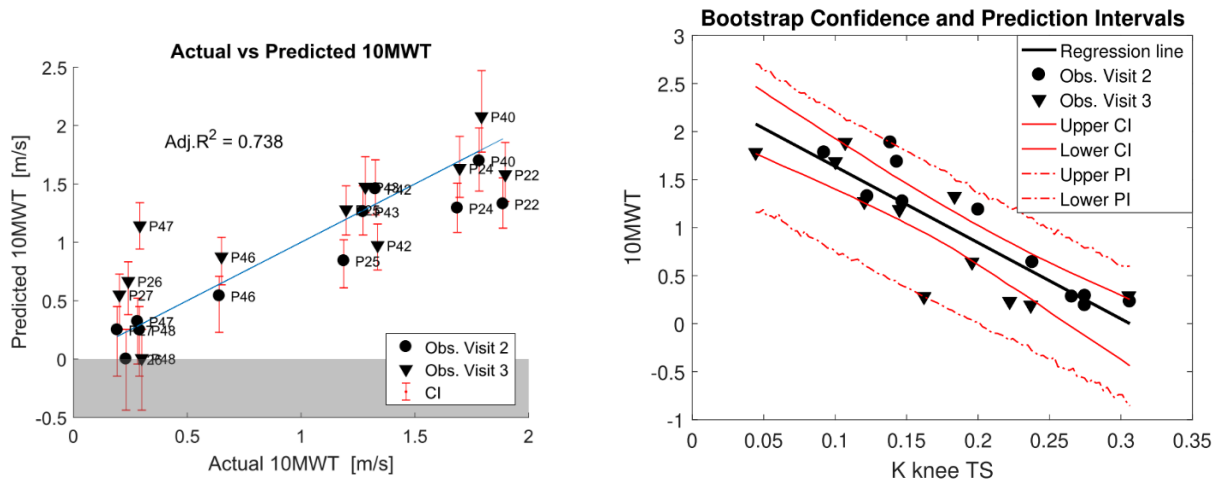
Figure 5.3: A: Actual vs Precited 10MWT: the unregularized linear model is created with the variable selected with Bolasso, K knee TS. The error bars show the confidence interval of the predicted observations. In blue, the identity line is shown. B: The predictor K knee TS vs the predicted 10MWT (black line). CI (continuous red line) and PI (dashed red line) are calculated from the second round of bootstrapping.

5.4.2.2 Prediction of TUG

During bootstrapping for the prediction of TUG, K knee TS was again selected the most, but less often than for the prediction of the 10MWT (75.9% of the times in 1000 bootstrap runs – see Appendix C.1.2). The coefficient of K knee TS was negative, as for the 10MWT (-0.763, CI: [-1.098, -0.517]). In the unregularized model, K knee TS was a significant predictor (p < 0.001), with an adjusted R^2 of 0.606 (CI = [0.420, 0.936]) and an average PI of 0.166 s^{-1}.
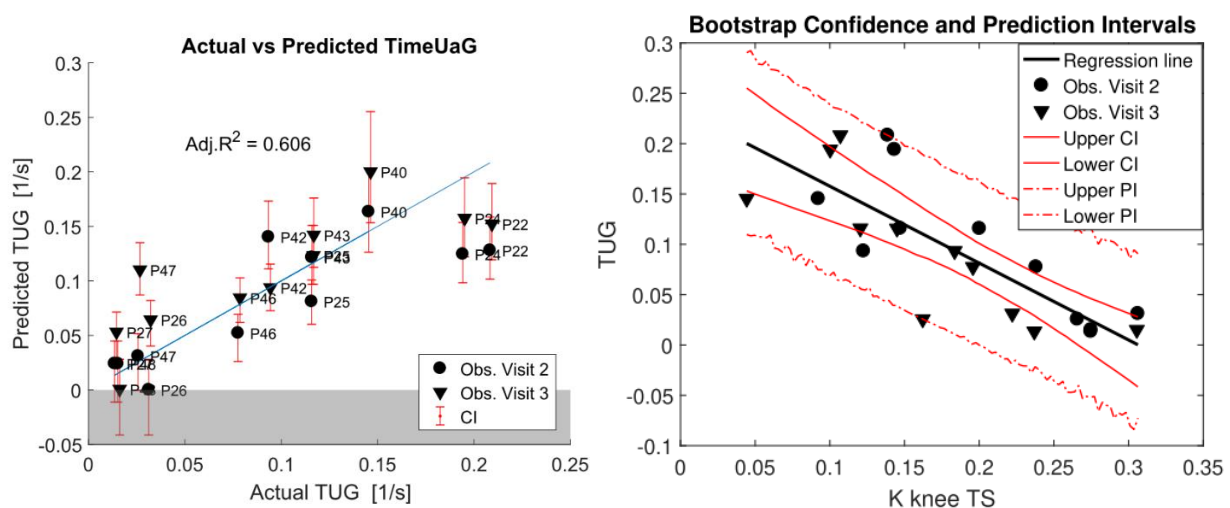
Figure 5.4: A: Actual vs Precited TUG: the unregularized linear model is created with the variable selected with Bolasso, K knee TS. The error bars show the confidence interval of the predicted observations. In blue, the identity line is shown. B: The predictor K knee TS vs the predicted TUG (black line). CI (continuous red line) and PI (dashed red line) are calculated from the second round of bootstrapping. The reciprocal of the TUG data in seconds are used for the model, to make it consistent with the 10MWT data, which are expressed as speed.

5.4.3 Interpretation

In ambulatory subjects, the support (in particular, the stiffness K) required from the knee at terminal swing alone could predict the 10MWT with a PI of 1.410 m/s and explained 74% of the variance in the data.

The relevance of terminal swing was already suggested from the technical validation experiment that we performed in a previous study [302]. There, we simulated different levels of weakness on a robotic test bench and we studied how the AAN controller would react to them. We observed that the stiffness increased proportionally to the level of simulated weakness, but only in two phases of the gait cycle: on the transition between stance and swing and at terminal swing.

In real life conditions, while walking in the Lokomat, only the support required at terminal swing seems to be related to the level of impairment of the patient. This is also confirmed by gait literature, where a smooth transition from swing to stance and an adequate step length are considered two requirements of functional gait [29, 31, 33]. In EMG studies, it is shown that a burst of muscle activity at the quadriceps is required to complete knee extension before heel strike [28, 29].

The AAN algorithm implemented a dead band around the reference trajectory to allow for some deviations (Fig. 6 in [314]); the patient had, therefore, the possibility and the need to control foot placement and step length at terminal swing. When looking at the position error in foot placement, we could see that subjects with SCI tended to have a shorter step length than able-bodied subjects. The increased support required in this phase was likely needed to extend adequately the knee before foot contact. Moreover, in this phase a more precise tracking of the reference trajectory was required because, for safety reasons, we used narrower dead bands at terminal swing (Fig. 6 in [314]). It may be that where the task demand is increased, the impairment becomes more evident.

The TUG could not be predicted as accurately as the 10MWT from the AAN-based assessment. The TUG was originally developed as a balance assessment for elderly people and applied later also in SCI patients [254]. The correlation between 10MWT and TUG is excellent in SCI, but their relationship changes over time after injury [254]. In chronic patients one year after SCI, 78% of the variance in the TUG can be explained by the 10MWT [254]. However, it is likely that the TUG captures other components required for standing up and walking which are not observable while walking in the Lokomat (e.g. balance and/or force – see section 5.5.2.2).

5.5 DOES FORCE CONTRIBUTE TO THE PREDICTION OF WALKING ABILITY?

5.5.1 Methods

Muscle strength of the lower limbs is highly related to walking speed [16, 323]. Therefore, we investigated if measures of isometric forces (L-FORCE) improve the prediction of walking speed as measured in the 10MWT and TUG and if they are better predictors than the AAN outcome measures, i.e. will L-FORCE measures be chosen in the Bolasso procedure instead of the AAN outcome measures?

To check this, we added the maximum voluntary isometric torque values (Hip Flexion (LF_HF), Hip Extension (LF_HE), Knee Flexion (LF_KF), Knee Extension (LF_KE)) to the dataset described in the previous section. For every joint and direction, we took the average torque among left and right leg and

we z-normalized each variable. We then applied the same method described in Table 5.6 to select the best predictor(s) of walking speed among the AAN outcome measures and the isometric force data. Also in this case, only ambulatory patients were included. The same procedure was applied to predict the TUG[-1].

5.5.2   Results

5.5.2.1   Prediction of 10MWT

In 1000 bootstrap replications of Lasso with the larger set of variables, the variable K knee TS was again selected in most of the cases (81.4% - see Appendix C.1.3). The second most selected variable was hip force LF_HF (66.1%). When both variables were used to generate an unregularized linear model to predict the 10MWT, the Adjusted R^2 was 0.857 (CI = [0.661, 0.980]).

The coefficient of LF_HF was positive (β = 1.405, CI = [0.336, 2.295], p<0.001), since, as expected, higher isometric force at the hip leads to higher speed in the 10MWT. The average PI decreased to 1.147 m/s (-0.263 m/s) compared to the model with a single predictor.
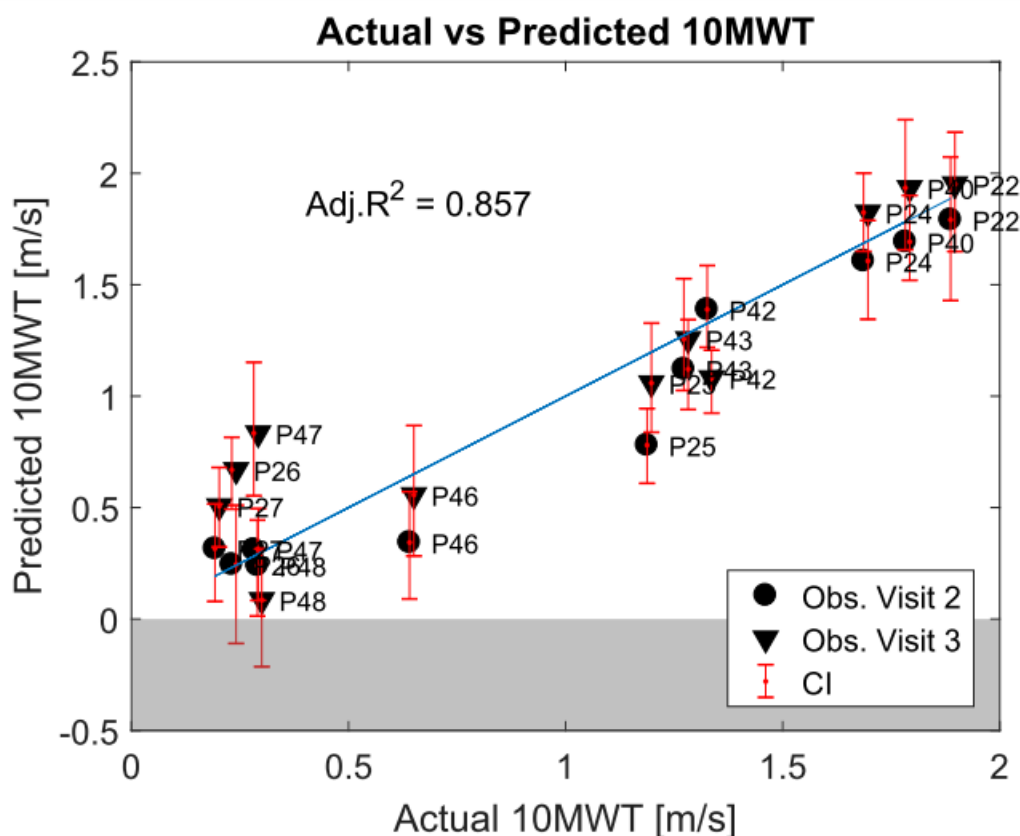
Figure 5.5: Unregularized linear model for predicting the 10MWT with 2 predictors (K knee TS and LF HF). In blue, the identity line is shown.

5.5.2.2   Prediction of TUG

In the prediction of the TUG, instead, LF_KF was selected 75.9% of the times in 1000 bootstrap replications, while K knee at terminal swing only 62.8% (see Appendix C.1.4). When looking at the

percentage of selection of the other L-FORCE measures, we found that LF_HF was selected 50% of the times. We know that the maximum knee flexion torque was highly correlated with maximum hip flexion ($\rho = 0.92$). It may be, therefore, that this other L-FORCE variable could be used to predict the TUG with a similar accuracy. While Lasso is suggested as technique to handle datasets with multicollinearity [324], it cannot completely solve this issue. We removed LF_KF from the analysis and we ran again the Bolasso procedure to check if other force measures were picked over the AAN outcome measures: the hip flexion LF_HF was selected 82.9% of the times, while K knee TS only 60.7%.

We created, therefore, one model using LF_KF and K knee TS as predictors and one using LF_HF and K knee TS. Compared with the model using only the K knee TS (Figure 5.4), both models perform better (LF_KF: average PI = 0.106 s^{-1}, Adj. R^2 = 0.854 (CI = [0.622, 0.976]); LF_HF: average PI = 0.134 s^{-1}, Adj. R^2 = 0.796 (CI = [0.590, 0.954])). The coefficients of LF_KF and LF_HF were positive (LF_KF: β = 0.146, CI = [0.053, 0.203]; LF_HF: β = 0.185, CI = [0.032, 0.288]) and statistically significant ($p < 0.001$), meaning that higher force leads to better performance in the TUG (since we predicted TUG^{-1}). We chose the model with LF_KF due to its smaller PI and higher Adj. R^2.
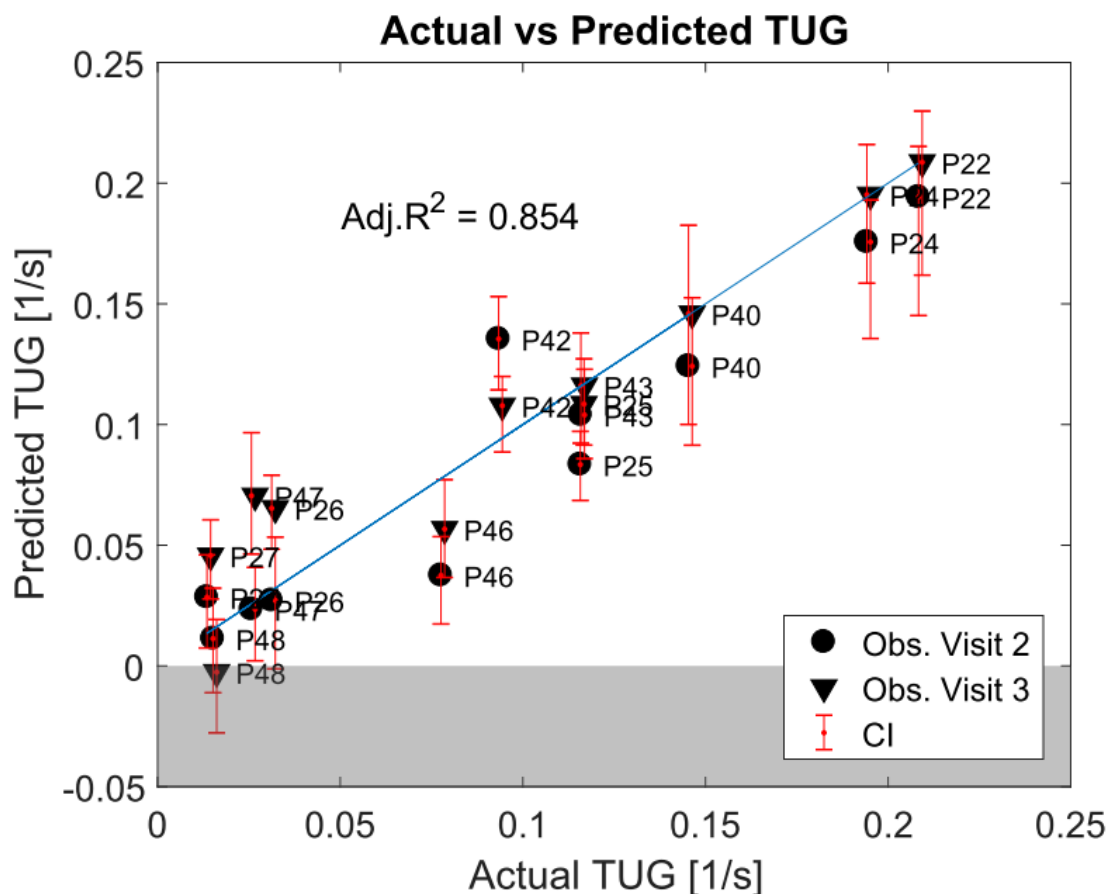
Figure 5.6: Unregularized linear model for predicting TUG. Data are taken from subjects that could perform the TUG (n=11). Predictors: LK_KF and K knee TS. In blue, the identity line is shown.

5.5.3 Interpretation

Adding the maximum isometric torque of the hip flexors as predictor increased the explained variance of the model for predicting speed in the walking tests (ΔR^2 10MWT = +0.119, ΔR^2 TUG = +0.248). The ability to walk is a composite, multifactorial construct consisting of factors such as motor control and coordination, muscle strength, balance and posture, range of motion, proprioception and muscle tone [16]. It is likely that the Lokomat AAN algorithm captures aspects more related to motor control and coordination (i.e. the ability to follow a reference trajectory), while the L-FORCE obviously measures the torque produced by muscle groups acting at the hip and at the knee joints. The first variable of muscle force chosen by the regression procedure was the maximum hip flexion isometric torque. This is in line with literature, where the strength of the hip flexors at the less affected side has been found to correlate well with gait speed as measured by the 10MWT [323]. A study using neuromusculoskeletal model of gait also found that gait performance is most affected by weakness at the hip flexors (together with ankle plantar flexors and hip abductors) [325].

Concerning the TUG, either the maximum isometric knee flexion torque or the maximum isometric hip flexion torque contributed more significantly to the prediction than any other AAN outcome measure. The TUG is more challenging than the 10MWT, since it includes standing up from a chair, turning and sitting down. Despite being highly correlated with the 10MWT (Section 5.4.3), the TUG requires other factors to be completed successfully, such as balance and force [326, 327]. It is reasonable, therefore, that information related to muscle force improved highly the prediction of the TUG, with respect to variables related to motor control alone. Lower limb muscle strength was associated with longer sit-to-walk duration in the TUG in elderly subjects (knee extensors [327]) and in stroke patients (affected ankle plantar flexors [328]), however in those studies the hip and knee flexors were not tested.

5.6 CAN WE RELIABLY MEASURE THE AAN OUTCOME MEASURES AND PREDICT THE WALKING SCORES?

5.6.1 Methods

In this section we studied the reliability of the AAN outcome measures in two sessions executed within 7 days. The sessions were performed by the same examiner (intra-rater reliability). It is essential to determine the consistency of the measures in different sessions to determine whether the measurement error is acceptable for practical applications. We examined both the relative reliability and the absolute reliability of the measure. Relative reliability refers to the degree to which individuals maintain their position in a sample over repeated measurements [77] and it can be measured with the Spearman correlation coefficient [90]. Absolute reliability refers to the degree to which repeated measurements vary for individuals, irrespective of their ranks in a sample [90], and it can be measured with the Bland-Altman plot and the 95% Limits of Agreement (LOAs) [90, 92]. The Bland-Altman plot shows the mean of the two measures plotted against their difference and it can be used to examine the presence of

systematic bias and the magnitude of the error compared to the mean value of the measure. The presence of systematic bias is tested with a t-test. The LOAs indicate the range where, for a new individual from the studied population, the difference between any two tests will lie within a 95% probability [90]. If the test is administered to the same individual to detect changes between sessions, these changes are considered significant only if they fall outside the LOAs. Therefore, the LOAs are strictly related to the minimal detectable change (MDC) of a test [77]. We examined the Bland-Altman plot for the K knee TS using the free package *BlandAltman* in Matlab [329]. Only ambulatory patients were included in the analysis.

We had the subjects perform the L-FORCE test only once in Visit 1, therefore we cannot give indication of its reliability in this study, but we refer to the work of Bolliger at al. [84], where the L-FORCE showed a fair to good reliability (intra-rater reliability for LF_HF and LF_KF ranged from 0.50 to 0.91; the SEM ranged between 6.5 Nm and 11.6 Nm for single measures).

5.6.2 Results
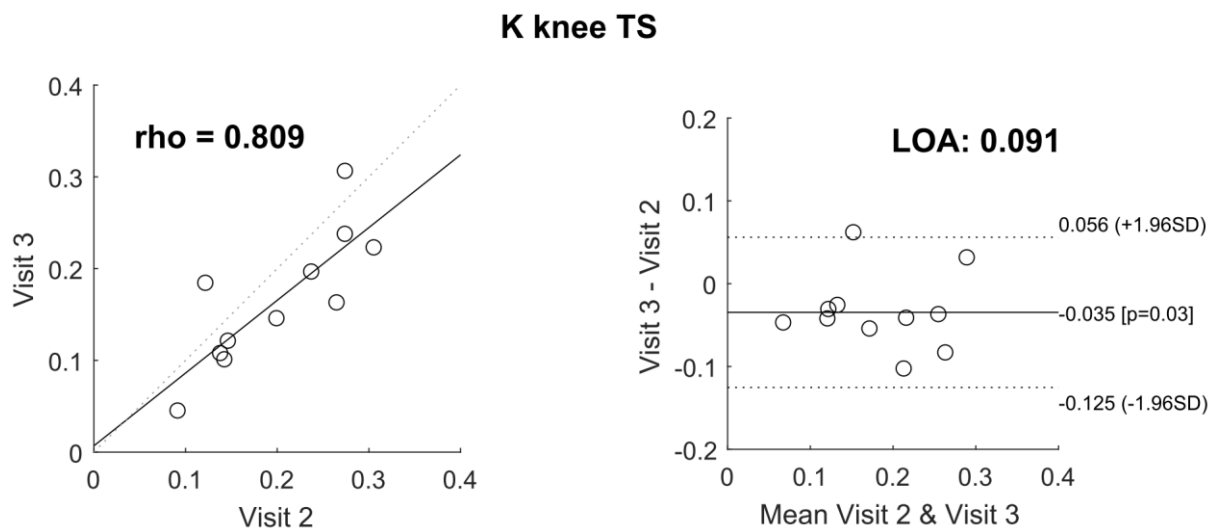
Figure 5.7: Correlation and Bland-Altman plot for K knee TS in ambulatory patients. Rho: Spearman's coefficient, LOA: Limits of Agreement

The relative reliability of K knee TS in ambulatory patients was good (ρ=0.809), and the LOAs (absolute reliability) indicate that any change smaller than 0.091 cannot be considered significant. To give an idea of what this value means in terms of prediction, we calculated the interval created by such LOAs when K knee TS was used in the models to predict the 10MWT and TUG (section 5.4). The LOAs of the K knee TS resulted in an interval of $\pm$ 0.722 m/s in the 10MWT and to an interval of $\pm$ 0.069 s^{-1} in the TUG^{-1} (corresponding to 14.395 s). Note that this estimation did not consider the uncertainty in the model coefficients. The t-test for systematic bias indicated that the observations of K knee TS from the second measurement (Visit 3) were slightly lower than the observations from the first measurement (Δ = -0.035, p = 0.03).

5.6.3   Interpretation

The Limits of Agreement indicate that a change in the measurement can be considered true only if it falls outside these limits [90]. Therefore, a difference of 0.091 in normalized K knee TS will be necessary to show a significant improvement in the test. Considering that the maximum normalized stiffness is 1, this difference corresponds to 9.1% change in stiffness.

The Minimal Detectable Change in SCI in the standard 10MWT is 0.13 m/s and in the TUG is 10.8 s [4]. Our intervals determined from the reliability of the predictor K knee TS are higher, however the aim of our study is not to replace the standard timed tests, but rather to use the timed tests as a reference to identify the variables measured in the Lokomat that can provide more information on the patient's walking ability.

The significant difference between the two visits may indicate the presence of a learning effect from the first to the second measurement.

Interestingly, the Spearman correlation between the AAN outcome measured in Visit 2 and 3 was rather high ($\rho = 0.809$), confirming how the high inter-subject variability masked the intra-subject error [91] and showing once more how important it is to consider both the relative and absolute reliability when validating a new measurement tool.

5.7   DO THESE VARIABLES CHANGE MONOTONICALLY FROM NON-AMBULATORY TO ABLE-BODY INDIVIDUALS?

5.7.1   Methods

In the previous sections, we focused on the prediction of walking in ambulatory patients (patients that had a 10MWT > 0). We identified the Lokomat variables able to provide more information on the walking function of the subjects, as measured by the 10MWT and TUG. We would like here to study if these results apply also to non-ambulatory subjects, on one side, and to unimpaired subjects, on the other side of the spectrum.

We applied the model generated in Section 5.5 for predicting the speed in the 10MWT to the four subjects who could not perform the test, to check if we could obtain a "virtual 10MWT".

Furthermore, we identified then among all the AAN outcome measures those which clearly distinguish ambulatory from non-ambulatory patients. We created boxplots for the ambulatory subjects' data. We then calculated the median of all the outcome measures in the non-ambulatory subjects. We selected the variables in which the non-ambulatory subjects had a median higher than $q_3 + 1.5 \cdot (q_3 - q_1)$ – with q_1 and q_3 first and third quartile - of the distribution generated from the ambulatory subjects' data. Having only 4 non-ambulatory subjects, we limited our analysis to the observation of how their data differ from those of the patients that could walk overground.

We were also interested to see if the results found in patients applied to able-bodied subjects, therefore we used the model generated from the patients' data to predict the speed of the unimpaired subject in the 10MWT.

We then used the same method described in Section 5.4 to identify which predictors explain better the 10MWT in able-bodied subjects, including both AAN outcome measures and L-FORCE measures as possible predictors.

5.7.2 Results

5.7.2.1 Prediction of 10MWT in all subjects

The predicted 10MWT for all the subjects participating in the study is shown in Figure 5.8 (see Appendix C.2 for the predicted TUG).The model used is that generated from ambulatory subjects in Section 5.5, based on K knee TS and LF_HF.
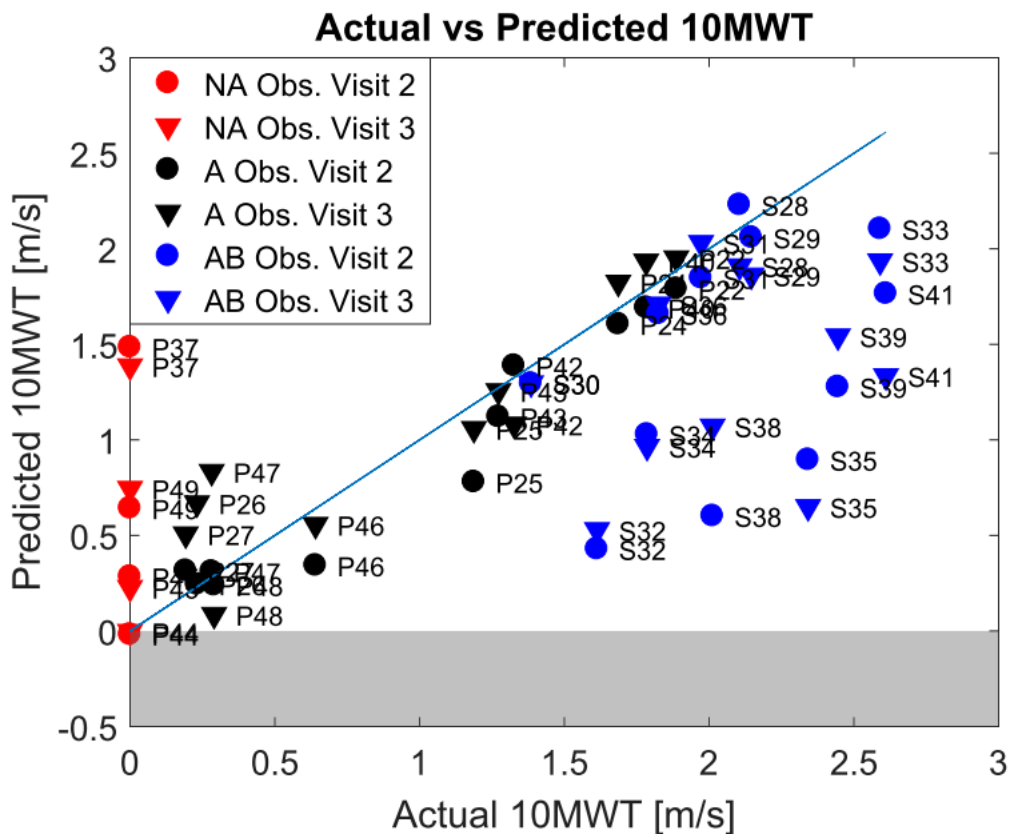
Figure 5.8: Prediction of "virtual 10MWT" of non-ambulatory subjects (red markers, "NA"), of 10MWT of ambulatory patients (black markers, "A") and of able-bodied control subjects (blue markers, "AB"). The model used has 2 predictors (K knee term swing and LF HF) and it was generated from the data of ambulatory patients in section 5.5.2.1.

The variable K knee TS reflects the guidance at terminal swing required in the Lokomat to extend the knee right before foot placement. While examining case by case the four non-ambulatory patients, we can see that P37 had a high knee extension isometric torque (LF_KE) and MMT=5 for both knee extensors: he was therefore able to extend the knee actively at the end of swing phase and required low robotic support. For this reason, this patient scored high on the "virtual 10MWT". The prediction of

10MWT for the other subjects was in the range of the wheelchair-dependent walkers (P44), supervised walkers-walkers indoor (P45) and walkers with aid (P49) [43]. P44 and P45 would be classified as unable to walk independently in the community (according to the cutoff speed of 0.59 m/s determined in [330]). However, P45 had a complete lesion at T10 and no motor function below the lesion level. P44, despite being classified as ASIA D, was at an advanced stage of Multiple Sclerosis and he/she was not able to stand or walk. P49, despite not being able to exert force at the knee joint, had some residual motor function at the hip flexors level (MMT hip flexors = 3), but he/she was not able to walk.

It seems, therefore, that the model missed some important information to correctly assign to the non-ambulatory patients a speed close to 0: K knee TS and LF_HF were not sufficient to describe the level of function in non-ambulatory patients. We looked, therefore, at the other AAN outcome measures to identify in which ones these patients showed a marked difference from the ambulatory subjects (Figure 5.9). Two main phases showed a clear separation between the groups: the single stance phase (BWS, K hip SS) and the second double support phase (B hip DS2). The second double support phase was already highlighted in our previous study performed with a robotic test bench: the higher the simulated impairment, the higher the support required during the preparation of swing phase [302].

The non-ambulatory patients needed a BWS higher than 64% of their body weight (BWS was normalized by the maximum achievable BWS, equal to 80% of the body weight). For the other variables mentioned above, the non-ambulatory patients showed a residual support in a higher range of values compared to the other patients. However, given the very few observations collected, it is not possible to show in this study if these variables would be able to correctly assess the level of function within the non-ambulatory subjects.

The models created from patients' data with one predictor (K knee TS) and two predictors (K knee TS and LF_HF) performed very poorly in predicting the 10MWT in able bodied subjects (Figure 5.8).
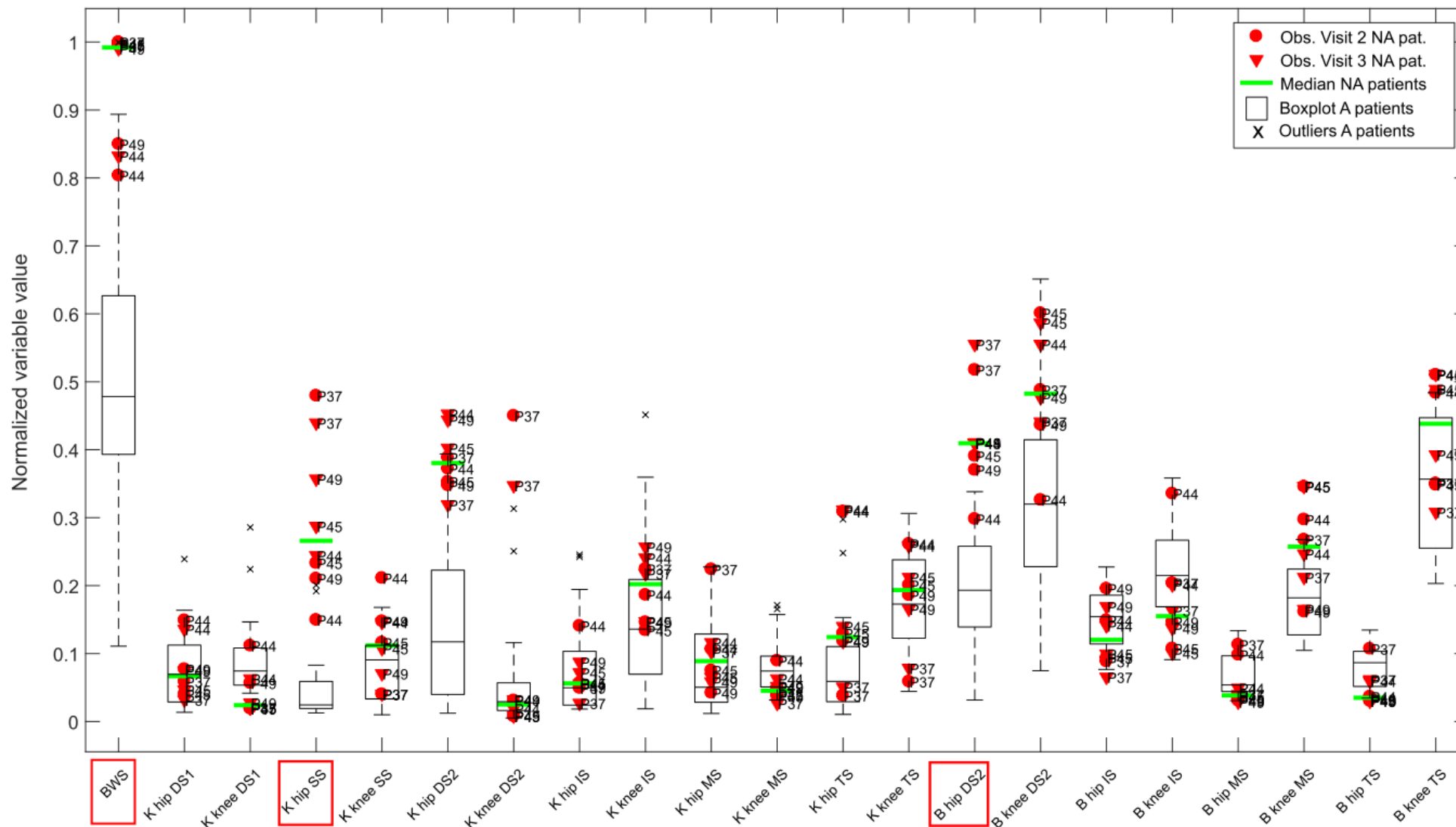
Figure 5.9: Boxplots for each variable show the distribution for each variable in ambulatory (A) subjects. Observations for non-ambulatory subjects are shown in red. The highlighted variables are those in which the median of the data of the non-ambulatory (NA) patients was higher than the q3 + 3/2 IQR of the data of the ambulatory subjects.

5.7.2.2   *Bolasso for prediction of 10MWT in AB subjects*

L-FORCE at Hip Flexion was chosen 63.5% of the times (see Appendix C.1.5) and it was found to be a significant predictor of walking speed in able-bodied subjects ($\beta = 1.612$ (CI = [1.169, 1.888]), p = 0.002, Adj. $R^2 = 0.567$ (CI = [0.225, 0.826])). The model average PI is 0.834 m/s. Bolasso selected as first most frequent predictors the four L-FORCE measures.
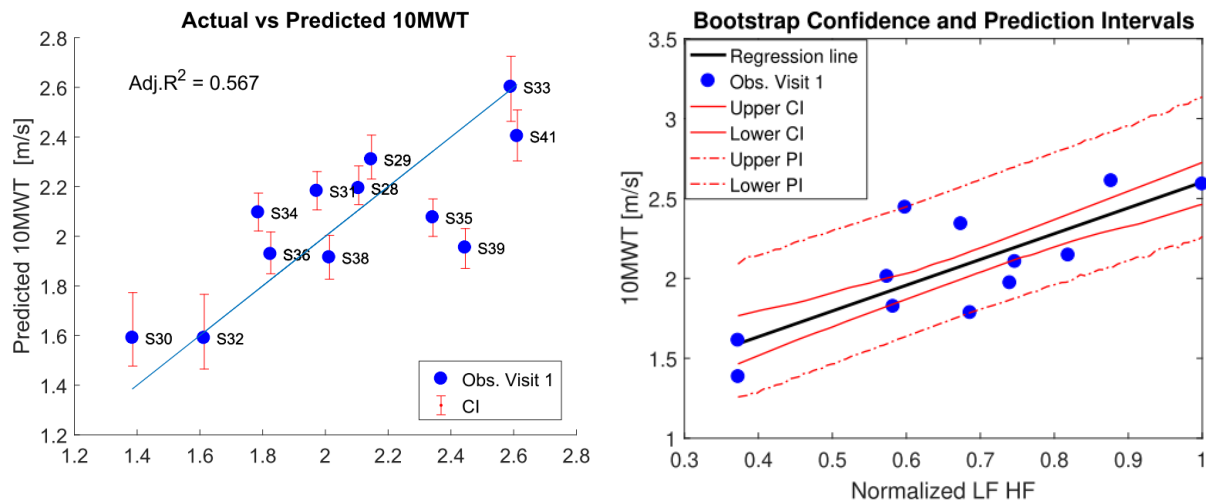
Figure 5.10: Prediction of 10MWT in AB subjects using LF HF as only predictor

5.7.3   Interpretation

The model generated from the data of the ambulatory patients is only partially able to give meaningful information on the people that cannot walk without the robotic gait trainer. Since the model does not take into account variables related to the stance phase, it overestimates the "virtual" walking ability of the subjects given their residual function measured during swing phase in the robotic gait trainer (P37 and P49).

There are likely other important predictors for gait and gait-related functions in the non-ambulatory population and some of them could be measured in a robotic gait trainer, as suggested in Section 5.7.2.1. Measures relative to the stance phase and push-off phase could be good candidates to investigate. The support of the upper body is one of the main determinants of gait [28, 29] and it is common practice for the physiotherapists to train standing before walking [17]. Our data confirms that the ability to support the body weight is a necessary but not sufficient condition to walk. If this condition is not met, the importance of other functions, such as the ability to place the foot correctly at the end of swing, is negligible.

At push-off most of the power during gait cycle is generated [28, 29]. The conditions at push-off, especially the rate of knee flexion, determine the knee flexion peak during swing phase and the consequent ability to clear the ground during swing [36]. The main muscles that influence knee flexion velocity during the double support phase are the gastrocnemius (ankle plantarflexor) and iliopsoas (hip flexor)[331]. However, due to the use of foot-lifters in the Lokomat, the activation of the gastrocnemius

is partly reduced [332–334]. This requires, as compensation, to produce an increased hip flexion rate and quadriceps EMG activity at the end of stance phase to lift the foot above the treadmill [271, 333]. While the less impaired patients were able to cope with this demand, the more severely affected patients could not reach the knee flexion velocity required by the Lokomat during the double support phase, as suggested by the high residual damping required at DS2.

We believe that, if more data from non-ambulatory subjects with different level of function were collected, it would be possible to generate a model (possibly adding one or two other predictors) that explains continuously the "walking ability" as shown in Figure 1.1. In non-ambulatory patients, this assessment would show how close they are to recover walking. However, it would be challenging to validate this assessment, since we would need a way to measure how close non-ambulatory subjects are to regain some walking function. Possibly, a study in acute and sub-acute patients, rather than chronic, will help address this question. One could follow the same patients longitudinally and see if improvements in functional and impairment scales are paralleled by improvements in the AAN outcome measures.

It is also not possible to explain the 10MWT of able-bodied subjects with the AAN outcome measures. The performance in the AAN-based assessment is affected by the underlying impairment of the subjects and it is not capturing physiological differences in walking speed in unimpaired individuals, therefore this result should not be surprising. Moreover, able-bodied subjects often try to impose their own foot trajectory while walking in the Lokomat, thereby deviating from the reference trajectory imposed by the device. While the deadband implemented in this adaptive algorithm tried to address this problem, it may be insufficient to accommodate completely the physiological variability in gait pattern expressed by able-bodied subjects.

The main predictor selected in the patient population (K knee TS) was specific for the impairment, while the isometric torque at hip flexion seemed to be an important predictor of speed both in the patients and able-bodied populations. There is evidence in literature that maximum isometric hip joint torque is a significant predictor of gait speed in people after stroke [335] and spinal cord injury [323]. In able-bodied subjects, there is some evidence that lower limb muscle strength correlates with gait speed [336–338]. Our unimpaired subjects had a mean age of 42.3 ± 15.5 years, with the oldest being 64 years old. It was shown that preferred walking speed decreases on average by 16% per decade after age 60 [330], therefore the age effect was likely not relevant for our sample.

5.8 DISCUSSION

In this study we showed the relationship between data measured with a robot-aided gait assessment and clinical scores measuring walking ability. We also examined how measures of isometric joint torques would contribute to the assessment of walking. The AAN-based assessment tested in this study

could be performed by ambulatory and non-ambulatory patients during training and it is feasible in everyday clinical practice. The isometric joint torques could be measured with the same device.

We were able to identify an informative predictor of overground walking speed in ambulatory patients: the support (stiffness of the impedance controller) required from the robotic exoskeleton at the knee during terminal swing. This predictor was consistently selected during the bootstrap procedure and, alone, it could be used to generate a model able to explain 74% of the variance in the 10MWT data and 61% in the TUG data. The ability to correctly place the foot on the treadmill at the end of swing phase seemed to relate directly to the walking ability of the patients as measured by the 10MWT and TUG.

The assessment of isometric joint torque added an important predictor to the model and improve the accuracy of prediction of speed of both tests, but especially in the TUG, where it seemed to be even more important than the predictor K knee TS.

It can be hypothesized that the performance measured in the AAN-based assessment is mainly due to motor control and to the ability of modulating the force, rather than to the ability of applying high forces. The task of following a reference trajectory with the ankle requires indeed a timely accurate coordination of the hip and knee joints and the ability to process the visual information displayed on the screen while providing the correct motor commands. In order to walk, we need, however, more than motor control, and force is undoubtedly one of the other main components of walking function [16]. The isometric torque assessment seemed, thus, a good complementary assessment to the AAN-based assessment.

Regarding non-ambulatory patients, we could identify some promising outcome measures to explore in future studies: stance phase and double support phase seemed to clearly separate non-ambulatory subjects from the others and they will likely also carry the information useful to differentiate between non-ambulatory patients with different level of function.

The fact that unimpaired subjects did not conform to the model suited for the ambulatory patients confirms that what we found within this study is a sign of impairment rather than due to individual speed variations. The predictor selected among the isometric torque values (hip flexors maximum torque) seemed to be instead a common predictor of speed in both populations.

One of the concerns that clinicians have about robotic gait trainers is that the environment where the people train is too artificial and different from overground gait and that, therefore, the assessments performed in a robotic gait trainer are not ecologically valid. Moreover, the support provided by the device may mask what the patient can actively do. We showed, instead, that it is possible to measure in a robotic gait trainer functions that are related to overground performance in walking tests such as the 10MWT and TUG.

5.8.1 Limitations and Challenges

Despite being able to identify two good predictors of walking speed (robotic stiffness required at terminal swing and isometric hip flexor force), we cannot state, with the available data, that a robotic assist-as-needed control as we implemented it in the Lokomat, is valid and reliable enough to be used as assessment of 'walking ability' in the clinic.

The intra-rater reliability between two sessions needs to be improved before the test can be used in clinical practice. Several factors may have affected the reliability of the measures. First, a learning effect between sessions was still present despite having included in the protocol a first session of familiarization. Second, the measurements of joint angles in the Lokomat depends on the alignment between the robotic and the human joints. Even if we tried to position the subject always in the same way and to use always the same hardware and software setting, it is challenging to have perfectly reproducible conditions. Third, the AAN-based assessment relied on subjective attention and concentration during the task. It is likely that cognitive and visual aspects had an influence on the outcomes, as already noticed in literature [339]. Lastly, the reference gait trajectory used in the study was subjectively adapted to the subject's individual gait pattern in the first visit, according to the experience of the examiner that performed the test. It may be that the additional challenge of following a gait pattern different from one's own resulted in a more variable performance that impacted negatively the validity and the reliability of the assessment. Based on these considerations, more practice should be allowed before performing the assessment and a personalized reference gait trajectory should be determined prior to the start of the assessment. The trajectory could be defined based on anthropometric measures [22] or on database-driven methods, taking a pool of physiological trajectories as templates [340]. Alternatively, the error metric for the adaptation of the impedance, which is now based on the kinematic deviation between reference and actual trajectory, should be based, for example, on the success in different sub-tasks of walking (e.g. stability in stance, foot placement) [341].

The adaptation algorithm theoretically adapted the GF in a range between 0 and 100%. However, we saw that, depending on the weight of the patient's limbs, on the severity of impairment and on the BWS value, a value of GF much lower than the maximum is sufficient to walk in the Lokomat. The highest hip and knee GF required by a subject in our study, average during the whole gait cycle, was 20% (with a BWS equal to 80% of the body weight). This means that the actual range where the subjects can show the impairment is limited and meaningful information can only be seen after the GF has reached this low value (after 15 steps).

One of the major weaknesses of this study is that we could not develop a model to predict the walking-related functions of the patients continuously from the non-ambulatory to the ambulatory phase. The robotic gait trainers seem to provide better therapeutic results in people with severe gait impairments [19], who are also the most frequent users of these devices. Moreover, these patients have fewer possibilities of being assessed since they cannot perform the timed tests. More data from non-ambulatory

subjects with different level of severity needs to be collected to see if the variables identified in Section 5.7.2.1 are meaningful predictors of function in severely and moderately affected patients. A longitudinal study in patients with acute or sub-acute lesions should be carried out to understand how the AAN outcome measures change over time in the same patients. Studying the recovery within the same patients will show if individual changes can be measured by the AAN-based assessment. Other populations with neurological impairments need to be tested to check if the predictors of walking speed identified for SCI are applicable also to other pathologies.

One important question that this study raises is how to validate novel objective assessments. We faced the conundrum of trying to validate an assessment that claims to be more objective than existing assessments against the same standard assessments that we were trying to improve. The 10MWT and TUG had a clear floor effect that prevented to assess people that could not walk. The other scores (WISCI II, BBS, FAC, MMT, AIS) were ordinal-based and too coarse-grained to be directly compared with the Lokomat measures. To address this issue, one should either include in the validation study more sophisticated assessments of gait (e.g. motion capture gait analysis) or, as we demonstrate in 0, develop a controlled environment to simulate known neuromotor impairments and study if the novel assessment can correctly measure them.

Lastly, the model used to predict the walking tests is a simple linear regression: it may be that a generalized linear model with another link function would lead to better predictions. Also, the interaction between different variables, especially between the BWS and the other AAN outcome measures needs to be better explored.

5.8.2 Implications for Walking Training Paradigms

We could demonstrate that the robotic support correctly adapted to different level of impairment, from the most severely affected patients to the individuals with a walking function close to normal. The software was safe and challenging at the same time, and all the patients could use it.

The identification of certain predictors for speed of walking overground leads to the question: do individuals improve their walking speed when the values of their predictor variables change in the appropriate direction? This question is worth further investigation, but it is beyond the scope of this study. The data confirmed the importance of standing stability in the early phase of gait recovery and the need to develop a more precise control of the step to improve, once the basic standing function is recovered. Secondly, the patients should be able to provide an adequate propulsion of the leg during double support phase. As a last requirement, a correct foot placement at terminal swing seems to be important. These functions could be trained with the help of robots that allow to reduce the support unevenly throughout the gait cycle and to visualize on the screen the performance for a proper feedback to the patient and therapist.

Robotic gait trainers allow the therapists to adapt the support parameters (e.g. limb guidance and body weight support) manually to challenge the patient in an optimal way. However, these functions are not often used in clinical practice because clear guidelines on the progression of these parameters are lacking and the consequences of the changes on the therapeutic outcomes are not clear. Adaptive algorithms, such as the one developed for this study, can be used safely for determining the optimal level of assistance for every patient. They could be integrated as standard training modalities and be used as assist-as-needed training paradigms, rather than as assessment.

5.9 CONCLUSION

We showed in this study that one variable alone measured during training in the Lokomat can explain most of the variance of the timed walking tests. The addition of an isometric force measure collected in a specific test available in the Lokomat (L-FORCE) makes the explained variance of the models increase above 85%. These results are very promising because they show that walking ability can be measured in a robotic gait trainer in a safe and efficient way. Further efforts should improve the model to predict the clinical scores from the AAN outcome measures, extending this also to patients that cannot walk yet, and increase the reliability of the measures. These steps will help to move closer to the long-term goal of developing a valid and reliable test that, with a standardized protocol and few measures, can assess walking ability in patients will all levels of severity and be quickly and easily administered during training. Accessible assessments mean personalized therapy, possibility of demonstrating improvements to insurances and increased patient's motivation with positive effects on his/her recovery.

Chapter 6   HYBRID JOINT/END-POINT SPACE CONTROLLER

The content of this chapter is partly extracted from the following publication and it was adapted to ensure consistency within the chapter and with the rest of the document and to avoid repetitions:

Maggioni S, Reinert N, Lünenburger L, Melendez-Calderon A. *An Adaptive and Hybrid End-Point/Joint Impedance Controller for Lower Limb Exoskeletons.* Front Robot AI. 2018;5. © 2018 Maggioni, Reinert, Lünenburger and Melendez-Calderon. Reprinted under the terms of the Creative Commons Attribution 4.0 International License[3].

Foreword

The clinical study pointed out that the most important AAN outcome measure to explain walking ability is related to the control of the foot at terminal swing. It also raised the concern that the joint space controller was not compliant enough to physiological deviations not considered as errors. This led to the development of a hybrid joint/end-point space controller, which combined the strengths of the implementation in joint space and those of the implementation in end-point space. This approach – combined with the AAN controller in end-point space – allows the end-point impedance to adapt to the magnitude and the direction of the error performed in the foot trajectory, providing a resulting end-point force acting only in the direction of the error.

---

[3] http://creativecommons.org/licenses/by/4.0/

6.1 INTRODUCTION

In Chapter 5, we tested an assist-as-needed controller implemented in joint space as described in Chapter 3. The analysis of the data collected during the experiments with Spinal Cord Injury patients revealed that foot contact is the most informative gait phase on walking ability in ambulatory subjects.

In the second place, we realized that validity and reliability may have been negatively affected from some controller characteristics: the deadbands around the reference joint trajectory were defined ad-hoc and not based on safety constrains such as minimum step length and height to avoid contacts with the treadmill. The joint space controller was not able to be compliant in directions where support was not needed and people with high level of function often tried to impose their own gait trajectory, resulting in an increased impedance generated from the AAN controller.

These critical points led us to consider the development of an advanced modified version of the AAN controller implemented in joint space, by exploring the possibility of adding an end-point impedance adaptation mechanism to the original joint impedance adaptation algorithm.

In this chapter, we analyze the characteristics and limitations of controllers defined in two commonly used formulations: joint and end-point space, exploring especially the implementation of an AAN algorithm. We propose then, as a proof-of-concept, an AAN impedance controller that combines the strengths of working in both spaces: a hybrid joint/end-point impedance controller. This approach gives the possibility to adapt the end-point stiffness in magnitude and direction in order to provide a support that targets the kinematic deviations of the end-point with the appropriate force vector. This controller was implemented on the Lokomat®Pro V5 (Hocoma AG, Switzerland) and tested on 5 able-bodied subjects and 1 subject with Spinal Cord Injury. Our experiments show that the hybrid controller is a feasible approach for exoskeleton devices and that it could exploit the benefits of the end-point controller in shaping a desired end-point stiffness and those of the joint controller to promote the correct angular changes in the trajectories of the joints. The adaptation algorithm is able to adapt the end-point stiffness based on the subject's performance in different gait phases, i.e. the robot can render a higher stiffness selectively in the direction and gait phases where the subjects perform with larger kinematic errors. The proposed approach can potentially be generalized to other robotic applications for rehabilitation or assistive purposes.

The choice of how an adaptive impedance controller is formulated inevitably determines how complex it is to address any potential hazard situation arising from reduced impedance. Here, we analyze the characteristics and limitations of controllers defined in two commonly used formulations: joint and end-point space, exploring especially the implementation of AAN controllers in these two spaces. A comparative analysis of these two approaches has been reported for industrial manipulators [342, 343] but, to the best of our knowledge, such comparison has not been extensively examined within the context of rehabilitation robotics and even less in *lower limb* applications.

After analyzing the properties of these two approaches for the control of lower limb exoskeletons, we propose an AAN impedance controller that combines the strengths of working in both spaces: a hybrid joint/end-point impedance controller. This controller gives the possibility to adapt the end-point stiffness in magnitude and direction, to provide a support that targets end-point deviations with the appropriate force vector. We present the proof-of-concept for this hybrid controller based on simulations and tests conducted with five able-bodied subjects and one subject with walking impairment due to a complete spinal cord injury. The proposed approach can potentially be generalized to other robotic applications for rehabilitation or assistive purposes.

6.2 JOINT VS END-POINT SPACE FORMULATIONS

To analyze the impedance properties of the joint and end-point control approaches for the control of lower limb exoskeletons, we present the impact that these two formulations have on the end-point stiffness. The stiffness can be visualized as an ellipse, whose major axis indicates the direction of maximum stiffness [344, 345]. The stiffness ellipse captures the geometrical features of the force field around a reference position of the end-point. In the force field representation, we can visualize the direction and magnitude of the restoring forces for displacements around the reference trajectory. For further details on the calculation of stiffness ellipses and force field, see the Appendix E .

6.2.1 Impedance Control Based on Joint Space Formulation

In most exoskeleton devices, the actuators control the flexion and extension of the robotic joints, which roughly align to the human joints. Therefore, the impedance controllers normally are implemented to compute the actuators torques in order to follow reference trajectories defined in joint space (e.g. hip and knee angles). A joint controller can be applied both in the stance and the swing phase of gait, because the actual joint trajectory q_{act} and the reference trajectory q_{ref} are defined continuously during the whole gait cycle and do not depend on the kinematic configuration (e.g. open chain in swing phase or closed chain in double-support phase). A joint space formulation avoids problems that might arise from inverse kinematics/dynamics calculations, especially in kinematic configurations (specific combinations of hip/knee angles) where the Jacobian matrix is singular.

A detailed description of a controller formulated in joint space for a lower limb exoskeleton can be found in Chapter 3 of this thesis.

6.2.1.1 Impact of Joint Space Formulation on End-Point Stiffness

Potential hazards during walking can come from unwanted interactions between the foot and the floor (or treadmill). Therefore, we examined the forces at the ankle level that may result in such unwanted interactions. These forces were generated by a controller defined in joint space, given foot displacements of different amplitude and directions throughout the swing phase. We obtained the

resulting end-point forces (force field) using the Jacobian matrix of the two-links robot (see Appendix E).
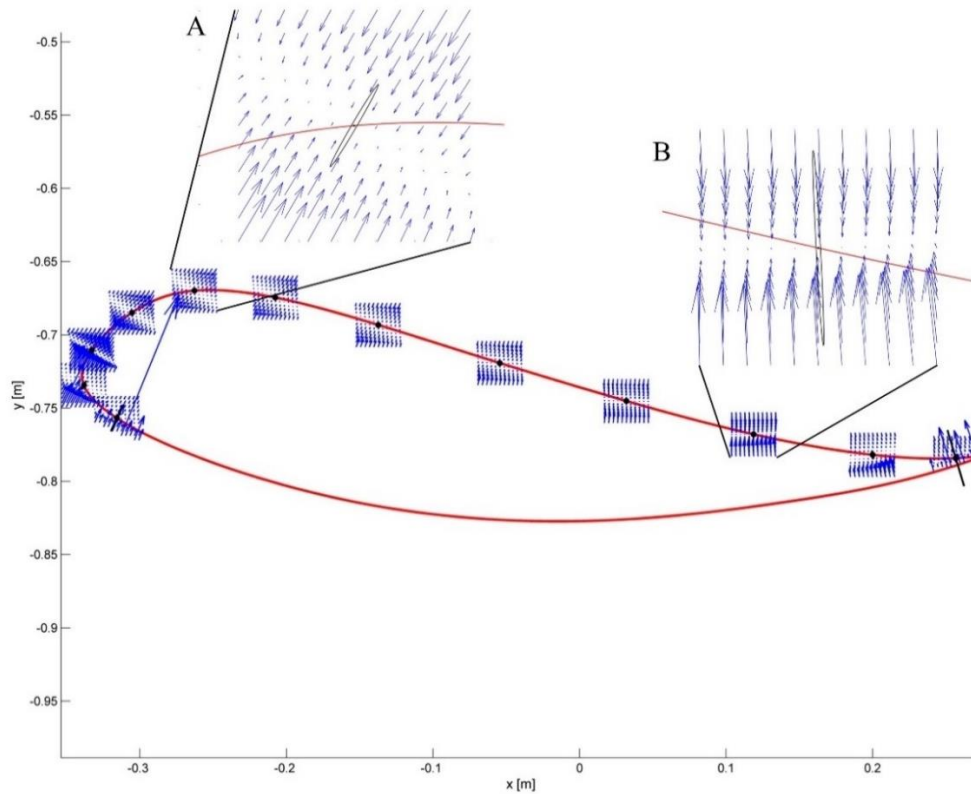

Figure 6.1: The force field resulting from a joint space impedance controller is shown at some selected points along the ankle trajectory. The restoring forces do not always point towards the reference position. Two critical points are magnified. A) Point of maximum foot clearance: the vectors show that enough support is guaranteed if the ankle is below the reference trajectory. The ellipse in black represents the end-point stiffness resulting from the joint stiffness. B) At the end of the swing phase, if the subject is late with respect to the reference point, it can experience forces directed downwards instead of forward. © 2018 Maggioni, Reinert, Lünenburger and Melendez-Calderon. Reprinted, with permission, from the original article [314]*.*

In Figure 6.1, we show the force field for different points during the pre-swing and swing phase. In this case, hip and knee stiffness are constant throughout the gait cycle, but the resulting end-point stiffness varies depending on the angular configuration of the joints. The magnitude and direction of joint torques and end-point forces applied by a joint controller on a real trajectory are presented in Figure 6.2. Two main requirements for functional walking are adequate foot clearance and foot placement at the end of swing [30, 33]. Therefore, we examined these two phases in detail. As the reader can appreciate, the restoring forces around the foot are not always directed towards the reference trajectory (note that the reference trajectory is defined in joint space, but it is transformed to end-point space for visualization purposes). Consider the situation where a subject is not able to sufficiently lift the foot from the ground at the beginning of swing phase: as we can see in Figure 6.1A and Figure 6.2B, the joint controller is able to provide forces that are directed towards an adequate foot clearance position. On the other hand, if the subject is not able to perform a sufficiently long step (e.g. due to insufficient hip flexion or reduced knee extension at the end of swing), or if his foot is lagging behind the reference position, the actual position of his ankle can fall in an area where the forces rendered by the controller direct the foot towards the ground, instead of lifting it to guarantee a sufficient step length. It is

interesting to compare how the same controller acts in the two different spaces; we can obtain insights that are not possible by studying the joint torques and end-point forces in isolation.
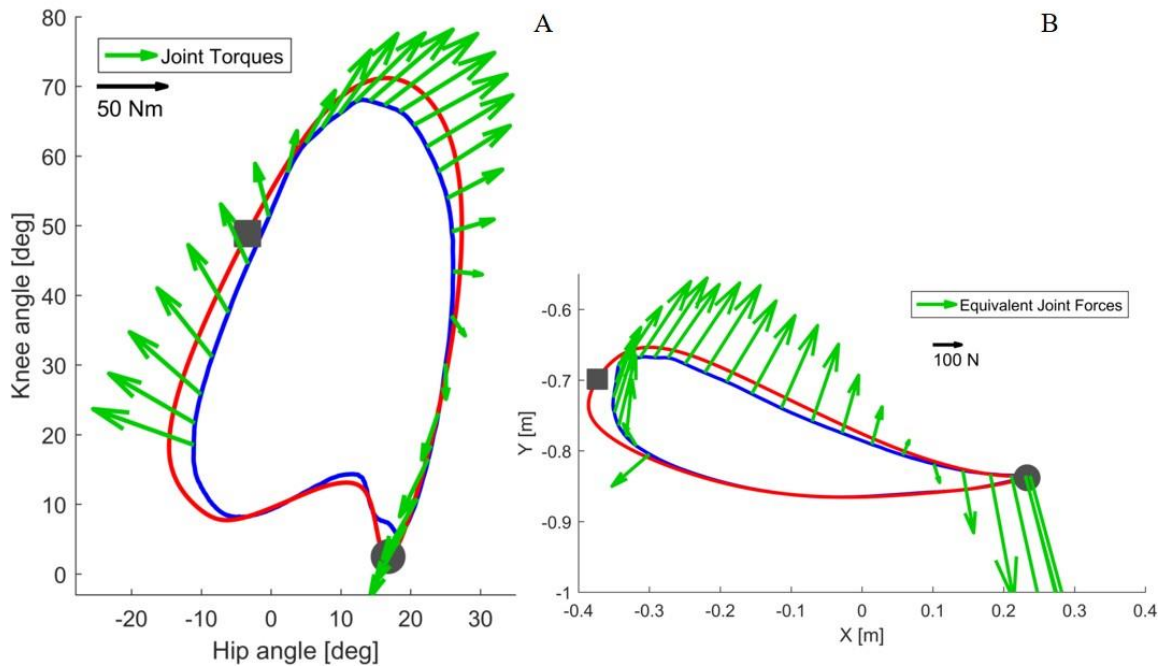
Figure 6.2: In correspondence of a real trajectory (blue line) deviating from the reference trajectory (red line), the joint controller generates the torques shown in Panel A. The same torques can be visualized in end-point space (Panel B) as equivalent end-point forces (see Appendix for calculation (A.4)). Refer to the scale for information on the magnitude of the torques and forces. The beginning of the stance phase is marked with a grey circle, while the beginning of the swing phase is marked with a grey square. © 2018 Maggioni, Reinert, Lünenburger and Melendez-Calderon. Reprinted, with permission, from the original article [314].

6.2.1.2   *Joint Space Formulation of an AAN Controller*

In Chapter 3, we presented an AAN algorithm that automatically adapts the Lokomat actuators' impedance based on the ability of the subject to follow a reference gait trajectory. The estimator of the subject's performance relied on the kinematic deviation between the actual trajectory and the reference. The error weighting function $f_1(\mathbf{e})_w$ consisted of a hyperbolic tangent function of the kinematic error e defined for each window w, which allowed physiological deviations from the reference trajectories of the hip and knee joint, while ensuring safety (Figure 3.4). This means that for each time point of the gait cycle, the subject's hip and knee are allowed to deviate from the reference trajectory within the deadbands defined for each joint, independently from each other and irrespective of the position of the end-point. To study how the angular boundaries defined in joint space result in end-point space, we apply forward kinematics (see Appendix E) to render the resulting boundaries around the end-point (i.e. at the ankle), as illustrated in Figure 6.3.

Figure 6.3: In the joint controller hip and knee deadbands are defined independently from each other, as shown in the panel A (hip angle) and B (knee angle). The reference trajectory (red) is taken from [55]. The deadbands (black lines) are calculated from the standard deviation of the trajectories of 10 able-bodied subjects walking in the Lokomat with impedance set to 5% of the maximum, which allows freedom of movement. 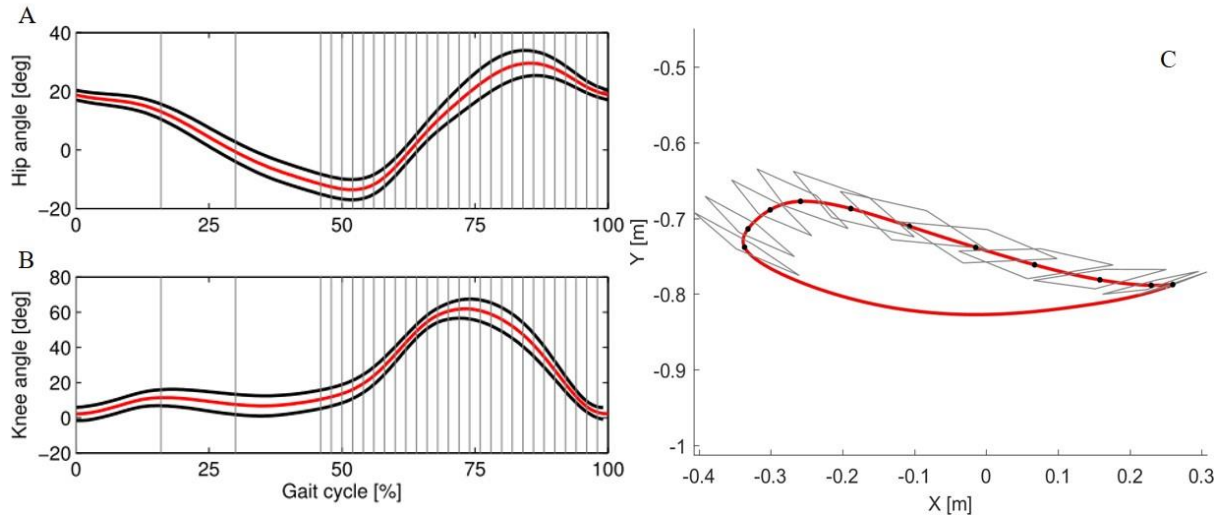In the AAN algorithm, deviations occurring within the deadbands lead to a null error. The gait cycle is divided in 30 windows (grey lines show the windows' limits). In panel C, the resulting reference trajectory (red) and the corresponding deadbands in end-point space are shown. For each window along the swing phase (only 15 are shown for clarity of representation), the grey rhomboid shows the area including all the possible combinations of hip and knee angles within the deadbands shown in Panel A and B. © 2018 Maggioni, Reinert, Lünenburger and Melendez-Calderon. Reprinted, with permission, from the original article [314].

Due to the non-linearity of the kinematic transformation and its dependency on the joint configuration, the shape of the boundaries resulting at the end-point is hardly predictable from what can be seen in joint space. During the push-off phase and at the beginning of swing, the boundaries are extremely narrow along the direction of the foot motion. This results in a very strict timing requirement for the subject walking in the robot (i.e. the subject must closely follow the desired ankle position at any time). Even small deviations along the directions of motion can result in a high error, which causes the algorithm to increase the impedance in this specific gait phase. However, in the direction perpendicular to the reference trajectory, higher deviations are allowed, and they could potentially result in insufficient foot clearance. Conversely, during mid-swing, the resulting shape of the joint space deadbands is less conservative along the direction of the trajectory, allowing increased leading or lagging of the foot with respect to a reference position. At the end of swing, again the shape of the boundaries in end-point space changes: here the boundaries allow the subject to perform longer or shorter steps than desired.

6.2.2 Impedance Control Based on End-Point Space Formulation

An alternative option to a joint space formulation is an *end-point space formulation* (sometimes referred to as *task space formulation*), in which the reference trajectory is defined according to an anatomical landmark around an end-point. In walking, the definition of end-point depends on the kinematic configuration, e.g. lateral malleolus or foot metatarsal during swing phase; or trochanter during stance phase, as the foot is already placed on the ground. Thus, formulating the problem in end-point space for lower limb exoskeletons may require two different control approaches: one for stance and another one for swing. While implementation of this approach may be cumbersome in practice, a

controller during swing that relies on an end-point space formulation may provide additional benefits compared to a joint space approach. In this paper, we are interested in studying the control of the end-point impedance only in the swing phase of gait.

In an end-point space formulation, the torque applied to the exoskeleton actuators is derived from an end-point force $\mathbf{F}_x$ (Eq. 6.1). This force depends on a set of stiffness, $\mathbf{K}_x = [K_{xx}, K_{xy}; K_{yx}, K_{yy}]$, and damping, $\mathbf{B}_x = [B_{xx}, B_{xy}; B_{yx}, B_{yy}]$, parameters and a kinematic error between a measured end-point trajectory, $\mathbf{x}_{act} = \left[x_{act}, y_{act}\right]$, and a reference trajectory, $\mathbf{x}_{ref} = \left[x_{ref}, y_{ref}\right]$. Note that x_{ref} and x_{act} can be calculated in real-time by using forward kinematic equations that depend on the measured joint angles q_{ref} and q_{act} and known limb segment lengths of the user (see Appendix E). The accuracy of this calculation, however, depends on the correct measurement of the segments' lengths and on the alignment between the robotic joints and the human joints.

$$F_x = K_x \cdot \left(x_{ref} - x_{act}\right) + B_x \cdot \left(\dot{x}_{ref} - \dot{x}_{act}\right); \qquad (6.1)$$

Using the Jacobian matrix $\mathbf{J}(\mathbf{q}_{act})$, we obtain through inverse dynamics the torque that the joint actuators need to render the force F_x:

$$\tau_x = J^T\left(q_{act}\right) \cdot F_x; \qquad (6.2)$$

6.2.2.1 Impact of End-Point Space Formulation on End-Point Stiffness

Similar to Section 6.2.1.1, we would like now to examine the forces acting at the level of the foot when end-point control is used. By design (Eq. 6.1), at each point of the swing phase, the restoring force for every deviation in Cartesian space is directed towards the reference end-point position (Figure 6.4), which is the point that could have potentially critical collisions with the environment (e.g. stumbling). The axes of the stiffness ellipse can be modified in magnitude and direction as desired. For example, a higher stiffness in the direction of gravity can be designed. However, singularities exist which prevent the end-point controller from generating joint torques in correspondence of those points (i.e. when the knee is completely extended at the end of swing).

Now consider the end-point forces generated when an end-point controller is used with a real trajectory. The force field set as shown in Figure 6.4 leads, in the case of the real trajectory presented in Figure 6.5B, to forces directed towards the reference trajectory in end-point space. Figure 6.5A shows the same forces transformed to torques (Eq. A.19). As visible in the graph, the joint torques in this case do not always point towards the joint reference trajectory, especially at initial swing, the phase that is crucial for determining a safe foot clearance through an appropriate knee flexion. When the foot is lagging behind the reference trajectory in end-point space, the end-point controller tries to push the foot forward by increasing the hip flexion, while not acting on the knee. This is evident in Figure 6.5A where, at the point of maximum knee flexion, the torques have an almost null component acting on the knee.

This problem might cause insufficient foot clearance and potential undesired foot contact with the treadmill.
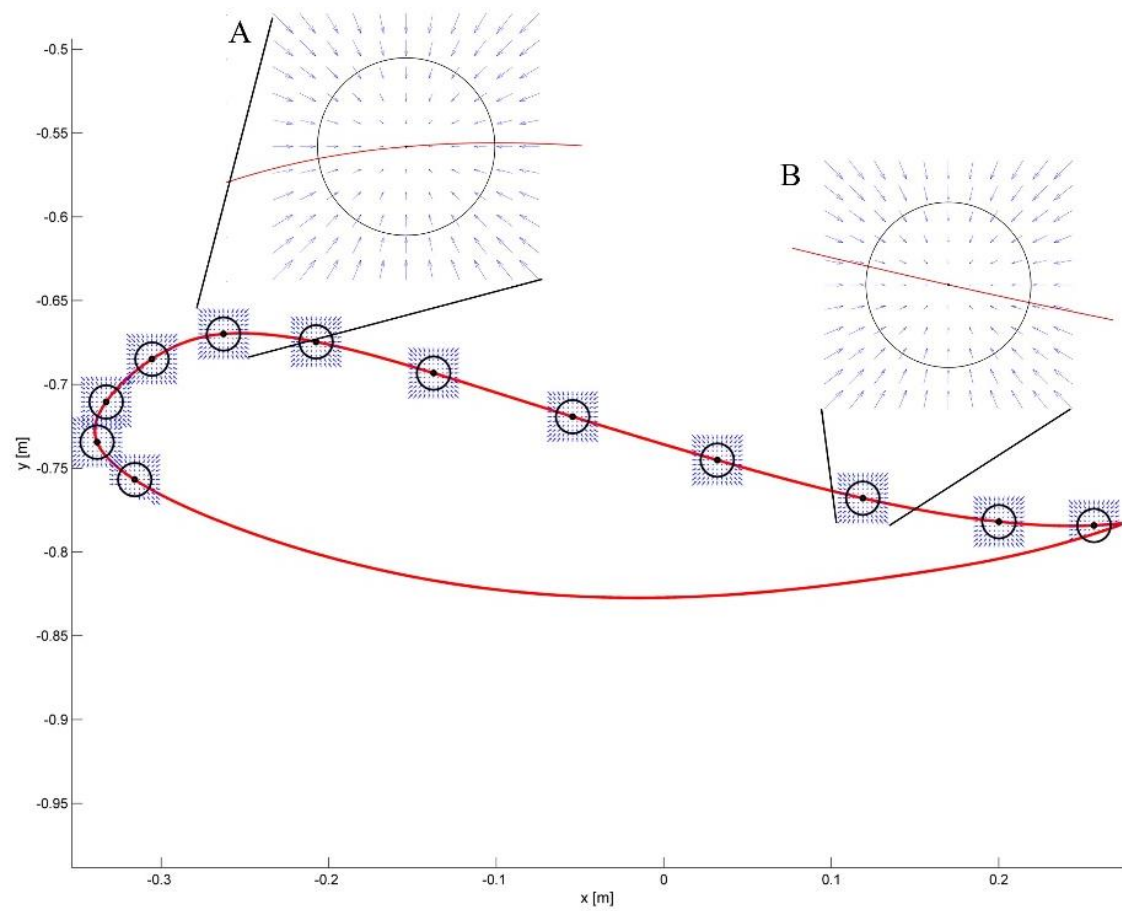
Figure 6.4: The desired force field in task-space is shown at some selected points along the end-point trajectory. The force field always points towards the reference position. Two critical areas are magnified. A) Point of maximum foot clearance: the circle in black represents the desired end-point stiffness. The arrows show that regardless of the deviation from the reference point, the restoring force results always in a force directed to the reference point. B) At the end of the swing phase, the desired characteristics of the force field are the same as in A. © 2018 Maggioni, Reinert, Lünenburger and Melendez-Calderon. Reprinted, with permission, from the original article [314].
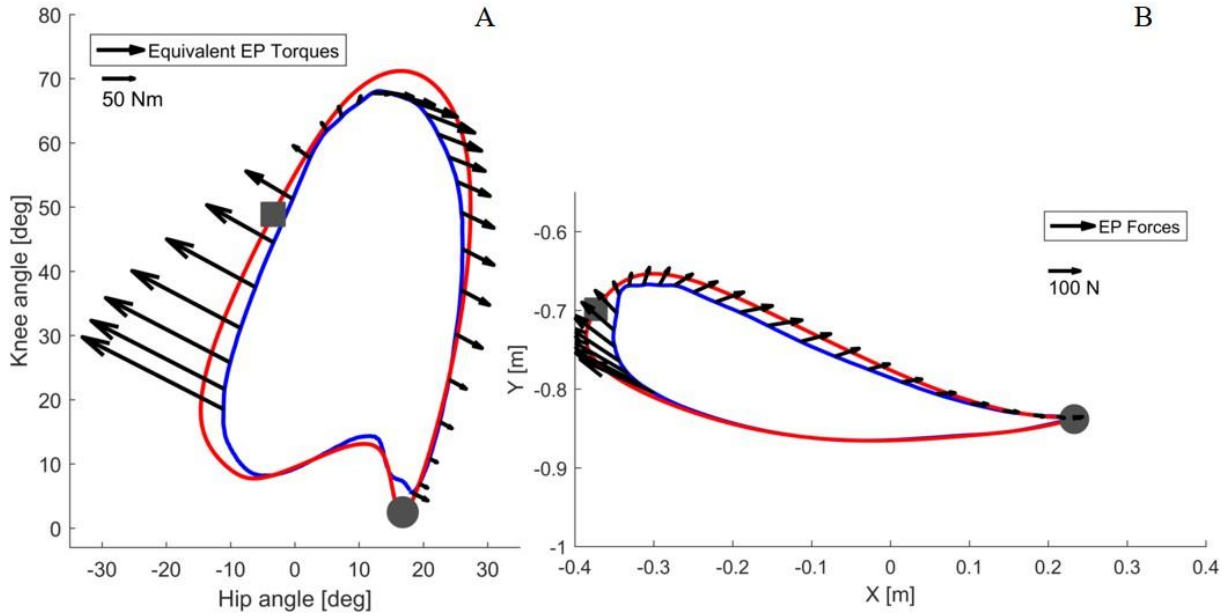
Figure 6.5: In correspondence of a real trajectory (blue line) deviating from the reference trajectory (red line), the end-point controller generates the forces shown in Panel B. The same forces can be visualized in joint space (Panel A) as equivalent joint torques (see Appendix for calculation (A.6)). Refer to the scale for information on the magnitude of the torques and forces. The beginning of the stance phase is marked with a grey circle, while the beginning of the swing phase is marked with a grey square. © 2018 Maggioni, Reinert, Lünenburger and Melendez-Calderon. Reprinted, with permission, from the original article [314].

6.2.2.2   End-Point Space Formulation of an AAN Controller

In this type of controller, the parameters P adapted based on Eq. 3.2 are the end-point stiffness and damping ($\mathbf{K}_x$ and $\mathbf{B}_x$). Having control over the task space impedance allows the implementation of AAN controllers that provide optimal assistance to the end-point. Indeed, the task space force field can be shaped in order to support the foot only in the directions that are needed. Furthermore, designing the deadbands in end-point space allows requirements such as minimum foot clearance or minimum step length to be set directly.

6.2.3   Summary of Working in Different Spaces

The two controllers show very different features when applied to a two-link exoskeleton and it is not possible to prefer one over the other independently of the application. In Table 6.1, we summarized the strengths and weaknesses of the two control formulations. The symbols "+" and "-" indicate whether the formulation can adequately address the specific features listed. These aspects have also been nicely addressed in [342], where the performance of joint and end-point controllers is compared in an industrial manipulator.

PERFORMANCES OF JOINT AND END-POINT SPACE FORMULATION

Features	Joint space formulation	End-point space formulation
Use in stance and swing phase	+	-
Intuitive definition of foot clearance and foot placement as safety parameters	-	+
Intuitive definition of deadbands for an ANN controller	-	+
Directional adaptation of end-point stiffness to provide adequate foot guidance	-	+
Intuitive control of robot (e.g. no need of inverse kinematic calculations)	+	-
Easy to deal with singular kinematic configurations	+	-

Table 6.1: Summary of the performances of joint and end-point formulations for the control of a two-link exoskeleton

6.3 HYBRID JOINT/END-POINT SPACE CONTROLLER WITH ASSIST-AS-NEEDED

In Section 6.2, we highlighted strengths and weaknesses of the two formulations: joint and end-point space. Here, we propose an adaptive controller that is formulated in both spaces ("hybrid" formulation) and aims to combine the strengths of both approaches. An end-point space component aims at adapting the end-point stiffness in both magnitude and direction to provide a guided foot placement; while a joint space component aims at providing appropriate temporal coordination between hip and knee angles, especially when the kinematic configuration of the exoskeleton is close to a singularity. This hybrid approach also gives the possibility of defining deadbands more intuitively (based on foot position), which gives more control over the interactions with the environment.

The torques applied during the swing phase of gait, $\boldsymbol{\tau}_{swing}$, are the sum of torques generated by a PD controller based on the end-point position and end-point velocity error (Eq. (6.4)), torques generated by a D controller based on the angular velocity error in joint space (Eq. 6.5), and compensation, as illustrated in Figure 6.6:

$$\boldsymbol{\tau}_{swing} = \boldsymbol{\tau}_{xPD} + \boldsymbol{\tau}_{qD} + \boldsymbol{\tau}_{comp} \tag{6.3}$$

$$\boldsymbol{\tau}_{xPD} = J[\boldsymbol{q}_{act}]^T \cdot \boldsymbol{K}_x \cdot (\boldsymbol{x}_{ref} - \boldsymbol{x}_{act}) + J[\boldsymbol{q}_{act}]^T \cdot \boldsymbol{B}_x \cdot (\dot{\boldsymbol{x}}_{ref} - \dot{\boldsymbol{x}}_{act}); \tag{6.4}$$

$$\boldsymbol{\tau}_{qD} = \boldsymbol{B}_q \cdot (\dot{\boldsymbol{q}}_{ref} - \dot{\boldsymbol{q}}_{act}); \tag{6.5}$$

The end-point controller is designed to control the magnitude and direction of the forces required in task-space. Since the reference trajectories in joint space are derived from trajectories in task space, one can express the controller terms as:

$$\boldsymbol{\tau}_{xPD} + \boldsymbol{\tau}_{qD} = \boldsymbol{K}_{tot} \cdot (\boldsymbol{q}_{ref} - \boldsymbol{q}_{act}) + \boldsymbol{B}_{tot} \cdot (\dot{\boldsymbol{q}}_{ref} - \dot{\boldsymbol{q}}_{act}) \tag{6.6}$$

$$\boldsymbol{K}_{tot} = \boldsymbol{J}[\boldsymbol{q}_{act}]^T \cdot \boldsymbol{K}_x \cdot \boldsymbol{J}[\boldsymbol{q}_{act}] \tag{6.7}$$

$$\boldsymbol{B}_{tot} = \boldsymbol{J}[\boldsymbol{q}_{act}]^T \cdot \boldsymbol{B}_x \cdot \boldsymbol{J}[\boldsymbol{q}_{act}] + \boldsymbol{B}_q \tag{6.8}$$
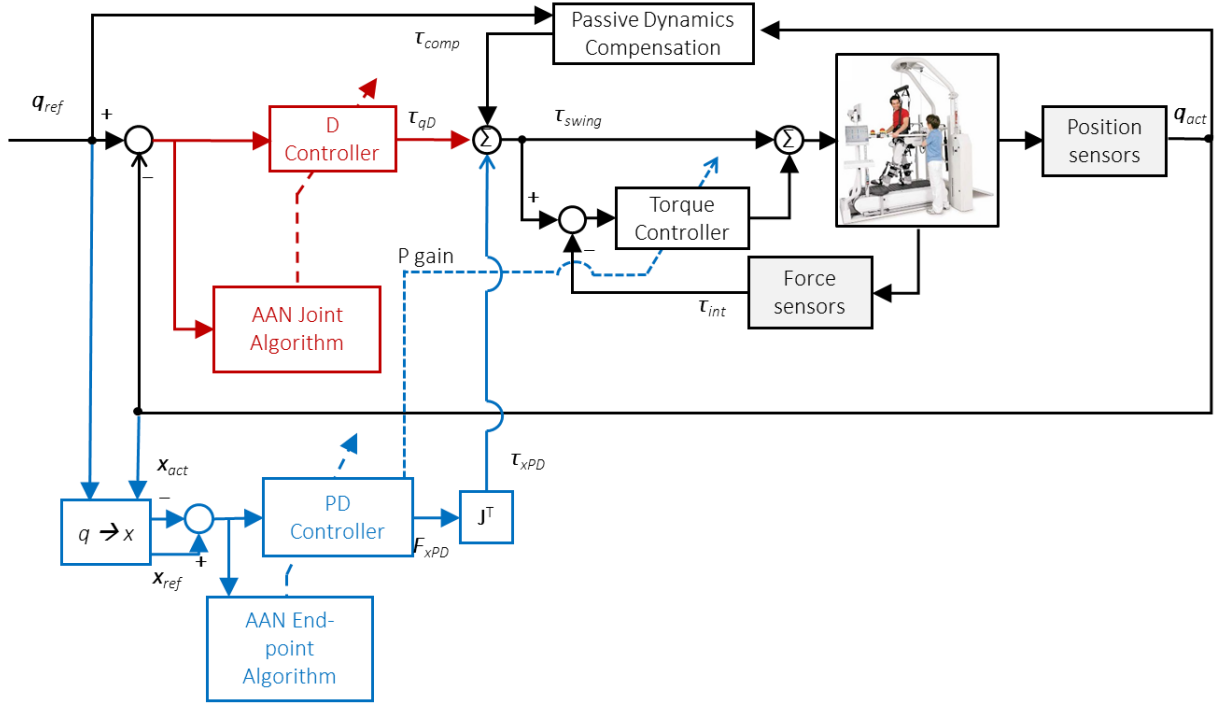
Figure 6.6: Control diagram of the adaptive hybrid joint / end-point controller during the swing phase of gait. The transparency of the exoskeleton is obtained through a torque feedback loop (torque controller). The torque controller provides a torque proportional to the error between the desired torque τswing and the measured torque τint, in order to minimize this same error. Transparency is improved through the optimization of passive dynamics with a method called Generalized Elasticities [283]. Detailed information on the low-level control architecture can be found in [284] and [346]. © 2018 Maggioni, Reinert, Lünenburger and Melendez-Calderon. Reprinted, with permission, from the original article [314].

The actual stiffness and damping in end-point space, $\mathbf{K}_x$[N/m] and $\mathbf{B}_x$[Ns/m], are obtained from a normalized stiffness and damping $\overline{\mathbf{K}}_x$ and $\overline{\mathbf{B}}_x$ matrices, which are then scaled according to the specific characteristics of the robot. The normalized joint damping term $\overline{\mathbf{B}}_q$ can be adapted according to Eq. 3.4. $\overline{\mathbf{B}}_x$ can be adapted either with a similar algorithm or coupled to $\overline{\mathbf{K}}_x$.

For the term $\overline{\mathbf{K}}_x$ we would like an AAN algorithm that adapts both the magnitude and direction of the equivalent stiffness ellipse based on the kinematic errors performed throughout the swing phase.

To achieve this the swing phase is divided into equally sized windows. For each window w and for each step s, we adapt the stiffness based on the weighted error at the previous step, both in magnitude and in direction, as:

$$\overline{K}_{x_{s+1,w}} = \gamma_x \cdot \overline{K}_{x_{s,w}} + f_{K_x}[e_{x_{s,w}}] \cdot R[\alpha_{s,w}] \cdot G_K \cdot R[\alpha_{s,w}]^T; \tag{6.9}$$

$$e_{x_{s,w}} = \begin{bmatrix} x_{ref_{s,w}} - x_{act_{s,w}} \\ y_{ref_{s,w}} - y_{act_{s,w}} \end{bmatrix}; \tag{6.10}$$

$$\alpha_{s,w} = arctan(\boldsymbol{e}_{x_{s,w}}); \tag{6.11}$$

$$\boldsymbol{R}[\alpha_{s,w}] = \begin{bmatrix} cos\,\alpha_{s,w} & -sin\,\alpha_{s,w} \\ sin\,\alpha_{s,w} & cos\,\alpha_{s,w} \end{bmatrix}. \tag{6.12}$$

The first term, $\gamma_x \cdot \overline{\mathbf{K}}_{x_{s,w}}$, reduces the stiffness ellipse in all directions given a constant forgetting factor, $\gamma_x = 0.9$. The second term increases the stiffness in the direction of the kinematic error. The magnitude of this change is controlled by a gain matrix $\mathbf{G}_K = [0.1\ 0;\ 0\ 0.01]$, which can be seen as a predefined ellipse with axes of fixed length. This ellipse $\mathbf{G}_K$ is (i) rotated along the direction of the error, (ii) scaled according to the magnitude of the weighted error $f_{K_x}[\boldsymbol{e}_{x_{s,w}}]$ and (iii) summed to the stiffness ellipse $\gamma_x \cdot \overline{\mathbf{K}}_{x_{s,w}}$. The error function f_{K_x} ($f_{K_x}: \boldsymbol{e}_{x_{s,w}} \to [0,1]$) is defined for each window w with different shape characteristics (Figure 6.7). The error functions $f_{K_x}[\boldsymbol{e}_{x_{s,w}}]$ can be defined with deadbands designed in end-point space. In this way, it is possible to identify requirements for the foot trajectory that ensure a safe interaction between the foot and the treadmill, for example, minimum foot clearance [347] and minimum step length [348]. One way of defining the error weighting functions $f_{K_x}[\boldsymbol{e}_{x_{s,w}}]$ is by using Asymmetric Generalized Gaussian functions (AGGF) [349] which can be designed to have a different variance depending on the gait cycle window. The AGGF allows the width of tolerated kinematic deviations to be defined in all directions independently. An example is presented in Figure 6.7. By design, $\overline{\mathbf{K}}_{x_{s,w}}$ and $f_{K_x}[\boldsymbol{e}_{x_{s,w}}]$ are bounded above by 1, therefore, even in presence of high errors, the eigenvalues of the stiffness matrix will never increase above the initial values. The change in the stiffness matrix between consecutive time steps is bounded. We implemented a series of safety measures to prevent undesired robot behaviors. First and foremost, we made sure that the controller was stable with constant stiffness and damping values throughout the task space. Second, software mechanisms were in place to constrain the stiffness and damping values to some boundaries. The damping was tied to the stiffness to guarantee a critically damped (or overdamped) system throughout the different kinematic configurations. The rate of change of stiffness and damping parameters was constrained. Finally, the safety hardware and software mechanisms of the Lokomat prevented to reach singular configurations and shut down the motors whenever an excessive force or an excessive deviation from the reference trajectory was detected. Before the tests in humans, the controller was tested in real-life simulations on a test-bench as described in section 6.4.
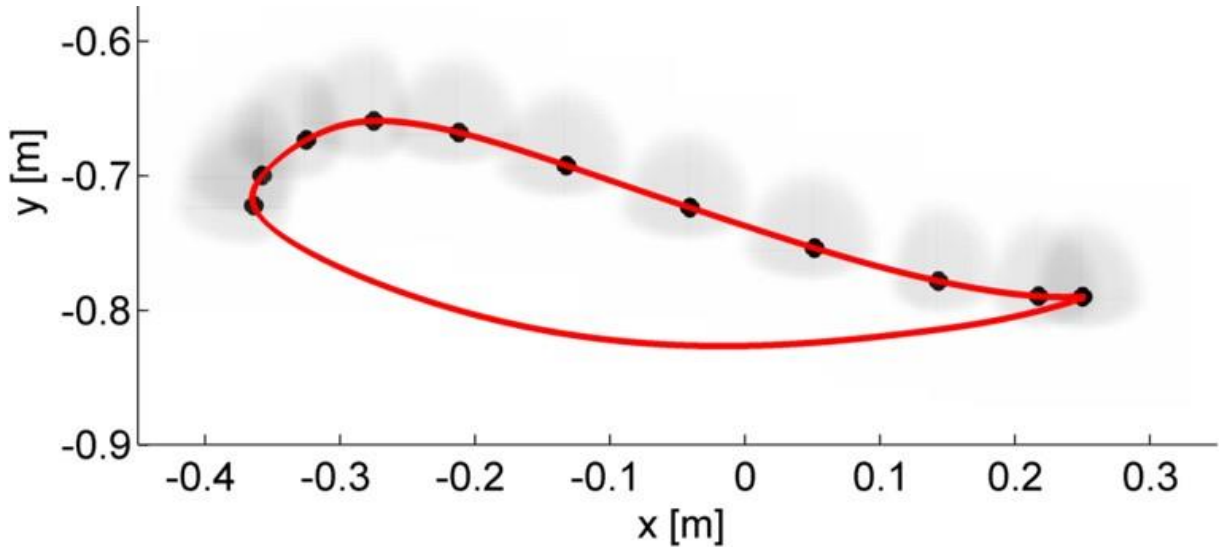
Figure 6.7: In end-point space the deadbands have been designed as asymmetric Generalized Gaussian functions (AGGF). The weighting functions are shaped differently in different points of the swing phase to prevent kinematic deviations that could result in unsafe interactions with the treadmill (e.g. reduced foot clearance and step length). For each window during the swing phase an AGGF is defined (for clarity of representation, only half of the windows are displayed). Kinematic errors falling within the borders of the respective AGGF result in a null weighted error. Otherwise, the weighted error saturates to 1. © 2018 Maggioni, Reinert, Lünenburger and Melendez-Calderon. Reprinted, with permission, from the original article [314].

6.4 SIMULATION RESULTS

Before testing the AAN hybrid joint/end-point controller in human subjects, we performed simulations of the expected behavior using Matlab (v2013b, Mathworks).

We started from the simple case of a point along the reference trajectory and simulated different types of kinematic error. We wanted to test whether the AAN algorithm in the hybrid controller ensures an adaptation of the stiffness matrix to the direction and magnitude of the error. We simulated two cases: (i) error of unitary magnitude and constant direction (angle α between the error vector and the x axis equals 0) and (ii) error of unitary magnitude but variable direction (with α varying randomly at each step in the interval $[0, \pi /2]$). The resulting stiffness ellipses are described in terms of *size, shape* and *orientation* [345], whereby *size* indicates the length of the major axis of the ellipse, *shape* the ratio between the major and minor axis of the ellipse, and *orientation* the angle between the major axis and the x axis.

In the first simulation (Figure 6.8 – first line), the size along the error direction (length of the ellipse major axis) does not decrease since the error function $f_{K_x}\left[\mathbf{e}_{x_{s,w}}\right]$ gives a constant unitary result. The orientation of the ellipse's major axis aligns with the error direction, inducing a force field with maximal restoring forces along the direction of the error and very low forces in every other direction, guaranteeing a compliant behavior of the controller against disturbances in directions other than the error. In the second simulation, as shown in Figure 6.8 – second line, the ellipse orientation follows the error direction and so does the relative force field. The shape of the ellipse depends on how variable the direction of the error was in the previous steps (Eq. 6.9).
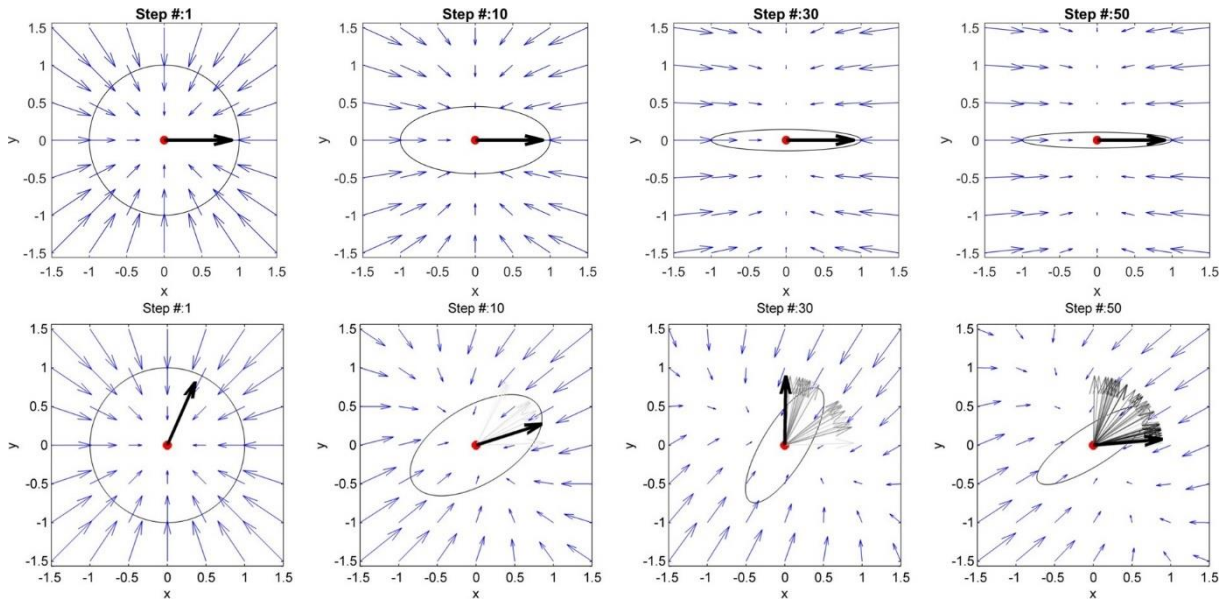
Figure 6.8: First line: Simulation of an error with constant magnitude and direction (black vector) around a reference point (in red). The stiffness ellipse initial configuration is a circle which adapts step by step to the error. The central force field visible at step 1 consequently changes its characteristics. At step 50, the force field is directed mainly along the direction of the error. This implies that the stiffness is high only in directions parallel to the error. Second line: Simulation of an error with constant magnitude and variable direction. The error angle variates randomly between 0 and 90°. The error of the current step is shown in bold black, while the previous vectors are shown in grey. The stiffness ellipse adapts its orientation based on the error direction. The force field represented by the blue vectors adapts accordingly. © 2018 Maggioni, Reinert, Lünenburger and Melendez-Calderon. Reprinted, with permission, from the original article [314].
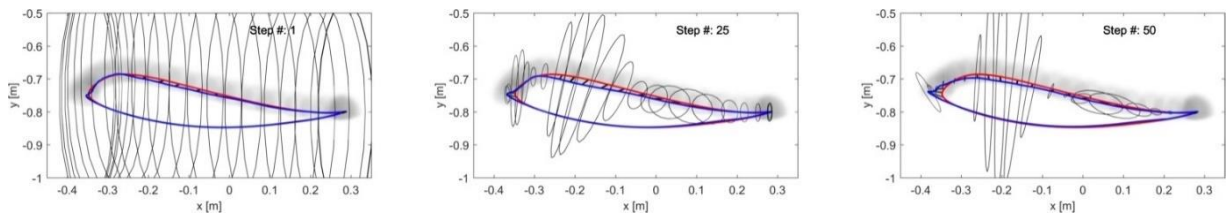
Figure 6.9: Adaptation of the end-point stiffness of the test orthosis during the simulation of a spastic-like behavior in the simulated human leg of the test bench. The initial stiffness ellipses are shown in the first box. The simulated velocity-dependent torque caused deviations of the foot trajectory at mid-swing and at the end of the swing phase. The hybrid controller adapted the stiffness ellipses magnitude and direction to provide targeted support to these deviations. © 2018 Maggioni, Reinert, Lünenburger and Melendez-Calderon. Reprinted, with permission, from the original article [314].

In a second phase, we used a robotic test bench to simulate neurological impairments such as spasticity. The test bench uses a bio-inspired model of a human leg implemented on the leg orthosis of a robotic gait trainer (the Lokomat, in this case). In this setup, one leg orthosis is controlled to simulate a human leg (*simulated human leg*), while the second orthosis (*test orthosis*) is controlled by the hybrid end-point/joint controller with AAN. The two orthoses are then rigidly connected using two aluminum bars, simulating a physical attachment of the robot to the user's leg. A spastic-like behavior was implemented on the simulated human leg by adding a velocity-dependent torque at the level of the knee joint, which was applied when the knee angular velocity exceeded a certain threshold. A detailed description of the test bench and of the impairment simulation can be found in [302]. The physical connection between the two orthoses allowed the hybrid controller implemented on the test orthosis to control the simulated human leg by shaping the stiffness ellipses to the simulated impairment. As expected, the test orthosis with the hybrid joint/end-point controller adapted the end-point stiffness to

counteract the deviations of the simulated human leg caused by the spastic-like simulated impairment (Figure 6.9).

6.5 EXPERIMENTAL RESULTS

The adaptive hybrid joint/end-point controller and the adaptive joint controller were tested with five able-bodied subjects (1 female, age = 27 ± 4.7 years) and one subject with a chronic motor complete Spinal Cord Injury (male, age = 37 years, ASIA B, level of injury = T4, WISCI II = 0/20). The Kantonale Ethikkommission Zürich and Swissmedic approved the study. The aim of this test was first to determine the feasibility and safety of the novel hybrid controller, and subsequently compare the performances of the adaptive hybrid controller to the existing joint adaptive controller [277]. In particular, we hypothesized (i) that this novel controller adapts the magnitude of the stiffness to the subject's ability to follow the reference trajectory and, at the same time, (ii) that the orientation of the stiffness ellipses aligns to end-point deviations. We decided not to test the pure end-point controller on human subjects, due to safety concerns that emerged while doing preliminary tests with a dummy. As foreseen in Section 6.2.2.1, the end-point controller alone was not able to guarantee sufficient foot clearance and avoid potential undesired foot contact with the treadmill.

6.5.1 Methods

Subjects were instructed to follow a given foot trajectory in time and space, which was projected on a screen positioned in front of the Lokomat. The actual and reference ankle trajectories were displayed in different colors and two dots indicated the reference and actual position at every time point. After being set up in the Lokomat, the subjects were allowed to familiarize themselves with walking in the device with the standard impedance controller (impedance was set at the maximum available value). The visual feedback was constantly presented to the subject. In this familiarization phase, the Lokomat gait pattern was adjusted to the subject's gait pattern by tuning the ROM and the offset of the hip and knee angular trajectories. These settings were then kept constant during the subsequent experiment. Once comfortable and accustomed to walking inside the robot, the subject was presented with a familiarization round with the novel AAN hybrid controller as described in Section 6.3. The subject was instructed to follow the reference trajectory as closely as possible while the adaptation algorithm adapted the impedance based on the kinematic error of the ankle trajectory. After the familiarization phase, the AAN control was active on the leg under test for 50 steps, while the impedance of the other leg was kept at the maximum available value. To ensure a safe foot clearance during swing, the stiffness in the vertical direction was made 5 times higher than the stiffness in the horizontal direction. While this is not a problem in the case of high impedance, it might become apparent when the adaptation algorithm reduces the impedance below a certain level, especially in patients with walking impairments. The implemented stiffness $\widetilde{\mathbf{K}}_x$ and damping $\widetilde{\mathbf{B}}_x$ in the Lokomat were:

$$\boldsymbol{K}_x = \boldsymbol{M}_K \cdot \overline{\boldsymbol{K}}_x \tag{6.13}$$

$$M_K = [1500\ 0; 0\ 7500]\frac{N}{m} \tag{6.14}$$

$$\widetilde{K}_x = \frac{(K_x + K_x{}^T)}{2} \tag{6.15}$$

$$\widetilde{B}_x = M_B \cdot \bar{B}_x \tag{6.16}$$

$$M_B = [40\ 0; 0\ 40]\frac{Ns}{m} \tag{6.17}$$

The transformation in Eq. 6.15 guarantees that stiffness matrix is symmetric. In addition, to guarantee the stiffness matrix to remain positive definite after this transformation the following constraint was implemented:

$$\left(-\sqrt{K_{11} \cdot K_{22}} + \rho\right) < K_{ij} < \left(\sqrt{K_{11} \cdot K_{22}} - \rho\right) \tag{6.18}$$

For $i \neq j; i, j = 1,2$, where

$$\rho = 0.1\sqrt{K_{11} \cdot K_{22}} \tag{6.19}$$

The performance of the AAN hybrid controller was then compared with that of the AAN joint controller (see Section 3.3.1 and [277]). For this comparison, subjects were tested in a separate session (scheduled within 4 weeks), while performing the same task using the AAN joint controller.

In the AAN hybrid controller, the magnitude of the end-point stiffness was calculated as the maximum eigenvalue of the stiffness matrix (i.e. the length of the major axis of the stiffness ellipse), averaged over all the windows during the swing phase of each step. The major axis of the stiffness ellipse indicates the direction where the end-point stiffness is maximal. To obtain a measure of the alignment between the direction of maximum stiffness and the position error at the ankle, we calculated the angle between the major axis of the stiffness ellipse and the vector of the end-point error. Only the swing phase of the gait is considered, since the hybrid controller is active only during swing. The weighted kinematic error $f_{K_x}\left[\mathbf{e}_{x_{s,w}}\right]$ equals zero when the actual deviation is within the defined deadbands. In this case, the adaptation algorithm (Eq. 6.9) decreases the size of the stiffness ellipse but does not change its orientation. Therefore, we only calculated the alignment in those windows where the weighted error $f_{K_x}\left[\mathbf{e}_{x_{s,w}}\right]$ was greater than 0.1. The data of the last 5 steps of the adaptive task were used for the analysis of the final stiffness alignment determined by the algorithm. An average value over all subjects was calculated.

In the joint controller, the magnitude of the stiffness was calculated as the mean of the hip and knee joint stiffness during the swing phase. We then obtained the equivalent end-point stiffness resulting from the joint stiffness matrix (Eq. A.24). The angle between the major axis of the resulting stiffness ellipse and the direction of the error in end-point space was calculated to estimate the alignment of the force field perceived at the ankle with the error.

6.5.2 Results

All subjects were able to perform the experiment with the adaptive hybrid controller; the subject with SCI required a fixed body weight support equal to 70% of his body weight to use the adaptive hybrid controller.
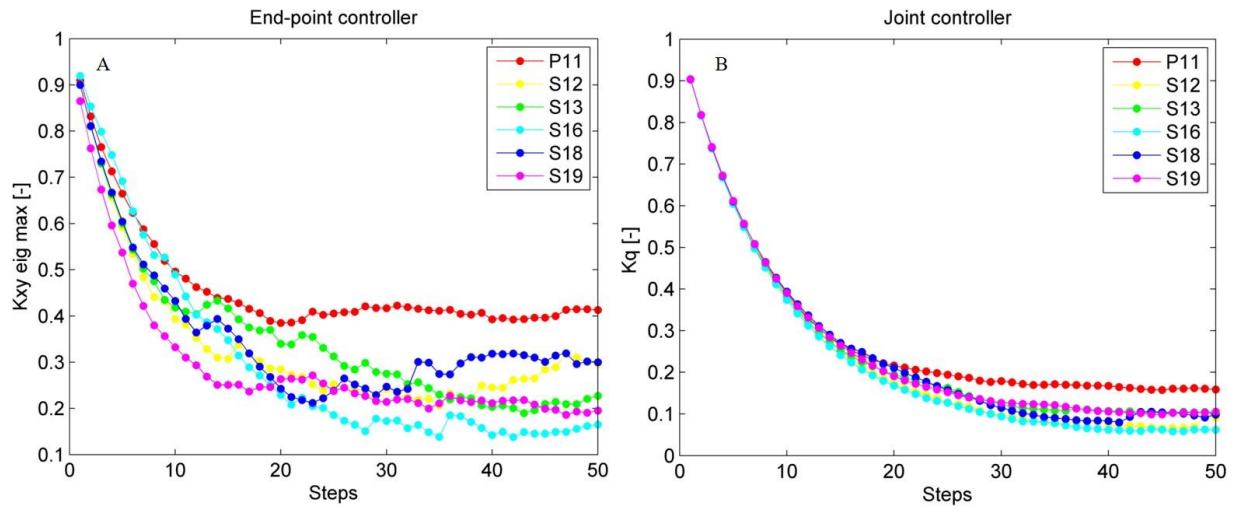
Figure 6.10: In this figure, the normalized adaptive stiffness of the two types of controller (AAN hybrid controller and AAN joint controller) is shown over 50 steps. Each data point represents the mean value over the swing phase of one step. In Panel A, the adaptive stiffness of the hybrid controller (i.e. the maximum eigenvalue of the ellipse) is displayed. In Panel B, the adaptive stiffness of the joint controller (i.e. the mean of the normalized hip and knee stiffness) is shown. The data of the patient are visualized in red. © 2018 Maggioni, Reinert, Lünenburger and Melendez-Calderon. Reprinted, with permission, from the original article [314].

The overall end-point stiffness decreased over time and converged to a specific value for each subject. The patient reached, as expected, a higher final value than the able-bodied subjects did.

Results confirmed that the stiffness ellipses start from an initial size and shape (ratio major/minor axis = 5) and, based on Eq. 6.9, subsequently adapt in shape, orientation and size to the errors at the ankle (Figure 6.11). During adaptation, the size of the stiffness ellipses adapts gradually to the kinematic error occurring in that gait phase. At every step, the orientation of the stiffness ellipses tends to align to the direction of the error in that gait window (Eq. 6.9, second term).
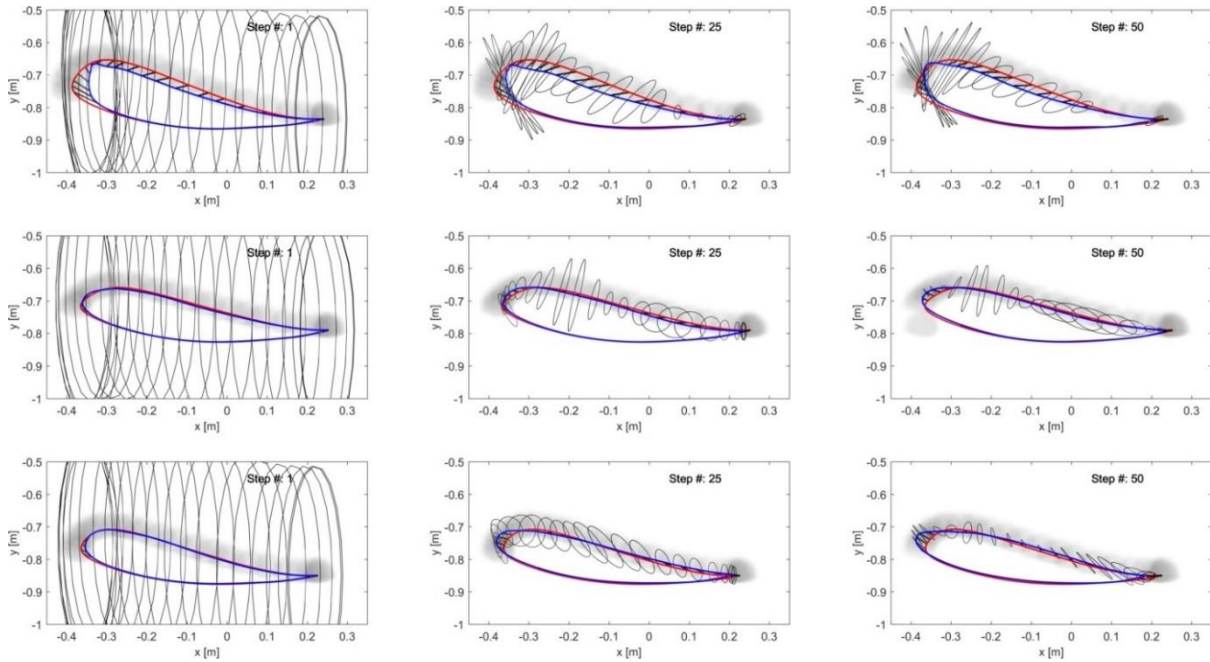
Figure 6.11: Adaptation of the end-point stiffness during the experiment for three different subjects. The initial stiffness ellipses are shown in the first column. To ensure a safe foot clearance during swing, the vertical stiffness maximum value was set higher than the horizontal stiffness. After 25 steps (2nd column) the stiffness ellipses are adapting to the error size and direction. At the last step of the adaptation (3rd column), the ellipses reached their final configuration. On the 1st line, data from the subject with SCI are shown: as expected, the final stiffness ellipses have a bigger size than those achieved by the able-bodied subjects in the 2nd and 3rd line. © 2018 Maggioni, Reinert, Lünenburger and Melendez-Calderon. Reprinted, with permission, from the original article [314].

In contrast, Figure 6.12 shows the results for the joint controller, whereby hip and knee joint stiffness adapt separately (described in section 3.3.1) and no coupling terms are present. Hence, the size, shape and orientation of the resulting end-point stiffness depend not only on the actual joint stiffness but also on the configuration of the leg segments (therefore, on the gait phase). It is clear that there is little or no correspondence between the errors performed in task space and the resulting end-point stiffness.
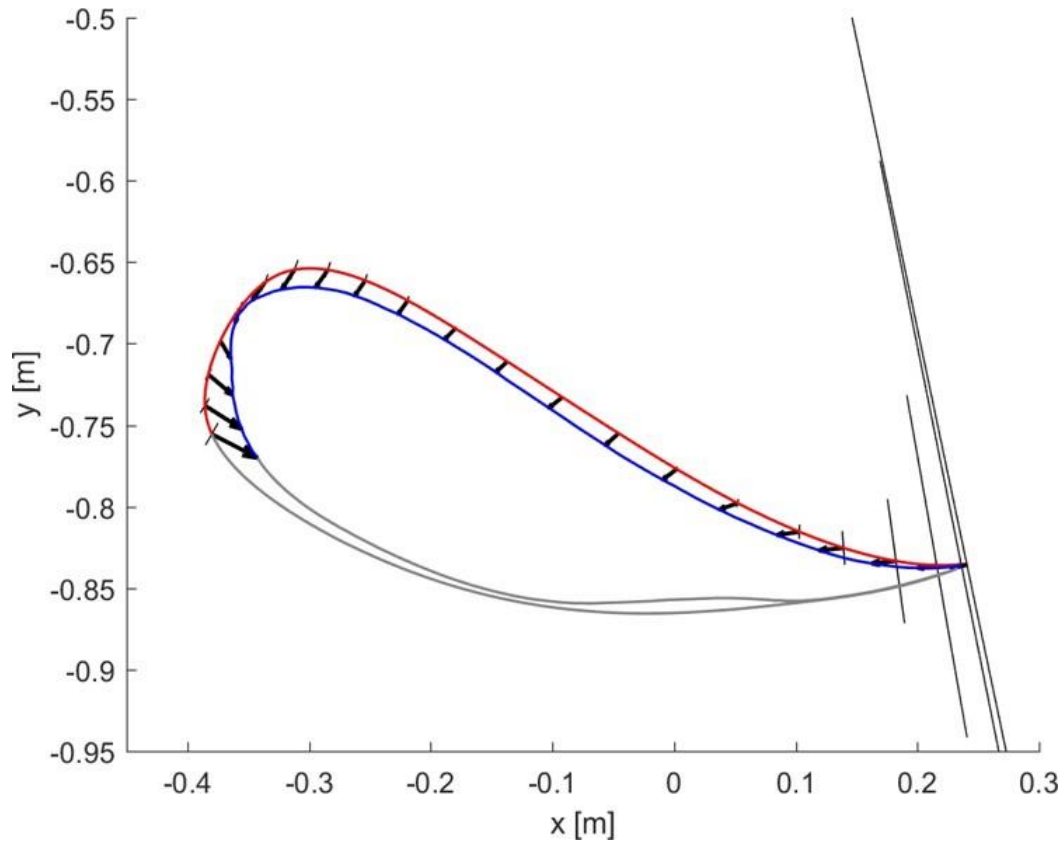
Figure 6.12: Resulting end-point stiffness ellipses caused by the joint controller in the subject with SCI. The resulting end-point stiffness is calculated from the hip and knee stiffness during the last step (50th) of the adaptation. The ellipses appear in the figure as lines since the minor axis is close to a null length. The kinematic error between the reference trajectory (red) and the actual trajectory (blue) of the ankle joint during swing phase is shown by the black vectors. © 2018 Maggioni, Reinert, Lünenburger and Melendez-Calderon. Reprinted, with permission, from the original article [314].

The alignment between the major axes of the ellipses and the error in the respective time window in the last 5 steps is greater (i.e. the angle is minimum) in the ideal hybrid controller (for $C = [1\ 0;\ 0\ 1]$) (Figure 6.13). The joint controller showed the worst performance in terms of alignment.
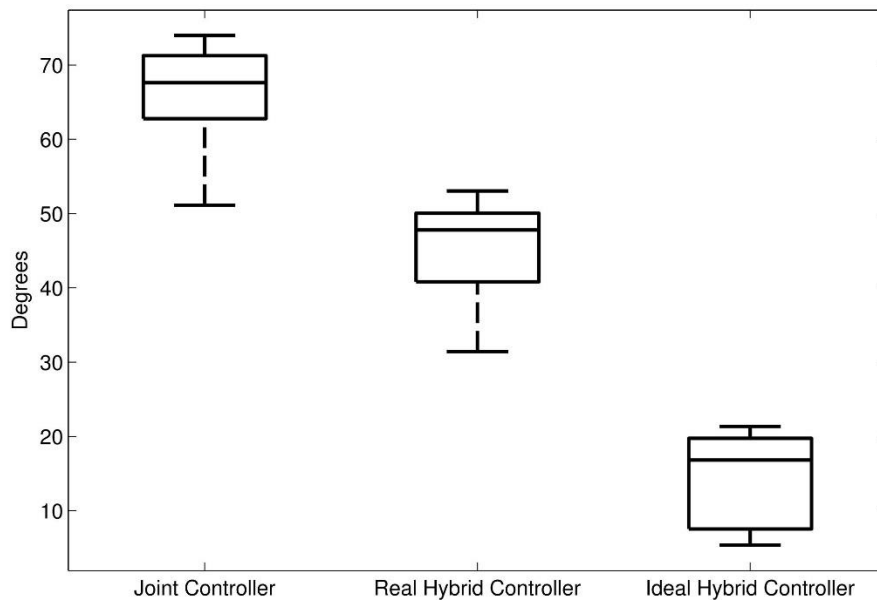
Figure 6.13: Average alignment (angle) between the major axis of the end-point stiffness ellipses and the direction of the error in the same gait window. First boxplot: alignment of the end-point stiffness ellipses resulting from the joint controller. Second boxplot: alignment of the end-point stiffness ellipses obtained in the experiments with the hybrid controller. Third boxplot: alignment of the end-point stiffness ellipses in the ideal case where the initial vertical stiffness of the hybrid control was set equal to the horizontal stiffness. © 2018 Maggioni, Reinert, Lünenburger and Melendez-Calderon. Reprinted, with permission, from the original article [314].

If we examine one of the critical points of the late swing phase, i.e. right before heel strike, in further detail (Figure 6.11), it becomes apparent that, especially in the subject with SCI, the hybrid controller generates an end-point stiffness ellipse rotated in the direction of the error (i.e. the stiffness is higher in the direction along which the error occurred). The adaptive joint controller (Figure 6.12) instead shows a very small stiffness value in that direction, but a high stiffness in a direction that does not apparently require any support.

6.6 DISCUSSION

The aim of our work was to develop an AAN controller for a lower limb exoskeleton which could optimally adapt the support based on the patient's ability to follow a reference trajectory. To achieve this, we examined and discussed the features and disadvantages of joint and end-point space formulation to control exoskeleton robots for the lower limbs. Then, we developed a proof-of-concept novel controller that combines the benefits of joint and end-point formulations: an adaptive hybrid joint/end-point space controller. We presented the results of a software simulation and, finally, the results of the tests on able-bodied subjects and one subject with SCI.

When developing a controller for gait exoskeletons, the choice of the formulation (joint or end-point) highly influences the apparent stiffness and damping rendered by the robot and it has an impact on how the reference trajectories (and safety features around them) are designed. While gait trajectories defined in joint space are closer to the hardware structure of the exoskeleton and similar to what gait analysis presents us, the trajectory of the foot during gait is a precise end-point control task [35]. The human

achieves certain trajectories in task-space thanks to the fact that the internal models take care of the proper muscle activations that guarantee the correct joint movements [299]. In both healthy and pathological conditions, different joint kinematic solutions are adopted to control the position and orientation of the end-point and, in particular, to achieve a safe trajectory of the foot during the swing phase [35]. It has thus been hypothesized that the control of the foot trajectory during swing is a major focus of our central nervous system (CNS) during human locomotion [350], as also supported by animal studies [351]. In contrast to trajectories defined in joint space, end-point trajectories of able-bodied subjects during swing show very little variability during walking on firm level ground and on the treadmill [25, 35, 352]. Instead, during stance phase the main task is not control of the foot trajectory, but rather the support and balance of the body weight. These functional tasks are accomplished by the control of hip, knee and ankle angles in a so called "support synergy" [353]. The different tasks performed during swing and stance phase and the different models used for these two phases, support the use of the end-point formulation only during the swing phase of gait.

Depending on the formulation used in the controller, the resulting stiffness properties of the exoskeleton can vary significantly. This results in different magnitudes and directions of supportive torques. Considering the strengths and weaknesses of the joint and end-point formulation for impedance controllers, we proposed a hybrid joint/end-point controller in order to exploit the benefits of the end-point controller in shaping a desired end-point stiffness, while using an additional joint component to guarantee the correct angular trajectories of the joints. In previous research, the concept of a hybrid controller was introduced for an industrial manipulator that was programmed to follow a given end-point trajectory in the presence of external disturbances (both at the end-effector and at the joint level) [342]. The torques calculated by the end-point controller were complemented with the torques obtained from a joint impedance controller only at those joints that were affected by large disturbance forces. This approach was proven more effective than either end-point or joint control alone to reduce the tracking error in the presence of end-effector and joint level perturbations.

The control over the end-point stiffness also opens new possibilities when developing a controller with assist-as-needed characteristics. The AAN implemented in end-point space can be directly programmed to adapt the magnitude and the direction of the stiffness based on the error of the subject in task space. Our experiments showed that the controller could adapt the end-point stiffness based on the deviation of the subject from the foot reference trajectory. As expected, the application with a subject with SCI resulted in a higher final end-point stiffness than the able-bodied subjects. When comparing the alignment of the end-point stiffness ellipses generated by the different controllers, we saw that in the hybrid joint/end-point controller the stiffness was better aligned with the error direction. In this way, the controller directs the restoring forces in the direction where they are needed, thus providing a more "specific" support.

Emken employed a similar approach on the end-effector robotic gait trainer ARTHuR [272]. The end-point stiffness of the robot was adapted with an AAN algorithm that separately adapted horizontal and vertical stiffness. Our approach differs in that the end-point stiffness ellipses align to the direction where the maximum stiffness is required (i.e. the direction of the error). Interestingly, this behavior is close to the way humans adapt their stiffness in response to external disturbances: as shown by Burdet and colleagues [354], the central nervous system can voluntarily control the magnitude, shape and orientation of the end-point stiffness in the upper limb. Moreover, several studies have found that the control of the foot trajectory is the major focus of our central nervous system during locomotion, both in the unimpaired [35, 352] and in the impaired spinal cord [25, 350]. Therefore, a controller for robotic exoskeletons that is shaping the end-point position and the end-point stiffness can be considered as a "bioinspired" solution for the control of robotic devices for human interaction.

A further advantage of the adaptive end-point controller is that the error metric for the algorithm can be defined in task space. This allows us to consider explicitly the interaction between the foot and the environment and the spatio-temporal features of the foot trajectory. As Winter showed [35], foot clearance is sensitive to very small angular deviations in any of the joints of the lower limb kinematic chain. This means that, in order to guarantee a safe minimum toe clearance, one would have to design very restrictive deadbands in joint space, which would have a negative impact on freedom of movement for physiological deviations. In contrast, deadbands in task space can be designed to be restrictive only in the directions that are needed for safety, determining how much deviation can be tolerated in the vertical direction (crucial for avoiding stumbling) and in the horizontal direction, which corresponds to leading or lagging with respect to the reference trajectory. Moreover, with the end-point controller, it is possible to present the subjects with visual feedback on the errors in end-point space, which is much easier to process than feedback on joint position [21, 22, 274], and use the same representation within the error metric of the adaptation algorithm. When used in the experiments with subjects, the adaptive hybrid joint/end-point controller required the use of an additional term to support against gravity: the vertical stiffness was set 5 times higher than the horizontal stiffness. Alternatively, an additional feed-forward term for compensating the effect of gravity could be added. Furthermore, lighter robots (e.g. LOPES [116]) would reduce the role of gravity and inertia of the system and thus the need to counteract them. The accuracy of the end-point position can be increased by adding a position sensor which measures directly the x coordinates of the ankle, instead of estimating them from the joint angles. While we derived necessary conditions for stability based on the approach proposed by [355] and we took several precautions to guarantee safety, the stability of the AAN hybrid controller is something that requires further investigation.

The single subject with SCI with whom we tested the adaptive and hybrid end-point / joint controller did not show abnormal muscle activation synergies. Extra care should be taken when using the hybrid control with patients that present abnormal synergies or other strong compensatory movements. There might be cases where, despite an almost physiological end-point trajectory, hip and knee angles remain

anomalous [25]. In such cases the hybrid control should be extended by a term that counteracts joint position deviations, as in the approach proposed by Smith [342], where a joint impedance term was added only when large disturbances at the joint level were detected. Before drawing any conclusions on the benefits of this novel controller in treating subjects with gait disabilities, more tests are needed to study how the controller would react to different impairments such as spasticity.

As a future step, the application of our adaptive hybrid joint/end-point controller concept to other rehabilitation robots, e.g. upper limb exoskeletons (such as the ARMin [356], Armeo®Power (Hocoma AG) or ALEx [357]) would be of great interest, because a vast body of literature has investigated how humans adapt their upper-limb stiffness based on the task and on external disturbances [344, 354] and it would be instructive to use an adaptive controller similar to the one presented in this work to test its interaction with the human arm.

6.7 CONCLUSION

The adaptive controller presented in this chapter implemented our ideas of a safe controller combining an end-point impedance controller with a joint damping controller into a "hybrid" joint/end-point controller. The controller was tested successfully with able-bodied human subjects and one subject with spinal cord injury. With this approach, it was possible to implement a controller that shapes the end-point stiffness according to the direction and the magnitude of the error performed at the ankle. In contrast to other applications, the hybrid controller adapted the end-point stiffness to selectively counteract certain errors while leaving the robot compliant in other directions. The adaptive controller proposed in this chapter is a patient-cooperative, bio-inspired solution for more human-oriented rehabilitation robots , which fulfilled the requirement of "adaptability" identified by many studies in the field of rehabilitation robotics [358] and may be used on other devices, including upper extremity rehabilitation robots.

Chapter 7   GENERAL CONCLUSION AND OUTLOOK

7.1 CONCLUSION

Walking impairments affect in countries like the USA 22.5% of the population over 65 years old [2]. The WHO has promoted a call for action named "Rehabilitation 2030", calling for concerted and coordinated global action by all stakeholders to scale up rehabilitation [359]. To provide suitable and targeted rehabilitation to patients in need, we need state-of-the-art treatments, trained health professionals and assessments to measure and track recovery. Current assessments of sensorimotor functions present still several issues which prevent their regular use in clinical practice and limit the benefit that the individuals can obtain from rehabilitation. The most pressing issues are the subjectivity and poor sensitivity of the measures, and the time required for executing them. New technologies, and, in particular, robotic gait trainers, have become a real possibility for locomotor therapy after neurological injuries. Robotic gait trainers allow creating standard protocols within the training sessions, measure objective data with the integrated sensors, and support patients with all levels of severity. Thus, researchers have tried to take advantage of this new form of training to develop objective, reliable and sensitive measures to assess recovery of walking and walking-related functions.

The long-term goal of this project is to develop a valid, reliable and sensitive assessment of walking activity in a robotic gait trainer that can be used in clinical practice to measure patients during every stage of rehabilitation. **The <u>specific aims</u> of this thesis** were: *i)* to review current conventional and robotic assessments of walking and walking-related functions in order to understand how they can be improved and what is important to measure, *ii)* to design and implement an algorithm in a treadmill-based robotic gait trainer which allows safe and objective assessment of patients' walking ability, *iii)* to test and validate the robotic assessment on a robotic test bench and in a neurological population against established clinical scores.

7.1.1   Requirements for Functional Walking

We identified which aspects of walking need to be assessed by identifying the requirements for functional walking. Gait experts and physiotherapists agreed that stance phase stability, control of foot trajectory, especially at the transitions swing-stance and stance-swing, energy conservation and absorption, propulsion and endurance are at the basis of functional walking. This critical review laid the foundation for designing a robot-aided gait assessment of walking ability which could target some of these walking-related functions (Table 3.3).

7.1.2   Assessment of Lower Limb Functions

When developing and adopting assessments for research and/or clinical practice these psychometric properties that need to be considered: validity, reliability and responsiveness. We reviewed existing

conventional and technology-based assessments of sensorimotor function focusing on the lower limb. While examining requirements and barriers for their clinical application, we found out that the reason for their limited adoption can be ascribed to the lack of proper validation studies with an adequate sample size, to the administrative burden (cost and time) and to the uncertainty on the usefulness of a new measure for decisions on patient's treatment. The review of the assessments available for gait pattern and walking activity highlighted the limits of current gait assessment tests (e.g. floor and ceiling effects, limited sensitivity or, on the other side of the spectrum, high complexity and administrative burden). The overview of the state of the art of technology-based walking assessments provided us with ideas on how to tackle the problem with an assist-as-needed (AAN) software implemented in a robotic gait trainer.

7.1.3 AAN-Based Approach for Walking Assessment

In Chapter 3, we proposed our solution for an assessment of walking ability implemented in a treadmill-based robotic exoskeleton. The algorithm was designed to be used during training from patients with all level of severity, by providing enough support to walk safely, but also enough freedom to assess how much the patient actively contributed to the movements. To achieve this, we developed an AAN real-time controller, which adapted the impedance of the robotic joints and the body weight support based on the patient's ability to follow a reference trajectory. We hypothesized that the residual robotic support determined by the algorithm, after convergence, would be proportional to the walking impairment of the patient. The pilot tests with able-bodied subjects confirmed that the approach was feasible and suggested some changes in the protocol to be implemented before performing the study in patients, such as improving the clarity of the visual feedback, increasing the efforts for personalizing the trajectory, including a longer familiarization phase in the protocol and analyzing the outcome measures per gait phase.

7.1.4 Validation of the AAN-Based Assessment

The validity of the approach based on AAN algorithm was tested first in a controlled situation (Chapter 4), using a robotic test bench simulating typical neurological impairments (weakness and spastic-like behavior). The test bench setup relied on a simple but innovative solution that took advantage of the hardware structure of the Lokomat. One leg orthosis was programmed to emulate a 'human leg' with a superimposed impairment, the second leg implemented the AAN software under test. The two orthoses were connected with metal bars to reproduce the connection between a human leg and the robot, which is normally achieved by the cuffs. A combination of feedforward and feedback control components was used for simulating a human leg. Weakness and spastic-like behavior could be separately tuned and added to the simulation of the human leg (only simulation of swing phase was possible). In the experiments, we checked if the AAN controller deployed on one orthosis was able to assess correctly the impairment simulated on the other orthosis. Simulated weakness and spastic-like behavior led to specific, different profiles of residual robotic stiffness. Increased simulated weakness

resulted in a proportionally higher residual robotic stiffness during initial and terminal swing. Increased severity of spastic-like behavior led to increased residual stiffness at initial swing, but reduced stiffness at terminal swing. The results confirmed that our method was sensitive enough to capture differences in the simulated impairments, but that the measures were affected by speed and were dependent on the gait phase.

The AAN robotic controller was tested in 15 patients with SCI and 12 able-bodied control subjects (Chapter 5). The main purpose was to verify if the residual robotic impedance, determined by the algorithm, was able to provide information on walking ability. We found that one variable alone (the residual stiffness at the knee at terminal swing) measured during training in the Lokomat could explain most of the variance of the timed walking tests (10MWT and TUG). The robotic stiffness required by the knee joint at terminal swing is needed to produce an adequate step length and have a smooth swing-to-stance transition, which are two of the requirements for walking identified by gait analysis experts (Table 1.1). In non-ambulatory patients, this predictor did not seem to relate to their functional level. It is likely that other factors, such as the ability to support the body weight and to perform an adequate push-off, are necessary before the foot placement becomes relevant. However, the limited amount of data in non-ambulatory patients prevented us to draw any further conclusion. The inclusion of an additional isometric force variable into the linear models increased the explained variance of the models to above 85%, indicating that muscle force provides an important and distinct information from the AAN outcome measures. These results show that walking ability could be measured in a robotic gait trainer in a safe and efficient way with few measurements required. A change of 9.1% (between two different sessions) in the robotic knee stiffness at terminal swing would be required to indicate a significant change in a patient's walking ability. This is a limitation on the responsiveness of the assessment, because changes smaller than this are within the range of test-retest variability. Based on experience, this value is still rather high, and the reliability of the AAN-based assessment would need further improvement before the test can provide any useful information in clinical practice. Low reliability may have been caused by an insufficient familiarization time, by the high cognitive-motor demand of the tasks and/or by the request of following a reference trajectory that was only partially adapted to the individual patient. Finally, we demonstrated that the AAN software was safe and feasible for patients with all levels of walking impairment and it could adapt the level of support as required by the individual patient: these characteristics make it an ideal solution as training software that challenges the patients as needed.

7.1.5 Towards a Hybrid Joint/End-Point AAN Controller

The importance of the control of the foot trajectory emerged in the clinical study and the need to provide a more transparent controller, safe but at the same time compliant in the directions were no support was needed, led us to the development of an alternative type of controller based on end-point impedance adaptation. In Chapter 6, we presented the technical details of a "hybrid joint/end-point space

controller with AAN" and the feasibility tests in 5 able-bodied subjects and one patient with a complete SCI. The concept of a hybrid controller combined the benefits of joint space controllers and end-point space controllers, in an attempt to overcome the weaknesses of both. The adaptive controller shaped the end-point stiffness according to the direction and the magnitude of the error performed at the ankle. The resulting end-point force selectively counteracted certain foot position errors while leaving the robot compliant in other directions. We demonstrated the feasibility of the hybrid controller and the safety in able-bodied subjects, however additional gravity compensation was needed to support the severely impaired patient. Improvement of this aspect is needed before further tests in patients.

Overall, we were able to design, develop and test a novel software for a treadmill-based robotic exoskeleton that can be used to determine the support required by a patient while performing gait training. The support determined by the algorithm provides information on the patient's walking ability which can be used to assess the patient's recovery, to provide motivation and to adjust the therapy consequently.

7.2 OUTLOOK

The work carried out in this thesis led the field closer to the achievement of the long-term goal of developing an objective, valid and reliable assessment of walking ability. However, several aspects still need to be addressed to be able to reach that goal.

The clinical study on 15 SCI patients gave a good first evaluation of the validity and reliability of the AAN-based assessment of walking ability. However, the validity of the test needs to be evaluated in patients that are not yet able to walk overground by using other clinical outcome measures as reference. These patients cannot be assessed with the standard timed tests and they are in utmost need of an alternative to measure how close they are to recover walking, despite not being able to walk yet. Overall, more data need to be collected from ambulatory and non-ambulatory patients to increase the statistical power of the tests and to confirm that the model created to predict the timed tests is generalizable to a broader patient population. Surely, data from other neurological populations (e.g. stroke, cerebral palsy children) need to be collected to evaluate if the Lokomat outcome measures identified in our study is specific for the SCI population or could be extended to other groups of patients with walking impairments.

A smarter solution for validating novel assessments of sensorimotor functions, where no gold standard is present, needs to be established. We proposed the use of a robotic test bench where controlled conditions and impairments can be simulated. This approach requires refinement in the way the model of the human is built, for example by applying existing sophisticated neuromuscular-skeletal models [313].

Our clinical study also showed that reliability of the AAN approach was not yet sufficient for its use as an assessment battery in the clinical practice. The reliability can be increased by allowing more familiarization time for the patient to get used to walking in the Lokomat, since a trend of learning from one visit to the next was found in our data. We believe that validity and reliability will greatly benefit from implementing a personalized reference trajectory in the Lokomat. This will allow the test to be independent of effects due to learning a new trajectory. For example, a database-driven reference trajectory adaptation algorithm can be built and fed with a pool of physiological trajectories of different types of individuals [340]. The algorithm can record some sample steps from a patient walking in the Lokomat and assign the closest matching reference trajectory from the database. Otherwise, anthropometric and walking speed data can be used to determine from a model the most likely reference trajectory for the individual [360].

The cross-sectional clinical study identified the Lokomat measures able to explain most of the variance (more than 84%) of the timed test in ambulatory chronic SCI subjects: will the same outcome measures be able to capture improvements in acute and sub-acute patients in a longitudinal study? It can also be hypothesized that a within-subject analysis may lead to improved responsiveness of the assessment due to the lower variability in the measures. It would be then extremely interesting to study whether any Lokomat measure captured at an early point after injury would be able to *predict* walking recovery in patients undergoing rehabilitation. This information would be of very useful for determining the best possible therapy for the patient.

The AAN software was used in this project for assessing patients' walking ability, but it is able to provide only as much support as needed for the patient to walk safely, while challenging him/her at the same time. This is a perfect characteristic for a training software, since it is known that shaping the therapy to the patient's ability enhances motor learning [361]. The AAN software can easily be added as an exercise in the Lokomat library and address therapy goals such as foot trajectory control, ability to support the body weight and endurance. Moreover, the software will be able to measure the support required from the patient to walk and provide this information as feedback for the patient and the therapist. The ability to determine the training parameters (e.g. amount of body weight support and guidance force) based on the patient's needs would close the loop between therapy and assessment and provide an assessment procedure seamlessly integrated in the training.

Appendix A

In this section we report the tables with the psychometric properties of clinical assessments (Table A.1) and robotic assessments (Table A.2) that have been published in the paper:

Maggioni S, Melendez-Calderon A, van Asseldonk E, Klamroth-Marganska V, Lünenburger L, Riener R, et al. *Robot-aided assessment of lower extremity functions: a review.* J Neuroeng Rehabil. 2016; 13:72. doi:10.1186/s12984-016-0180-3. Reprinted under the terms of the Creative Commons Attribution 4.0 International License[4].

VALIDITY, RELIABILITY AND RESPONSIVENESS OF CLINICAL ASSESSMENTS OF LOWER LIMB FUNCTIONS AND ACTIVITIES

Measure	Instrument / test	Properties				Study
		Validity	Inter-rater reliability	Intra-rater reliability	Responsiveness	
pROM	Universal goniometer	Knee angle : ICC ≥ 0.98 [362]	Hip flex: 0.56 ≤ ICC ≥ 0.91, SEM = 6.16° [112, 363, 364] Hip ext: 0.20 ≤ ICC ≥ 0.68, SEM = 4.45° [112, 363, 364] Hip abduction: 0.45 ≤ ICC ≥ 0.63, SEM = 6.08°[363, 364] Hip adduction: 0.14 ≤ ICC ≥ 0.65, SEM = 4.4° [363, 364] Knee flex: 0.84 ≤ ICC ≤ 0.93, SEM = 8.21° [112, 363] Knee ext: 0.59 ≤ ICC ≤ 0.86, SEM = 3.48° [112, 363] Ankle DF: 0.26 ≤ ICC ≤ 0.87 [112] Ankle PF: ICC=0.74 [112]	Knee flex: 0.97 ≤ ICC ≥ 0.99 Knee ext: 0.91 ≤ ICC ≥ 0.98 [365, 366] Hip sagittal angle: 0.51 ≤ ICC ≥ 0.54, SEM = 4° [367] Ankle DF: 0.72 ≤ ICC ≥ 0.89 [114]	-	[112, 114, 362–367]
aROM	Universal goniometer	Knee flex: r ≥ 0.975 Knee ext: r ≥ 0.390	Knee flex: ICC ≥ 0.977 Knee ext: ICC ≥ 0.893	Knee flex: ICC = 0.997 Knee ext: ICC ≥ 0.972	-	[109]
End-feel	Manual examination	-	Hip flex: 0.21 ≤ κ ≤ 0.41 Hip ext: κ = - 0.13 Knee flex: - 0.01 ≤ κ ≤ 0.31 Knee ext: 0.25 ≤ κ ≤ 0.43	Knee flex: κ = 0.76 Knee ext: κ = 1.00	-	[112], [368]
Muscle strength	MMT	Knee flex (vs isokinetic dynamometer): ρ = 0.74 Knee ext: r = 0.70 [85]	Lower extremities: 0.66 ≤ ICC ≤ 1 [369] MRC score: 0.62 ≤ ICC ≤ 0.88 [370]	Lower extremities: 0.77 ≤ ρ ≤ 0.99 [371]	External resp.: Sensitivity: 60.9% to 70.3% [156]	[85, 156, 369–371]

	HHD	Knee ext: 0.43 ≤ r ≤ 0.99 Knee flex: 0.83 ≤ ICC ≤ 0.85 Ankle PF: r = 0.93 Ankle DF: r = 0.60 [158]	Knee flex: ICC = 0.95 Knee ext: ICC = 0.88 Ankle DF: ICC = 0.69 [157]	Hip: ICC = 0.82 (belt), ICC = 0.80 (therapist) [372] Knee flex: ICC = 0.97 Knee ext: ICC = 0.93 Ankle DF: ICC = 0.91 [157]	95%CI = 32.5 N (72%) 95%CI = 57.1 N (79%) [372]	[157, 158, 372]
Proprioception	Romberg test	-	-	-	-	
	Toe-test	-	-	-	-	
Joint impedance	MAS	vs ankle measurement device: r = 0.09 vs H-reflex: r = 0.47 vs Pendulum test: r = - 0.69	0.16 ≤ κ ≤ 0.61 Ankle PF: r = 0.727	0.4 ≤ ICC ≤ 0.75	-	[373]
	Pendulum test	vs MAS: - 0.63 ≤ ρ ≤ -0.89	-	0.651 ≤ ICC ≤ 0.844	-	[233]
Walking activity / Gait pattern	WISCI II	Construct validity: vs TUG: r = -0.76 vs 10MWT: r = -0.68 vs 6MWT: r = 0.60	0.98 ≤ ICC ≤ 1	ICC = 1	MDC: 1 level Effect size 2.05, moderate change – discrimination between 1 and 3 months post injury Effect size 0.73, small change – discrimination between 3 and 6 months post injury	[373]
	10MWT	vs TUG: ρ = 0.89 vs 6MWT: ρ = - 0.95 vs WISCI II: ρ = 0.795	r = 0.97 LOA = ± 7.0 s	r = 0.98 LOA = ± 6.0 s	Effect size: 0.92 - discrimination between 1 and 3 months post injury Effect size: 0.47 - discrimination between 3 and 6 months post injury	[4, 254, 373]

Table A.14: In the table: ρ indicates Spearman rank correlation, r Pearson's correlation, κ Cohen's Kappa, CI confidence intervals, DF dorsiflexion, PF plantarflexion

Measure	Instrument	Properties				Study and population tested
		Validity	Inter-rater reliability	Intra-rater reliability	Responsiveness	
pROM	Lokomat	-	-	-	-	-
	Isokinetic dynamometer (Biodex System 3 Pro dynamometer - Biodex Medical Systems Inc., Shirley, NY, USA)	-	Ankle DF: ICC ≥ 0.938 SEM = 1.4°	Ankle DF: ICC ≥ 0.930 SEM = 0.8°	MDC = 2.2°-3.3°	[114], 15 stroke patients
	Manual spasticity evaluator	-	ρ = 0.95	ICC = 0.86	-	[127], 12 children with CP, 5 able-bodied (AB) adults
	Anklebot	Mean absolute error over two planes ≤1°	-	-	-	[129], validation vs electrogoniometer using a mock-up foot
	Ankle assessment device	-	-	Ankle DF: ICC = 0.846 Ankle PF: ICC = 0.958	Ankle DF: MDC = 3.27° Ankle PF: MDC = 3.81°	[374], 9 AB subjects
aROM	-	-	-	-	-	No studies found
Muscle strength	Isokinetic dynamometer (Biodex System 3)	-	-	Isometric peak torque control subjects: ICC ≥ 0.92; SEM ≤ 25.1 Nm Peak torque patients, contralesional limb ICC ≥ 0.86, SEM ≤ 23.9 Nm	-	[375], 17 subjects with stroke, 13 AB subjects
	Lokomat, isometric test	-	Hip: ICC ≥ 0.87, SEM ≤ 11.2 Nm; Knee: ICC ≥ 0.85, SEM ≤ 7.9 Nm.	Hip: ICC≥ 0.79, SEM ≤ 10.5 Nm; Knee: ICC ≥ 0.84, SEM ≤ 8.2 Nm.	-	[84], 14 subjects with neurological movement disorders, 16 AB subjects
	Ankle assessment device	-	-	Ankle DF: ICC = 0.949 Ankle PF: ICC = 0.858	Ankle DF: MDC = 1.69 Nm Ankle PF: MDC = 1.68 Nm	[374], 9 AB subjects
Proprioception	Modified Biodex chair, TTDPM test	-	-	Knee frontal plane: ICC≥0.40	-	[183], 17 AB subjects
	Chair with knee actuator, TTDPM test	-	OA: ICC=0.91, SEM=2.13°, AB: ICC = 0.89, SEM = 0.43°	OA: ICC=0.91, SEM=2.26°, AB: ICC = 0.86, SEM = 0.39°	-	[192] 24 subjects with OA, 26 AB subjects

	Lokomat, JPR test	vs clinical score: Hip: ρ = 0.507, Knee: ρ = 0.790	-	SCI, Hip: ICC= 0.55, Knee: ICC= 0.882 AB, Hip: ICC= 0.493, Knee: ICC= 0.656	-	[185], 23 SCI and 23 AB subjects
	Lokomat, TTDPM test	vs manual kinesthesia assessment: left hip, r = −0.71; left knee, r = −0.86; right hip, r = −0.47; right knee, r = −0.57	-	AB, hip: ICC = 0.88 left, ICC = 0.94 right; knee ICC = 0.90 left, ICC = 0.91 right. SCI, hip: ICC = 0.97 left, ICC = 0.96 right; knee: ICC = 0.95 left, ICC = 0.96 right	-	[193], 17 SCI and 17 AB subjects Manual kinesthesia assessment: 1 point for each correct movement detection
Abnormal joint synergies	-	-	-	-	-	No studies found
Passive ankle stiffness	Manual spasticity evaluator	-	Ankle DF 4°: r = 0.81	Ankle DF 4°: ICC = 0.82	-	[127], 12 children with CP
	Ankle perturbator	Repeated testing of known static torque: ICC = 0.994	ICC = 0.767-0.943			[376], 10 AB subjects
	Ankle assessment device	-	-	Ankle DF 20°: ICC = 0.863 Ankle DF 30°: ICC = 0.865	Ankle DF 20°: MDC = 0.0686 Nm/° Ankle DF 30°: MDC = 0.1323 Nm/°	[374], 9 AB subjects
Active ankle stiffness	Ankle perturbator	-	-	r>0.8	-	[242], 11 AB subjects
	Ankle perturbator	-	Between-trial: ICC = 0.76–0.99 and between-day: ICC = 0.64–0.95	-	-	[243], 38 children with CP and 35 AB subjects
Walking function / Gait pattern	Exosuit: strain sensors	Mean absolute error ≤ 8°	-	-	-	[139], 1 AB subject
	Soft ankle orthosis: strain sensors, IMUs	Mean error strain sensor: 0.255±1.63° Mean error IMUs: 0.135±2.85°	-	-	-	[275], 1 AB subject

Table A.3: in the table: ρ indicates Spearman's rank correlation, r Pearson's correlation, DF dorsiflexion, PF plantarflexion

Appendix B

In 0, an Adaptive Feedforward Controller (AFFC) is used to determine the parameters of the Lokomat. The Lokomat orthosis in swing phase is modeled as one double pendulum (Figure A.1). The equations of motion of the Lokomat orthosis were derived using the Lagrangian formulation.
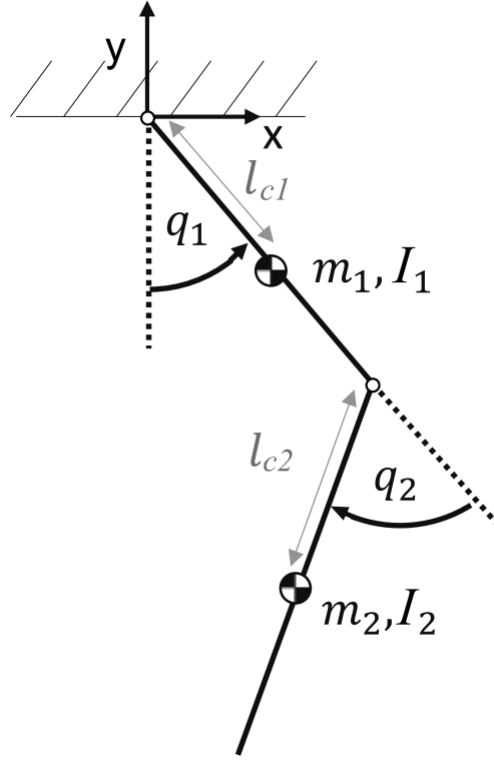
Figure A.7.1: Lokomat model in swing phase (no contact with the treadmill). Note the sign of q_2 due to the anatomical convention used for the knee angle. m represents the mass, I the moment of inertia, l_m the distance of the center of gravity from the joint.

The general equation of the feedforward torques:

$$\boldsymbol{\tau}_{FF} = H(\boldsymbol{q}) \cdot \ddot{\boldsymbol{q}} + C(\boldsymbol{q}, \dot{\boldsymbol{q}}) + G(\boldsymbol{q}) + F(\dot{\boldsymbol{q}}) \tag{A.1}$$

is composed by the inertia matrix $H(\boldsymbol{q})$:

$$H(\boldsymbol{q}) = \begin{bmatrix} I_1 + I_2 + m_1 l_{c1}{}^2 + m_2(l_1^2 + l_{c2}{}^2 + 2l_1 l_{c2} \cos(q_2)) & I_2 - m_2\left(l_1 l_{c2} \cos(q_2) + l_{c2}{}^2\right) \\ I_2 - m_2\left(l_1 l_{c2} \cos(q_2) + l_{c2}{}^2\right) & I_2 + m_2 l_{c2}{}^2 \end{bmatrix} ; \tag{A.2}$$

the Coriolis matrix $C(\boldsymbol{q}, \dot{\boldsymbol{q}})$:

$$C(\boldsymbol{q}, \dot{\boldsymbol{q}}) = \begin{bmatrix} -m_2 l_1 l_{c2} \sin(q_2) \dot{q}_2(2\dot{q}_1 - \dot{q}_2) \\ m_2 l_1 l_{c2} \sin(q_2) \dot{q}_1^2 \end{bmatrix} ; \tag{A.3}$$

and the gravity matrix $G(\boldsymbol{q})$:

$$G(\boldsymbol{q}) = g \begin{bmatrix} m_1 l_{c1} \sin(q_1) + m_2 l_1 \sin(q_1) + m_2 l_{c2} \sin(q_1 - q_2) \\ -m_2 l_{c2} \sin(q_1 - q_2) \end{bmatrix} . \tag{A.4}$$

The friction component includes a static and a dynamic term:

$$F(\dot{q}) = \begin{bmatrix} f_1\dot{q}_1 + k_1 \tanh(\dot{q}_1) \\ f_2\dot{q}_2 + k_2 \tanh(\dot{q}_2) \end{bmatrix}. \tag{A.5}$$

The AFFC algorithm requires the model to be linear in the parameters to be identified. Such parameters, initially set to 0, are then identified in real-time according to gradient descent of the tracking error function (Eq. 4.5). Eq. A.1 can be linearized as:

$$\tau_{FF} = \varphi(q, \dot{q}, \ddot{q}) \cdot \lambda \tag{A.6}$$

The unknown parameters λ are identified in real time with the AFFC learning rule. In the following equations, I represents the moment of inertia, m the mass, l the length, l_c the distance to the center of gravity from the joint along the segment (Figure A.7.1).

$$\lambda_{HC} = \begin{bmatrix} \lambda_1 \\ \lambda_2 \\ \lambda_3 \\ \lambda_4 \end{bmatrix} = \begin{bmatrix} I_1 + m_1 l_{c1}^2 + m_2 l_1^2 \\ m_2 l_1 l_{c2} \\ I_2 \\ -m_2 l_{c2}^2 \end{bmatrix} \tag{A.7}$$

$$\lambda_G = \begin{bmatrix} \lambda_5 \\ \lambda_6 \end{bmatrix} = \begin{bmatrix} m_2 l_{c2} \\ m_1 l_{c1} + m_2 l_1 \end{bmatrix} \tag{A.8}$$

$$\lambda_F = \begin{bmatrix} \lambda_7 \\ \lambda_8 \\ \lambda_9 \\ \lambda_{10} \end{bmatrix} = \begin{bmatrix} f_1 \\ k_1 \\ f_2 \\ k_2 \end{bmatrix} \tag{A.9}$$

The matrix $\boldsymbol{\Phi}(q, \dot{q}, \ddot{q})$ is composed by the following elements:

$$\boldsymbol{\Phi}_{HC} = \begin{bmatrix} \ddot{q}_1 & 2\cos(q_2)\ddot{q}_1 - \cos(q_2)\ddot{q}_2 - \sin(q_2)\dot{q}_2(2\dot{q}_1 - \dot{q}_2) & \ddot{q}_1 + \ddot{q}_2 & -\ddot{q}_2 \\ 0 & -\cos(q_2)\ddot{q}_1 + \sin(q_2)\dot{q}_1^2 & \ddot{q}_1 + \ddot{q}_2 & -\ddot{q}_1 \end{bmatrix}, \tag{A.10}$$

$$\boldsymbol{\Phi}_G = g \begin{bmatrix} \sin(q_1 - q_2) & \sin(q_1) \\ -\sin(q_1 - q_2) & 0 \end{bmatrix}, \tag{A.11}$$

$$\boldsymbol{\Phi}_F = \begin{bmatrix} \dot{q}_1 & \tanh(\dot{q}_1) & 0 & 0 \\ 0 & 0 & \dot{q}_2 & \tanh(\dot{q}_2) \end{bmatrix}, \tag{A.12}$$

resulting in:

$$\boldsymbol{\Phi}(q, \dot{q}, \ddot{q}) = [\boldsymbol{\Phi}_{HC} \quad \boldsymbol{\Phi}_G \quad \boldsymbol{\Phi}_F]. \tag{A.13}$$

Appendix C

C.1   SELECTION OF PREDICTORS IN BOLASSO

In Chapter 5, Bolasso was used as feature selection method to identify which AAN-outcome measure(s) could better predict the timed walking tests. Here the variables selected in 1000 bootstrap runs are presented.

C.1.1   Prediction of 10MWT using only AAN outcome measures
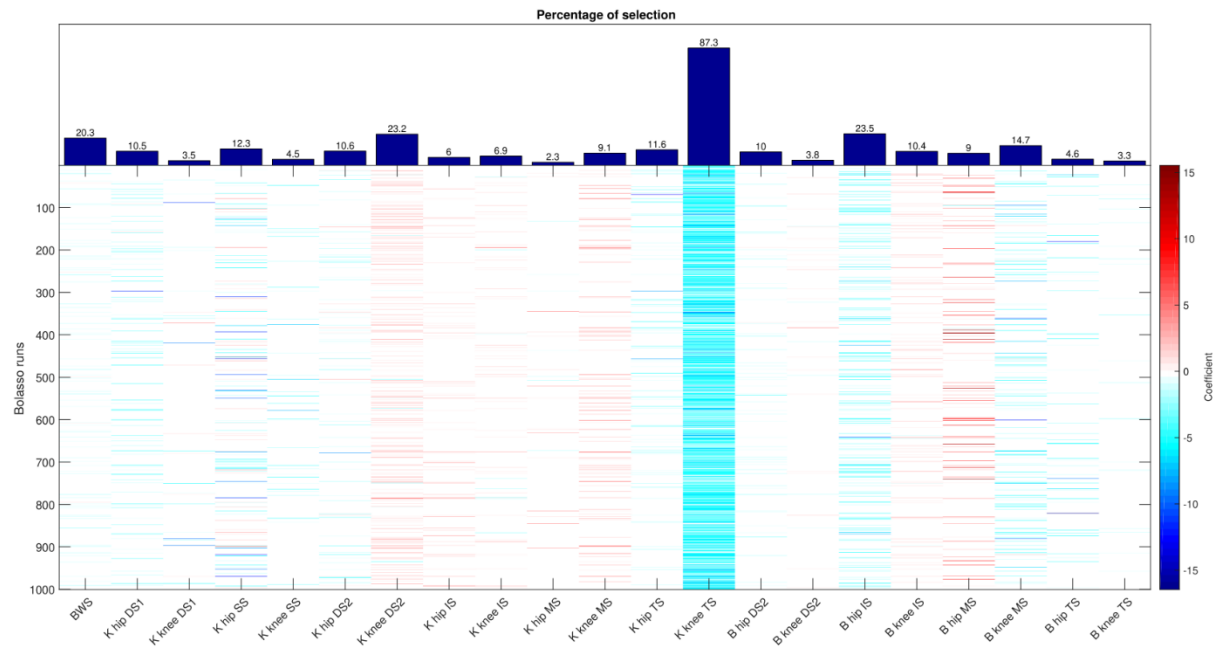
Figure A.7.2: Output of the Bolasso algorithm for the prediction of 10MWT in ambulatory patients. The colored bars indicate if the coefficient of the predictor in a certain Bolasso run was different from 0, positive (red) or negative (blue). The percentage of selection is shown in the bar plot above.

C.1.2 Prediction of TUG using only AAN outcome measures
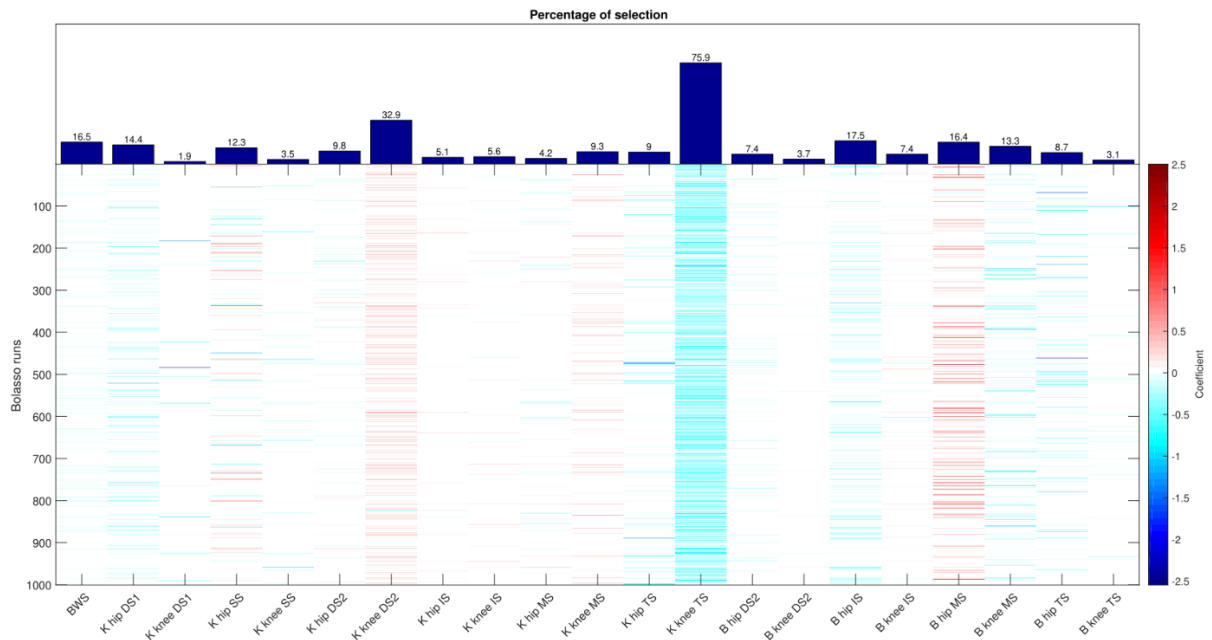
Figure A.7.3: Output of the Bolasso algorithm for the prediction of TUG in ambulatory patients. The colored bars indicate if the coefficient of the predictor in a certain Bolasso run was different from 0, positive (red) or negative (blue). The percentage of selection is shown in the bar plot above.

C.1.3 Prediction of 10MWT using AAN outcome measures and L-FORCE measures
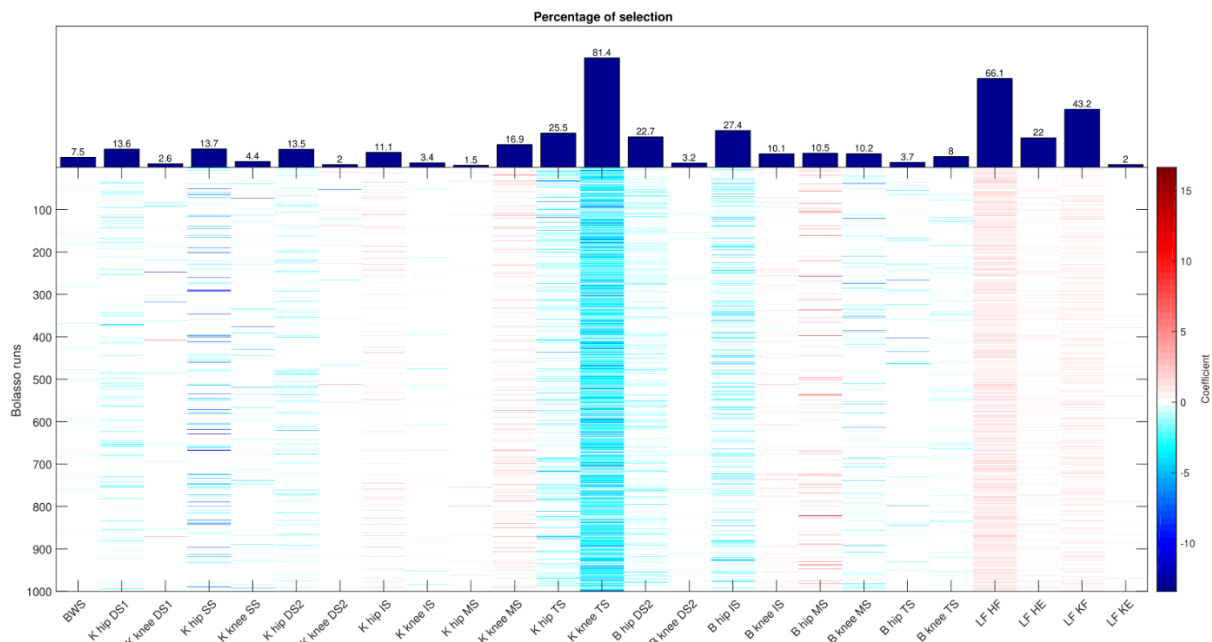
Figure A.7.4: Output of the Bolasso algorithm for the prediction of 10MWT in ambulatory patients when also the L-FORCE measures are added to the pool of possible predictors. The colored bars indicate if the coefficient of the predictor in a certain Bolasso run was different from 0, positive (red) or negative (blue). The percentage of selection is shown in the bar plot above.

C.1.4 Prediction of TUG using AAN outcome measures and L-FORCE measures
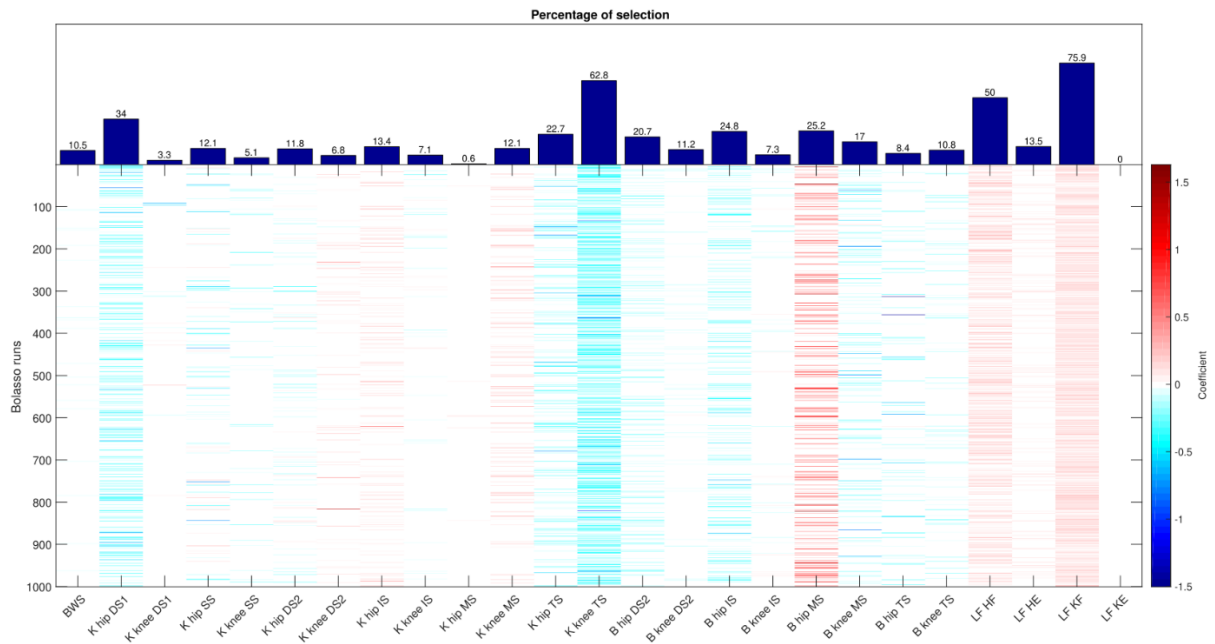
Figure A.7.5: Output of the Bolasso algorithm for the prediction of TUG in ambulatory patients when also the L-FORCE measures are added to the pool of possible predictors. The colored bars indicate if the coefficient of the predictor in a certain Bolasso run was different from 0, positive (red) or negative (blue). The percentage of selection is shown in the bar plot above.

C.1.5 Prediction of 10MWT in able-bodied subjects using AAN outcome measures and L-FORCE measures
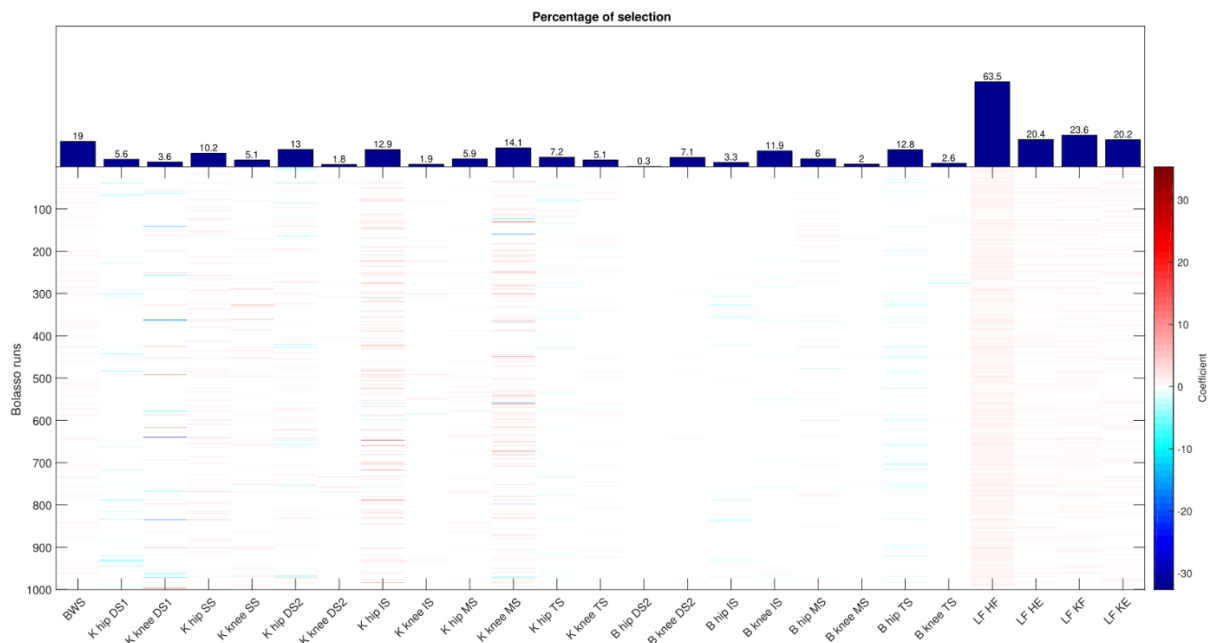
Figure A. 7.6: Output of the Bolasso algorithm for the prediction of 10MWT in able-bodied subjects when also the L-FORCE measures are added to the pool of possible predictors. The colored bars indicate if the coefficient of the predictor in a certain Bolasso run was different from 0, positive (red) or negative (blue). The percentage of selection is shown in the bar plot above.

C.2 Prediction of TUG in Non-ambulatory Patients and in Able-bodied Subjects
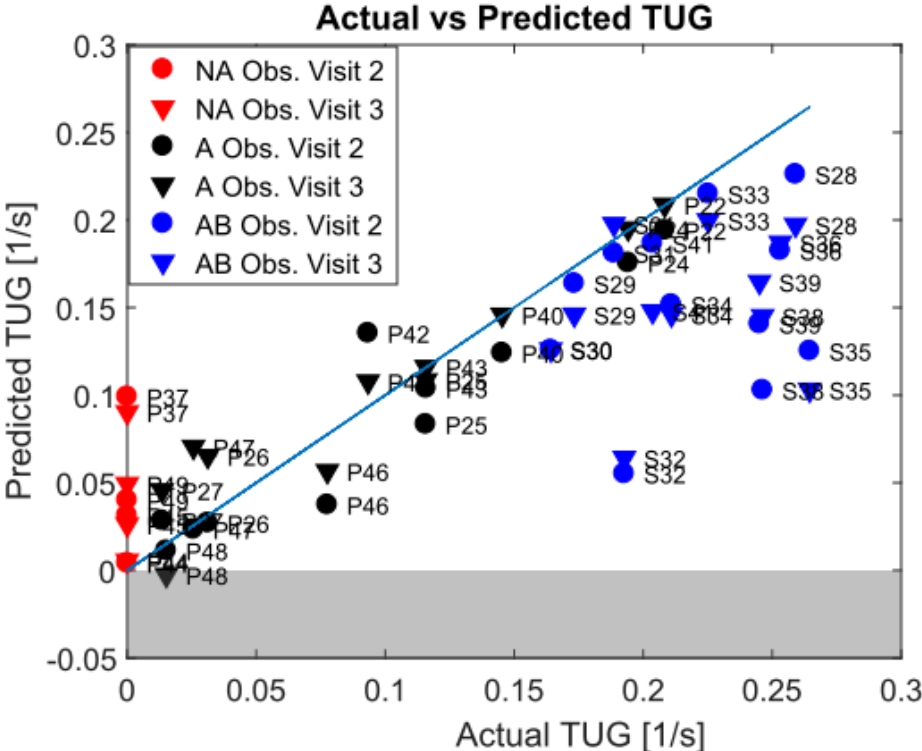

Figure A.7.7: Prediction of virtual TUG using model with 2 predictors (K knee TS and LF KF). In blue, the identity line is shown.

Appendix D

In Chapter 5, the results of the clinical study on the AAN-based assessment were presented. At the end of Visit 2 and 3, the participants were asked to fill the NASA Task Load Index (TLX)[5] questionnaire (Table A.4).

An overview of the answers grouped by visits and per participants group is presented in Figure A.7.8.

[5] https://humansystems.arc.nasa.gov/groups/TLX/tlxpaperpencil.php

NASA Task Load Index	
Mental Demand	How mentally demanding was the task?
	Very Low ⊢—————————————————————⊣ Very High
Physical Demand	How physically demanding was the task?
	Very Low ⊢—————————————————————⊣ Very High
Temporal Demand	How hurried or rushed was the pace of the task?
	Very Low ⊢—————————————————————⊣ Very High
Performance	How successful were you in accomplishing what you were asked to do?
	Very Low ⊢—————————————————————⊣ Very High
Effort	How hard did you have to work to accomplish your level of performance?
	Very Low ⊢—————————————————————⊣ Very High
Frustration	How insecure, discouraged, irritated, stressed, and annoyed were you?
	Very Low ⊢—————————————————————⊣ Very High

Table A.4: NASA TLX questionnaire used in the study. Participants were asked to fill in this questionnaire after performing the AAN-based assessment on both visits.
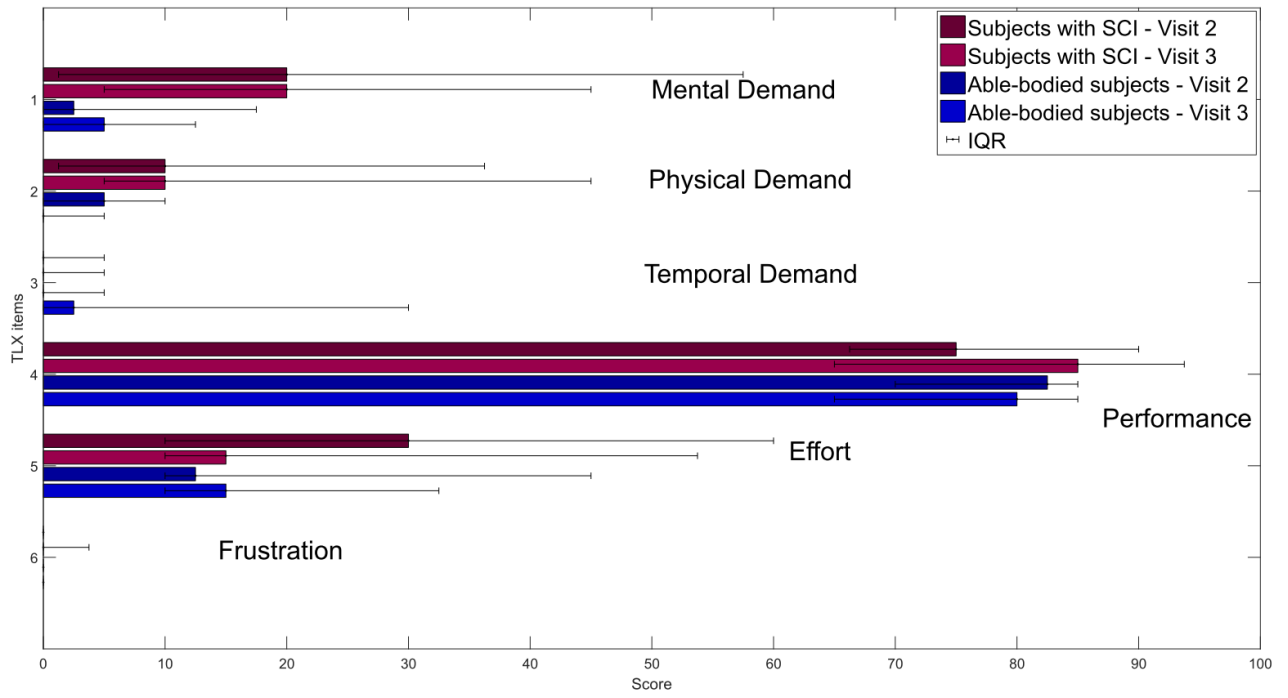
Figure A.7.8: Mean and Interquartile Range of the answers to the NASA TLX questionnaire, grouped by visit and participant group.

Figure A. 7.9: Correlation plot between clinical scores (10MWT [m/s], TUG [1/s], WISCI II) and TLX questionnaire collected after the second AAN-based assessment visit (Visit 3). The values indicated the Spearman correlation coefficient. The significant correlations coefficients (p<0.05) are indicated in red. Only ambulatory subjects are included in the analysis.

Appendix E

In Chapter 6, the hybrid joint/end-point space controller was introduced. The equations below explain the relationships between joint space and end-point space formulations.

RELATIONSHIP BETWEEN JOINT AND END-POINT SPACES

E.1   FORWARD KINEMATICS

In this paper we examine the behavior of two controllers applied to a two-segment robotic device with two actuated joints, which correspond to the hip and knee joint of the human subject.

In the paper we referred to joint angular trajectories, **q**:

$$q = \begin{bmatrix} q_{hip} \\ q_{knee} \end{bmatrix}. \tag{A.14}$$

We calculate the position of the end-point of the two-segment kinematic chain in Cartesian space, using the sign convention shown in Figure A.1:

$$x = \begin{bmatrix} l_1 \cdot sin(q_{hip}) + l_2 \cdot sin(q_{hip} + q_{knee}) \\ -l_1 \cdot cos(q_{hip}) - l_2 \cdot cos(q_{hip} + q_{knee}) \end{bmatrix} = \begin{bmatrix} x \\ y \end{bmatrix}. \tag{A.15}$$

E.2   TRANSFORMATIONS BETWEEN END-POINT FORCES AND JOINT TORQUES

In our system, a set of commanded joint torques, **τ**, are used to control the robotic joints:

$$\tau = \begin{bmatrix} \tau_{hip} \\ \tau_{knee} \end{bmatrix}; \tag{A.16}$$

We can obtain the resulting forces applied at the end-point, F_x, in correspondence of a given set of applied joint torques, through this transformation:

$$F_x = (J[q]^T)^{-1}\tau_q , \tag{A.17}$$

where **J[q]** is the Jacobian matrix, that represents the differential relationship between the joint displacements and the resulting end-point motion (i.e. the sensitivity of each individual end-point coordinate to individual joint displacement). The Jacobian matrix is defined for each set of joint coordinates. The Jacobian matrix for our system can be calculated as follows:

$$J(q_{act}) = \begin{bmatrix} l_1 \cdot cos(q_{hip}) + l_2 \cdot cos(q_{hip} + q_{knee}) & l_2 \cdot cos(q_{hip} + q_{knee}) \\ l_1 \cdot sin(q_{hip}) + l_2 \cdot sin(q_{hip} + q_{knee}) & l_2 \cdot sin(q_{hip} + q_{knee}) \end{bmatrix} \tag{A.18}$$

On the other side, to obtain the joint torques necessary to provide the desired end-point forces, we can use the inverse of Eq. A.4:

$$\tau_q = J[q]^T F_x \tag{A.19}$$

E.3 TRANSFORMATIONS BETWEEN JOINT STIFFNESS AND END-POINT STIFFNESS

For each set point along the angular reference trajectory, we want to study the relationship between torque and angular displacement; this relationship is represented by the joint stiffness matrix $\boldsymbol{K}_j$ [344]:

$$K_j = \frac{d\tau}{dq}. \tag{A.20}$$

Therefore, for small angular displacement around the set point we can calculate the desired restoring torques:

$$\begin{bmatrix} \tau_{hip} \\ \tau_{knee} \end{bmatrix} = \boldsymbol{K}_j \cdot \begin{bmatrix} dq_{hip} \\ dq_{knee} \end{bmatrix} = \begin{bmatrix} K_{hh} & K_{hk} \\ K_{kh} & K_{kk} \end{bmatrix} \cdot \begin{bmatrix} dq_{hip} \\ dq_{knee} \end{bmatrix} \tag{A.21}$$

In a similar way, in task space, the end-point stiffness matrix $\mathbf{K}_x$ represents the ratio between linear force and linear displacement:

$$K_x = \frac{dF}{dx} \tag{A.22}$$

The desired restoring forces can be calculated knowing the end-point stiffness matrix:

$$\begin{bmatrix} F_x \\ F_y \end{bmatrix} = \boldsymbol{K}_x \cdot \begin{bmatrix} dx \\ dy \end{bmatrix} = \begin{bmatrix} K_{xx} & K_{xy} \\ K_{yx} & K_{yy} \end{bmatrix} \cdot \begin{bmatrix} dx \\ dy \end{bmatrix} \tag{A.23}$$

The joint and end-point stiffness matrices are symmetric [344], therefore $K_{xy} = K_{yx}$ and $K_{hk} = K_{kh}$.

To calculate the perceived stiffness $\mathbf{K}_x$ at the end-point we can apply this calculation to the joint stiffness $\mathbf{K}_j$:

$$K_x = (J[q]^T)^{-1} K_q (J[q])^{-1} \tag{A.24}$$

E.4 STIFFNESS ELLIPSES

As shown in [345], if we take d$\mathbf{x}$ as a unitary vector with a direction that changes gradually from $0°$ to $360°$ and we multiply it for $\mathbf{K}_x$, we obtain the corresponding output force vectors. They describe an ellipse, where the major axis indicates the direction along which the stiffness is higher, whereas the minor axis is the direction of minimum stiffness. These directions are the eigenvectors of the stiffness matrix and the magnitude of the major and minor axes are its eigenvalues.

We can also visually represent the stiffness around a set point using force and torque fields in end-point and joint space, respectively. For small displacements around a set point, we can plot the restoring forces or torques as shown above (Eqs. A.21 and A.23). It is interesting to notice that, except for the directions of the major and minor axes of the ellipse, the restoring forces and torques are not co-linear with the correspondent displacement vectors.

Appendix F

Four students contributed to the work presented in this thesis. Their topics are presented in the table below.

Contribution	Student work
Technical validation on a robotic test bench, clinical pilot tests	Simon Stucki (MT), *Validation of a novel robot-aided gait assessment algorithm,* October 2015
Hybrid joint/end-point controller, technical validation on a robotic test bench and clinical pilot tests	Nils Reinert (MT), *End-point Impedance Adaptation for Robotic Gait Devices,* May 2016
Clinical study (experiments and data analysis)	Jasmin Egloff (ST), *Clinical Validation of a novel Robot-aided Walking Assessment*, June 2016
Clinical study (experiments and data analysis)	Carole Köchli (I), *Clinical validation of a novel Robot-aided Gait Assessment*, December 2016

Table A.5: Four students contributed to the work listed in the left column, with the theses listed in the right column. MT: Master Thesis, ST: Semester Thesis, I: Internship.

BIBLIOGRAPHY

1. World Report on Disability. Geneva; 2011. https://www.who.int/disabilities/world_report/2011/en/.

2. Kraus, L., Lauer, E., Coleman, R., & Houtenville A. 2017 Disability Statistics Annual Report. Durham, NH: University of New Hampshire; 2018. https://www.mendeley.com/catalogue/2017-disability-statistics-report/.

3. Li S, Francisco GE, Zhou P. Post-stroke hemiplegic gait: New perspective and insights. Front Physiol. 2018;9 AUG:1–8.

4. Lam T, Noonan VK, Eng JJ, SCIRE Research Team. A systematic review of functional ambulation outcome measures in spinal cord injury. Spinal Cord. 2008;46:246–54. doi:10.1038/sj.sc.3102134.

5. GBD 2016 Traumatic Brain Injury and Spinal Cord Injury Collaborators. Global, regional, and national burden of traumatic brain injury and spinal cord injury, 1990–2016: a systematic analysis for the Global Burden of Disease Study 2016. Lancet Neurol. 2019;18:56–87.

6. Mirelman A, Bonato P, Camicioli R, Ellis TD, Giladi N, Hamilton JL, et al. Gait impairments in Parkinson's disease. Lancet Neurol. 2019;18:697–708. doi:10.1016/S1474-4422(19)30044-4.

7. Larocca NG. Impact of walking impairment in multiple sclerosis: perspectives of patients and care partners. Patient. 2011;4:189–201.

8. Williams G, Morris ME, Schache A, McCrory PR. Incidence of gait abnormalities after traumatic brain injury. Arch Phys Med Rehabil. 2009;90:587–93.

9. Esquenazi A, Maier IC, Aurich Schuler, Tabea Beer SM, Borggraefe I, Campen K, Luft AR, et al. Clinical Application of Robotics and Technology in the Restoration of Walking. In: Reinkensmeyer DJ, Dietz V, editors. Neurorehabilitation Technology. 2nd Editio. Springer International Publishing; 2016. p. 223–48.

10. Burns SP, Gelding DG, Rolle WA, Graziani V, Ditunno JF. Recovery of Ambulation in Motor-Incomplete Tetraplegia. Arch Phys Med Rehabil. 1997;78 November:1169–72.

11. Winstein CJ, Stein J, Arena R, Bates B, Cherney LR, Cramer SC, et al. Guidelines for Adult Stroke Rehabilitation and Recovery: A Guideline for Healthcare Professionals from the American Heart Association/American Stroke Association. Stroke. 2016;47:e98–169.

12. Sezer N, Akkuş S, Uğurlu FG. Chronic complications of spinal cord injury. World J Orthop.

2015;6:24–33.

13. Scivoletto G, Di Donna V. Prediction of walking recovery after spinal cord injury. Brain Res Bull. 2009;78:43–51. doi:10.1016/j.brainresbull.2008.06.002.

14. Bohannon RW, Horton MG, Wikholm JB. Importance of four variables of walking to patients with stroke. Int J Rehabil Res. 1991;:246–50.

15. Ditunno PL, Patrick M, Stineman M, Ditunno JF. Who wants to walk? Preferences for recovery after SCI: a longitudinal and cross-sectional study. Spinal Cord. 2008;46:500–6. doi:10.1038/sj.sc.3102172.

16. Barbeau H, Nadeau S, Garneau C. Physical Determinants, Emerging Concepts, and Training Approaches in Gait of Individuals with Spinal Cord Injury. J Neurotrauma. 2006;23:571–85.

17. Wirz M, van Hedel HJA. Balance, gait, and falls in spinal cord injury. In: Day BL, Lord SR, editors. Handbook of Clinical Neurology. Elsevier B.V.; 2018.

18. Awai L, Curt A. Comprehensive assessment of walking function after human spinal cord injury. 1st edition. Elsevier B.V.; 2015. doi:10.1016/bs.pbr.2014.12.004.

19. Mehrholz J, Thomas S, Werner C, Kugler J, Pohl M, Elsner B. Electromechanical-assisted training for walking after stroke (Review). Cochrane Database Syst Rev. 2017.

20. Lünenburger L, Colombo G, Riener R, Dietz V. Clinical assessments performed during robotic rehabilitation by the gait training robot Lokomat. In: Proceedings of the 2005 IEEE 9th International Conference on Rehabilitation Robotics. 2005. p. 345–8.

21. Banala SK, Kim SH, Agrawal SK, Scholz JP. Robot Assisted Gait Training With Active Leg Exoskeleton (ALEX). IEEE Trans neural Syst Rehabil Eng. 2009;17:2–8.

22. Koopman B, van Asseldonk EH, van der Kooij H. Selective control of gait subtasks in robotic gait training: foot clearance support in stroke survivors with a powered exoskeleton. J Neuroeng Rehabil. 2013;10:3. doi:10.1186/1743-0003-10-3.

23. World Health Organization. Towards a Common Language for Functioning , Disability and Health ICF. 2002. http://www.who.int/classifications/icf/training/icfbeginnersguide.pdf.

24. Emken JL, Bobrow JE, Reinkensmeyer DJ. Robotic Movement Training As an Optimization Problem: Designing a Controller That Assists Only As Needed. In: Proceedings of the 2005 IEEE 9th International Conference on Rehabilitation Robotics. Chicago, IL, USA; 2005. p. 307–12. doi:10.1109/ICORR.2005.1501108.

25. Awai L, Curt A. Intralimb coordination as a sensitive indicator of motor-control impairment after spinal cord injury. Front Hum Neurosci. 2014;8 March:148. doi:10.3389/fnhum.2014.00148.

26. World Health Organization. ICF Browser. 2017. http://apps.who.int/classifications/icfbrowser/. Accessed 26 Aug 2019.

27. Miller-Keane, O'Toole MT. Miller-Keane Encyclopedia & Dictionary of Medicine, Nursing & Allied Health, 7th Edition. 2005.

28. Perry J. Gait Analysis. Normal and Pathological Function. Thorofare, NJ, USA: SLACK Incorporated; 1992.

29. Winter DA. Biomechanics and motor control of human gait: normal, elderly and pathological. 2nd edition. Waterloo, Canada: Waterloo Biomechanics; 1991.

30. Baker R. Measuring Walking: A Handbook of Clinical Gait Analysis. 1st edition. London: Mac Keith Press; 2013.

31. Baker R. Why we walk the way we do 1 (framework). 2013. https://www.youtube.com/watch?v=iG6KfzoqWyg. Accessed 5 Aug 2019.

32. Baker R. Walking with Richard. Personal reflections on lower limb biomechanics. 2019. https://wwrichard.net/. Accessed 26 Aug 2019.

33. Gage JR. Gait Analysis in Cerebral Palsy. Oxford: Cambridge University Press; 1991.

34. Horak FB. Postural orientation and equilibrium: what do we need to know about neural control of balance to prevent falls? Age Ageing. 2006;35 suppl_2:ii7-ii11. doi:10.1093/ageing/afl077.

35. Winter DA. Foot trajectory in human gait: a precise and multifactorial motor control task. Phys Ther. 1992;72:45–53;

36. Goldberg SR, Sylvia O, Arnold AS, Gage JR, Delp SL. Kinematic and kinetic factors that correlate with improved knee flexion following treatment for stiff-knee gait. J Biomech. 2006;39:689–98.

37. Baker R. Why we walk the way we do 6 (Step length). 2013. https://www.youtube.com/watch?v=1EYnQ7kwY5Y. Accessed 26 Aug 2019.

38. Baker R. Why we walk the way we do 4 (energy). 2013. https://youtu.be/hDt6QsErrX8. Accessed 26 Aug 2019.

39. Kuo AD, Donelan JM. Dynamic Principles of Gait and Their Clinical Implications. Phys Ther.

2010;90:157–74.

40. Steuer I, Rouleau P, Guertin PA. Pharmacological approaches to chronic spinal cord injury. Curr Pharm Des. 2013;19:4423–36.

41. Wagner FB, Mignardot J-B, Le Goff-Mignardot CG, Demesmaeker R, Komi S, Capogrosso M, et al. Targeted neurotechnology restores walking in humans with spinal cord injury. Nature. 2018;563:65–71.

42. Steeves JD, Lammertse D, Curt A, Fawcett JW, Tuszynski MH, Ditunno JF, et al. Guidelines for the conduct of clinical trials for spinal cord injury (SCI) as developed by the ICCP panel: clinical trial outcome measures. Spinal Cord. 2007;45:206–21.

43. van Hedel H. Gait speed in relation to categories of functional ambulation after spinal cord injury. Neurorehabil Neural Repair. 2009;23:343–50.

44. Furlan JC, Noonan V, Singh A, Fehlings MG. Assessment of disability in patients with acute traumatic spinal cord injury: a systematic review of the literature. J Neurotrauma. 2011;28:1413–30. doi:10.1089/neu.2009.1148.

45. French B, Lh T, Coupe J, Ne M, Connell L, Harrison J, et al. Repetitive task training for improving functional ability after stroke (Review). Cochrane Database Syst Rev. 2016.

46. Behrman AL, Harkema SJ. Physical Rehabilitation as an Agent for Recovery After Spinal Cord Injury. Phys Med Rehabil Clin N Am. 2007;18:183–202.

47. Jones ML, Evans N, Tefertiller C, Backus D, Sweatman M, Tansey K, et al. Activity-based therapy for recovery of walking in individuals with chronic spinal cord injury: results from a randomized clinical trial. Arch Phys Med Rehabil. 2014;95:2239–46.e2.

48. Barbeau H. Locomotor training in neurorehabilitation: emerging rehabilitation concepts. Neurorehabil Neural Repair. 2003;17:3–11.

49. Wolpaw JR, Tennissen AM. Activity-Dependent Spinal Cord Plasticity in Health and Disease. Annu Rev Neurosci. 2001;24:807–43.

50. Dietz V, Muller R, Colombo G. Locomotor activity in spinal man: significance of afferent input from joint and load receptors. Brain. 2002;125 Pt 12:2626–34.

51. Dietz V, Harkema SJ. Locomotor activity in spinal cord-injured persons. J Appl Physiol. 2004;96:1954–60.

52. Lünenburger L, Bolliger M, Czell D, Muller R, Dietz V. Modulation of locomotor activity in complete spinal cord injury. Exp brain Res. 2006;174:638–46. doi:10.1007/s00221-006-0509-4.

53. Visintin M, Barbeau H, Korner-Bitensky N, Mayo N. A new approach to retrain gait in stroke patients through body weight support and treadmill stimulation. Stroke. 1998;29:1122--8.

54. Esquenazi A, Lee S, Wikoff A, Packel A, Toczylowski T, Feeley J. A Randomized Comparison of Locomotor Therapy Interventions: Partial Body Weight Supported Treadmill, Lokomat® and G-Eo® Training in Traumatic Brain Injury. Pm&R. 2017;8:S154.

55. Colombo G, Joerg M, Schreier R, Dietz V. Treadmill training of paraplegic patients using a robotic orthosis. J Rehabil Res Dev. 2000;37:693–700.

56. Gassert R, Dietz V. Rehabilitation robots for the treatment of sensorimotor deficits: A neurophysiological perspective. J Neuroeng Rehabil. 2018;15:1–15.

57. Colombo G, Wirz M, Dietz V. Driven gait orthosis for improvement of locomotor training in paraplegic patients. Spinal Cord. 2001;:252–5.

58. Hwang J, Shin Y, Park J-H, Cha YJ, You JSH. Effects of Walkbot gait training on kinematics, kinetics, and clinical gait function in paraplegia and quadriplegia. NeuroRehabilitation. 2018;42:481–9.

59. Diaz I, Gil JJ, Sanchez E. Lower-Limb Robotic Rehabilitation : Literature Review and Challenges. J Robot. 2011.

60. Esquenazi A, Talaty M, Jayaraman A. Powered Exoskeletons for Walking Assistance in Persons with Central Nervous System Injuries: A Narrative Review. Phys Med Rehabil. 2017;9:46–62. doi:10.1016/j.pmrj.2016.07.534.

61. Schrade SO, Dätwyler K, Stücheli M, Studer K, Türk D-A, Meboldt M, et al. Development of VariLeg, an exoskeleton with variable stiffness actuation: first results and user evaluation from the CYBATHLON 2016. J Neuroeng Rehabil. 2018;15:18. doi:10.1186/s12984-018-0360-4.

62. Lee S, Kim J, Baker L, Long A, Karavas N, Menard N, et al. Autonomous multi-joint soft exosuit with augmentation-power-based control parameter tuning reduces energy cost of loaded walking. J Neuroeng Rehabil. 2018;15:66. doi:10.1186/s12984-018-0410-y.

63. Schmidt K, Duarte JE, Grimmer M, Sancho-Puchades A, Wei H, Easthope CS, et al. The Myosuit: Bi-articular anti-gravity exosuit that reduces hip extensor activity in sitting transfers. Front Neurorobot. 2017;11 OCT:1–16.

64. Bannwart M, Emst D, Easthope C, Bolliger M, Rauter G. Automated stand-up and sit-down

detection for robot-assisted body-weight support training with the FLOAT. IEEE Int Conf Rehabil Robot. 2017;2017:412–7.

65. Nam KY, Kim HJ, Kwon BS, Park JW, Lee HJ, Yoo A. Robot-assisted gait training (Lokomat) improves walking function and activity in people with spinal cord injury: a systematic review. J Neuroeng Rehabil. 2017;14:1–13.

66. Wirz M, MacH O, Maier D, Benito-Penalva J, Taylor J, Esclarin A, et al. Effectiveness of Automated Locomotor Training in Patients with Acute Incomplete Spinal Cord Injury: A Randomized, Controlled, Multicenter Trial. J Neurotrauma. 2017;34:1891–6.

67. Esclarín-Ruz A, Alcobendas-Maestro M, Casado-Lopez R, Perez-Mateos G, Florido-Sanchez MA, Gonzalez-Valdizan E, et al. A comparison of robotic walking therapy and conventional walking therapy in individuals with upper versus lower motor neuron lesions: a randomized controlled trial. Arch Phys Med Rehabil. 2014;95:1023–31. doi:10.1016/j.apmr.2013.12.017.

68. Alcobendas-Maestro M, Esclarín-Ruz A, Casado-López RM, Muñoz-González A, Pérez-Mateos G, González-Valdizán E, et al. Lokomat robotic-assisted versus overground training within 3 to 6 months of incomplete spinal cord lesion: randomized controlled trial. Neurorehabil Neural Repair. 2012;26:1058–63. doi:10.1177/1545968312448232.

69. Donati ARC, Shokur S, Morya E, Campos DSF, Moioli RC, Gitti CM, et al. Long-Term Training with a Brain-Machine Interface-Based Gait Protocol Induces Partial Neurological Recovery in Paraplegic Patients. Sci Rep. 2016;6:30383. https://doi.org/10.1038/srep30383.

70. Lam T, Wirz M, Lünenburger L, Dietz V. Swing phase resistance enhances flexor muscle activity during treadmill locomotion in incomplete spinal cord injury. Neurorehabil Neural Repair. 2009;22:438–46. doi:10.1177/1545968308315595.

71. Mirbagheri MM, Kindig MW, Niu X. Effects of robotic-locomotor training on stretch reflex function and muscular properties in individuals with spinal cord injury. Clin Neurophysiol. 2015;126:997–1006. doi:10.1016/j.clinph.2014.09.010.

72. Chang WH, Kim MS, Huh JP, Lee PKW, Kim Y-H. Effects of robot-assisted gait training on cardiopulmonary fitness in subacute stroke patients: a randomized controlled study. Neurorehabil Neural Repair. 2012;26:318–24.

73. Husemann B, Muller F, Krewer C, Heller S, Koenig E. Effects of locomotion training with assistance of a robot-driven gait orthosis in hemiparetic patients after stroke: a randomized controlled pilot study. Stroke. 2007;38:349–54.

74. Bergmann J, Krewer C, Bauer P, Koenig A, Riener R, Muller F. Virtual reality to augment robot-assisted gait training in non-ambulatory patients with a subacute stroke: a pilot randomized controlled trial. Eur J Phys Rehabil Med. 2018;54:397–407.

75. Veneri D, Tartaglia J. Determining Important Dosage Parameters to Improve Gait Speed and Distance Using Mechanical Gait Support for Persons with Stroke: A Meta-Analysis. Crit Rev Phys Rehabil Med. 2014;26.

76. Aurich-Schuler T, Grob F, Van Hedel HJA, Labruyère R. Can Lokomat therapy with children and adolescents be improved? An adaptive clinical pilot trial comparing Guidance force, Path control, and FreeD. J Neuroeng Rehabil. 2017;14:1–14.

77. Maggioni S, Melendez-Calderon A, van Asseldonk E, Klamroth-Marganska V, Lünenburger L, Riener R, et al. Robot-aided assessment of lower extremity functions: a review. J Neuroeng Rehabil. 2016;13:72. doi:10.1186/s12984-016-0180-3.

78. Duncan EA, Murray J. The barriers and facilitators to routine outcome measurement by allied health professionals in practice: a systematic review. BMC Health Serv Res. 2012;12:96.

79. Jette DU, Halbert J, Iverson C, Miceli E, Shah P. Use of standardized outcome measures in physical therapist practice: perceptions and applications. Phys Ther. 2009;89:125–35.

80. Copeland J. Outcome measures: why physiotherapists must use them. Phys Ther Rev. 2009;14:367–8. doi:10.1179/108331909X12488667117131.

81. Hedel HJA Van. Improvement in function after spinal cord injury : the black-box entitled rehabilitation. Swiss Med Wkly. 2012; September.

82. Lambercy O, Maggioni S, Lünenburger L, Gassert R, Bolliger M. Robotic and wearable sensor technologies for measurements/clinical assessments. In: Dietz V, Reinkensmeyer DJ, editors. Neurorehabilitation Technology. 2nd edition. Springer International; 2016.

83. Keller U, Schölch S, Albisser U, Rudhe C, Curt A, Riener R, et al. Robot-Assisted Arm Assessments in Spinal Cord Injured Patients: A Consideration of Concept Study. PLoS One. 2015;10:e0126948. doi:10.1371/journal.pone.0126948.

84. Bolliger M, Banz R, Dietz V, Lünenburger L. Standardized voluntary force measurement in a lower extremity rehabilitation robot. J Neuroeng Rehabil. 2008;5:23. doi:10.1186/1743-0003-5-23.

85. Tiffreau V, Ledoux I, Eymard B, Thévenon A, Hogrel J-Y. Isokinetic muscle testing for weak patients suffering from neuromuscular disorders: a reliability study. Neuromuscul Disord. 2007;17:524–31. doi:10.1016/j.nmd.2007.03.014.

86. Shirota C, Van Asseldonk E, Matjačić Z, Vallery H, Barralon P, Maggioni S, et al. Robot-supported assessment of balance in standing and walking. J Neuroeng Rehabil. 2017;14:1–19.

87. Zhang M, Davies TC, Zhang Y, Xie S, Eng P. Reviewing effectiveness of ankle assessment techniques for use in robot-assisted therapy. J Rehabil Res Dev. 2014;51:517–34.

88. Raghavendra P, Bornman J, Granlund M, Björck-Akesson E. The World Health Organization's International Classification of Functioning, Disability and Health: implications for clinical and research practice in the field of augmentative and alternative communication. Augment Altern Commun. 2007;23:349–61. doi:10.1080/07434610701650928.

89. Rauch A, Cieza A, Stucki G. How to apply the ICF for rehabilitation management in clinical practice.pdf. 2008;44:329–42.

90. Atkinson G, Nevill A. Statistical Methods for Assessing Measurement Error (Reliability) in Variables Relevant to Sports Medicine. Sport Med. 1998;26:217–38.

91. Weir JP. Quantifying Test-Retest Reliability Using the Intraclass Correlation Coefficient and the SEM. J Strength Cond Res. 2005;19:231–40.

92. Altman DG, Bland JM. Measurement in Medicine : the Analysis of Method Comparison Studies. Stat. 1983;32 July 1981:307–17.

93. Andresen EM. Criteria for assessing the tools of disability outcomes research. Arch Phys Med Rehabil. 2000;81:S15–20. doi:10.1053/apmr.2000.20619.

94. Roach KE. Measurement of Health Outcomes : Reliability , Validity and Responsiveness. J Prosthetics Orthot. 2006;18:1–5. http://www.oandp.org/jpo/library/2006_01S_008.asp.

95. Cook CE. Clinimetrics Corner: The Minimal Clinically Important Change Score (MCID): A Necessary Pretense. J Man Manip Ther. 2008;16:E82–3.

96. Hallgren KA. Computing Inter-Rater Reliability for Observational Data: An Overview and Tutorial. Tutor Quant Methods Psychol. 2012;8:23–34. doi:10.1016/j.biotechadv.2011.08.021.Secreted.

97. Shrout PE, Fleiss JL. Intraclass Correlations : Uses in Assessing Rater Reliability. Psychon Bull. 1979;86:420–8.

98. Shrout PE. Measurement reliability and agreement in psychiatry. Stat Methods Med Res. 1998;7:301–17.

99. McHugh ML. Interrater reliability: the kappa statistic. Biochemia Medica. 2012;22:276–82.

172

100. Sivan M, Connor RJO, Makower S, Hons BA, Phys D, Levesley M, et al. Systematic review of outcome measures used in the evaluation of robot-assisted upper limb exercise in stroke. J Rehabil Med. 2011;43:181–9.

101. Husted JA, Cook RJ, Farewell VT, Gladman DD. Methods for assessing responsiveness : a critical review and recommendations. J Clin Epidemiol. 2000;53:459–68.

102. Wright A, Hannon J, Hegedus EJ, Kavchak AE. Clinimetrics corner : a closer look at the minimal clinically important difference (MCID). J Man Manip Ther. 2012;20:160–6.

103. Clarkson H. Joint Motion and Function Assessment: A Research-based Practical Guide. Philadelphia: Lippincott Williams and Wilkins; 2000.

104. Rowe PJ, Myles CM, Walker C, Nutton R. Knee joint kinematics in gait and other functional activities measured using flexible electrogoniometry: how much knee motion is sufficient for normal daily life? Gait Posture. 2000;12:143–55.

105. Charbonnier C, Chagué S, Schmid J, Kolo FC, Bernardoni M, Christofilopoulos P. Analysis of hip range of motion in everyday life: a pilot study. Hip Int. 2015;25:82–90.

106. Anderson FC, Goldberg SR, Pandy MG, Delp SL. Contributions of muscle forces and toe-off kinematics to peak knee flexion during the swing phase of normal gait : an induced position analysis. J Biomech. 2004;37:731–7.

107. Ribbers G. Brain Injury: Long term outcome after traumatic brain injury. In: Stone J, Blouin M, editors. International Encyclopedia of Rehabilitation. 2010. http://cirrie.buffalo.edu/encyclopedia/en/article/338/.

108. Pohl M, Mehrholz J, Rockstroh G, Rückriem S, Koch R. Contractures and involuntary muscle overactivity in severe brain injury. Brain Inj. 2007;21:421–32.

109. Brosseau L, Balmer S, Tousignant M, O'Sullivan JP, Goudreault C, Goudreault M, et al. Intra- and intertester reliability and criterion validity of the parallelogram and universal goniometers for measuring maximum active knee flexion and extension of patients with knee restrictions. Arch Phys Med Rehabil. 2001;82:396–402.

110. Gajdosik RL, Bohannon RW. Clinical measurement of range of motion. Review of goniometry emphasizing reliability and validity. Phys Ther. 1987;67:1867–72. http://www.ncbi.nlm.nih.gov/pubmed/3685114.

111. Piriyaprasarth P, Morris ME. Psychometric properties of measurement tools for quantifying knee joint position and movement: a systematic review. Knee. 2007;14:2–8.

doi:10.1016/j.knee.2006.10.006.

112. van Trijffel E, van de Pol RJ, Oostendorp R a B, Lucas C. Inter-rater reliability for measurement of passive physiological movements in lower extremity joints is generally low: A systematic review. J Physiother. 2010;56:223–35. doi:10.1016/S1836-9553(10)70005-9.

113. Dijkstra PU, de Bont LG, van der Weele LT BG. Joint mobility measurements: reliability of a standardized method. Cranio J Craniomandib Pract. 1994;12:52:57.

114. Jung I-G, Yu I-Y, Kim S-Y, Lee D-K, Oh J-S. Reliability of ankle dorsiflexion passive range of motion measurements obtained using a hand-held goniometer and Biodex dynamometer in stroke patients. J Phys Ther Sci. 2015;27:1899–901.

115. Bok S-K, Lee TH, Lee SS. The effects of changes of ankle strength and range of motion according to aging on balance. Ann Rehabil Med. 2013;37:10–6.

116. Veneman JF, Kruidhof R, Hekman EEG, Ekkelenkamp R, Asseldonk EHF Van, van der Kooij H. Design and Evaluation of the LOPES Exoskeleton Robot for Interactive Gait Rehabilitation. IEEE Trans neural Syst Rehabil Eng. 2007;15:379–86.

117. Emken JL, Wynne JH, Harkema SJ, Reinkensmeyer DJ. Robotic device for manipulating human stepping. IEEE Trans Robot. 2006;22:185–9.

118. Farris RJ, Quintero H a., Goldfarb M. Preliminary evaluation of a powered lower limb orthosis to aid walking in paraplegic individuals. IEEE Trans Neural Syst Rehabil Eng. 2011;19:652–9.

119. del-Ama AJ, Gil-Agudo A, Pons JL, Moreno JC. Hybrid FES-robot cooperative control of ambulatory gait rehabilitation exoskeleton. J Neuroeng Rehabil. 2014;11:27. doi:10.1186/1743-0003-11-27.

120. Esquenazi A, Talaty M, Packel A, Saulino M. The ReWalk Powered Exoskeleton to Restore Ambulatory Function to Individuals with Thoracic-Level Motor-Complete Spinal Cord Injury. Am J Phys Med Rehabil. 2012;91:911–21.

121. Strausser KA, Swift TA, Zoss AB, Kazerooni H, Bennett BC. Mobile Exoskeleton for Spinal Cord Injury: Development and Testing. In: ASME 2011 Dynamic Systems and Control Conference. Arlington, VA, USA; 2011. doi:10.1115/DSCC2011-6042.

122. Bortole M, Venkatakrishnan A, Zhu F, Moreno JC, Francisco GE, Pons JL, et al. The H2 robotic exoskeleton for gait rehabilitation after stroke: early findings from a clinical study. J Neuroeng Rehabil. 2015;12:54. doi:10.1186/s12984-015-0048-y.

123. Bartenbach V, Wyss D, Seuret D, Riener R. A Lower Limb Exoskeleton Research Platform to Investigate Human-Robot Interaction. In: IEEE International Conference on Rehabilitation Robotics. Singapore; 2015.

124. Riener R, Lünenburger L, Maier IC, Colombo G, Dietz V. Locomotor Training in Subjects with Sensori-Motor Deficits: An Overview of the Robotic Gait Orthosis Lokomat. J Healthc Eng. 2010;1:197–216. doi:10.1260/2040-2295.1.2.197.

125. Waldman G, Yang C-Y, Ren Y, Liu L, Guo X, Harvey RL, et al. Effects of robot-guided passive stretching and active movement training of ankle and mobility impairments in stroke. NeuroRehabilitation. 2013;32:625–34. doi:10.3233/NRE-130885.

126. Zhang L-Q, Chung SG, Bai Z, Xu D, Rey EMT Van, Rogers MW, et al. Intelligent Stretching of Ankle Joints With Contracture/Spasticity. IEEE Trans Neural Syst Rehabil Eng. 2002;10:149–57.

127. Peng Q, Park H-S, Shah P, Wilson N, Ren Y, Wu Y-N, et al. Quantitative evaluations of ankle spasticity and stiffness in neurological disorders using manual spasticity evaluator. J Rehabil Res Dev. 2011;48:473–81.

128. Giacomozzi C, Cesinaro S, Basile F, De Angelis G, Giansanti D, Maccioni G, et al. Measurement device for ankle joint kinematic and dynamic characterisation. Med Biol Eng Comput. 2003;41:486–93.

129. Roy A, Krebs HI, Williams DJ, Bever CT, Forrester LW, Macko RM, et al. Robot-aided neurorehabilitation: A novel robot for ankle rehabilitation. IEEE Trans Robot. 2009;25:569–82.

130. Borsa PA, Sauers EL, Herling DE, Manzour WF. In Vivo Quantification of Capsular End- point in the Nonimpaired Glenohumeral Joint Using an Instrumented Measurement System. J Orthop Sports Phys Ther. 2001;31:419–31.

131. McQuade K, Price R, Liu N, Ciol MA. Objective Assessment of Joint Stiffness: A Clinically Oriented Hardware and Software Device with an Application to the Shoulder Joint. J Nov Physiother. 2012;2.

132. Jarrassé N, Proietti T, Crocher V, Robertson J, Sahbani A, Morel G, et al. Robotic Exoskeletons: A Perspective for the Rehabilitation of Arm Coordination in Stroke Patients. Front Hum Neurosci. 2014;8 December:1–13. doi:10.3389/fnhum.2014.00947.

133. van Dijk W, van der Kooij H, Koopman B, van Asseldonk EHF. Improving the transparency of a rehabilitation robot by exploiting the cyclic behaviour of walking. IEEE Int Conf Rehabil Robot. 2013;2013:6650393. doi:10.1109/ICORR.2013.6650393.

134. Weiselfish-Giammatteo S, Giammatteo T. Integrative Manual Therapy for Biomechanics: Application of Muscle Energy and "beyond" Technique : Treatment of the Spine, Ribs, and Extremities. North Atlantic Books; 2003.

135. Rowe P, Myles C, Hillmann S, Hazlewood M. Validation of Flexible Electrogoniometry as a Measure of Joint Kinematics. Physiotherapy. 2001;87:479–88.

136. Tesio L, Monzani M, Gatti R, Franchignoni F. Flexible electrogoniometers: kinesiological advantages with respect to potentiometric goniometers. 1995;10:2–4.

137. Bronner S, Agraharasamakulam S, Ojofeitimi S. Reliability and validity of electrogoniometry measurement of lower extremity movement. J Med Eng Technol. 2010;34:232–42. doi:10.3109/03091900903580512.

138. Piriyaprasarth P, Morris ME, Winter A, Bialocerkowski AE. The reliability of knee joint position testing using electrogoniometry. BMC Musculoskelet Disord. 2008;9:6. doi:10.1186/1471-2474-9-6.

139. Menguc Y, Park YL, Martinez-Villalpando E, Aubin P, Zisook M, Stirling L, et al. Soft wearable motion sensing suit for lower limb biomechanics measurements. Proc - IEEE Int Conf Robot Autom. 2013;:5309–16.

140. Donno M, Palange E, Nicola F Di, Member S, Bucci G, Ciancetta F. A New Flexible Optical Fiber Goniometer for Dynamic Angular Measurements : Application to Human Joint Movement Monitoring. IEEE Trans Instrum Meas. 2008;57:1614–20.

141. Favre J, Jolles BM, Aissaoui R, Aminian K. Ambulatory measurement of 3D knee joint angle. J Biomech. 2008;41:1029–35. doi:10.1016/j.jbiomech.2007.12.003.

142. Luinge HJ, Veltink PH. Inclination measurement of human movement using a 3-D accelerometer with autocalibration. IEEE Trans Neural Syst Rehabil Eng. 2004;12:112–21. doi:10.1109/TNSRE.2003.822759.

143. Dejnabadi H, Jolles BM, Aminian K. A new approach to accurate measurement of uniaxial joint angles based on a combination of accelerometers and gyroscopes. IEEE Trans Biomed Eng. 2005;52:1478–84. doi:10.1109/TBME.2005.851475.

144. Djurić-Jovičić MD, Jovičić NS, Popović DB, Djordjević AR. Nonlinear optimization for drift removal in estimation of gait kinematics based on accelerometers. J Biomech. 2012;45:2849–54. doi:10.1016/j.jbiomech.2012.08.028.

145. MeSH - Muscle Strength. http://www.ncbi.nlm.nih.gov/mesh/68053580. Accessed 28 Dec

2015.

146. Neckel N, Pelliccio M, Nichols D, Hidler J. Quantification of functional weakness and abnormal synergy patterns in the lower limb of individuals with chronic stroke. J Neuroeng Rehabil. 2006;3:17. doi:10.1186/1743-0003-3-17.

147. Tiffreau V, Ledoux I, Eymard B, Thévenon A, Hogrel J-Y. Isokinetic muscle testing for weak patients suffering from neuromuscular disorders: a reliability study. Neuromuscul Disord. 2007;17:524–31. doi:10.1016/j.nmd.2007.03.014.

148. Wirz M, van Hedel HJ, Rupp R, Curt A, Dietz V. Muscle force and gait performance: relationships after spinal cord injury. Arch Phys Med Rehabil. 2006;87:1218–22. doi:10.1016/j.apmr.2006.05.024.

149. Kim C, Eng J. The relationship of lower-extremity muscle torque to locomotor performance in people with stroke. Phys Ther. 2003;:49–57.

150. Cho KH, Bok SK, Kim YJ, Hwang SL. Effect of lower limb strength on falls and balance of the elderly. Ann Rehabil Med. 2012;36:386–93.

151. Newham DJ, Hsiao SF. Knee muscle isometric strength, voluntary activation and antagonist co-contraction in the first six months after stroke. Disabil Rehabil. 2001;23.

152. Noreau L, Vachon J. Comparison of three methods to assess muscular strength in individuals with spinal cord injury. Spinal Cord. 1998;36:716–23. http://www.ncbi.nlm.nih.gov/pubmed/9800275.

153. Paternostro-Sluga T, Grim-Stieger M, Posch M, Schuhfried O, Vacariu G, Mittermaier C, et al. Reliability and Validity of the Medical Research Council (MRC) Scale and a Modified Scale for Testing Muscle Strength in Patients with Radial Palsy. J Rehabil Med. 2008;40:665–71.

154. Beasley W. Quantitative muscle testing: principles and applications to research and clinical services. Arch Phys Med Rehabil. 1961;42:398–425.

155. Herbison GJ, Isaac Z, Cohen ME, Ditunno JF. Strength post-spinal cord injury: myometer vs manual muscle test. Spinal Cord. 1996;34:543–8. doi:10.1038/sc.1996.98.

156. Bohannon RW. Manual muscle testing: does it meet the standards of an adequate screening test? Clin Rehabil. 2005;19:662–7.

157. Merlini L, Mazzone ES, Solari A, Morandi L. Reliability of hand-held dynamometry in spinal muscular atrophy. Muscle and Nerve. 2002;26:64–70.

158. Stark T, Walker B, Phillips JK, Fejer R, Beck R. Hand-held dynamometry correlation with the gold standard isokinetic dynamometry: a systematic review. PM R. 2011;3:472–9. doi:10.1016/j.pmrj.2010.10.025.

159. Marmon AR, Pozzi F, Alnahdi AH, Zeni J a. The validity of plantarflexor strength measures obtained through hand-held dynamometry measurements of force. Int J Sports Phys Ther. 2013;8:820–7.

160. Kim WK, Kim DK, Seo KM, Kang SH. Reliability and validity of isometric knee extensor strength test with hand-held dynamometer depending on its fixation: A pilot study. Ann Rehabil Med. 2014;38:84–93.

161. Meldrum D, Cahalane E, Keogan F, Hardiman O. Maximum voluntary isometric contraction: investigation of reliability and learning effect. Amyotroph Lateral Scler Other Motor Neuron Disord. 2003;4:36–44.

162. Colombo R, Mazzini L, Mora G, Parenzan R, Creola G, Pirali I, et al. Measurement of isometric muscle strength: a reproducibility study of maximal voluntary contraction in normal subjects and amyotrophic lateral sclerosis patients. Med Eng Phys. 2000;22:167–74. doi:10.1016/S1350-4533(00)00024-2.

163. Lauermann SP, Lienhard K, Item-Glatthorn JF, Casartelli NC, Maffiuletti N a. Assessment of quadriceps muscle weakness in patients after total knee arthroplasty and total hip arthroplasty: methodological issues. J Electromyogr Kinesiol. 2014;24:285–91. doi:10.1016/j.jelekin.2013.10.018.

164. Lienhard K, Lauermann SP, Schneider D, Item-Glatthorn JF, Casartelli NC, Maffiuletti N a. Validity and reliability of isometric, isokinetic and isoinertial modalities for the assessment of quadriceps muscle strength in patients with total knee arthroplasty. J Electromyogr Kinesiol. 2013;23:1283–8. doi:10.1016/j.jelekin.2013.09.004.

165. Lum PS, Patten C, Kothari D, Yap R. Effects of velocity on maximal torque production in poststroke hemiparesis. Muscle and Nerve. 2004;30:732–42.

166. Knapik JJ, Wright JE, Mawdsley RH, Braun J. Isometric, isotonic, and isokinetic torque variations in four muscle groups through a range of joint motion. Phys Ther. 1983;63:938–47. http://www.ncbi.nlm.nih.gov/pubmed/6856681.

167. Whiteley R, Jacobsen P, Prior S, Skazalski C, Otten R, Johnson A. Correlation of isokinetic and novel hand-held dynamometry measures of knee flexion and extension strength testing. J Sci Med Sport. 2012;15:444–50. doi:10.1016/j.jsams.2012.01.003.

168. Campen A Van, Groote F De, Jonkers I, Schutter J De. An Extended Dynamometer Setup to Improve the Accuracy of Knee Joint Moment Assessment. IEEE Trans Biomed Eng. 2013;60:1202–8.

169. Van Campen A, De Groote F, Jonkers I, De Schutter J. An extended dynamometer setup to improve the accuracy of knee joint moment assessment. IEEE Trans Biomed Eng. 2013;60:1202–8. doi:10.1109/TBME.2012.2228643.

170. Clark DJ, Condliffe EG, Patten C. Reliability of concentric and eccentric torque during isokinetic knee extension in post-stroke hemiparesis. Clin Biomech (Bristol, Avon). 2006;21:395–404. doi:10.1016/j.clinbiomech.2005.11.004.

171. Hidler J. Robotic-assessment of walking in individuals with gait disorders. Conf Proc . Annu Int Conf IEEE Eng Med Biol Soc IEEE Eng Med Biol Soc Annu Conf. 2004;7:4829–31. doi:10.1109/IEMBS.2004.1404336.

172. Neckel ND, Blonien N, Nichols D, Hidler J. Abnormal joint torque patterns exhibited by chronic stroke subjects while walking with a prescribed physiological gait pattern. J Neuroeng Rehabil. 2008;5:19. doi:10.1186/1743-0003-5-19.

173. Forrester LW, Roy A, Goodman RN, Rietschel J, Barton JE, Krebs HI, et al. Clinical application of a modular ankle robot for stroke rehabilitation. NeuroRehabilitation. 2013;33:85–97.

174. Bohannon RW. Knee extension strength and body weight determine sit-to-stand independence after stroke. Physiother Theory Pract. 2007;23:291–7. doi:10.1080/09593980701209428.

175. Bohannon RW. Relevance of Muscle Strength to Gait Performance in Patients with Neurologic Disability. Neurorehabil Neural Repair. 1989.

176. Nadler SF, DePrince ML, Hauesien N, Malanga G a., Stitik TP, Price E. Portable dynamometer anchoring station for measuring strength of the hip extensors and abductors. Arch Phys Med Rehabil. 2000;81:1072–6.

177. Drouin JM, Valovich-mcLeod TC, Shultz SJ, Gansneder BM, Perrin DH. Reliability and validity of the Biodex system 3 pro isokinetic dynamometer velocity, torque and position measurements. Eur J Appl Physiol. 2004;91:22–9. doi:10.1007/s00421-003-0933-0.

178. Rothstein JM, Lamb RL, Mayhew TP. Clinical uses of isokinetic measurements. Critical issues. Phys Ther. 1987;67:1840–4. http://www.ncbi.nlm.nih.gov/pubmed/3685109.

179. Han J, Waddington G, Adams R, Anson J, Liu Y. Assessing proprioception: A critical review of methods. J Sport Heal Sci. 2015. doi:10.1016/j.jshs.2014.10.004.

180. Suetterlin KJ, Sayer AA. Proprioception: where are we now? A commentary on clinical assessment, changes across the life course, functional implications and future interventions. Age Ageing. 2013;:1–6. doi:10.1093/ageing/aft174.

181. Goble DJ. Proprioceptive acuity assessment via joint position matching: from basic science to general practice. Phys Ther. 2010;90:1176–84. doi:10.2522/ptj.20090399.

182. Proske U, Gandevia SC. The Proprioceptive Senses: Their Roles in Signaling Body Shape, Body Position and Movement, and Muscle Force. Physiol Rev. 2012;92:1651–97.

183. Cammarata ML, Dhaher YY. Proprioceptive acuity in the frontal and sagittal planes of the knee: a preliminary study. Eur J Appl Physiol. 2011;111:1313–20. doi:10.1007/s00421-010-1757-3.

184. Allet L, Kim H, Ashton-Miller J, De Mott T, Richardson JK. Frontal plane hip and ankle sensorimotor function, not age, predicts unipedal stance time. Muscle Nerve. 2012;45:578–85. doi:10.1002/mus.22325.

185. Domingo A, Lam T. Reliability and validity of using the Lokomat to assess lower limb joint position sense in people with incomplete spinal cord injury. J Neuroeng Rehabil. 2014;11:167. doi:10.1186/1743-0003-11-167.

186. Elangovan N, Herrmann A, Konczak J. Assessing proprioceptive function: evaluating joint position matching methods against psychophysical thresholds. Phys Ther. 2014;94:553–61.

187. Clark NC, Röijezon U, Treleaven J. Proprioception in Musculoskeletal Rehabilitation. Part 2: Clinical Assessment and Intervention. Man Ther. 2015;20:378–87. doi:10.1016/j.math.2015.01.009.

188. Sanford J, Moreland J, Swanson LR, Stratford PW, Gowland C. Reliability of the Fugl-Meyer assessment for testing motor performance in patients following stroke. Phys Ther. 1993;73:447–54.

189. Hillier S, Immink M, Thewlis D. Assessing Proprioception : A Systematic Review of Possibilities. Neurorehabil Neural Repair. 2015;29:933–49.

190. Refshauge KM, Taylor JL, Mccloskey DI, Gianoutsos M, Mathews P, Fitzpatrick RC. Movement detection at the human big toe. J Physiol. 1998;513:307–14.

191. Refshauge KM, Chan R, Taylor JL, Mccloskey DI. Detection of movements imposed on human hip , knee , ankle and toe joints. 1995;:231–41.

192. Hurkmans EJ, van der Esch M, Ostelo RWJG, Knol D, Dekker J, Steultjens MPM. Reproducibility of the measurement of knee joint proprioception in patients with osteoarthritis of the knee. Arthritis Rheum. 2007;57:1398–403. doi:10.1002/art.23082.

193. Chisholm AE, Domingo A, Jeyasurya J, Lam T. Quantification of Lower Extremity Kinesthesia Deficits Using a Robotic Exoskeleton in People With a Spinal Cord Injury. Neurorehabil Neural Repair. 2015. doi:10.1177/1545968315591703.

194. Brunnstrom S. Movement Therapy in Hemiplegia—A Neurophysiological Approach. New York: Harper & Row Publishers, Inc.; 1970.

195. Fugl-Meyer AR, Jääskö L, Leyman I, Olsson S, Steglind S. The post-stroke hemiplegic patient. 1. a method for evaluation of physical performance. Scand J Rehabil Med. 1975;7:13–31.

196. Duncan PW, Propst M, Nelson SG. Reliability of the Fugl-Meyer Assessment of Sensorimotor Recovery Following Cerebrovascular Accident. Phys Ther. 1983;63:1606–10.

197. Hsueh I-P, Hsu M-J, Sheu C-F, Lee S, Hsieh C-L, Lin J-H. Psychometric comparisons of 2 versions of the Fugl-Meyer Motor Scale and 2 versions of the Stroke Rehabilitation Assessment of Movement. Neurorehabil Neural Repair. 2008;22:737–44. doi:10.1177/1545968308315999.

198. Dettmann MA, Linder MT, Sepic SB. Relationships among walking performance, postural stability, and functional assessments of the hemiplegic patient. Am J Phys Med. 1987;66:77–90.

199. Tan AQ, Dhaher YY. Evaluation of lower limb cross planar kinetic connectivity signatures post-stroke. J Biomech. 2014;:1–8.

200. Cruz TH, Dhaher Y. Evidence of Abnormal Lower-Limb Torque Coupling After Stroke: An Isometric Study. Stroke. 2008;39:139–47.

201. Krishnan C, Dhaher Y. Corticospinal responses of quadriceps are abnormally coupled with hip adductors in chronic stroke survivors. Exp Neurol. 2012;233:400–7.

202. Thelen DD, Riewald S a, Asakawa DS, Sanger TD, Delp SL. Abnormal coupling of knee and hip moments during maximal exertions in persons with cerebral palsy. Muscle Nerve. 2003;27:486–93. doi:10.1002/mus.10357.

203. Hidler JM, Carroll M, Federovich EH. Strength and Coordination in the Paretic Leg of Individuals Following Acute Stroke. 2007;15:526–34.

204. Sanchez N, Dewald JPA. Constraints imposed by the lower extremity extensor synergy in chronic hemiparetic stroke: Preliminary findings. Conf Proc Annu Int Conf IEEE Eng Med Biol Soc IEEE Eng Med Biol Soc Conf. 2014;2014:5804–7. doi:10.1109/EMBC.2014.6944947.

205. Lunardini F, Casellato C, D'Avella A, Sanger T, Pedrocchi A. Robustness and Reliability of Synergy-Based Myocontrol of a Multiple Degree of Freedom Robotic Arm. IEEE Trans Neural Syst

Rehabil Eng. 2015. doi:10.1109/TNSRE.2015.2483375.

206. Sanchez N, Acosta A, Stienen A, Dewald J. A Multiple Degree of Freedom Lower Extremity Isometric Device to Simultaneously Quantify Hip, Knee and Ankle Torques. IEEE Trans Neural Syst Rehabil Eng. 2015;23:765–75. doi:10.1109/TNSRE.2014.2348801.

207. Cruz TH, Lewek MD, Dhaher YY. Biomechanical impairments and gait adaptations post-stroke: multi-factorial associations. J Biomech. 2009;42:1673–7. doi:10.1016/j.jbiomech.2009.04.015.

208. Dewald JP, Beer R. Abnormal joint torque patterns in the paretic upper limb of subjects with hemiparesis. Muscle Nerve. 2001;24:273--83.

209. Ellis MD, Sukal T, DeMott T, Dewald JPA. Augmenting clinical evaluation of hemiparetic arm movement with a laboratory-based quantitative measurement of kinematics as a function of limb loading. Neurorehabil Neural Repair. 2008;22:321–9. doi:10.1177/1545968307313509.

210. Latash M, Zatsiorsky VM. Biomechanics and Motor Control: Defining Central Concepts. Academic P. 2015.

211. Hogan N. Mechanical impedance of single- and multi-articular systems. In: Winters JM, Woo S.-Y, editors. Multiple Muscle Systems. New York: Springer-Verlag; 1990. p. 149–64.

212. Latash ML, Zatsiorsky VM. Joint stiffness: Myth or reality? Hum Mov Sci. 1993;12:653–92. doi:10.1016/0167-9457(93)90010-M.

213. Ludvig D, Perreault EJ. Estimation of joint impedance using short data segments. Conf Proc Annu Int Conf IEEE Eng Med Biol Soc IEEE Eng Med Biol Soc Conf. 2011;2011:4120–3. doi:10.1109/IEMBS.2011.6091023.

214. Kearney RE, Hunter IW. System identification of human joint dynamics. Crit Rev Biomed Eng. 1990;18:55–87.

215. Mirbagheri MM, Barbeau H, Kearney RE. Intrinsic and reflex contributions to human ankle stiffness: variation with activation level and position. Exp brain Res. 2000;135. doi:10.1007/s002210000534.

216. Sinkjaer T, Magnussen I. Passive, intrinsic and reflex-mediated stiffness in the ankle extensors of hemiparetic patients. Brain. 1994;117:355–63. http://brain.oxfordjournals.org/content/117/2/355.short.

217. Chung SG, Van Rey E, Bai Z, Roth EJ, Zhang L-Q. Biomechanic changes in passive properties of hemiplegic ankles with spastic hypertonia. Arch Phys Med Rehabil. 2004;85:1638–46.

182

218. Mirbagheri MM, Barbeau H, Ladouceur M, Kearney RE. Intrinsic and reflex stiffness in normal and spastic, spinal cord injured subjects. Exp brain Res. 2001;141.

219. Hunter I, Kearney R. Dynamics of human ankle stiffness: Variation with mean ankle torque. J Biomech. 1982;15:747–52.

220. Gottlieb GL, Agarwal GC. Response to sudden torques about ankle in man: myotatic reflex. J Neurophysiol. 1979;42 1 Pt 1:91–106.

221. Weiss P, Kearney R, Hunter I. Position dependence of ankle joint dynamics-II. Active mechanics. J Biomech. 1986;19:737–51.

222. Weiss P, Kearney R, Hunter I. Position dependence of ankle joint dynamics-I. Passive mechanics. J Biomech. 1986;19:727–35.

223. Kearney R, Hunter I. Dynamics of human ankle stiffness: Variation with displacement amplitude. J Biomech. 1982;15:753–6. http://www.scopus.com/inward/record.url?eid=2-s2.0-0020353013&partnerID=40.

224. de Vlugt E, van Eesbeek S, Baines P, Hilte J, Meskers CGM, de Groot JH. Short range stiffness elastic limit depends on joint velocity. J Biomech. 2011;44:2106–12. doi:10.1016/j.jbiomech.2011.05.022.

225. Zhang LQ, Nuber G, Butler J, Bowen M, Rymer WZ. In vivo human knee joint dynamic properties as functions of muscle contraction and joint position. J Biomech. 1998;31:71–6. doi:10.1016/S0021-9290(97)00106-1.

226. Kearney RE, Hunter IW. Nonlinear identification of stretch reflex dynamics. Ann Biomed Eng. 1988;16:79–94.
http://eutils.ncbi.nlm.nih.gov/entrez/eutils/elink.fcgi?dbfrom=pubmed&id=3408053&retmode=ref&cmd=prlinks.

227. Powers RK, Marder-Meyer J, Rymer WZ. Quantitative relations between hypertonia and stretch reflex threshold in spastic hemiparesis. Ann Neurol. 1988;23:115–24. doi:10.1002/ana.410230203.

228. Mugge W, Abbink DA, van der Helm FCT. Reduced power method: how to evoke low-bandwidth behaviour while estimating full-bandwidth dynamics. 2007;:575–81. http://ieeexplore.ieee.org/xpls/abs_all.jsp?arnumber=4428483.

229. Bohannon RW, Smith MB. Interrater reliability of a modified Ashworth scale of muscle spasticity. Phys Ther. 1987;67:206–7.

230. Blackburn M, van Vliet P, Mockett SP. Reliability of measurements obtained with the modified Ashworth scale in the lower extremities of people with stroke. Phys Ther. 2002;82:25–34.

231. Wartenberg R. Pendulousness of the legs as a diagnostic test. Neurology. 1951;1:18.

232. Fowler EG, Nwigwe AI, Ho TW. Sensitivity of the pendulum test for assessing spasticity in persons with cerebral palsy. Dev Med Child Neurol. 2000;42:182–9.

233. Bohannon RW, Harrison S, Kinsella-Shaw J. Reliability and validity of pendulum test measures of spasticity obtained with the Polhemus tracking system from patients with chronic stroke. J Neuroeng Rehabil. 2009;6:30. doi:10.1186/1743-0003-6-30.

234. Kearney E, Weiss L, Morier R. System identification of human ankle dynamics: Intersubject variability and intrasubject reliability. Clin Biomech. 1990;5:205–17.

235. Wilken J, Rao S, Estin M, Saltzman CL, Yack HJ. A new device for assessing ankle dorsiflexion motion: reliability and validity. J Orthop Sports Phys Ther. 2011;41:274–80.

236. Chesworth BM, Vandervoort BM. Reliability of a torque motor system for measurement of passive ankle joint stiffness in control subjects. Physiother Canada. 1988;40:300–3.

237. Franzoi AC, Castro C, Cardone C. Isokinetic assessment of spasticity in subjects with traumatic spinal cord injury (ASIA A). Spinal Cord. 1999;37:416–20.

238. McHugh MP, Hogan DE. Effect of knee flexion angle on active joint stiffness. Acta Physiol Scand. 2004;180:249–54. doi:10.1046/j.0001-6772.2003.01240.x.

239. Blackburn JT, Padua DA, Riemann BL, Guskiewicz KM. The relationships between active extensibility, and passive and active stiffness of the knee flexors. J Electromyogr Kinesiol. 2004;14:683–91. doi:10.1016/j.jelekin.2004.04.001.

240. de Vlugt E, de Groot JH, Schenkeveld KE, Arendzen JH, van der Helm FCT, Meskers CGM. The relation between neuromechanical parameters and Ashworth score in stroke patients. J Neuroeng Rehabil. 2010;7:35. doi:10.1186/1743-0003-7-35.

241. Androwis GJ, Michael PA, Strongwater A, Foulds RA. Estimation of intrinsic joint impedance using quasi-static passive and dynamic methods in individuals with and without Cerebral Palsy. In: IEEE Engineering in Medicine and Biology Society. Annual Conference. 2014. p. 4403–6.

242. Mirbagheri MM, Kearney RE, Barbeau H. Quantitative, objective measurement of ankle dynamic stiffness: Intrasubject reliability and intersubject variability. In: Annual International Conference of the IEEE Engineering in Medicine and Biology - Proceedings. 1996. p. 585–6.

243. Sloot LH, van der Krogt MM, de Gooijer-van de Groep KL, van Eesbeek S, de Groot J, Buizer AI, et al. The validity and reliability of modelled neural and tissue properties of the ankle muscles in children with cerebral palsy. Gait Posture. 2015;42:7–15. doi:10.1016/j.gaitpost.2015.04.006.

244. Loram I, Lakie M, Maganaris C. Reply from Ian D. Loram, Constantinos N. Maganaris and Martin Lakie. J Physiol. 2005;569:706.

245. Vlutters M, Boonstra TA, Schouten AC, Van der Kooij H. Direct measurement of the intrinsic ankle stiffness during standing. J Biomech. 2015;48:1258–63. doi:10.1016/j.jbiomech.2015.03.004.

246. Koopman B, van Asseldonk EHF, van der kooij H. In vivo measurement of human knee and hip dynamics using MIMO system identification. In: Proceedings of 32nd Annual Internation conference of the IEEE EMBS. Buenos Aires; 2011. p. 3426–9. doi:10.1109/IEMBS.2010.5627893.

247. Pfeifer S, Vallery H, Hardegger M, Riener R, Perreault EJ. Model-based estimation of knee stiffness. IEEE Trans Biomed Eng. 2012;59:2604–12. doi:10.1109/TBME.2012.2207895.

248. Ludvig D, Pfeifer S, Hu X, Perreault EJ. Time-varying system identification for understanding the control of human knee impedance. In: IFAC Proceedings Volumes (IFAC-PapersOnline). 2012. p. 1306–10.

249. Ludvig D, Starret Visser T, Giesbrecht H, Kearney R. Identification of time-varying intrinsic and reflex joint stiffness. IEEE Trans Biomed Eng. 2011;:1. http://ieeexplore.ieee.org/xpls/abs_all.jsp?arnumber=5711650.

250. Ludvig D, Perreault EJ. System identification of physiological systems using short data segments. IEEE Trans Biomed Eng. 2012;59:3541–9. doi:10.1109/TBME.2012.2220767.

251. Tucker MR, Moser A, Lambercy O, Sulzer J, Gassert R. Design of a wearable perturbator for human knee impedance estimation during gait. IEEE Int Conf Rehabil Robot 2013. 2013;2013:6650372. doi:10.1109/ICORR.2013.6650372.

252. Hedel HJA Van, Wirz M, Curt A. Improving walking assessment in subjects with an incomplete spinal cord injury : responsiveness. 2006;:352–6.

253. van Hedel HJ a, Wirz M, Dietz V. Standardized assessment of walking capacity after spinal cord injury: the European network approach. Neurol Res. 2008;30:61–73. doi:10.1179/016164107X230775.

254. Hedel HJ Van, Wirz M, Dietz V. Assessing Walking Ability in Subjects With Spinal Cord Injury : Validity and Reliability of 3 Walking Tests. Arch Phys Med Rehabil. 2005;86 February:190–6.

255. Jackson AB, Carnel CT, Ditunno JF, Read MS, Boninger ML, Schmeler MR, et al. Outcome Measures for Gait and Ambulation in the Spinal Cord Injury Population. J Spinal Cord Med. 2008;31:487–99.

256. Schmid A, Duncan PW, Studenski S, Lai SM, Richards L, Perera S, et al. Improvements in speed-based gait classifications are meaningful. Stroke. 2007;38:2096–100. doi:10.1161/STROKEAHA.106.475921.

257. Awai L, Bolliger M, Ferguson AR, Courtine G, Curt A. Influence of Spinal Cord Integrity on Gait Control in Human Spinal Cord Injury. Neurorehabil Neural Repair. 2015; OCTOBER. doi:10.1177/1545968315600524.

258. Jasiewicz JM, Allum JHJ, Middleton JW, Barriskill A, Condie P, Purcell B, et al. Gait event detection using linear accelerometers or angular velocity transducers in able-bodied and spinal-cord injured individuals. Gait Posture. 2006;24:502–9. doi:10.1016/j.gaitpost.2005.12.017.

259. Rueterbories J, Spaich EG, Larsen B, Andersen OK. Methods for gait event detection and analysis in ambulatory systems. Med Eng Phys. 2010;32:545–52.

260. Aminian K, Najafi B, Büla C, Leyvraz P-F, Robert P. Spatio-temporal parameters of gait measured by an ambulatory system using miniature gyroscopes. J Biomech. 2002;35:689–99. http://www.ncbi.nlm.nih.gov/pubmed/11955509.

261. Bilney B, Morris M, Webster K. Concurrent related validity of the GAITRite walkway system for quantification of the spatial and temporal parameters of gait. Gait Posture. 2003;17:68–74.

262. Micó-Amigo ME, Kingma I, Ainsworth E, Walgaard S, Niessen M, van Lummel RC, et al. A novel accelerometry-based algorithm for the detection of step durations over short episodes of gait in healthy elderly. J Neuroeng Rehabil. 2016;13:38. doi:10.1186/s12984-016-0145-6.

263. Boutaayamou M, Schwartz C, Stamatakis J, Denoël V, Maquet D, Forthomme B, et al. Development and validation of an accelerometer-based method for quantifying gait events. Med Eng Phys. 2015;37:226–32.

264. Mariani B, Rouhani H, Crevoisier X, Aminian K. Quantitative estimation of foot-flat and stance phase of gait using foot-worn inertial sensors. Gait Posture. 2013;37:229–34. doi:10.1016/j.gaitpost.2012.07.012.

265. Hausdorff JM. Gait variability: methods, modeling and meaning. J Neuroeng Rehabil. 2005;9:1–9.

266. Allen JL, Kautz S a, Neptune RR. Step length asymmetry is representative of compensatory

mechanisms used in post-stroke hemiparetic walking. Gait Posture. 2011;33:538–43. doi:10.1016/j.gaitpost.2011.01.004.

267. Chen G, Patten C, Kothari DH, Zajac FE. Gait differences between individuals with post-stroke hemiparesis and non-disabled controls at matched speeds. Gait Posture. 2005;22:51–6. doi:10.1016/j.gaitpost.2004.06.009.

268. Olney SJ, Richards C. Hemiparetic gait following stroke . Part I : Characteristics. Gait Posture. 1996;4:136–48.

269. McRoberts. http://www.mcroberts.nl/. Accessed 5 Jun 2016.

270. GaitUp. http://www.gaitup.com/. Accessed 5 Jun 2016.

271. Hidler J, Wisman W, Neckel N. Kinematic trajectories while walking within the Lokomat robotic gait-orthosis. Clin Biomech (Bristol, Avon). 2008;23:1251–9. doi:10.1016/j.clinbiomech.2008.08.004.

272. Emken JL, Harkema SJ, Beres-jones JA, Ferreira CK, Reinkensmeyer DJ. Feasibility of Manual Teach-and-Replay and Continuous Impedance Shaping for Robotic Locomotor Training Following Spinal Cord Injury. IEEE Trans Biomed Eng. 2008;55:322–34.

273. Duschau-Wicke A, von Zitzewitz J, Caprez A, Luenenburger L, Riener R. Path control: a method for patient-cooperative robot-aided gait rehabilitation. IEEE Trans neural Syst Rehabil Eng. 2010;18:38–48. doi:10.1109/TNSRE.2009.2033061.

274. Krishnan C, Ranganathan R, Dhaher YY, Rymer WZ. A Pilot Study on the Feasibility of Robot-Aided Leg Motor Training to Facilitate Active Participation. PLoS One. 2013;8.

275. Park YL, Chen BR, Young D, Stirling L, Wood RJ, Goldfield E, et al. Bio-inspired active soft orthotic device for ankle foot pathologies. IEEE Int Conf Intell Robot Syst. 2011;:4488–95.

276. Bartenbach V, Schmidt K, Naef M, Wyss D, Riener R. Concept of a Soft Exosuit for the Support of Leg Function in Rehabilitation. In: IEEE International Conference on Rehabilitation Robotics. Singapore; 2015.

277. Maggioni S, Lünenburger L, Riener R, Melendez-Calderon A. Robot-Aided Assessment of Walking Function Based on an Adaptive Algorithm. In: 2015 IEEE 14th International Conference on Rehabilitation Robotics. Singapore; 2015. p. 804–9.

278. Duschau-Wicke A, Felsenstein S, Riener R. Adaptive body weight support controls human activity during robot-aided gait training. In: 2009 IEEE 11th International Conference on Rehabilitation

Robotics. Kyoto; 2009. p. 413–8.

279. Wolbrecht ET, Chan V, Reinkensmeyer DJ, Bobrow JE. Optimizing compliant, model-based robotic assistance to promote neurorehabilitation. IEEE Trans Neural Syst Rehabil Eng. 2008;16:286–97. doi:10.1109/TNSRE.2008.918389.

280. Reference Overview Lokomat. Hocoma. 2019. https://www.hocoma.com/partners/references/?products=Lokomat®Pro;Lokomat®Basic;Lokomat®Nanos. Accessed 25 Aug 2019.

281. Neckel ND, Blonien N, Nichols D, Hidler J. Abnormal joint torque patterns exhibited by chronic stroke subjects while walking with a prescribed physiological gait pattern. 2008;13:1–13.

282. Niu X, Varoqui D, Kindig M, Mirbagheri MM. Prediction of gait recovery in spinal cord injured individuals trained with robotic gait orthosis. J Neuroeng Rehabil. 2014;11:1–9. doi:10.1186/1743-0003-11-42.

283. Vallery H, Duschau-Wicke A, Riener R. Optimized passive dynamics improve transparency of haptic devices. In: Proceedings - IEEE International Conference on Robotics and Automation. 2009. p. 301–6.

284. Riener R, Lünenburger L, Jezernik S, Anderschitz M, Colombo G, Dietz V. Patient-cooperative strategies for robot-aided treadmill training: first experimental results. IEEE Trans neural Syst Rehabil Eng. 2005;13:380–94. doi:10.1109/TNSRE.2005.848628.

285. Stoquart G, Detrembleur C, Lejeune T. Effect of speed on kinematic, kinetic, electromyographic and energetic reference values during treadmill walking. Neurophysiol Clin. 2008;38:105–16.

286. Meuleman J, van Asseldonk E, van Oort G, Rietman H, van der Kooij H. LOPES II-Design and evaluation of an Admittance controlled gait raining robot with shadow-leg approach. IEEE Trans Neural Syst Rehabil Eng. 2016;24:352–63.

287. Marchal-Crespo L, Reinkensmeyer DJ. Review of control strategies for robotic movement training after neurologic injury. J Neuroeng Rehabil. 2009;6. doi:10.1186/1743-0003-6-20.

288. Emken JL, Benitez R, Reinkensmeyer DJ. Human-robot cooperative movement training: learning a novel sensory motor transformation during walking with robotic assistance-as-needed. J Neuroeng Rehabil. 2007;4. doi:10.1186/1743-0003-4-8.

289. Banala SK, Agrawal SK, Scholz JP. Active Leg Exoskeleton (ALEX) for Gait Rehabilitation of Motor-Impaired Patients. In: Proceedings of the 2007 IEEE 10th International Conference on Rehabilitation Robotics. Noordwijk, The Netherlands; 2007.

290. Hussain S, Xie SQ, Liu G. Robot assisted treadmill training: Mechanisms and training strategies. Med Eng Phys. 2011;33:527–33.

291. Cao J, Xie SQ, Das R, Zhu GL. Control strategies for effective robot assisted gait rehabilitation: the state of art and future prospects. Med Eng Phys. 2014;36:1555–66. doi:10.1016/j.medengphy.2014.08.005.

292. Hussain S, Xie SQ, Jamwal PK. Adaptive impedance control of a robotic orthosis for gait rehabilitation. IEEE Trans Cybern. 2013;43:1025–34.

293. Hussein S, Schmidt H, Krüger J. Adaptive control of an end-effector based electromechanical gait rehabilitation device. In: 2009 IEEE 11th International Conference on Rehabilitation Robotics. Kyoto, Japan; 2009. p. 366–71.

294. Jezernick S, Colombo G, Morari M. Rehabilitation With a 4-DOF Robotic Orthosis. IEEE Trans Robot Autom. 2004;20:574–82.

295. Atkinson G, Nevill AM. Measurement Error (Reliability) in Variables Relevant to Sports Medicine. Sport Med. 1998;26:217–38.

296. Balasubramanian S, Colombo R, Sterpi I, Sanguineti V, Burdet E. Robotic assessment of upper limb motor function after stroke. Am J Phys Med Rehabil. 2012;91.

297. Richter H, Simon D, Smith WA, Samorezov S. Dynamic modeling , parameter estimation and control of a leg prosthesis test robot. Appl Math Model. 2015;39:559–73. doi:10.1016/j.apm.2014.06.006.

298. Melendez-Calderon A, Piovesan D, Patton JL, Mussa-Ivaldi FA. Enhanced assessment of limb neuro-mechanics via a haptic display. Robot Biomimetics. 2014;1.

299. Shadmehr R, Mussa-Ivaldi F. Adaptive representation of dynamics during learning of a motor task. J Neurosci. 1994;14 May:3208–24.

300. Lam T, Anderschitz M, Dietz V. Contribution of feedback and feedforward strategies to locomotor adaptations. J Neurophysiol. 2006;95:766–73.

301. Kawato M. Internal models for motor control and trajectory planning. Curr Opin Neurobiol. 1999;9:718--27.

302. Maggioni S, Stucki S, Lünenburger L, Riener R, Melendez-Calderon A. A bio-inspired robotic test bench for repeatable and safe testing of rehabilitation robots. In: Proceedings of the IEEE RAS and EMBS International Conference on Biomedical Robotics and Biomechatronics. Singapore; 2016. p.

894–9.

303. Pfeifer SM. Biomimetic Stiffness for Transfemoral Prostheses. ETH Zürich; 2014.

304. Zhang L-Q, Nuber G, Butler J, Bowen M, Rymer WZ. In vivo human knee joint dynamic properties as functions of muscle contraction and joint position. J Biomech. 1997;31:71–6.

305. Honegger M, Codourey A, Burdet E. Adaptive Controller of the Hexaglide, a 6 dof Parallel Manipulator. In: IEEE International Conference on Robotics and Automation. 1997. doi:10.1109/ROBOT.1997.620093.

306. Mirbagheri M, Barbeau H, Ladouceur M, Kearney R. Intrinsic and reflex stiffness in normal and spastic, spinal cord injured subjects. Exp Brain Res. 2001;141. doi:10.1007/s00221-001-0901-z.

307. Park HS, Kim J, Damiano DL. Development of a haptic elbow spasticity simulator (HESS) for improving accuracy and reliability of clinical assessment of spasticity. IEEE Trans Neural Syst Rehabil Eng. 2012;20:361–70.

308. Ishikawa S, Okamoto S, Isogai K, Akiyama Y, Yanagihara N, Yamada Y. Assessment of robotic patient simulators for training in manual physical therapy examination techniques. PLoS One. 2015;10:1–16.

309. Wisse M, Schwab AL, van der Linde RQ, van der Helm FCT. How to keep from falling forward: Elementary swing leg action for passive dynamic walkers. IEEE Trans Robot. 2005;21:393–401.

310. Goldberg S, Ounpuu S, Delp S. The importance of swing-phase initial conditions in stiff-knee gait. J Biomech. 2003;36:1111–6.

311. Dietz V, Sinkjaer T. Spastic movement disorder: impaired reflex function and altered muscle mechanics. Lancet Neurol. 2007;6:725–33.

312. Rüdt S, Moos M, Seppey S, Riener R, Marchal-Crespo L. Towards More Efficient Robotic Gait Training: A Novel Controller to Modulate Movement Errors. In: 6th IEEE RAS/EMBS International Conference on Biomedical Robotics and Biomechatronics. Singapore; 2016.

313. OpenSim. National Center for Simulation in Rehabilitation Research (NCSRR). 2010. https://opensim.stanford.edu/. Accessed 29 Aug 2019.

314. Maggioni S, Reinert N, Lünenburger L, Melendez-Calderon A. An Adaptive and Hybrid End-Point/Joint Impedance Controller for Lower Limb Exoskeletons. Front Robot AI. 2018;5.

315. Wirz M, Muller R, Bastiaenen C. Falls in persons with spinal cord injury: validity and reliability

of the Berg Balance Scale. Neurorehabil Neural Repair. 2010;24:70–7.

316. Tindall B, Council MR. Aids to the investigation of the peripheral nervous system. Med Res Counc. 1986.

317. Marino RJ, Jones L, Kirshblum S, Tal J, Dasgupta A. Reliability and repeatability of the motor and sensory examination of the international standards for neurological classification of spinal cord injury. J Spinal Cord Med. 2008;31:166–70.

318. Bernhardt M, Frey M, Colombo G, Riener R. Hybrid force-position control yields cooperative behaviour of the rehabilitation robot LOKOMAT. Proc ICORR 2005 - IEEE Int Conf Rehabil Robot. 2005;:536–9.

319. Olney SJ, Griffin MP, McBride ID. Temporal, kinematic, and kinetic variables related to gait speed in subjects with hemiplegia: a regression approach. Phys Ther. 1994;74:872–85. http://www.ncbi.nlm.nih.gov/pubmed/8066114.

320. Tibshirani R. Regression Shrinkage and Selection via the Lasso. J R Stat Soc Ser B. 1996;58:267–88.

321. Bach FR, Project-team IW. Bolasso : Model Consistent Lasso Estimation through the Bootstrap. In: ICML '08 Proceedings of the 25th international conference on Machine learning. Helsinki, Finland; 2008.

322. Sauerbrei W. The use of resampling methods to simplify regression models in medical statistics. J R Stat Soc Ser C Appl Stat. 1999;48:313–29.

323. Kim CM, Eng JJ, Whittaker MW. Level walking and ambulatory capacity in persons with incomplete spinal cord injury: relationship with muscle strength. Spiinal Cord. 2004;42:156–62.

324. Gold D. Dealing With Multicollinearity: A Brief Overview and Introduction to Tolerant Methods. Water Programming: A Collaborative Research Blog. 2017. https://waterprogramming.wordpress.com/2017/02/22/dealing-with-multicollinearity-a-brief-overview-and-introduction-to-tolerant-methods/. Accessed 6 Aug 2019.

325. Labruyère R, Hedel HJA Van. Strength training versus robot-assisted gait training after incomplete spinal cord injury : a randomized pilot study in patients depending on walking assistance. J Neuroeng Rehabil. 2014;11:1–12.

326. Podsiadlo D, Richardson S. The Timed "Up & Go": A Test of Basic Functional Mobility for Frail Elderly Persons. J Am Geriatr Soc. 1991;39:142–8.

327. Chen T, Chou LS. Effects of Muscle Strength and Balance Control on Sit-to-Walk and Turn Durations in the Timed Up and Go Test. Arch Phys Med Rehabil. 2017;98:2471–6.

328. Ng S, Hui-Chan C. The timed up {&} go test: its reliability and association with lower-limb impairments and locomotor capacities in people with chronic stroke. Arch Phys Med Rehabil. 2005;86:1641–7.

329. Ran Klein. Bland-Altman and Correlation Plot. MATLAB Central File Exchange. 2019. http://www.mathworks.com/matlabcentral/fileexchange/45049-bland-altman-and-correlation-plot. Accessed 18 Aug 2019.

330. Van Silfhout L, Hosman AJF, Bartels RHMA, Edwards MJR, Abel R, Curt A, et al. Ten Meters Walking Speed in Spinal Cord-Injured Patients: Does Speed Predict Who Walks and Who Rolls? Neurorehabil Neural Repair. 2017;31:842–50.

331. Goldberg S, Anderson F, Pandy M, Delp S. Muscles that influence knee flexion velocity in double support: implications for stiff-knee gait. J Biomech. 2004;37:1189–96.

332. Van Kammen K, Boonstra AM, Van Der Woude LHV, Reinders-Messelink HA, Den Otter R. Differences in muscle activity and temporal step parameters between Lokomat guided walking and treadmill walking in post-stroke hemiparetic patients and healthy walkers. J Neuroeng Rehabil. 2017;14:1–11.

333. Hidler JM, Wall AE. Alterations in muscle activation patterns during robotic-assisted walking. Clin Biomech. 2005;20:184–93. doi:10.1016/j.clinbiomech.2004.09.016.

334. Coenen P, van Werven G, van Nunen MPM, Van Dieën JH, Gerrits KHL, Janssen TWJ. Robot-assisted walking vs overground walking in stroke patients: an evaluation of muscle activity. J Rehabil Med. 2012;44:331–7. doi:10.2340/16501977-0954.

335. Nadeau S, Arsenault AB, Gravel D, Bourbonnais D. Analysis of the clinical factors determining natural and maximal gait speeds in adults with a stroke. Am J Phys Med Rehabil. 1999;78.

336. Kwon IS, Oldaker S, Schrager M, Talbot LA, Fozard JL, Metter EJ. Relationship between muscle strength and the time taken to complete a standardized walk-turn-walk test. Journals Gerontol - Ser A Biol Sci Med Sci. 2001;56:B398–404.

337. Bohannon R. W. Comfortable and maximum walking speed of adults aged 20-79 years : reference values and determinants. Age Ageing. 2016;26 March:15–9.

338. Willén C, Stibrant Sunnerhagen K, Ekman C, Grimby G. How is walking speed related to muscle strength? A study of healthy persons and persons with late effects of polio. Arch Phys Med

Rehabil. 2004;85:1923–8.

339. Plummer P, Eskes G, Wallace S, Giuffrida C, Fraas M, Campbell G, et al. Cognitive-motor interference during functional mobility after stroke: state of the science and implications for future research. Arch Phys Med Rehabil. 2013;94:2565–74.

340. Haufe FL, Maggioni S, Melendez-Calderon A. Reference Trajectory Adaptation to Improve Human-Robot Interaction: A Database-Driven Approach. Proc Annu Int Conf IEEE Eng Med Biol Soc EMBS. 2018;2018–July:1727–30.

341. Bayón C, Fricke SS, Rocon E, Van Der Kooij H, Van Asseldonk EHF. Performance-Based Adaptive Assistance for Diverse Subtasks of Walking in a Robotic Gait Trainer: Description of a New Controller and Preliminary Results. Proc IEEE RAS EMBS Int Conf Biomed Robot Biomechatronics. 2018;2018–Augus:414–9.

342. Smith A, Yang C, Ma H, Culverhouse P, Cangelosi A, Burdet E. Novel hybrid adaptive controller for manipulation in complex perturbation environments. PLoS One. 2015;10:e0129281. doi:10.1371/journal.pone.0129281.

343. Smith A, Yang C, Ma H, Culverhouse P, Cangelosi A, Burdet E. Biomimetic Joint/Task Space Hybrid Adaptive Control for Bimanual Robotic Manipulation. In: Proceedings - IEEE International Conference on Control & Automation (ICCA). Taichung, Taiwan; 2014.

344. Shadmehr R. Control of Equilibrium Position and Stiffness Through Postural Modules. J Mot Behav. 1993;25:228–41.

345. Mussa-Ivaldi F, Hogan N, Bizzi E. Neural, mechanical, and geometric factors subserving arm posture in humans. J Neurosci. 1985;5:2732–43.

346. Vallery H, Duschau-Wicke A, Riener R. Generalized Elasticities Improve Patient-Cooperative Control of Rehabilitation Robots. In: 2009 IEEE 11th International Conference on Rehabilitation Robotics. 2009. p. 535–41.

347. Begg R, Best R, Dell'Oro L, Taylor S. Minimum foot clearance during walking: strategies for the minimisation of trip-related falls. Gait Posture. 2007;25:191–8. doi:10.1016/j.gaitpost.2006.03.008.

348. Sekiya N, Nagasaki H, Ito H, Furuna T. The invariant relationship between step length and step rate during free walking. J Hum Mov Stud. 1996;30:241–57.

349. Elguebaly T, Bouguila N. Finite asymmetric generalized Gaussian mixture models learning for infrared object detection. Comput Vis Image Underst. 2013;117:1659–71. doi:10.1016/j.cviu.2013.07.007.

350. Ivanenko YP, Grasso R, Zago M, Molinari M, Scivoletto G, Castellano V, et al. Temporal Components of the Motor Patterns Expressed by the Human Spinal Cord Reflect Foot Kinematics. J Neurophysiol. 2003;90:3555–65. doi:10.1152/jn.00223.2003.

351. Georgopoulos AP, Grillner S. Visuomotor coordination in reaching and locomotion. Science (80-). 1989;245:1209–10. doi:10.1126/science.2675307.

352. Ivanenko YP, Grasso R, Macellari V, Lacquaniti F. Control of Foot Trajectory in Human Locomotion: Role of Ground Contact Forces in Simulated Reduced Gravity. J Neurophysiol. 2002;87:3070–89.

353. Winter DA. Human balance and posture control during standing and walking. Gait Posture. 1995;3:193–214.

354. Burdet E, Osu R, Franklin D, Milner T, Kawato M. The central nervous system stabilizes unstable dynamics by learning optimal impedance. Nature. 2001;414:446–9.

355. Kronander K, Billard A. Stability Considerations for Variable Impedance Control. IEEE Trans Robot. 2016;32:1298–305.

356. Nef T, Mihelj M, Riener R. ARMin: a robot for patient-cooperative arm therapy. Med Biol Eng Comput. 2007;45:887–900. doi:10.1007/s11517-007-0226-6.

357. Pirondini E, Coscia M, Marcheschi S, Roas G, Salsedo F, Frisoli A, et al. Evaluation of a New Exoskeleton for Upper Limb Post-stroke Neuro-rehabilitation: Preliminary Results. In: Jensen W, Kæseler Andersen O, Akay M, editors. Replace, Repair, Restore, Relieve – Bridging Clinical and Engineering Solutions in Neurorehabilitation. 2014. p. 637–45. doi:10.1007/978-3-319-08072-7.

358. Iosa M, Morone G, Cherubini A, Paolucci S. The three laws of neurorobotics: A review on what neurorehabilitation robots should do for patients and clinicians. J Med Biol Eng. 2016;36:1–11.

359. WHO. Rehabilitation 2030. https://www.who.int/disabilities/care/rehab-2030/en/. Accessed 14 Oct 2019.

360. Koopman B, van Asseldonk EHF, van der kooij H. Speed-dependent reference joint trajectory generation for robotic gait support. J Biomech. 2014;47:1447–58. doi:10.1016/j.jbiomech.2014.01.037.

361. Homberg V. Neurorehabilitation approaches to facilitate motor recovery. Handb Clin Neurol. 2013;110:161–73.

362. Gogia PP, Braatz JH, Rose SJ, Norton BJ. Reliability and validity of goniometric measurements at the knee. Phys Ther. 1987;67:192–5.

363. Currier LL, Froehlich PJ, Carow SD, McAndrew RK, Cliborne A V, Boyles RE, et al. Development of a Clinical Prediction Rule to Identify Patients With Knee Pain and Clinical Evidence of Knee Osteoarthritis Who Demonstrate a Favorable Short-Term Response to Hip Mobilization. Phys Ther. 2007;87:1106–19. doi:10.2522/ptj.20060066.

364. Poulsen E, Christensen HW, Penny JØ, Overgaard S, Vach W, Hartvigsen J. Reproducibility of range of motion and muscle strength measurements in patients with hip osteoarthritis - an inter-rater study. BMC Musculoskelet Disord. 2012;:242.

365. Elveru RA, Rothstein JM, Lamb RL. Goniometric reliability in a clinical setting. Phys Ther. 1988;68:672.

366. Watkins MA, Riddle DL, Lamb RL, Personius WJ. Reliability of goniometric measurements and visual estimates of ankle joint active range of motion obtained in a clinical setting. Phys Ther. 1991;71:90–6.

367. Wakefield CB, Halls A, Difilippo N, Cottrell GT. Reliability of Goniometric and Trigonometric Techniques for Measuring Hip-Extension Range of Motion Using the Modified Thomas Test. J Athl Train. 2015;50:150219105224004. doi:10.4085/1062-6050-50.2.05.

368. Hayes KW, Petersen CM. Reliability of assessing end-feel and pain and resistance sequence in subjects with painful shoulders and knees. J Orthop Sports Phys Ther. 2001;31:432–45.

369. Fan E, Ciesla ND, Truong AD, Bhoopathi V, Zeger SL, Needham DM. Inter-rater reliability of manual muscle strength testing in ICU survivors and simulated patients. Intensive Care Med. 2010;36:1038–43. doi:10.1007/s00134-010-1796-6.

370. Escolar DM, Henricson EK, Mayhew J, Florence J, Leshner R, Patel KM, et al. Clinical evaluator reliability for quantitative and manual muscle testing measures of strength in children. Muscle and Nerve. 2001;24:787–93.

371. Jain M, Smith M, Cintas H, Koziol D, Wesley R, Harris-Love M, et al. Intra-Rater and Inter-Rater Reliability of the 10- Point Manual Muscle Test (MMT) of Strength in Children with Juvenile Idiopathic Inflammatory Myopathies (JIIM). Phys Occup Ther Pediatr. 2006;26:1541–3144.

372. Schache MB, McClelland JA, Webster KE. Reliability of measuring hip abductor strength following total knee arthroplasty using a hand-held dynamometer. Disabil Rehabil. 2015.

373. www.rehabmeasures.org. Rehabilitation Measures Database. http://www.rehabmeasures.org. Accessed 16 Jun 2016.

374. Zhang M, Davies TC, Nandakumar A, Quan S. A novel assessment technique for measuring

ankle orientation and stiffness. J Biomech. 2015;48:3527–9. doi:10.1016/j.jbiomech.2015.06.012.

375. Clark DJ, Condliffe EG, Patten C. Reliability of concentric and eccentric torque during isokinetic knee extension in post-stroke hemiparesis. Clin Biomech (Bristol, Avon). 2006;21:395–404. doi:10.1016/j.clinbiomech.2005.11.004.

376. Chesworth BM, Vandervoort AA. Age and passive ankle stiffness in healthy women. Phys Ther. 1989;69:217–24.

ABBREVIATIONS

10MWT	10-Meter-Walking-Test
AAN	Assist-as-Needed
AB	Able-bodied
AIS	ASIA Impairment Scale
BBS	Berg Balance Scale
BWS	Body Weight Support
CI	Confidence Interval
CoR	Center of Rotation
DS1	First Double Support
DS2	Second Double Support
FAC	Functional Ambulation Category
FB	Feedback
FF	Feedforward
HE	Hip Extension
HF	Hip Flexion
ICF	International Classification of Functioning, Disability and Health
IS	Initial Swing
KE	Knee Extension
KF	Knee Flexion
Lasso	Least Absolute Shrinkage and Selection Operator
LF	L-FORCE
LOA	Limits of Agreement
MAS	Modified Ashworth Scale
MDC	Minimum Detectable Change
MMT	Manual Muscle Test

MS	Mid-Swing
PD	Proportional-Derivative
PI	Prediction Interval
SCI	Spinal Cord Injury
SS	Single Support
TLX	Task Load Index
TS	Terminal Swing
TUG	Time-Up-and-Go
WHO	World Health Organization
WISCI	Walking Index for Spinal Cord Injury

SYMBOLS

B	Damping
g	Error Gain
I	Inertia Moment
J	Jacobian Matrix
K	Stiffness
l	Segment Length
l_c	Distance between center of gravity and joint
m	Segment Mass
P	Generic Parameter adapted in AAN equation
q	Joint Angles
R^2	Coefficient of Determination
γ	Forgetting Factor for AAN equation
δ	Lasso Penalty Parameter
ρ	Spearman's Correlation Coefficient
Φ	Linearized Equations of Motion

LIST OF PUBLICATIONS OF AUTHOR

Journal Publications

Maggioni S, Melendez-Calderon A, van Asseldonk E, Klamroth-Marganska V, Lünenburger L, Riener R, et al. *Robot-aided assessment of lower extremity functions: a review.* J Neuroeng Rehabil. 2016;13:72.

Maggioni S, Reinert N, Lünenburger L, Melendez-Calderon A. *An Adaptive and Hybrid End-Point/Joint Impedance Controller for Lower Limb Exoskeletons.* Front Robot AI. 2018;5.

In preparation: **Maggioni S**, Lünenburger L, Riener R, Curt A, Bolliger M, Melendez-Calderon A, *Gait features in a robotic gait trainer: what can they tell us about waking ability?.* 2020

Shirota C, Van Asseldonk E, Matjačić Z, Vallery H, Barralon P, **Maggioni S**, et al. *Robot-supported assessment of balance in standing and walking.* J Neuroeng Rehabil. 2017;14:1–19.

Marchal-Crespo L, Tsangaridis P, Obwegeser D, **Maggioni S**, Riener R. *Haptic Error Modulation Outperforms Visual Error Amplification When Learning a Modified Gait Pattern.* Frontiers in Neuroscience. 2019;13:61.

Conference Publications

Maggioni S, Lünenburger L, Riener R, Melendez-Calderon A. *Robot-Aided Assessment of Walking Function Based on an Adaptive Algorithm.* In: 2015 IEEE 14th International Conference on Rehabilitation Robotics. Singapore; 2015. p. 804–9.

Maggioni S, Stucki S, Lünenburger L, Riener R, Melendez-Calderon A. *A bio-inspired robotic test bench for repeatable and safe testing of rehabilitation robots.* In: Proceedings of the IEEE RAS and EMBS International Conference on Biomedical Robotics and Biomechatronics. Singapore; 2016. p. 894–9.

Haufe FL, **Maggioni S**, Melendez-Calderon A. *Reference Trajectory Adaptation to Improve Human-Robot Interaction: A Database-Driven Approach.* Proc Annu Int Conf IEEE Eng Med Biol Soc EMBS. 2018;2018–July:1727–30.

Tsangaridis P, Obwegeser D, **Maggioni S**, Riener R, Marchal-Crespo L. Visual and Haptic Error Modulating Controllers for Robotic Gait Training. In: 2018 7th IEEE International Conference on Biomedical Robotics and Biomechatronics (Biorob). 2018. p. 1050–5.

Book Chapters

Lambercy O, **Maggioni S**, Lünenburger L, Gassert R, Bolliger M. *Robotic and wearable sensor technologies for measurements/clinical assessments.* In: Dietz V, Reinkensmeyer DJ, editors. Neurorehabilitation Technology. 2nd edition. Springer International; 2016.

Bejarano NC, **Maggioni S**, Rijcke L De, Cifuentes CA, Reinkensmeyer DJ. *Robot-Assisted Rehabilitation Therapy: Recovery Mechanisms and Their Implications for Machine Design*. In: Pons JL, editor. Emerging Therapies in Neurorehabilitation II. Springer International Publishing; 2016. p. 197–223.

CURRICULUM VITAE

Serena Maggioni

Personal information

E-mail: serena.maggioni@hocoma.com; sere.maggioni@gmail.com

Nationality: Italian

Date and place of birth: Milano (MI), 30/04/1986

Education and training

- 2013 – 2019
  PhD student at ETH ZURICH, Sensory-Motor Systems (SMS) Lab
  Thesis: *"Robot-Aided Gait Assessment and Rehabilitation: an Assist-as-Needed Approach"*

- 2009 - 2012
  MASTER DEGREE IN BIOMEDICAL ENGINEERING at POLITECNICO DI MILANO
  Thesis: *"Effects of EMG-based vibro-tactile biofeedback on motor strategies in childhood dystonia: a preliminary study"*
  The project was carried out at the University of Southern California (Los Angeles) from November 2011 to April 2012.
  Final grade 105/110

- 2006 - 2009
  BACHELOR DEGREE IN BIOMEDICAL ENGINEERING at POLITECNICO DI MILANO
  Thesis: "*Functional quantitative assessment of dystonia in pediatric age".*
  The project was developed in collaboration with NEARlab (Politecnico di Milano) and Neurological Institute C. Besta.
  Final grade 107/110

- 2005-2006
  Course in Linguistic and Cultural Mediation at UNIVERSITA' DEGLI STUDI DI MILANO
  Languages: English and Hindi

- 2000 - 2005
  SCIENTIFIC HIGH SCHOOL LEAVING QUALIFICATION at LICEO SCIENTIFICO ARTURO TOSI, Busto Arsizio (VA)
  Final grade 91/100

Work experience

- 2017 – today
  Hocoma AG, Industriestrasse 4, 8604 Volketswil
  Clinical and Scientific Affairs Manager

- 2013 – 2017
  Hocoma AG, Industriestrasse 4, 8604 Volketswil
  Researcher in Software Engineering

- October - December 2012
  Politecnico di Milano - NearLab

Collaboration in a research study on a biofeedback paradigm based on the EMG activity in childhood dystonia.

- 2006 - 2013
  Cultural and youth association "Comunità Giovanile", Busto Arsizio (VA), Italy:
  member of executive council, cultural events organizer, personnel manager during festivals.

- February – July 2009
  Neurological Institute "C. Besta", Milano
  Internship at the Infantile Neuropsychiatric Unit.

- May – October 2009
  Politecnico di Milano
  Collaboration "150 hours" at Career Service

Fellowships

- March 2013 – March 2016
  Marie Curie Action FP7-ITN: Moving beyond

Recognitions

- IEEE/RAS-EMBS International Conference on Biomedical Robotics and Biomechatronics 2016 (Singapore): finalists in the category "**Best student conference paper award**" for the paper "A bio-inspired robotic test bench for repeatable and safe testing of rehabilitation robot" by S. Maggioni, S. Stucki, L. Lünenburger, R. Riener, A. Melendez-Calderon